ISSN 2587-6066

СИБИРСКИЙ ЖУРНАЛ НАУКИ И ТЕХНОЛОГИЙ

SIBERIAN JOURNAL OF SCIENCE AND TECHNOLOGY

Том 21, № 2
Vol. 21, № 2

КРАСНОЯРСК 2020

СИБИРСКИЙ ЖУРНАЛ НАУКИ И ТЕХНОЛОГИЙ

Том 21, № 2

Красноярск 2020

СИБИРСКИЙ ЖУРНАЛ НАУКИ И ТЕХНОЛОГИЙ

Том 21, № 2

SIBERIAN JOURNAL OF SCIENCE AND TECHNOLOGY

Vol. 21, No 2

К СВЕДЕНИЮ ЧИТАТЕЛЕЙ

«Сибирский журнал науки и технологий» является научным, производственно-практическим рецензируемым изданием. Свидетельство о регистрации средства массовой информации ПИ № ФС 77-70577 от 03.08.2017 г. выдано Федеральной службой по надзору в сфере связи, информационных технологий и массовых коммуникаций (Роскомнадзор).

ISSN 2587-6066.

Подписной индекс в каталоге «Пресса России» – 39263.
Зарегистрирован в Российском индексе научного цитирования (РИНЦ).

Включен в базу данных Ulrich's Periodicals Directory американского издательства Bowker.

Входит в перечень журналов ВАК по следующим научным специальностям:

05.07.02 Проектирование конструкция и производство летательных аппаратов (технические);

05.07.05 Тепловые электроракетные двигатели и энергоустановки летательных аппаратов (технические);

05.07.07 Контроль и испытание летательных аппаратов и их систем (технические);

05.13.01 Системный анализ, управление и обработка информации (по отраслям) (технические);

05.13.11 Математическое и программное обеспечение вычислительных машин, комплексов и компьютерных сетей (физико-математические науки).

Выпускается с 2000 года. До 2002 года журнал носил название «Вестник Сибирской аэрокосмической академии имени академика М. Ф. Решетнева» («Вестник САА»), до мая 2017 года – «Вестник Сибирского государственного аэрокосмического университета имени академика М. Ф. Решетнева».

Каждый выпуск журнала включает три раздела:

1 раздел. Информатика, вычислительная техника и управление.

2 раздел. Авиационная и ракетно-космическая техника.

3 раздел. Технологические процессы и материалы.

Статьи публикуются бесплатно после обязательного рецензирования и при оформлении их в соответствии с требованиями редакции (www.vestnik.sibsau.ru). Журнал выходит 4 раза в год.

Электронная версия журнала представлена на сайте Научной электронной библиотеки (http://www.elibrary.ru) и сайте журнала (www.vestnik.sibsau.ru)

При перепечатке или цитировании материалов из журнала «Сибирский журнал науки и технологий» ссылка обязательна.

Учредитель и издатель

ФГБОУ ВО «Сибирский государственный университет науки и технологий имени академика М. Ф. Решетнева» (СибГУ им. М. Ф. Решетнева)

АДРЕС РЕДАКЦИИ, УЧРЕДИТЕЛЯ И ИЗДАТЕЛЯ:
Сибирский государственный университет науки и технологий имени академика М. Ф. Решетнева,
Российская Федерация, 660037, г. Красноярск,
проспект имени газеты «Красноярский рабочий», 31,
П-408. Тел./ факс (391) 262-72-38
E-mail: vestnik@sibsau.ru

Редактор Н. Н. Голоскокова
Ответственный редактор английского текста
М. В. Савельева
Оригинал-макет и верстка М. А. Светлаковой
Подписано в печать 14.07.2020. Формат 70×108/16.
Бумага офсетная. Печать плоская. Усл. печ. л. 17,0
Уч.-изд. л. 22,0. Тираж 1000 экз. Заказ 2969. С 157/20.
Редакционно-издательский отдел СибГУ им. М.Ф. Решетнева.
Отпечатано в редакционно-издательском центре
СибГУ им. М. Ф. Решетнева.
Российская Федерация, 660037, г. Красноярск,
просп. им. газ. «Красноярский рабочий», 31.
Дата выхода в свет: 14.09.2020. Свободная цена

INFORMATION FOR AUTHORS AND SUBSCRIBERS

Siberian Journal of Science and Technology is a research, production and practical peer-reviewed journal. Included by the Higher Attestation Commission of the Russian Federation in the Index of Leading Russian Peer-Reviewed Journals and Periodicals, in which significant scientific dissertation results should be published when applying for a Dr.Sc. degree.
The journal is the official periodical of Reshetnev Siberian State University of Science and Technology.

Certificate of Registration as a Mass Media Resource. Certificate: PI No. FC 77-50577, dated 03 August 2017, given by Federal Supervision Agency for Information Technology, Communications and Mass Media.

The Journal is included in the following subscription catalogue 39263 – Pressa Rossii.

The journal is registered in the Russian Science Citation Index (RSCI).
The journal is indexed in the database of Ulrich's Periodicals Directory.

The journal was first published in 2000. Prior to 2002 it had the title *Vestnik Sibirskoi aerokosmicheskoi akademii imeni academika M. F. Reshetneva (Vestnik SAA)*, prior to may 2017 it had the title *Vestnik Sibirskogo gosudarstvennogo aerokosmicheskogo universiteta imeni akademika M. F. Reshetneva (Vestnik SibGAU)*.

The Journal is recommended for publishing the main results of research when applying for Cand. Sc. degree and Dr. Sc. degree upon the following specialties:

05.07.02 Engineering, Design and Manufacturing of Aircraft (Engineering);

05.07.05 Thermal Electric Jet Engines and Power Facilities of Aircraft (Engineering);

05.07.07 Control and Testing of Aircraft and its Systems (Engineering);

05.13.01 System Analysis, Management and Information Processing (branch-wise) (Engineering);

05.13.11 Mathematical Support and Software for Computers, Computer Systems and Computer Networks (Physical and Mathematical Sciences).

Each issue consists of three parts:

Part 1. Informatics, computer technology and management.

Part 2. Aviation and Spacecraft Engineering.

Part 3. Technological Processes and Material Science.

Papers prepared in accordance with the editorial guidelines (www.vestnik.sibsau.ru) are published free of charge after being peer reviewed.

The journal is published four times a year.

An online version can been viewed at http://www.elibrary.ru
Siberian Journal of Science and Technology should be cited when reprinting or citing materials from the journal.

CONTACTS. Website: www.vestnik.sibsau.ru
Address: Reshetnev Siberian State University of Science and Technology.
31, Krasnoyarsky Rabochy Av., Krasnoyarsk, 660037, Russian Federation.
Tel./ fax (391) 262-72-38; e-mail: vestnik@sibsau.ru

Editor N. N. Goloskokova
Executive editor (*English Language*) M. V. Savelyeva
Layout original M. A. Svetlakova
Signed (for printing): 14.07.2020. Format 70×108/16.
Offset Paper. Print flat. 17.0. Published sheets 22,0.
1000 copies. Order 2969. C 157/20.
Printing and Publication Department
Reshetnev University.
Printed in the Department of copying and duplicating equipment Reshetnev University.
31, Krasnoyarsky Rabochy Av., Krasnoyarsk, 660037, Russian Federation.
Date of publication: 14.09.2020. Free price

СОДЕРЖАНИЕ

CONTENTS

Раздел
Part
1

ИНФОРМАТИКА, ВЫЧИСЛИТЕЛЬНАЯ ТЕХНИКА И УПРАВЛЕНИЕ

INFORMATICS, COMPUTER TECHNOLOGY AND MANAGEMENT

UDC 004.89
Doi: 10.31772/2587-6066-2020-21-2-150-154

For citation: Buryachenko V. V., Pahirka A. I. Object tracking with deep learning. *Siberian Journal of Science and Technology.* 2020, Vol. 21, No. 2, P. 150–154. Doi: 10.31772/2587-6066-2020-21-2-150-154

Для цитирования: Буряченко В. В., Пахирка А. И. Методы слежения за объектами с применением глубокого обучения // Сибирский журнал науки и технологий. 2020. Т. 21, № 2. С. 150–154. Doi: 10.31772/2587-6066-2020-21-2-150-154

OBJECT TRACKING WITH DEEP LEARNING

V. V. Buryachenko*, A. I. Pahirka

Reshetnev Siberian State University of Science and Technology
31, Krasnoyarskii rabochii prospekt, Krasnoyarsk, 660037, Russian Federation
*E-mail: buryachenko@sibsau.ru

Tracking objects is a key task of video analytics and computer vision, which has many applications in various fields. A lot of tracking systems include two stages: detecting objects and tracking changes in the position of objects. At the first stage, objects of interest are detected in each frame of the video sequence, and at the second, the correspondence of the detected objects in neighboring frames is assessed. Nevertheless, in difficult conditions of video surveillance, this task has a number of difficulties associated with changing the illumination of the frame, changing the shape of objects, for example, when a person is walking, and the task is also complicated in the case of camera movement. The aim of the work is to develop a method for tracking objects on the basis of deep learning, which allows to track several objects in the frame, including those in the rough conditions of video surveillance. The paper provides an overview of modern methods for solving objects tracking tasks, among which the most promising one is deep learning neural networks application. The main approach used in this paper is neural networks for detecting regions (R-CNN), which has proven to be an effective method for solving problems of detection and recognition of objects in images. The proposed algorithm uses an ensemble containing two deep neural networks to detect objects and to refine the results of classification and highlight the boundaries of the object. The article evaluates the effectiveness of the developed system using the classical in the field MOT(Multi-Object tracking) metric for objects tracking based on the known databases available in open sources. The effectiveness of the proposed system is compared to other well-known works.

Keywords: intelligent systems, deep learning, motion estimation, convolutional network for regions classification (R-CNN).

МЕТОДЫ СЛЕЖЕНИЯ ЗА ОБЪЕКТАМИ С ПРИМЕНЕНИЕМ ГЛУБОКОГО ОБУЧЕНИЯ

В. В. Буряченко*, А. И. Пахирка

Сибирский государственный университет науки и технологий имени академика М. Ф. Решетнева
Российская Федерация, 660037, г. Красноярск, просп. им. газеты «Красноярский рабочий», 31
*E-mail: buryachenko@sibsau.ru

Слежение за объектами является ключевой задачей видеоаналитики и компьютерного зрения, которая имеет множество применений в различных областях. Большинство систем слежения включают в себя два этапа: обнаружение объектов и отслеживание изменения положения объектов. На первом этапе осуществляется обнаружение объектов интереса в каждом кадре видеопоследовательности, а на втором выполняется оценка соответствия обнаруженных объектов в соседних кадрах. Тем не менее в сложных условиях видеонаблюдения данная задача имеет ряд особенностей, связанных с изменением освещенности кадра, изменением формы объектов, например при ходьбе человека, а также усложняется в случае движения камеры. Целью работы является разработка метода слежения за объектами на основе нейронных сетей глубокого обучения, который позволяет осуществлять отслеживание нескольких объектов в кадре, в том числе и в сложных условиях видеонаблюдения. В работе выполнен обзор современных методов решения задач слежения за объектами, среди которых наиболее перспективным подходом является использование сетей глубокого обучения. Основным используемым подходом в данной статье являются нейронные сети для обнаружения регионов (R-CNN), которые показали себя эффективным методом для решения задач обнаружения и распознавания объектов на изображениях. Предложенный алгоритм использует ансамбль, содержащий две глубокие нейронные сети для обнаружения объектов и уточнения результатов классификации и выделения границ объекта. В статье выполнена оценка эффективности разработанной системы с использованием классической метрики MOT в области слежения за объектами на известных базах данных, доступных в открытых источниках. Проведено сравнение эффективности предложенной системы с другими известными работами.

Ключевые слова: интеллектуальные системы, глубокое обучение, оценка движения, сверточная сеть для классификации регионов.

Introduction. In recent years, methods of measuring motion and tracking objects have achieved impressive results. Works on monitoring the movement of people in public places, facial recognition methods, suspicious objects detection and people's deviant behavior are practical applications for improving security. Video sequence stabilization methods are also widely used in video analytics as well as to improve the convenience of operators' work with surveillance systems. Stabilization eliminates unintentional video jitter, while preserving directed motions and camera panning.

Most of the tasks discussed are based on the use of high-level video sequence analysis, motion estimation, and object tracking techniques, which require demanding tasks to detect and track special points in video sequence frames. The application form proposes to use modern deep learning technologies to improve quality and reduce computational and time costs for performing motion estimation and stabilizing video sequences.

Review of publications. Deep neural networks have proved to be one of the best technologies for solving numerous problems related to digital image processing. The greatest success was demonstrated by convolutional neural networks containing from 10 to 300 layers, when solving image recognition problems [1], semantic analysis of texts [2] and training with reinforcement [3]. Recent studies have shown the effectiveness of artificial neural networks of complex structures when solving problems of motion analysis [4; 5] and evaluating optical flow [6; 7], as well as the possibility of using such technologies to stabilize video sequences [8]. One known approach used to detect and track objects is to estimate the visibility in the frame [9; 10].

This paper examines methods of tracking moving objects using deep learning approaches. To improve the quality of the algorithm, a convolutional network is used to classify regions (R-CNN) and methods for stabilizing the received video material. Visual tracking of objects is a classical computer vision task in which the position of the target is determined in each frame. This area of research remains in demand due to the large number of practical tasks based on tracking various objects. The algorithms used in this field are also improving, and allow to solve highly complex problems, such as occlusion, changing the position and shape of objects, people's appearance, lighting and presence of a complex background with various textures. In this regard, the publications offer a number of algorithms and approaches aimed at solving various tracking problems and improving the overall performance of object tracking.

Tracking of objects. A typical tracking system consists of two main models, the motion model and the appearance model. The motion model is used to predict the target location in the subsequent frame, similarly to the use of the Kalman filter or particle filter to simulate the target motion. The motion model can also be simple, for example including linear motion, on the basis of which several more complex trajectories are built; and more complex, which track objects taking with respect to changes in direction and speed of movement. To speed up the motion evaluation process, a motion value assumption is proposed within the search box around the previous location of the object. On the other hand, the appearance model is used to describe the target and check the predicted location of the target in each frame. Appearance models can use generative and discriminatory methods. In generative methods, tracking is performed by searching for a region most similar to an object. Discriminatory methods use a classifier that allows to distinguish between the object and the background. In general, the appearance model can be updated during system operation, taking into account required changes to objects. This allows, for example, to continue tracking a person when turning or tilting a body.

Traditionally, motion tracking algorithms have used manually calculated functions based on pixel intensity, color, and histogram of oriented gradients (HOG) to represent the target in generative or discriminatory description models. Although they achieve satisfactory performance under certain conditions, they are not resistant to major changes in the appearance of objects. Deep training using Convolution Neural Networks (CNN) has recently significantly improved the performance of various computer vision applications.

This approach also affected visual tracking of objects and partially allowed to overcome difficulties and get better performance compared to the methods used earlier. In CNN-based tracking systems, the object appearance model is based on convolutional network training, and the classifier is used to mark the path on the image as belonging to the object or background. CNN-based systems have achieved a modern level of efficiency even using simple off-line motion models without retraining. However, such systems usually experience high computational loads due to the large number of possible trajectories of objects during the stages of neural network training and objects tracking.

A promising trend in the field of object tracking is the tasks associated with the analysis of a large number of people in a frame (Multi-object tracking (MOT)). This task has two stages: detecting objects and associating them in different frames. During the first stage, desired objects are detected in each frame of the video stream, where the objects may be different depending on the detector used. The quality of detection directly affects the performance of the tracking system. The second stage includes searching for a match between detected objects in the current frame and the previous one to estimate their motion paths. The high accuracy of the object detection system results in fewer missing objects and more stable trajectories. However, at the same time, excessive retraining of the detection system can reduce the quality of the system when changing object parameters. Applying additional approaches when solving the problem of associating objects in different frames can improve the quality of tracking complex objects with changing parameters. The accuracy of object detection can be increased by using a convolutional neural network based on deep learning. Objects are merged based on appearance and improved motion functions.

R-CNN-based object tracking system. One of the areas of research is the development of an algorithm that allows to improve tracking objects accuracy by using a convolutional network for classifying regions (R-CNN)

and increasing the speed of the system to close to real time evaluation. A convolutional network allows to classify an area as belonging to an object or background, and at the same time, the characteristic map obtained during the network operation is also used to perform approximate localization of objects and allows to reduce the time for evaluating matches between them.

Practical experiments were conducted applying the neural network to classify regions, the structure of which is shown in tab. 1. The main task is to track several types of objects in a frame: people and cars. Proposed method includes components of human detection, prediction of objects position in subsequent frames, association of detected objects and control of selected objects cycle. The most widely known object detection algorithm is YOLO [24], which is fast enough to detect several objects in real time, but has insufficient accuracy, leading to trajectories fragmentation and complexities with identifying detected objects.

The basic diagram of the developed system is shown in fig. 1. With the development of deep learning-based algorithms, detection of objects in complex conditions has become much easier. A key component of the algorithm is a convolutional region detection network (R-CNN).

During the first stage, a region proposal network (RPN) generates bindings to regions in the image that have a high probability of an object presence. This process is divided into three steps.

Table 1

Convolutional region network parameters

Layer name	Filter dimensions	Step	Number of layer outputs
Conv 1	3 × 3	1	32×128×6432×128×64
Conv 2	3 × 3	1	32×128×6432×128×64
Max pool 1	3 × 3	2	32×64×3232×64×32
Residual block 1	3 × 3	1	32×64×3232×64×32
Residual block 2	3 × 3	1	32×64×3232×64×32
Residual block 3	3 × 3	2	64×32×1664×32×16
Residual block 4	3 × 3	1	64×32×1664×32×16
Residual block 5	3 × 3	2	128×16×8128×16×8
Residual block 6	3 × 3	1	128×16×8128×16×8
Dense layer 1		–	128
Batch norm		–	128

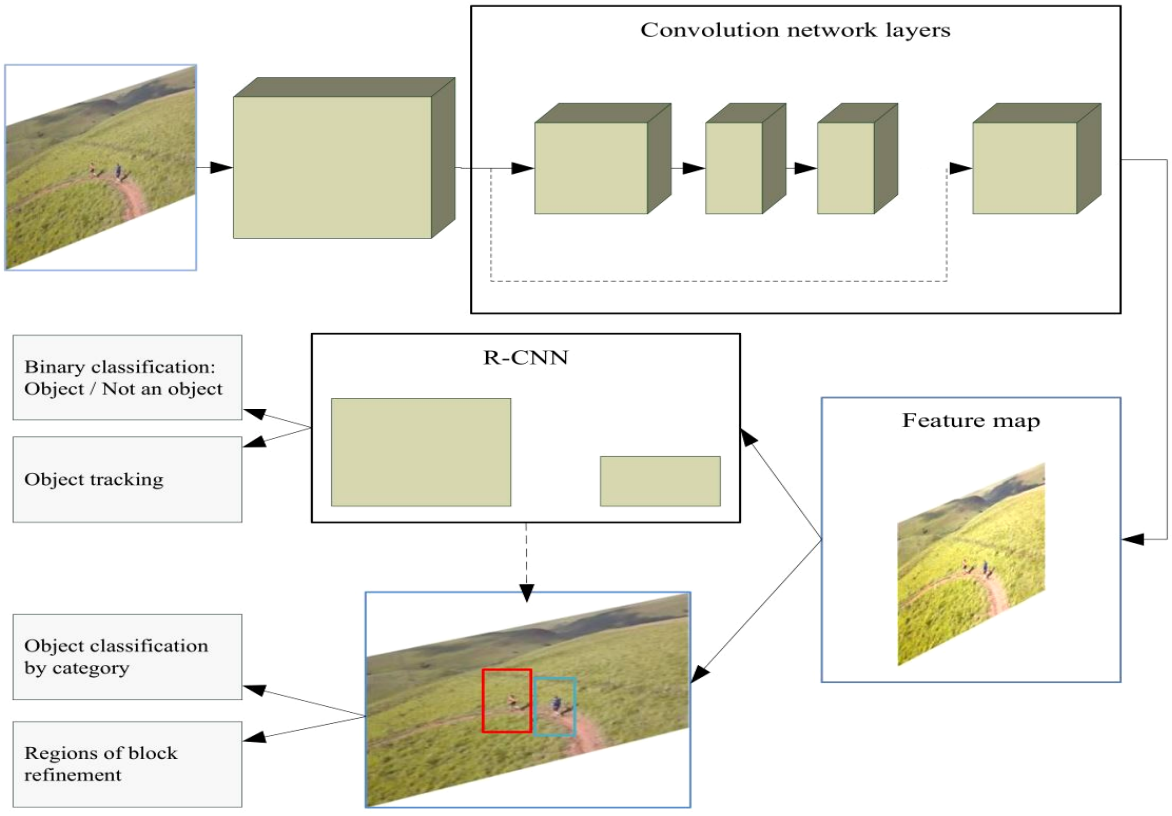

Fig. 1. The structure of the proposed object tracking system and objects classification

Рис. 1. Структура предложенной системы для отслеживания и классификации объектов

The first one includes a feature extraction process using a convolutional neural network. Convolution object maps are generated on the last layer. The second step uses the sliding window approach on these object maps to create blocks containing objects. The block parameters are refined in the next step to indicate the presence of objects in them.

Finally, in the third step, the generated masks are refined using a simpler network that calculates a loss function for selecting key blocks containing objects. For a neural network, proposing regions is a necessary step in extracting convolution functions that are calculated using the main network.

Pilot studies. Effectiveness of the object tracking algorithm was assessed using more than 10 video sequences from open databases: KITTI Vision Benchmark Suite [11], Drones Dataset [12], MOT16 [13], containing more than 20,000 frames for which the boundaries of objects of interest were indicated: people and machines. Scenes vary significantly in terms of background, lighting conditions, and how the camera moves. The study allows to determine the accuracy of detecting and tracking moving objects in accordance with the known metric Clear MOT (1), showing the ratio of correctly detected pixels in the image belonging to objects of interest to a known value (Ground Truth) [14]:

$$\mathrm{MOTA} = 1 - \frac{\sum_t \left(FP_t + FN_t + ID\_Sw_t \right)}{\sum_t GT_t},$$

where t – the frame number of the video sequence; GT – a valid value indicating the number of pixels containing the object of interest; FP and FN are false positive and false negative detectors respectively; ID_Sw is the threshold for changing object identity due to complex trajectories and noise during observation.

Tab. 2 shows the main results of object tracking system operation on various video sequences, as well as the scene parameters. Fig. 2 shows examples of object tracking.

Tab. 3 presents the assessment of the basic object tracking system quality parameters in comparison with other modern systems.

Table 2

Tracking system efficiency assessment

Video sequence name	Resolution	FPS	Number of frames	Camera motion	MOTA
MOT16_07 [13]	1920×1080	30	500	Y	64.1
DJI_0574 [12]	3840×2160	60	960	Y	78.5
Bluemlisalphutte Flyover [12]	1280×720	60	990	Y	75.8
Berghouse Leopard Jog [12]	1280×720	30	1110	N	63.2
Kitty_0016 [11]	1920×1080	30	509	Y	58.1
Kitty_0018 [11]	1920×1080	60	179	Y	61.4
Kitty_0024 [11]	1920×1080	30	315	N	63.7

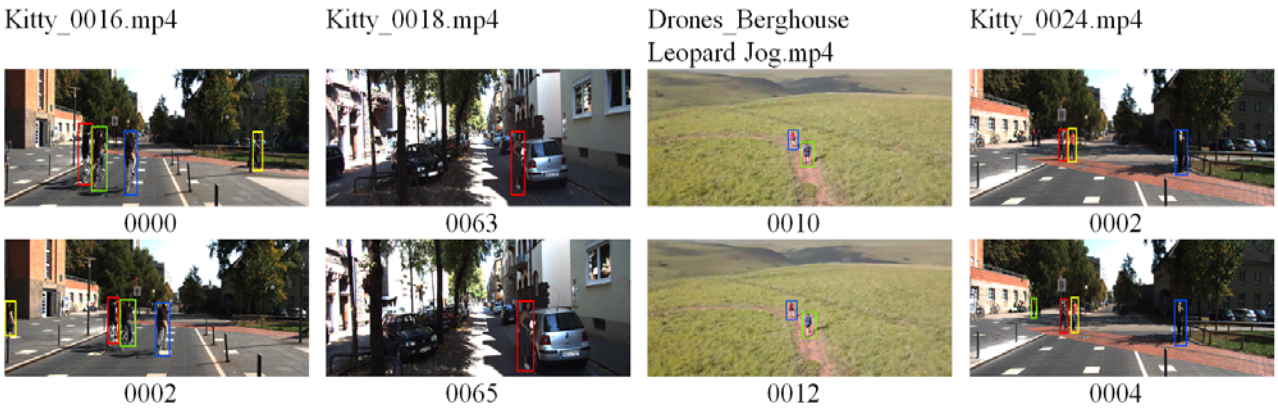

Fig. 2. Object racking examples of testing videos

Рис. 2. Примеры отслеживания объектов тестовых видеопоследовательностей

Table 3

Assessment of different object tracking systems efficiency

	MOTA	MOTP	FP	FN	Runtime
KNDT	68.2	79.4	11,479	45.605	0.7 Hz
POI	66.1	79.5	5061	55.914	10 Hz
SORT	59.8	79.6	8698	63.245	60 Hz
Deep Sort	61.4	79.1	12.852	56.668	40 Hz
Proposed system	60.8	79.8	3855	37.45	42 Hz

Conclusion. As a result, the system has been developed to track various objects for video surveillance and video analytics. Features of the algorithm are pseudo-real speed: 25–35 frames per second at the resolution of 1920 × 1080, as well as high quality of object tracking, which is associated with the use of the neural network to clarify the detected regions. To improve operator convenience and video analysis system quality, the system includes video sequence stabilization techniques that improve both real-time video and existing video by eliminating unintentional jitter.

References

1. Krizhevsky A., Sutskever I., Hinton G. E. ImageNet classification with deep convolutional neural networks. *Communications of the ACM*. 2017, Vol. 60, No. 6, P. 84–90.

2. Socher R., Perelygin A., Jean Y. Wu, Chuang J., Manning C. D., Ng A. Y., Potts C. Recursive Deep Models for Semantic Compositionality Over a Sentiment Treebank. *Proceedings of the Conference on Empirical Methods in Natural Language Processing (EMNLP)*. 2013. P. 1631–1642.

3. Mnih V., Kavukcuoglu K., Silver D. et al. Human-level control through deep reinforcement learning. *Nature.* 2015, Vol. 518, P. 529–533. Doi: 10.1038/nature14236.

4. Khan G., Tariq Z., Khan M. Multi-Person Tracking Based on Faster R-CNN and Deep Appearance Features, Visual Object Tracking with Deep Neural Networks, Pier Luigi Mazzeo, Srinivasan Ramakrishnan and Paolo Spagnolo, IntechOpen. 2019. Doi: 10.5772/intechopen.85215.

5. Ren S., He K., Girshick R., Sun J. Faster R-CNN: Towards Real-Time Object Detection with Region Proposal Networks Computer Vision and Pattern Recognition arXiv: 1506.01497, 04.01.2015.

6. Hui T.-W., Tang X., Loy C.-C. LiteFlowNet: A lightweight convolutional neural network for optical flow estimation. *IEEE Conference on Computer Vision and Pattern Recognition*, Salt Lake City, Utah, USA, 2018, P. 8981–8989.

7. Dosovitskiy A., Fischer P., Ilg E., Höusser P., Hazırbas C., Golkov V., van der Smagt P., Cremers D., Brox T. Flownet: Learning optical flow with convolutional networks. *IEEE International Conference on Computer Vision*, 2015, P. 2758–2766.

8. Wang M. et al. Deep Online Video Stabilization With Multi-Grid Warping Transformation Learning. *IEEE Transactions on Image Processing*, 2019, Vol. 28, No. 5, P. 2283–2292. Doi: 10.1109/TIP.2018.2884280.

9. Favorskaya M. N., Buryachenko V. V., Zotin A. G., Pahirka A. I. Video completion in digital stabilization task using pseudo-panoramic technique. *Int. Arch. Photogramm. Remote Sens. Spatial Inf. Sci*. 2017, Vol. XLII-2/W4, P. 83–90.

10. Favorskaya M. N., Buryachenko V. V. Background extraction method for analysis of natural images captured by camera traps. *Informatsionno-upravliaiushchie sistemy*. 2018, No. 6, P. 35–45. Doi: 10.31799/1684-8853-2018-6-35-45.

11. Geiger A., Lenz P., Urtasun R. Are we ready for autonomous driving? The KITTI vision benchmark suite. *IEEE 2012 Conference on Computer Vision and Pattern Recognition, Providence, RI*, 2012, P. 3354–3361,

12. Drone Videos DJI Mavic Pro Footage in Switzerland Available at: https://www.kaggle.com/kmader/ /drone-videos (accessed 05.05.2019).

13. Milan A., Leal-Taixé L., Reid I., Roth S., Schindler K. MOT16: A Benchmark for Multi-Object Tracking. arXiv:1603.00831 [cs], (arXiv: 1603.00831), 2016.

14. Sun S., Akhtar N., Song H., Mian A. S., Shah M. Deep Affinity Network for Multiple Object Tracking. *IEEE Transactions on Pattern Analysis and Machine Intelligence,* 2017, P. 1–15.

15. Zhou Xiangzeng, Xie Lei, Zhang Peng, Zhang Yanning. An Ensemble of Deep Neural Networks for Object Tracking. *IEEE International Conference on Image Processing, ICIP 2014*, 2014.

Buryachenko Vladimir Viktorovich – Cand. Sc., Associate Professor; Reshetnev Siberian State University of Science and Technology. E-mail: buryachenko@sibsau.ru.

Pahirka Andrei Ivanovich – Cand. Sc., Associate Professor; Reshetnev Siberian State University of Science and Technology. E-mail: pahirka@sibsau.ru.

Буряченко Владимир Викторович – кандидат технических наук, доцент; Сибирский государственный университет науки и технологий имени академика М. Ф. Решетнева. E-mail: buryachenko@sibsau.ru.

Пахирка Андрей Иванович – кандидат технических наук, доцент; Сибирский государственный университет науки и технологий имени академика М. Ф. Решетнева. E-mail: pahirka@sibsau.ru.

UDC 691.175
Doi: 10.31772/2587-6066-2020-21-2-155-162

For citation: Bychkovsky V. S., Butorin D. V., Bakanin D. V., Filippenko N. G., Livshits A. V. Volume temperature control at automated high-frequency processing of polymer and composite materials. *Siberian Journal of Science and Technology.* 2020, Vol. 21, No. 2, P. 155–162. Doi: 10.31772/2587-6066-2020-21-2-155-162

Для цитирования: Объемный контроль температуры при автоматизированной высокочастотной обработке полимерных и композиционных материалов / В. С. Бычковский, Д. В. Буторин, Д. В. Баканин и др. // Сибирский журнал науки и технологий. 2020. Т. 21, № 2. С. 155–162. Doi: 10.31772/2587-6066-2020-21-2-155-162

VOLUME TEMPERATURE CONTROL AT AUTOMATED HIGH-FREQUENCY PROCESSING OF POLYMER AND COMPOSITE MATERIALS

V. S. Bychkovsky*, D. V. Butorin, D. V. Bakanin, N. G. Filippenko, A. V. Livshits

Irkutsk State Transport University
15, Chernyshevsky Av., Irkutsk, 664074, Russian Federation
*E-mail: bikovskii_vs@mail.ru

The purpose of this work is to develop and justify a method for volumetric temperature control of a polymer and composite material in automated high-frequency processing. The developed method is implemented by introducing thermocouples into the prism-shaped or cube-shaped sample body according to a certain pattern of their location throughout the volume. This technique is cost-effective and easy to implement compared to expensive and specialized equipment with complex design, as well as to the cost of thermocouples having a simple design.

Methods to achieve the purpose of the research of the contact method of volumetric temperature of a polymer or composite sample control are development and outlining thermocouples throughout the volume so as to identify the most accurate temperature spectrum of the polymer or composite sample during automated high-frequency processing. Another method to achieve this purpose is the method of finding out how it will affect the measurements accuracy of the heating sample temperature from the introduction of thermocouples by making holes in it for installation. For this, a finite-difference mathematical calculation of the dependence of the sample temperature on the number of holes for thermocouples in it was performed in the MSC Patran Sinda software package. The calculation results were summarized and presented on graphic data. Further, a general mathematical calculation was performed according to the formulas for the process of heat and mass conductivity calculation, the results of which were table and graphic data.

At the end of the finite-difference and general mathematical calculation, a comparative analysis of the obtained error of temperature measurement from the introduction of thermocouples into the body of the sample was performed. Based on this analysis, the developed method is applicable for further research on automated high-frequency processing of polymer and composite materials, since the errors obtained do not exceed the permissible 3 %.

Keywords: polymers, high-frequency heating, finite-element mathematical model, general mathematical model.

ОБЪЕМНЫЙ КОНТРОЛЬ ТЕМПЕРАТУРЫ ПРИ АВТОМАТИЗИРОВАННОЙ ВЫСОКОЧАСТОТНОЙ ОБРАБОТКЕ ПОЛИМЕРНЫХ И КОМПОЗИЦИОННЫХ МАТЕРИАЛОВ

В. С. Бычковский*, Д. В. Буторин, Д. В. Баканин, Н. Г. Филиппенко, А. В. Лившиц

Иркутский государственный университет путей сообщения
Российская Федерация, 664074, г. Иркутск, ул. Чернышевского, 15
*E-mail: bikovskii_vs@mail.ru

Целью данной работы является разработать и обосновать способ объемного контроля температуры полимерного и композиционного материала при автоматизированной высокочастотной обработке. Разработанный способ реализуется путем внедрения термопар в тело образца по форме призмы или куба по определенной схеме их расположения по всему объему. Данная методика проста в реализации и экономически выгодна по сравнению со стоимостью дорогого и специализированного оборудования со сложной конструкцией и самих термопар, имеющих простую конструкцию.

Методами достижения поставленной цели исследований контактного способа объемного контроля температуры полимерного или композиционного образца являются разработка и построение схемы расположения термопар по всему объему так, чтобы выявить наиболее точно температурный спектр полимерного или композиционного образца при автоматизированной высокочастотной обработке. Разработана схема расположения термопар. Следующим методом для достижения поставленной цели стал метод выяснения влияния

на точность измерений температуры нагрева образца в зависимости от внедрения в него термопар за счет выполнения в нем отверстий для их установки. Для этого выполнен конечно-разностный математический расчет зависимости температуры образца от количества отверстий под термопары в нем в программном комплексе MSC Patran Sinda. Результаты расчета сведены и представлены на графических данных. Далее был выполнен общий математический расчет по формулам расчета процесса тепло- и массопроводности. Итогами данного расчета стали таблица и графические данные.

По окончании конечно-разностного и общего математического расчета произведен сравнительный анализ полученной погрешности измерения температуры от внедрения термопар в тело образца. Исходя из этого анализа, можно сказать, что разработанная методика применима для дальнейшего исследования автоматизированной высокочастотной обработки полимерных и композиционных материалов, так как полученные погрешности не превышают допустимых 3 %.

Ключевые слова: полимеры, высокочастотный нагрев, конечно-элементная математическая модель, общая математическая модель.

Introduction. To enhance operational and strength properties of increased durability achievement, to improve polymers and composites service life and to prevent dry start during operation, oil-filled polymer and composite antifriction materials are created using developed technology of high-frequency oil filling [1]. At the same time, implementation of the method has one problem in the course of process automation due to the need of constant sample temperature volumetric control during drying and self-filling [1–6]. Research in this field proves to be a pressing task.

Purpose and tasks. To develop a contact method for measuring a polymer sample temperature throughout the volume during high-frequency processing.

In order to achieve this goal, the following tasks were defined:

– outlining thermocouples location in the polymer sample body;

– constructing a finite-element mathematical model by calculating the effect of thermocouples quantity on the sample heating during high-frequency processing.

– constructing a general mathematical model by calculating the effect of thermocouples quantity on sample heating during high-frequency processing.

– making comparative analysis of the obtained results.

Background data. Sample from material PA6 Specification 224-001-78534599–2006; overall dimensions, 50 × 50 × 4 mm; density, 1120 kg/m3; specific heat capacity, 1601 J/kg K; thermal conductivity, 0.23 W/(m · K). Thermocouple (TC) chromel-alumel; weld diameter, 0.25 mm; wire diameter, 0.1 mm; hole dimensions, 0.25 × 25 mm [7–10].

Preliminary layout of thermocouples in the sample is shown in fig. 1.

Finite-difference mathematical calculation. Construction of a finite-difference mathematical model based on the calculation of the number of thermocouples effect on the sample heating during high-frequency processing was carried out in the MSC Patran Sinda software complex (fig. 2, tab. 1).

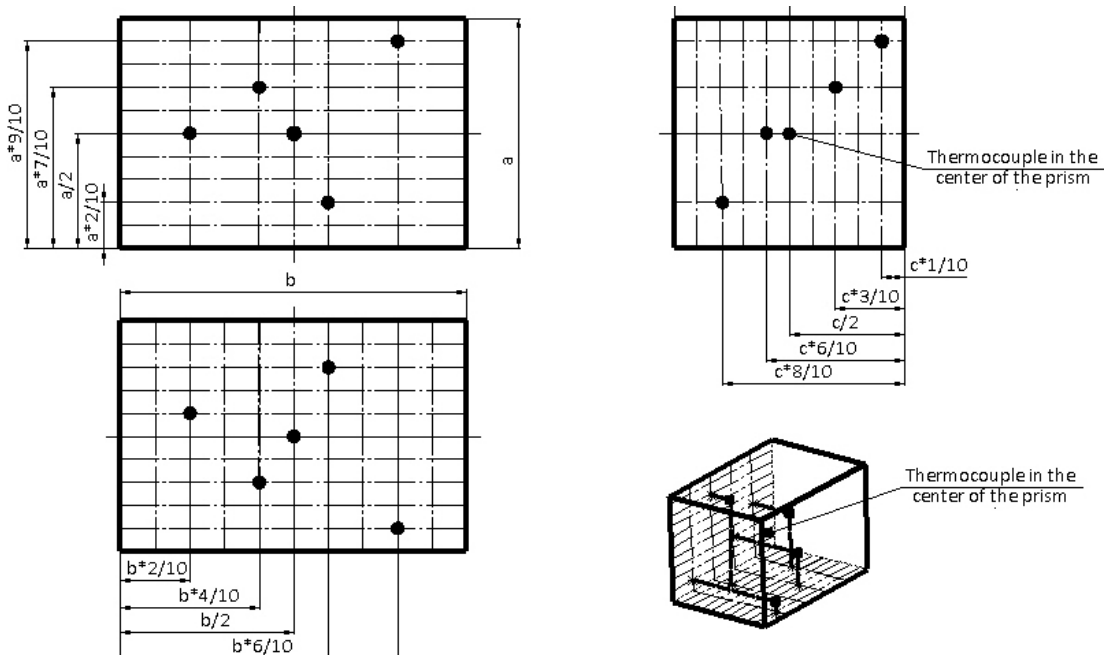

Fig. 1. Layout of thermocouples in the sample

Рис. 1. Схема расположения термопар в образце

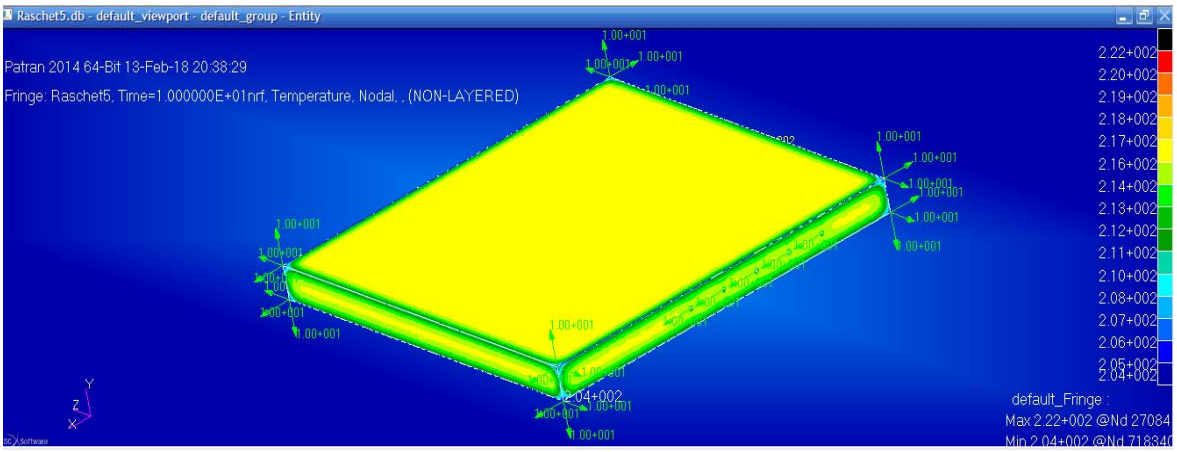

Fig. 2. The finite-difference mathematical model of the prototype

Рис. 2. Конечно-разностная математическая модель опытного образца

Table 1

Summary of calculation results MSC Patran Sinda

Quantity of thermo-couples, in pcs.	Symmetry plane temperature, °C	Body surface temperature, °C	Hole walls temperature, °C
0	220.746	202.701	–
1	221.500	203.516	220.251
2	221.546	203.538	220.263
3	221.625	203.569	220.282
4	221.630	203.558	220.271
5	221.678	203.575	220.293

As boundary conditions, the following ones were adopted: volumetric heating power constant, 10 W; convective thermal conductivity coefficient constant, 10 W/(K · m^2); ambient temperature, 20 °C [11–14].

According to the results of the calculations of MSC Patran Sinda given in tab.1, the diagram (fig. 3) of the temperature dependence on the number of holes for thermocouples in the polymer sample has been constructed.

From the obtained graphic data, it can be concluded that with high-frequency heating, as the number of holes in the body increases, the temperature of the polymer sample increases throughout the volume.

Calculation of error from thermocouples in polymer sample installation is done by formula

$$\Delta_1 = 100 - \frac{T_{\text{withoutTC}} \cdot 100}{T_{5\,\text{TC}}} = \\ = 100 - \frac{220,746 \cdot 100}{221,500} = 0,34\ \%, \qquad (1)$$

where $T_{\text{withoutTC}}$ – temperature in the body of a polymeric sample without holes, °C; $T_{5\text{TC}}$ – temperature in the polymeric sample body with 5 holes, °C.

Results of finite-element mathematical model construction showed that calculated error value does not exceed permissible value of 3 % [15].

General mathematical calculation. General mathematical model construction by calculating the effect of thermocouples number on sample heating during high-frequency processing.

The process of volumetric heating of the polymer sample with dimensions of 50×50×4 mm, from internal heat sources can be referred to as a particular case of thermal conductivity of a homogeneous plate.

Heat sources are evenly distributed throughout the volume, q_v = const. Convective heat transfer coefficient, α = const and ambient temperature T_{air} = const. Due to uniform cooling, the temperatures of both surfaces are the same [16; 17].

Under these conditions, the temperature of the plate will vary only along the x-axis (fig. 4) normal to the surface of the body.

The temperatures on the axis of the plate and on its surface are indicated through T_0 and $T_{surface}$, respectively; these temperatures are unknown. In addition, it is necessary to find the temperature distribution in the plate and the amount of heat supplied to the environment according to formula

$$T(x) = T_{air} + \frac{q_v \cdot \delta}{\alpha} + \frac{q_v}{2 \cdot \lambda}(\delta^2 - x^2), \quad -\delta \le x \le \delta, \qquad (2)$$

where T_{air} – ambient temperature (air), 20 °C; – convective heat transfer coefficient, 10 W/(deg m^2); λ – polymer thermal conductivity coefficient (PA 6), 0.26 W/(deg m); δ – extreme position of the point in

contact with the environment, 0.002 m; q_v – volumetric productivity of internal heat sources, W/m^3.

Volumetric capacity of internal heat sources is calculated according to formula

$$q_v = \frac{Q}{V}, \quad (3)$$

where Q – thermal power from each internal heat source, 10 W; V – body volume, m^3.

The results of internal heat sources volumetric productivity calculations are summarized in tab. 2.

Body surface temperature ($x = \delta$)

$$T_{surface} = T_{air} + \frac{q_v \cdot \delta}{\alpha}. \quad (4)$$

Symmetry plane temperature ($x = 0$)

$$T_0 = T_{surface} + \frac{q_v \cdot \delta^2}{2 \cdot \lambda}. \quad (5)$$

The results of temperature calculations on the surface of the body and on the plane of symmetry are summarized in tab. 3.

Let the boundary conditions of the third type be given, i. e. the ambient temperature on the outside surface and the constant heat transfer coefficient on the outside surface (fig. 5) [17–19].

Temperature field dependence, formula

$$T(r) = T_{air} + \frac{q_v \cdot \delta}{2\alpha} \times$$
$$\times \left[1 - \left(\frac{\delta_r}{\delta}\right)^2\right] + \frac{q_v \cdot \delta^2}{4\lambda} \cdot \left[1 + \left(\frac{\delta_r}{\delta}\right)^2 \cdot 2\ln\frac{r}{\delta} - \left(\frac{r}{\delta}\right)^2\right], \quad (6)$$
$$\delta_r \le r \le \delta,$$

where δ_r – radius of the hole for thermocouple, 0.000125 m.

Temperature difference between body surface and heat-release surface of the hole wall, formula

$$T_{hole} - T_{surface} = \frac{q_v \cdot \delta_r^2}{4\lambda} \cdot \left[\left(\frac{\delta}{\delta_r}\right)^2 - 2\ln\frac{\delta}{\delta_r} - 1\right], \quad (7)$$

hence

$$T_{hole} = \frac{q_v \cdot \delta_r^2}{4\lambda} \cdot \left[\left(\frac{\delta}{\delta_r}\right)^2 - 2\ln\frac{\delta}{\delta_r} - 1\right] + T_{surface} \cdot, \quad (8)$$

where T_{hole} – hole wall temperature,°C

The results of the hole wall temperature calculations are given in tab. 3, fig. 6.

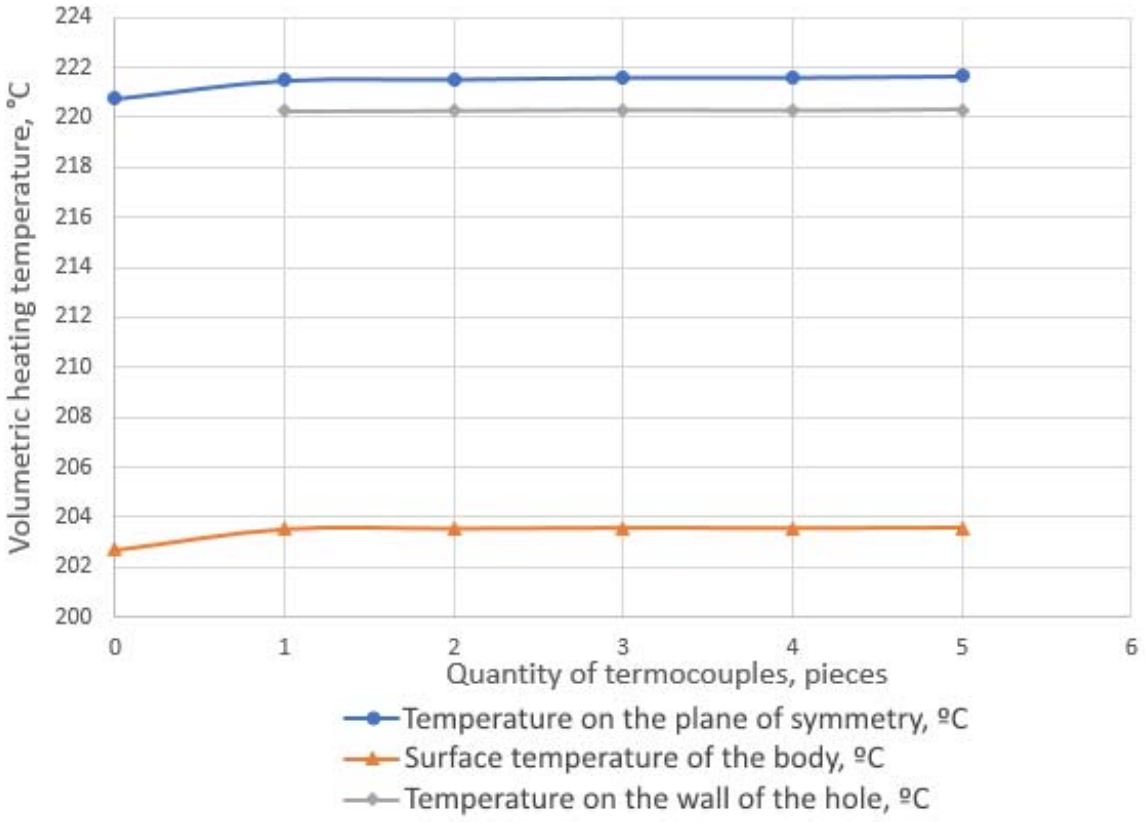

Fig. 3. Calculation results of MSC Patran Sinda

Рис. 3. Результаты расчетов MSC Patran Sinda

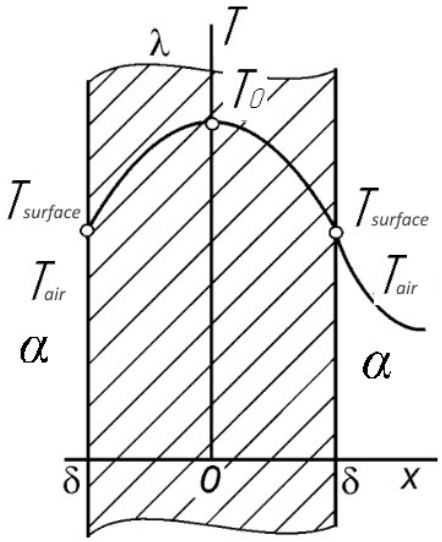

Fig. 4. Calculation scheme of thermal conductivity of a homogeneous plate

Рис. 4. Расчетная схема теплопроводности однородной пластины

Table 2

Summary of internal heat sources volumetric productivity calculations results

Quantity of thermocouples, pcs.	V, m^3	q_v, W/m^3
0	$1.00000 \cdot 10^{-5}$	$1.000 \cdot 10^6$
1	$9.99877 \cdot 10^{-6}$	$1.001 \cdot 10^6$
2	$9.99754 \cdot 10^{-6}$	$1.002 \cdot 10^6$
3	$9.99631 \cdot 10^{-6}$	$1.004 \cdot 10^6$
4	$9.99508 \cdot 10^{-6}$	$1.005 \cdot 10^6$
5	$9.99385 \cdot 10^{-6}$	$1.006 \cdot 10^6$

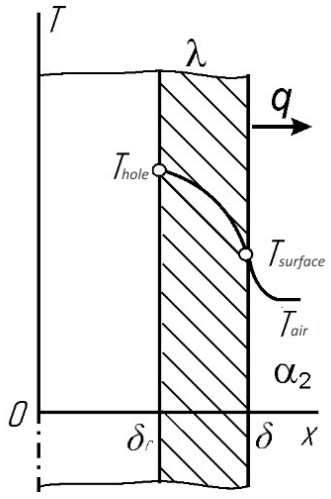

Fig. 5. Calculation diagram of the temperature on the wall of the hole

Рис. 5. Расчетная схема температуры на стенке отверстия

Table 3

The results of temperature calculations on the body surface, symmetry plane and on the walls of the hole

Quantity of thermocouples, pcs.	$T_{surface}$, °C	T_0 , °C	T_{hole},°C
0	220.000	227.692	–
1	220.246	227.948	224.029
2	220.493	228.204	224.280
3	220.741	228.462	224.553
4	220.989	228.719	224.785
5	221.238	228.978	225.039

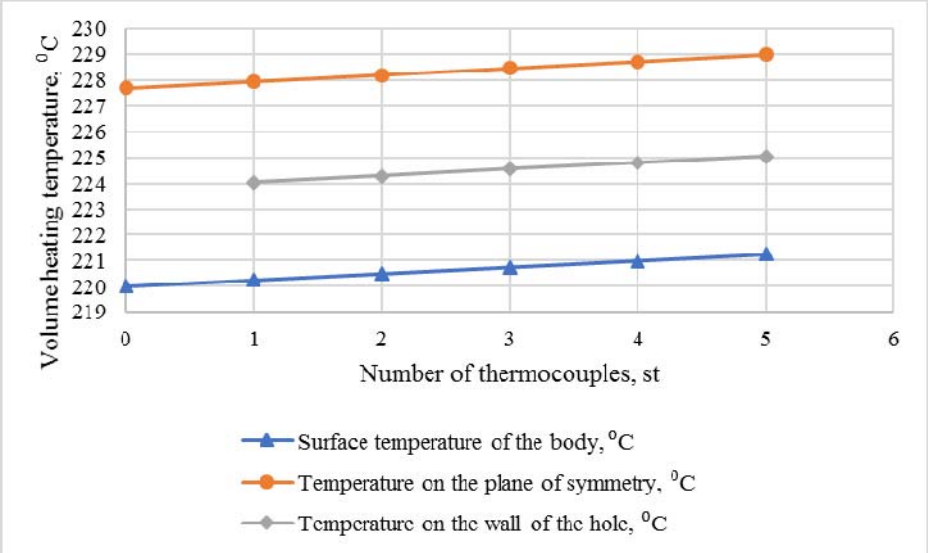

Fig. 6. Results of the General mathematical calculation

Рис. 6. Результаты общего математического расчета

From the obtained dependencies it can be seen that as the holes in the body increase, the temperature both on the surface of the sample and on the wall of the hole increases.

This can be explained by decrease in the sample volume, which entails an increase in the volumetric productivity of internal heat sources under continuous power.

Calculation of error from thermocouples installation in polymer sample (1)

$$\Delta_2 = 100 - \frac{T_{withoutTC} \cdot 100}{T_{5\,TC}} = 100 - \frac{227,692 \cdot 100}{228,978} = 0,57\ \%.$$

where $T_{withoutTC}$ – temperature inside the polymeric body sample without holes, °C; T_{5TC} – temperature inside the polymeric body with 5 holes, °C.

The results of the general mathematical model showed that the calculated error value does not exceed the permissible 3 %.

Comparative analysis. Error calculation from the number of holes for thermocouples was made applying the finite-element model in the software complex MSC Patran Sinda (0.34 %) and the general mathematical model according to the calculated formulas (0.57 %). The result of the study is the compliance of the chosen method of mathematical model construction with the result of finite-element analysis, as well as the correctness of polymer sample temperature measuring method.

Conclusion. In the present work, a method of determining the polymer sample body temperature throughout entire volume has been developed. This method has been implemented with the introduction of thermocouples into the polymer or composite body sample.

For the constructed layout of thermocouples in the body of the polymer sample to control the temperature of volumetric heating during high-frequency processing, the applicability of this scheme has been mathematically justified. Comparative analysis of measurement error due to sample volume change caused by the introduction of thermocouples not exceeding permissible 3 % [1] has been carried out.

This method has been planned for further application in automated high-frequency oil filling process [2], namely, for identification of the parameters of the filling process with a liquid plasticizer by monitoring the change in thermocouple readings.

References

1. Bychkovsiy V. S., Filippenko N. G., Popov S. I., Popov A. S. [Thermal vacuum deposition of a self-lubricating coating of polymeric materials of friction units

of machines and mechanisms of transport engineering]. *Sovremennye tekhnologii. Sistemnyy analiz. Modelirovanie.* 2018, Vol. 58, No. 2, P. 58–64 (In Russ.).

2. *Ustanovka dlya svarki plastmass., Pasport UZP 2500A, 412. 921.055.* [Installation for welding plastics. Passport UZP 2500A, 412.921.055]. 1987, 60 p.

3. Butorin D. V., Bakanin D. V., Bychkovskiy V. S., Filippenko N. G., Kuraytis A. S. Development and automation of the device for determination of thermophysical properties of polymers and composites. *Advances in Intelligent Systems and Computing*. 2020, Vol. 982, P. 731–740.

4. Chernyshov V. N., Chernyshova T. I. *Mikrovolnovyye metody i sistemy kontrolya teplofizicheskikh kharakteristik materialov i izdeliy. Monografiya* [Microwave methods and systems for monitoring the thermophysical characteristics of materials and products. Monograph]. Tambov, TGTU Publ., 2015, 124 p.

5. Kudryashov Yu. B., Perov Yu. F., Rubin A. B. *Radiatsionnaya biofizika radiochastotnyye i mikrovolnovyye elektromagnitnyye izlucheniya* [Radiation biophysics, radio-frequency and microwave electromagnetic radiation. Textbook for higher education]. Moscow, Fizmatlit Publ., 2008, 184 p.

6. Livshits A. V. [Process control of high-frequency electrothermal polymers]. *Problemy mashinostroeniya i avtomatizatsii*. Moscow, 2015, No. 3, P. 120–126 (In Russ.).

7. Larchenko A. G., Livshits A. V., Filippenko N. G., Popov S. I. *Ustroystvo diagnostiki detaley iz poliamidnykh materialov* [Diagnostic device for parts made of polyamide materials]. Patent RF, no. 2013115531/28, 2013.

8. Surzhikov A. P., Pritulov A. M., Gyngazov S. A., Lysenko E. N., Shabardin R. S. *Sposob izmereniya maksimal'noy temperatury ob"yekta pri nagrevanii yego oblucheniyem elektronnym puchkom* [The method of measuring the maximum temperature of an object when it is heated by irradiation with an electron beam]. Patent RF, no. 2168156, 1999.

9. Kalinchev E. L., Sokovtseva M. B. *Vybor plastmass dlya izgotovleniya i ekspluatatsii izdeliy. Spravochnoye izdaniye* [The choice of plastics for the manufacture and operation of products. Reference edition]. Leningrad, Khimiya Publ., 1987, 416 p.

10. GOST 10589–87 Polyamide 610 injection molding. Technical conditions Technology Information Center Russian State Library. Available at: http // www.rsl.ru (accessed 08.04.2020).

11. Bychkovsky V. S., Filippenko N. G., Bakanin D. V., Kuraitis A. S. [Investigation of the temperature change of a polymer sample during high-frequency heating depending on changes in body volume and the effect of convection]. *Molodaya nauka Sibiri.* 2018, Vol. 1, No. 1, P. 56–63 (In Russ.).

12. Palymsky I. B. *Chislennoye modelirovaniye slozhnykh rezhimov konvektsii Releya-Benara. Mekhanika zhidkosti, gaza i plazmy. Dokt. Diss.* [Numerical modeling of complex Rayleigh-Benard convection modes. Mechanics of fluid, gas and plasma. Doct. Diss.]. Novosibirsk, 2011, 206 p.

13. Butorin D. V., Filippenko N. G., Filatova S. N., Livshits A. V., Kargapoltsev S. K. [Development of a method for determining structural transformations in polymeric materials]. *Sovremennye tekhnologii. Sistemnyy analiz. Modelirovanie.* 2015, Vol. 48, No. 4, P. 80–86 (In Russ.).

14. Shastin V. I., Kargapoltcev S. K., Gozbenko V. E., Livshits A. V., Filippenko N. G. Results of the complex studies of microstructural, physical and mechanical properties of engineering materials using innovative methods. *International Journal of Applied Engineering Research*. 2017, Vol. 12, No. 24, P. 15269–15272.

15. Zaydel' A. N. *Pogreshnosti izmereniy fizicheskikh velichin. Uchebnik* [Errors of measurements of physical quantities. Textbook]. Leningrad, Nauka Publ., 1985, 112 p.

16. Gebkhart B., Dzhaluriya I., Makhadzhan R., Sammakiya B. *Svobodnokonvektivnyye techeniya, teplo- i massoobmen* [Free convective flows, heat and mass transfer]. Moscow, Mir Publ., 1991, 678 p.

17. Bryukhanov O. N., Shevchenko S. N. *Teplomassoobmen.* [Heat and mass transfer]. Moscow, INFRA-M Publ., 2013, 446 p.

18. Tsvetkov F. F. *Teplomassoobmen* [Heat and mass transfer]. Moscow, MEI Publ., 2011, 562 p.

19. Alexandrov A. A., Livshits A. V., Filippenko N. G., Popov S. I., Filatova S. N *Ustroystvo dlya opredeleniya koeffitsiyentov teplootdachi* [Device for determining heat transfer coefficients].. Patent RF, no. 2014154288/28, 2014.

Библиографические ссылки

1. Термовакуумное нанесение самосмазывающегося покрытия полимерных материалов узлов трения машин и механицизмов транспортного машиностроения / В. С. Бычковсий, Н. Г. Филиппенко, С. И. Попов, А. С. Попов // Современные технологии. Системный анализ. Моделирование. 2018. № 2 (58). С. 58–64.

2. Установка для сварки пластмасс. Паспорт УЗП 2500А, 412. 921.055. Завод «Промышленная электроника Габрово», 1987. 60 с.

3. Development and automation of the device for determination of thermophysical properties of polymers and composites / D. V. Butorin, D. V. Bakanin, V. S. Bychkovskiy et al. // Advances in Intelligent Systems and Computing. 2020. Vol. 982. P. 731–740.

4. Чернышов В. Н., Чернышова Т. И. Микроволновые методы и системы контроля теплофизических характеристик материалов и изделий : монография. Тамбов : Изд-во ФГБОУ ВПО «ТГТУ», 2015. 124 с.

5. Кудряшов Ю. Б., Перов Ю. Ф., Рубин А. Б. Радиационная биофизика радиочастотные и микроволновые электромагнитные излучения : учебник для вузов. М. : Физматлит, 2008. 184 с.

6. Лившиц А. В. Управление технологическими процессами высокочастотной электротермии полимеров // Проблемы машиностроения и автоматизации. 2015. № 3. С. 120–126.

7. Устройство диагностики деталей из полиамидных материалов / А. Г. Ларченко, А. В. Лившиц, Н. Г. Филиппенко, С. И. Попов ; заявитель и патентообладатель Иркутский государственный университет путей сообщения ; заявл. 05.04.2013 ; опубл. 10.09.2013.

8. Пат. 2168156 Российская Федерация[МПК7] G21C17/112. Способ измерения максимальной температуры объекта при нагревании его облучением электронным пучком / А. П. Суржиков, А. М. Притулов, С. А. Гынгазов, Е. Н. Лысенко, Р. С. Шабардин ; заявитель и патентообладатель Томский политехнич. ун-т ; заявл. 15.11.1999 ; опубл. 27.05.2002, Бюл. № 4. 6 с.

9. Калинчев Э. Л., Соковцева М. Б. Выбор пластмасс для изготовления и эксплуатации изделий : справоч. изд. Л. : Химия, 1987. 416 с.

10. ГОСТ 10589–87 Полиамид 610 литьевой. Технические условия. Центр информаций технологий Российская государственная библиотека / под ред. Т. В. ; Web-мастер Козлова Н. В. М. : 2007 [Электронный ресурс]. URL: http//www.rsl.ru (дата обращения: 08.04.2020).

11. Исследование изменения температуры полимерного образца при высокочастотном разогреве в зависимости от изменения объема тела и влияния конвекции / В. С. Бычковский, Н. Г. Филиппенко, Д. В. Баканин, А. С. Курайтис // Молодая наука Сибири. 2018. № 1(1). С. 56–63.

12. Палымский И. Б. Численное моделирование сложных режимов конвекции Рэлея-Бенара. Механика жидкости, газа и плазмы : дис. … д-ра физ.-мат. наук. Новосибирск, 2011. 206 с.

13. Разработка методики определения структурных превращений в полимерных материалах / Д. В. Бутерин, Н. Г. Филиппенко, С. Н. Филатова и др. // Современные технологии. Системный анализ. Моделирование. 2015. № 4 (48). С. 80–86.

14. Results of the complex studies of microstructural, physical and mechanical properties of engineering materials using innovative methods / V. I. Shastin, S. K. Kargapoltcev, V. E. Gozbenko et al. // International Journal of Applied Engineering Research. 2017. Vol. 12, No. 24. P. 15269–15272.

15. Зайдель А. Н. Погрешности измерений физических величин : учебник. Л. : Наука, 1985. 112 с.

16. Свободноконвективные течения, тепло- и массообмен / Б. Гебхарт, И. Джалурия, Р. Махаджан, Б. Саммакия : пер. с англ. Кн. 1. М. : Мир, 1991. 678 с.

17. Брюханов О. Н., Шевченко С. Н. Тепломассообмен : учебник. М. : Инфра-М, 2013. 464 с.

18. Цветков Ф. Ф. Тепломассообмен : учебник для вузов. М. : МЭИ, 2011. 562 с.

19. Пат. 2014154288/28 Российская ФедерацияМПК7 RU 155337 U1 на полезную модель. Устройство для определения коэффициентов теплоотдачи / А. А. Александров, А. В. Лившиц, Н. Г. Филиппенко, С. И. Попов, С. Н. Филатова ; заявитель и патентообладатель Иркутский гос. ун-т путей сообщения ; заявл. 10.10.2015 ; опубл. 30.12.2014.

Bychkovsky Vladimir Sergeevich – Ph. D. student, Irkutsk State Transport University. E-mail: bikovskii_vs@mail.ru.

Butorin Denis Vitalievich – Ph. D., Irkutsk State Transport University. E-mail: denis.den_butorin@mail.ru.

Bakanin Denis Viktorovich – Ph. D. student, Irkutsk State Transport University. E-mail: denis.bakan@mail.ru.

Filippenko Nikolay Grigoryevich – Ph. D, Irkutsk State Transport University. E-mail: denis. pentagon@mail.ru.

Livshits Alexander Valerievich – Doctor of Technical Sciences, Professor, Irkutsk State Transport University. E-mail: livnet@list.ru.

Бычковский Владимир Сергеевич – аспирант, Иркутский государственный университет путей сообщения. E-mail: bikovskii_vs@mail.ru.

Буторин Денис Витальевич – кандидат технических наук, доцент; Иркутский государственный университет путей сообщения. E-mail: den_butorin@mail.ru.

Баканин Денис Викторович – аспирант, Иркутский государственный университет путей сообщения. E-mail: denis.bakan@mail.ru.

Филиппенко Николай Григорьевич – кандидат технических наук, доцент, Иркутский государственный университет путей сообщения. E-mail: pentagon@mail.ru.

Лившиц Александр Валерьевич – доктор технических наук, профессор, Иркутский государственный университет путей сообщения. E-mail: livnet@list.ru.

UDC 629.58
Doi: 10.31772/2587-6066-2020-21-2-163-169

For citation: Volkov D. A., Sayapin A. V., Safonov K. V., Kuznetsov A. A. Remotely operated underwater vehicle in the form of a quadcopter: features of the design and control system. *Siberian Journal of Science and Technology.* 2020, Vol. 21, No. 2, P. 163–169. Doi: 10.31772/2587-6066-2020-21-2-163-169

Для цитирования: Дистанционно-управляемый подводный аппарат в форме квадрокоптера: особенности конструкции и системы управления / Д. А. Волков, А. В. Саяпин, К. В. Сафонов, А. А. Кузнецов // Сибирский журнал науки и технологий. 2020. Т. 21, № 2. С. 163–169. Doi: 10.31772/2587-6066-2020-21-2-163-169

REMOTELY OPERATED UNDERWATER VEHICLE IN THE FORM OF A QUADCOPTER: FEATURES OF THE DESIGN AND CONTROL SYSTEM

D. A. Volkov*, A. V. Sayapin, K. V. Safonov, A. A. Kuznetsov

Reshetnev Siberian State University of Science and Technology
31, Krasnoyarskii rabochii prospekt, Krasnoyarsk, 660037, Russian Federation
*E-mail: vlkden@yandex.ru

Inspection of underwater objects, such as underwater archaeological sites, sunken technical objects, and under water located technical structures, requires the use of specially trained divers, manned or unmanned, remotely operated or autonomous underwater vehicles.

A relatively rarely used design for such underwater vehicles is a design in the form of a quadrotor with positive buoyancy.

This article discusses the design and the control system of the remotely operated underwater vehicle in the form of a quadrotor. The aim of the work is the selection and justification of the shape of the vehicle, the selection of the optimal structure of the control system with the expectation of the subsequent use of the vehicle as an autonomous one.

The potential advantages of the selected design in the form of a quadcopter with a cylindrical body are described, in particular, the large volume of the sealed space of the vehicle, the possibility of installing capacious power sources, the potential for stabilizing the vehicle in a given position if there is a current at the place of work.

The sealed case of the device is designed to place control electronics, power electronics and battery power of the device. The selection and justification of the shape of the sealed enclosure were made using a hydrostatic modeling apparatus and theoretical mechanics. A solid cylinder made of polycarbonate was selected as a form of the sealed housing of the vehicle. The advantage of the selected form in comparison with the parallelepiped-shaped case is shown under the condition of the same material parameters.

The control system of the device includes software and hardware components. The choice of hardware components is justified, their key characteristics are described. As the control device of the top level, a single board computer (SBC, Single Board Computer) Orange Pi PC was selected, the direct control of the motor of the vehicle is performed using the Cortex-M3 microcontroller. The software architecture of the device is described. The choice of architecture is determined by the requirements of poorly connected components (which makes it easy to replace particular software elements without the need to modify the other elements), the simplicity of the potential replacement of the top-level control modules (which potentially allows switching from a remote control model to an autonomous control model). Some software components are described. The control system is implemented with the high-level language Python version 3.7, the basis of the control mechanism is message passing, the MQTT protocol maintained by the Mosquitto server is selected as a messaging mechanism.

Testing of the vehicle was carried out in pools with standing water and with a simulated current. Testing showed the need to gain experience to control the underwater vehicle.

The study will allow us to further develop a new version of the underwater vehicle, taking into account the wishes and identified problems.

Keywords: robotics, underwater archaeology, underwater vehicle, quadcopter, control system, hardware-software complex.

ДИСТАНЦИОННО-УПРАВЛЯЕМЫЙ ПОДВОДНЫЙ АППАРАТ В ФОРМЕ КВАДРОКОПТЕРА: ОСОБЕННОСТИ КОНСТРУКЦИИ И СИСТЕМЫ УПРАВЛЕНИЯ

Д. А. Волков*, А. В. Саяпин, К. В. Сафонов, А. А. Кузнецов

Сибирский государственный университет науки и технологий имени академика М. Ф. Решетнева
Российская Федерация, 660037, г. Красноярск, просп. им. газ. «Красноярский рабочий», 31
*E-mail: vlkden@yandex.ru

Обследование подводных объектов, таких как подводные археологические памятники, затонувшие технические объекты, технические сооружения, расположенные под водой, требует использования специально подготовленных водолазов, обитаемых или необитаемых дистанционно-управляемых или автономных подводных аппаратов.

Относительно редко используемой конструкцией для таких подводных аппаратов является конструкция квадрокоптера с положительной плавучестью.

В предлагаемой статье рассматривается конструкция и система управления подводного необитаемого дистанционно-управляемого аппарата в форме квадрокоптера. Целью работы является выбор и обоснование формы корпуса аппарата, оптимальной структуры системы управления с расчетом на последующее использование аппарата в качестве автономного.

Описаны потенциальные преимущества выбранной конструкции в форме квадрокоптера с цилиндрическим корпусом, в частности, большой объем герметичного пространства аппарата, возможность установки емких источников питания, потенциальная возможность стабилизации аппарата в заданном положении при наличии течения в месте проведения работ.

Герметичный корпус аппарата предназначен для размещения управляющей электроники, силовой электроники и элементов питания аппарата. Выбор и обоснование формы герметичного корпуса выполнены с использованием аппарата гидростатического моделирования и теоретической механики. В качестве формы герметичного корпуса аппарата выбран цельный цилиндр, выполненный из поликарбоната. Показано преимущество выбранной формы по сравнению с корпусом в форме параллелепипеда при условии одинаковых параметров материала.

Управляющая система аппарата включает в себя программные и аппаратные компоненты. Обоснован выбор аппаратных компонентов, описаны их ключевые характеристики. В качестве управляющего устройства верхнего уровня выбран одноплатный компьютер (SBC, Single Board Computer) Orange Pi PC, непосредственно управление двигателями аппарата осуществляется при помощи микроконтроллера Cortex-M3. Описана архитектура программного обеспечения аппарата. Выбор архитектуры обусловлен требованиями слабой связности компонентов (что позволяет легко заменять отдельные элементы программного обеспечения без необходимости модификации остальных элементов), простотой потенциальной замены управляющих модулей верхнего уровня (что потенциально позволяет перейти от модели дистанционного управления аппаратом к автономной модели управления). Описаны отдельные компоненты программного обеспечения. Управляющая система реализована на языке высокого уровня Python версии 3.7, основой механизма управления является передача сообщений, в качестве среды обмена сообщениями выбран протокол MQTT с реализацией в виде сервера Mosquitto.

Тестирование аппарата проводилось в бассейнах со стоячей водой и имитацией течения. Тестирование показало необходимость получения опыта для управления подводным аппаратом.

Проведённое исследование позволит в дальнейшем разработать новую версию подводного аппарата с учётом пожеланий и выявленных проблем.

Ключевые слова: робототехника, подводная археология, подводный аппарат, квадрокоптер, система управления, программно-аппаратный комплекс.

Introduction. In 2016 Alexander Goncharov and Nikolay Karelin (historians and lecturers at Reshetnev Siberian State University of Science & Technology) went on a research expedition to the north of the Krasnoyarsk Territory in search of the sunken English ship „Thames". They passed along the Yenisei River and the Yenisei Bay [1]. As a result of the undertaken studies, the location of this ship was determined. It is at the mouth of the Salnaya Kurya River [2].

Alexander Goncharov offered an idea to develop a remotely operated underwater vehicle designed for the exploration of underwater objects that have cultural, historical or other value.

The development team of Reshetnev Siberian State University of Science & Technology elaborated the concept of a remotely operated underwater vehicle in the form of a quadcopter. In 2018, they developed and presented a prototype of this device (fig. 1), as well as software for its use [3].

The main purpose of this underwater vehicle is the ability to conduct underwater archaeological research.

The advantage of the proposed design of the vehicle in the form of a quadcopter is the ability to hold a predetermined position and position in moving aquatic environment.

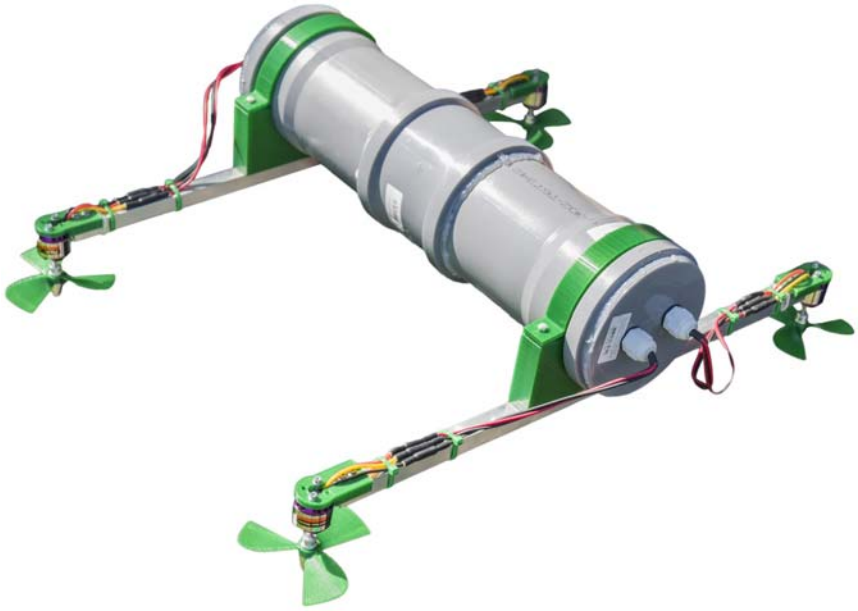

Fig. 1. The developed prototype of the underwater vehicle

Рис. 1. Разработанный прототип подводного аппарата

The originality of this development consists in the whole of the following distinctive features:

– the implementation of the design of the underwater vehicle in the form of a quadcopter and its control system is based on the idea of the implementation of aircraft;

– to control the underwater vehicle special software is used, it is available for use on mobile devices and personal computers;

– the proposed concept of an underwater vehicle combines the advantages of tethered and unmanned underwater vehicles.

Case design. The exoskeletal structure of the underwater vehicle is constructed as a hollow cylinder made of plastic.

This form allows the vehicle to withstand high pressure of the water column, and the calculations show that the maximum immersion depth of the vehicle is not caused by the shape and material of the exoskeletal structure, but by the sealing features of the side flanges.

The first prototype of the device was made in the form of polypropylene pipes connected by means of a socket joint, closed with sealed lids.

We have also considered the case made entirely with the use of 3D printing technology, however, the anisotropy of the case and its relatively low structural strength forced to abandon this approach.

In the future, it is planned to make the case as a single element in the form of a cylinder made of polycarbonate, with an external diameter of 110 mm and a wall thickness of 3 mm.

For this option, we made the calculations of the strength of the case using the methodology published in [4; 5], which showed the structural stability of the case at depth of immersion of up to 100 m.

A perforated metal plate serves as a chassis for the components located inside the body.

The following elements are placed on the plate:

– high-current Li-ion (lithium-ion) battery used as a main power source;

– on-board computer Orange Pi PC;

– MultiWii NanoWii control module based on a microcontroller with an ATmega32U4 processor;

– four electronic speed controllers (ESCs) that control the brushless motors located outside the case.

The metal plate chassis also serves as a heat sink, evenly distributing the heat released during the operation of the speed controllers, which contributes to its removal outside the case.

Two square aluminum profiles are attached to the main part of the case, at the ends of which brushless motors with propellers are installed, designed for the movement of the underwater vehicle in the aquatic environment.

Some elements of the case, including driving propellers, were developed in the OpenSCAD 3D modeling program and printed using a 3D printer. Upon the availability of a 3D printer, this approach makes it possible to get a kit of necessary elements for the purpose of their replacement in case of failure.

The speed controller wires connecting the motors to the on-board control system are routed through sealed lead-ins (seals), which prevent water from entering the case.

An important task is the transmission of video from the underwater vehicle. For these purposes, it is planned to install an on-board camera connected to the main control computer. This will allow using the device distantly as remotely operated. In the future it will be possible to put into operation the system of autonomous control of the device as well.

Two methods of installing a camera on the device are considered: inside the exoskeleton structure (since it is

transparent), and in a separate case on the external structures of the device. Each approach has its own advantages and disadvantages. Thus, installing a camera inside the case allows reducing the number of tight joints, which increases the reliability of the device as a whole. However, it causes the need for post-processing of the image from the camera, since the cylindrical body of the device introduces distortions. Installing a camera from the outside will reduce the distortions introduced by the body of the device (or, more precisely, it reduces the requirements for the amount of post-processing of the image from a camera, since a camera is supposed to be placed under a spherical dome), but it creates potential leakage spots.

It is planned to perform optimization of the shape of a driving propeller and the vehicle case as well [6].

Control system development. The main components of the control system are:

– an operator whose workplace is located on board an expedition escort ship or on shore; the workplace is equipped with the means for displaying the video stream from the board of the underwater vehicle, as well as with controls;

– a top-level control software module receiving operator's commands (or from an autonomous control system) and translates them into the values of the state space variables of the device;

– software of a low-level controller, ensuring the maintenance of set values of state space variables that controls the operation of electronic speed controllers.

Let us consider the components of the control system of the underwater vehicle in more detail. The control system complex consists of the following components:

– an operator using a device with installed software designed to control the underwater vehicle;

– a control device, which can be used as a smartphone, tablet or personal computer with installed software developed as part of this project, designed to send messages (commands) and receive video from an on-board camera;

– Wi-Fi router, which is used to establish communication between the control device and the on-board computer;

– an on-board computer designed to broadcast video from an on-board camera and receive messages (commands) from a control device, in order to transmit them to the multirotor controller for moving the underwater vehicle;

– a webcam designed to transmit video in order to monitor the environment;

– a multirotor controller used to transmit speed values and the position of the vehicle in space to speed controllers;

– electronic speed controllers (4 pcs.) that allow us to control the motors of an underwater vehicle with a given thrust;

– motors (4 pcs.) that allow us to perform the movement of the underwater vehicle in the aquatic environment.

Fig. 2 shows the scheme of interaction of components of the control system complex.

Four HobbyWing FlyFun 30A speed controllers and four RCX D2830/14 750kv brushless motors connected to them are used to move the device in the aquatic environment.

The electronic components of the underwater vehicle are powered by a high-current Li-ion (lithium-ion) battery with the capacity of 1800 mAh.

As an on-board computer, a single-board computer (microcomputer) with an operating system based on the Linux kernel is used. Initially, the Raspberry Pi Model B+ microcomputer was used in the underwater vehicle prototype, however, later it was replaced by the model Orange Pi PC to make it possible to install and use a webcam designed to monitor the environment and (potentially) recognize objects, since for broadcasting video images of optimal quality and the operation of a computer vision system, higher performance is required.

The software structure of the vehicle is described in [7].

Up to date, the following control mechanisms for the underwater vehicle are developed:

– a web server for using a joystick (gamepad) through the Gamepad API;

– control of the underwater vehicle using a mobile device with the Android operating system.

The connection of the operator's workstation with the top-level control application is made using wireless and wire technologies, which include a Wi-Fi network to connect the operator's workplace with a Wi-Fi router, which, in turn, is connected to the on-board computer by an Ethernet cable. The on-board computer and Wi-Fi router use a wire connection to form a single access point. Thus, the necessary flexibility of communication of all system components is provided.

For the exchange of messages (commands) between the control device and the on-board computer, the MQTT protocol is used with the implementation in the form of a Mosquitto server.

To receive messages via the MQTT protocol from the control device and transmit them to the on-board computer, and then send them to the multirotor controller, a program for the use on the on-board computer was developed in the Python programming language.

The control of the vehicle motors is performed using the Arduino-compatible MultiWii NanoWii multirotor controller. The software being used makes it possible to cyclically receive values from the on-board computer and transfer them to speed controllers to operate the motors of the device with preselected thrust. The operation is performed in the fixed coordinate system (roll, pitch, yaw). The program also allows keeping the horizontal position of the device in space, using the values of the gyroscope and accelerometer from the MPU-6050 sensor, embedded into the multirotor controller. When the underwater vehicle deviates from the horizon, the rotation speed of the respective motors changes automatically in order to return the vehicle to a horizontal position. This ability protects the device from tipping over.

To control this underwater vehicle, software for mobile devices with the Android operating system and for personal computers with the Windows operating system are developed and tested [8].

The software for controlling the underwater vehicle allows performing the following tasks:

– control of the movement of the vehicle in the aquatic environment;

– displaying streaming video from an installed camera;

– displaying the information received from installed sensors.

It is possible to control the movement of the device using the program interface or a connected joystick (gamepad).

Testing. This underwater vehicle has been repeatedly tested in pools with standing water, as well as in the water with simulated current. To test the device, two weight plates for a rod weighing 0.2 and 0.5 kg were attached to the case, since at the moment the device design has excessive positive buoyancy. In the future, this will make it possible to equip the underwater vehicle with additional attached implements, such as equipment for sampling water, temperature sensors, salt sensors, etc.

Testing in a pool with standing water showed that to control the underwater vehicle it is necessary to have an experienced operator with control skills. The installed motors had a high speed margin, therefore the speed of the motors was limited by software. When the underwater vehicle was submerged to the depth of 6 meters, there were not any problems. After a few minutes the vehicle was in the aquatic environment, there was no moisture inside the case.

Testing the device in the pool with a simulated current of a depth of 0.5 m showed that it is difficult to control the underwater vehicle in such conditions.

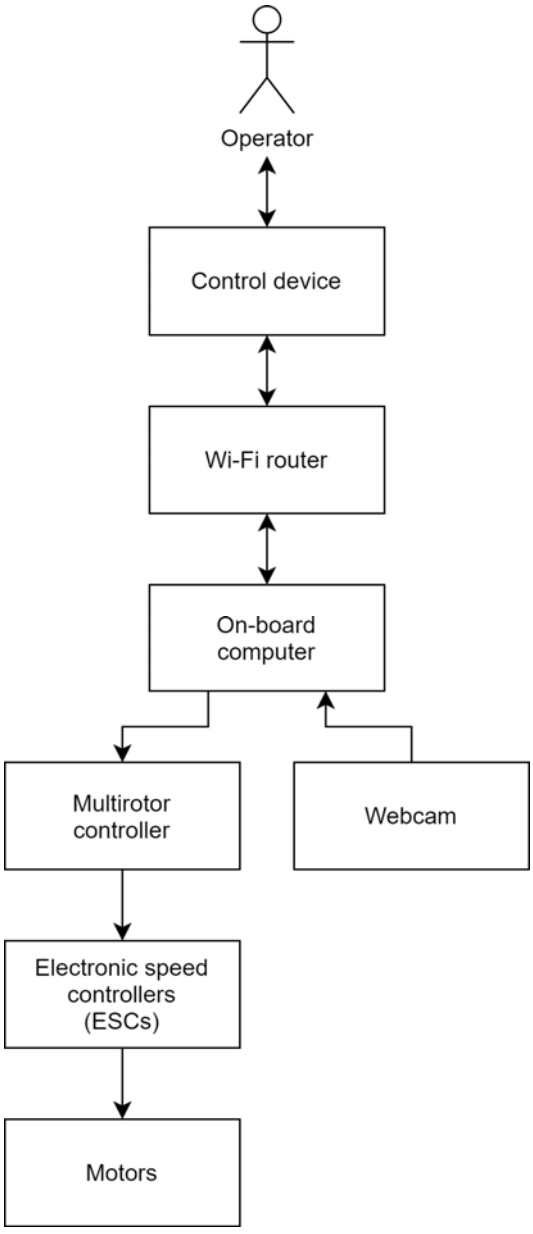

Fig. 2. Scheme of interaction of components of the control system complex

Рис. 2. Схема взаимодействия компонентов комплекса системы управления

Fig. 3. Testing the underwater vehicle prototype

Рис. 3. Тестирование прототипа подводного аппарата

However, under these conditions, the device stabilizes well and it is able to actively move. After several tests of the underwater vehicle, there were no problems with the penetration of water inside it.

Fig. 3 shows an image of testing the prototype of an underwater vehicle in a pool.

Conclusion. The developed prototype of a remotely operated underwater vehicle in the form of a quadcopter made it possible to determine the viability of the selected device design and the structure of its control system. In the future, it is planned to develop a waterproof case for installing a camera, add some necessary sensors. Is planned to install lighting package as well. In connection with the installation of new components, the underwater vehicle control system and software will be further elaborated. The studies will allow us to develop a new version of the underwater vehicle, taking into account the wishes and identified problems.

Acknowledgment. The participants of this project express their gratitude to the Palace of Water Sports of Reshetnev Siberian State University of Science and Technology and the Department of Water Use of the Faculty of Forest Engineering of Reshetnev Siberian State University of Science and Technology for their assistance in testing the underwater vehicle.

Благодарности. Участники данного проекта выражают благодарность за помощь в проведении тестирования подводного аппарата Дворцу водного спорта СибГУ им. М. Ф. Решетнева и кафедре использования водных ресурсов Лесоинженерного факультета СибГУ им. М. Ф. Решетнева.

References

1. Goncharov A. E., Karelin N. M., Mednikov D. M., Nasyrov I. R. [GIS and satellite remote sensing for archeology: exploring polar history]. *Vestnik SibGAU.* 2016, Vol. 17, No. 4, P. 956–963 (In Russ.).

2. Goncharov A. E., Mednikov D. M., Karelin N. M., Nasyrov I. R. Prospects for using sonar for underwater archeology on the Yenisei: surveying a 19th century shipwreck. *IOP Conf. Ser.: Mater. Sci.* 2016, Vol. 155. Doi: 10.1088/1757-899X/155/1/012037.

3. Volkov D. A., Sayapin A. V. [Remotely operated underwater vehicle for an archaeological survey]. *Materialy X Vseros. nauch.-tekhn. konf. s mezhdunar. uchastiem "Robototekhnika i iskusstvennyi intellect"* [Materials X All-Russian Scientific-Technical Conf. with Intern. Participation "Robotics and Artificial Intelligence"]. Krasnoyarsk, 2018, P. 21–25 (In Russ.).

4. *GOST 34233.2–2017. Raschet tsilindricheskikh i konicheskikh obechaek, vypuklykh i ploskikh dnishch i kryshek* [State Standard 34233.2–2017. Calculation of cylindrical and conical shells, convex and flat bottoms and covers]. Moscow, Standartinform Publ., 2018. 58 p.

5. *GOST R 54522–2011. Raschet tsilindricheskikh obechaek, dnishch, flantsev, kryshek. Rekomendatsii po konstruirovaniyu* [State Standard R 54522–2011. Calculation of cylindrical shells, bottoms, flanges, covers. Design Recommendations]. Moscow, Standartinform Publ., 2012. 27 p.

6. Volkov D. A., Fedotova L. D. [Geometrical and paramateral characteristics of an unmanned underwater vehicle]. *Materialy V Mezhdunarodnoy nauchno-prakticheskoy konferentsii "Aktual'nye problemy aviatsii i kosmonavtiki"* [Materials V Intern. Scientific-Practical Conf. "Topical Issues in Aeronautics and Astronautics"]. Krasnoyarsk, 2019, Vol. 2, P. 266–267 (In Russ.).

7. Sayapin A. V., Volkov D. A. [Software of remotely operated underwater vehicle for an archaeological survey]. *Materialy X Vseros. nauch.-tekhn. konf. s mezhdunar. uchastiem "Robototekhnika i iskusstvennyi intellect"* [Materials X All-Russian Scientific-Technical Conf. with Intern. Participation "Robotics and Artificial Intelligence"]. Krasnoyarsk, 2018, P. 72–77 (In Russ.).

8. Volkov D. A. [Development of the application software for an underwater vehicle control]. *Materialy V Mezhdunarodnoy nauchno-prakticheskoy konferentsii "Aktual'nye problemy aviatsii i kosmonavtiki"* [Materials V Intern. Scientific-Practical Conf. "Topical Issues in

Aeronautics and Astronautics"]. Krasnoyarsk, 2019, Vol. 2, P. 268–270 (In Russ.).

Библиографические ссылки

1. Проблемы использования ГИС и ДЗЗ из космоса для выявления памятников полярного судоходства / А. Е. Гончаров, Н. М. Карелин, Д. М. Медников и др. // Вестник СибГАУ. 2016. № 4 (17). С. 956–963.

2. Prospects for using sonar for underwater archeology on the Yenisei: surveying a 19th century shipwreck / A. E. Goncharov, D. M. Mednikov, N. M. Karelin, I. R. Nasyrov // IOP Conf. Ser.: Mater. Sci., 2016, Vol. 155. Doi: 10.1088/1757-899X/155/1/012037.

3. Волков Д. А., Саяпин А. В. Дистанционно-управляемый подводный аппарат для археологических исследований // Робототехника и искусственный интеллект : материалы X Всерос. науч.-техн. конф. с междунар. участием (08 декабря 2018, г. Железногорск) / под науч. ред. В. А. Углева ; Красноярск : ЛИТЕРА-принт, 2018. С. 21–25.

4. ГОСТ 34233.2–2017. Расчет цилиндрических и конических обечаек, выпуклых и плоских днищ и крышек. Введ. 2018–08–01. М. : Стандартинформ, 2018. 58 с.

5. ГОСТ Р 54522–2011. Расчет цилиндрических обечаек, днищ, фланцев, крышек. Рекомендации по конструированию. Введ. 2012–06–01. М. : Стандартинформ, 2012. 27 с.

6. Волков Д. А., Федотова Л. Д. Геометрические и параметрические характеристики дистанционно-управляемого подводного аппарата // Актуальные проблемы авиации и космонавтики : сб. материалов V Междунар. науч.-практ. конф., посвящ. дню космонавтики (08–12 апреля 2019, г. Красноярск) : в 3 т. / под общ. ред. Ю. Ю. Логинова ; Красноярск : СибГУ им. М. Ф. Решетнева, 2019. Т. 2. С. 266–267.

7. Саяпин А. В., Волков Д. А. Программное обеспечение дистанционно-управляемого подводного аппарата для археологических исследований // Робототехника и искусственный интеллект : материалы X Всерос. науч.-техн. конф. с междунар. участием (08 декабря 2018, г. Железногорск) / под науч. ред. В. А. Углева ; Красноярск : ЛИТЕРА-принт, 2018. С. 72–77.

8. Волков Д. А. Разработка прикладного программного обеспечения для управления подводным аппаратом // Актуальные проблемы авиации и космонавтики : сб. материалов V Междунар. науч.-практ. конф., посвящ. дню космонавтики (08–12 апреля 2019, г. Красноярск) : в 3 т. / под общ. ред. Ю. Ю. Логинова ; Красноярск : СибГУ им. М. Ф. Решетнева, 2019. Т. 2. С. 268–270.

Volkov Denis Andreevich – Master's Degree Student; Reshetnev Siberian State University of Science and Technology. E-mail: vlkden@yandex.ru.

Sayapin Aleksandr Vladimirovich – Cand. Sc., Associate Professor at the Department of Applied Mathematics; Reshetnev Siberian State University of Science and Technology. E-mail: alstutor@gmail.com.

Safonov Konstantin Vladimirovich – D. Sc., Professor, Head of the Department of Applied Mathematics; Reshetnev Siberian State University of Science and Technology. E-mail: safonovkv@rambler.ru.

Kuznetsov Aleksandr Alekseevich – D. Sc., Professor, Director of the Institute of Space Research and High Technologies; Reshetnev Siberian State University of Science and Technology. E-mail: alex_kuznetsov80@mail.ru.

Волков Денис Андреевич – магистрант; Сибирский государственный университет науки и технологий имени академика М. Ф. Решетнева. E-mail: vlkden@yandex.ru.

Саяпин Александр Владимирович – кандидат технических наук, доцент кафедры прикладной математики; Сибирский государственный университет науки и технологий имени академика М. Ф. Решетнева. E-mail: alstutor@gmail.com.

Сафонов Константин Владимирович – доктор физико-математических наук, профессор, заведующий кафедрой прикладной математики; Сибирский государственный университет науки и технологий имени академика М. Ф. Решетнева. E-mail: safonovkv@rambler.ru.

Кузнецов Александр Алексеевич – доктор физико-математических наук, профессор, директор Института космических исследований и высоких технологий; Сибирский государственный университет науки и технологий имени академика М. Ф. Решетнева. E-mail: alex_kuznetsov80@mail.ru.

UDC 519.21
Doi: 10.31772/2587-6066-2020-21-2-170-175

For citation: Egorythev G. P., Shiryaeva T. A., Shlepkin A. K., Filippov K. A., Savostyanova I. L. On the location of spacecraft in a given number of orbit. *Siberian Journal of Science and Technology.* 2020, Vol. 21, No. 2, P. 170–175. Doi: 10.31772/2587-6066-2020-21-2-170-175

Для цитирования: О распределении космических аппаратов по заданному числу орбит / Г. П. Егорычев, Т. А. Ширяева, А. К. Шлепкин и др. // Сибирский журнал науки и технологий. 2020. Т. 21, № 2. С. 170–175. Doi: 10.31772/2587-6066-2020-21-2-170-175

ON THE LOCATION OF SPACECRAFT IN A GIVEN NUMBER OF ORBITS

G. P. Egorythev[1], T. A. Shiryaeva[2], A. K. Shlepkin[2]*, K. A. Filippov[2], I. L. Savostyanova[3]

[1] Siberian Federal University
70, Svobodny Av., Krasnoyarsk, 660074, Russian Federation
[2] Krasnoyarsk State Agrarian University
90, Mira Av., Krasnoyarsk, 660049, Russian Federation
[3] Reshetnev Siberian State University of Science and Technology
31, Krasnoyarskii rabochii prospekt, Krasnoyarsk, 660037, Russian Federation
*E-mail: ak_kgau@mail.ru

Space vehicles are an expensive product. For example, just putting such a device into orbit costs at least one hundred million dollars plus the cost of the satellite itself and scientific equipment it carries. However, the current state of human civilization does not allow us to do without the presence of satellites in orbit. There were 2,062 active satellites in the international database as of March 2019. Compared to 2018, the number of new devices increased by 15 %. Experts warn that in the coming years, the world is expecting a «satellite boom» with a projected increase in the number of devices of about 15–30 % annually. All these satellites are rather different. Currently, several orbits are used for placing satellites on them, depending on the tasks they solve. A geostationary orbit is used for live television broadcasting. Low satellite orbits are used for communication between satellite phones. There are some orbits for navigation systems (GPS, Navstar, GLONASS). Naturally, under these conditions, there is a problem of placing spacecraft over a given number of orbits, with some restrictions on the location of the spacecraft in certain orbits, depending on the purpose of the spacecraft. The solution to this problem is considered on the condition that the number of spacecraft coincides with the number of possible orbits in which they can be placed with some additional restrictions on the possibility of their placement in orbit. Several solutions to this problem are obtained that allow us to calculate the number of possible combinations for such placement of spacecraft over a given number of orbits.

Keywords: satellite, orbit, substitution, permanent.

О РАСПРЕДЕЛЕНИИ КОСМИЧЕСКИХ АППАРАТОВ ПО ЗАДАННОМУ ЧИСЛУ ОРБИТ

Г. П. Егорычев[1], Т. А. Ширяева[2], А. К. Шлепкин[2]*, К. А. Филлипов[2], И. Л. Савостьянова[3]

[1] Сибирский федеральный университет
Российская Федерация, 660074, г. Красноярск, просп. Свободный, 70
[2] Красноярский государственный аграрный университет
Российская Федерация, 660049, г. Красноярск, просп. Мира, 90
[3]Сибирский государственный университет науки и технологий имени академика М. Ф. Решетнева
Российская Федерация, 660037, г. Красноярск, просп. им. газ. «Красноярский рабочий», 31
*E-mail: ak_kgau@mail.ru

Космические аппараты – дорогостоящий продукт. Например, только вывод такого аппарата на орбиту обходится минимум в сто миллионов долларов плюс стоимость самого спутника и научной аппаратуры, которую он несет. Однако современное состояние человеческой цивилизации уже не позволяет обходиться без наличия космических аппаратов на орбите. В международной базе данных на март 2019 г. числилось 2062 действующих спутника. По сравнению с 2018 г. рост числа новых аппаратов составил 15 %. Эксперты предупреждают, что в ближайшие годы мир ожидает «спутниковый бум» с прогнозируемым приростом количества аппаратов порядка 15–30 % ежегодно. Все эти космические аппараты сильно отличаются друг от друга. В настоящее время используется несколько орбит для размещения на них спутников в зависимости от решаемых ими задач. Геостационарная орбита используется для прямого телевещания. Низкие спутниковые орбиты используются для связи между спутниковыми телефонами. Свои орбиты существуют для спут-

ников систем навигации (GPS, Navstar, ГЛОНАСС), военных спутников, спутников для различных научных исследований. Естественно, в этих условиях возникает задача распределения космических аппаратов по заданному числу орбит при некоторых ограничениях на нахождении космического аппарата на некоторых орбитах в зависимости от назначения космического аппарата. Рассматривается решение данной задачи при условии, что число космических аппаратов совпадает с числом возможных орбит, на которых эти космические аппараты могут находиться при некоторых дополнительных ограничениях на возможность расположения спутника на орбите. Получено несколько решений этой задачи, позволяющих вычислить число возможных комбинаций для таких распределений космических аппаратов по заданному числу орбит.

Ключевые слова: спутник, орбита, подстановка, перманент.

1. Introduction. In the international database as for March 2019, there were 2062 active satellites. Compared to 2018, the growth of the number of new devices is 15 %. Experts warn that in the coming years the world is expecting a "satellite boom" with a projected increase of the number of devices of about 15–30 % annually. At present, some companies such as SpaceX and OneWeb are implementing an extensive program to launch satellites into low Earth orbits to put into action the plans for creating a global Internet broadcasting network.

In this case, a number of problems naturally arise [1–6], in particular, the problem of choosing the most favorable orbits for satellites of one class or another, as well as the problem of allocating a given number of satellites over a given set of orbits with existing prohibitions on placing a satellite in some orbit.

The article provides a solution to the second problem under the following conditions: the number of satellites *n* coincides with the number of possible orbits in which they are placed; each satellite is forbidden to be in exactly one orbit; two satellites cannot be in the same orbit. There is a formula that allows us to calculate the number of possible combinations for such satellite distributions in orbits.

The mathematical model of the problem. By permutation we mean the dimension matrix $2\times n$

$$\begin{pmatrix} 1 & 2\cdots & n \\ i_1 & i_2\cdots & i_n \end{pmatrix}. \qquad (1)$$

A permutation is called regular if $k \neq i_k$, i. e.

$$i_1 \neq 1, i_2 \neq 2, \cdots, i_n \neq n. \qquad (2)$$

Thus, in accordance with the restrictions indicated above, exactly one regular permutation of degree *n* will correspond to each option for the placement of satellites in orbits. The problem of finding the number of regular permutations of degree *n* belongs to an extensive class of problems of enumerating permutations with restrictions on positions (with forbidden positions), and it is referred to as the problem of derangements (le problem des rencontres); [7]).

It is equivalent to the classical problem of enumerating Latin rectangles having the size $2\times n$; for it, as the problem of combinatorics, many solutions of various types are known ([8], chapters 7, 8). The article presents several such solutions made using various methods, each of which has an independent value.

2. Recurrence formula for calculating the number of regular permutations. The number of regular permutations of degree *n* will be denoted by D_n.

Theorem 1. If $n=1$, then $D_1=0$. If $n=2$, then $D_2=1$. If $n>2$, then

$$D_n = n!-C_n^1 D_{(n-1)} - C_n^2 D_{(n-2)} - \cdots - C_n^{(n-2)} D_{n-(n-2)} - 1.$$

Proof. The first two conclusions of the theorem are a direct consequence of the definition of a regular permutation. Let $n>2$. Let us consider the irregular permutation

$$\begin{pmatrix} 1\cdots n_1\cdots n_k\cdots & n \\ \alpha_1\cdots n_1\cdots n_k\cdots & \alpha_n \end{pmatrix},$$

which holds fixed precisely *k* symbols of $n_1, n_2, \cdots, n_k$, and it moves all the remaining symbols (in quantity $k-1$). At fixed $n_1, n_2, \cdots, n_k$ the number of such permutations is D_{n-k}. Since the number of different sets without reiteration of the length *k* from the range $\{1, \cdots, n\}$ equals C_n^k, then the total number of irregular permutations of this kind equals C_n^k. To complete the proof of the theorem, it is enough to subtract all irregular permutations of the form considered above for all *k* from the total number of permutations of the degree *n* (and this is exactly $n!$).

The theorem is proved.

Let us verify the conclusions of the theorem for some initial values $n=1, 2, 3, 4, 5, 6$. The values $D_1=0$ and $D_2=1$ follow directly from the definition

$$D_3 = 3!-C_3^1 D_2 - 1 = 6-3-1 = 2,$$

$$D_4 = 4!-C_4^1 D_3 - C_4^2 D_2 - 1 = 24-4\cdot 2-6\cdot 1-1 = 9,$$

$$D_5 = 5!-C_5^1 D_4 - C_5^2 D_3 - C_5^3 D_2 - 1 = $$
$$= 120-5\cdot 9-10\cdot 2-10-1 = 44,$$

$$D_6 = 6!-C_6^1 D_5 - C_6^2 D_4 - C_6^3 D_3 - C_6^4 D_2 - 1 = $$
$$= 720-6\cdot 44-15\cdot 9-20\cdot 2-15\cdot 1-1 = 265.$$

The results have been confirmed by listing all the regular permutations for the specified values $n=1, 2, 3, 4, 5, 6$.

3. The formulae for calculating the number of regular permutations based on the concept of a permanent matrix. Here we consider the original task as an enumeration problem when calculating the number of the permutations with fixed positions and we use the means of permanents (cyclic) (0,1) of incidence matrices [9; 10]. By the permanent of a square $n\times n$ matrix $A=\left(a_{i,j}\right)$ over a commutative ring we mean the expression

$$per\left(A\right) = \sum_{\sigma\in S_n} a_{1\sigma(1)}\cdots a_{n\sigma(n)}, \qquad (3)$$

where summation is carried out for all S_n permutations $\sigma = (\sigma(1), \cdots, \sigma(n))$ n-of the range $\{1, 2, \cdots, n\}$, as well as on all the diagonals of the matrix A.

Let I_n be identity $n \times n$ matrix, J_n – $n \times n$ -the matrix, in which each element equals $1/n$, and $A_n = (nJ_n - I_n)$ – the following matrix of order n:

$$A_n = \begin{pmatrix} 0 & 1 & \cdots & 1 & 1 \\ 1 & 0 & & 1 & 1 \\ \vdots & & \ddots & \vdots & \\ 1 & 1 & & 0 & 1 \\ 1 & 1 & \cdots & 1 & 0 \end{pmatrix} \quad (4)$$

Theorem 2. The following formula for the number D_n is valid

$$D_n = per(A_n) = per(nJ_n - I_n), n = 2, 3, \cdots. \quad (5)$$

Proof. The incidence matrix $A_n = (a_{ij})$ of the order n in (4) is constructed in the way that in accordance with the conditions (2) it has $a_{ij} = 0$, if $i = j$, and $a_{ij} = 1$, if $i \neq j$. We can easily see that for each "identity" diagonal of the matrix A_n in (4), each element of which equals 1, the permutation of the type (2) corresponds one-to-one. On the other hand, it is obvious that the multiplication of n units equal to *1* corresponds to each such diagonal in the permanent sum (3) for $per(A_n)$. At the same time, the corresponding multiplications of the elements for each diagonal of the matrix A_n containing at least one zero element equal zero.

The theorem is proved.

Theorem 3. The following formula for the number D_n is valid

$$D_n = n!\left(1 - \frac{1}{1!} + \frac{1}{2!} - \cdots + \left((-1)^n \frac{1}{n!}\right), n = 2, 3, \cdots. \quad (6)\right.$$

Proof. By the "permanent" Laplace formula, decomposing $per(A_n)$ into the elements of the first line, we have

$$D_n = per(A_n) = \sum_{k=2}^{n} per\left(A_n\left(1/k\right)\right), n = 3, 4, \cdots. \quad (7)$$

Here $per\left(A_n\left(1/k\right)\right)(k = 2, 3, \cdots, n)$ – permanental minors from (0,1) matrices $A_n\left(1/k\right)$ of the order $(n-1)$, which differ only in the arrangement of the same (0,1)-lines.

Herewith each matrix $A_n\left(1/k\right)$ contains precisely $(n-2)$ zeros, and no two of them are contained in one line or in one column. It follows that at any $k = 2, 3, \cdots, n$ the following equation is valid

$$per\left(A_n\left(1/k\right)\right) = per(A_{n-1}) - per(A_{n-2}),$$

and according to (7) and (5) we obtain

$$\begin{aligned} D_n &= (n-1)\left(per(A_{n-1}) - per(A_{n-2})\right) = \\ &= (n-1)(D_{n-1} + D_{n-2}), n = 3, 4, \cdots, n. \end{aligned} \quad (8)$$

Therefore, by induction, taking into account the initial conditions $D_1 = 0, D_2 = 1,$ the formula (6) follows.

From here it follows that

The theorem is proved.

4. Derivation of the formula for calculating the number of regular permutations based on the inclusion-exclusion formula. This solution is related to the classical inclusion-exclusion formula (please see, for example, [10], § 3.2) by breaking the set S_n into disjoint sets $P_0, P_1, \cdots, P_n$, where P_i – set of permutations from S_n with precisely i fixed positions, $i = 1, 2, \cdots, n$ or, the same with $(n-i)$ constraint positions. Since

$$S_n = n! = \sum_{i=0}^{n} |P_i|, |P_i| = \binom{n}{i} D_{n-i},$$

$$\binom{n}{i} = \frac{n!}{i!(n-i)!}, \; i = 1, 2, \cdots, n,$$

We have

$$1 = \sum_{i=o}^{n} D_{n-i} \frac{1}{i!(n-i)!}. \quad (9)$$

Let

$$\tilde{D}_z = \sum_{i=0}^{\infty} \frac{D_i}{i!}$$

– generating function of a power (exponential) type for a numerical sequence $\left\{D_i / i!\right\}$, and consequently,

$$D_i = i! rez\left\{\tilde{D}(z) z^{-i-1}\right\}, i = 1, 2, \cdots, n \quad (10)$$

Here by formal deduction operator $res_z\{A(z)\}$ for the power Laurent series

$$A(z) = \sum_{k=r}^{\infty} a_k z^k, r \in Z,$$

we mean the coefficient at z^{-1} of the range $A(z)$, i. e., by convention,

$$res_z\{A(z)\} = a_{-1}. \quad (11)$$

Further, according to the coefficient method [11], we have in (9)

$$\frac{1}{i!} = res_w\left\{e^w w^{-i-1}\right\}, \frac{D_{n-i}}{(n-1)!} = res_z\left\{\tilde{D}(z) z^{-(n-k)-1}\right\},$$

and we sequentially obtain

$$1 = \sum_{i=0}^{n}\left(res_w\left\{e^w w^{-i-1}\right\} \times res_z\left\{\tilde{D}(z) z^{-(n-k)-1}\right\}\right) = \sum_{i=0}^{n} \cdots,$$

where in the last equation the added elements of the sum equal 0 by the definition of the operator res_z. Further, by regrouping the terms of the sum and putting the operator Σ under the symbol of the operator res_z, we obtain

$$1 = res_z\{\tilde{D}(z)z^{-n-1}[\sum_{i=0}^{\infty} z^w \left(res_w\left\{e^w w^{-i-1}\right\}\right]\}) =$$

(summation in square brackets by index *i*: substitution rule, substituting $w = z$)

$$= res_z\{\tilde{D}(z)z^{-n-1}[e^w]_{w=z}\} = res_z\left\{e^z\,\tilde{D}(z)z^{-n-1}\right\}.$$

That is, we have

$$res_z\left\{e^z\,\tilde{D}(z)z^{-n-1}\right\} = 1 \to := res_z\left\{\frac{1}{1-z}z^{-n-1}\right\}, n = 0,1,\cdots$$

It immediately follows that

$$e^z\,\tilde{D}(z) = \frac{1}{1-z},\ \tilde{D}(z) = \frac{e^{-1}}{1-z},$$

and according to (10)

$$D_n = n!res_z\left\{\tilde{D}(z)z^{-n-1}\right\} = n!res_z\left\{e^z\frac{1}{1-z}z^{-n-1}\right\} =$$

$$= n!res_z\left\{\left(1+\sum_{i=0}^{\infty}(-1)^i\frac{z^i}{i!}\right)\times\left(1+\sum_{i=0}^{\infty}(-1)^i z^i\right)z^{-n-1}\right\} =$$

(according to the operator res_z)

$$= n!(1-\frac{1}{1!}+\frac{1}{2!}-\cdots+\left(-1\right)^n\frac{1}{n!}), n = 1,2,3,\cdots.$$

5. Derivation of a formula for calculating the number of regular permutations based on combinatorial methods. This solution is connected to the use of traditional means of combinatorial analysis and generating functions of a power type related to the use of operations on power series (please see, for example [8–12]). Let Q_n – the set of all *n*-permutations of type (2), and $Q_n(k)$ – the set of these permutations from Q_n that have $1 \to k\,(k = 2,3,\cdots,n)$. Obviously, the class of sets $Q_n(k)$ – the partition of the set S_n. Let

$$Q_n(k) = Q_n^1(k) \cup Q_n^2(k),$$

where the set $Q_n^1(k)$ contains all the permutations from $Q_n(k)$ whose *k* does not image into 1, and the set $Q_n^2(k)$ contains all the permutations from $Q_n(k)$ whose *k* images into 1.

It stands to reason that for each fixed *k* we have

$$\left|Q_n^1(k)\right| = D_{n-1}, \left|Q_n^2(k)\right| = D_{n-2},$$

and consequently,

$$Q_n(k) = D_{n-1} + D_{n-2}.$$

Thus, we have

$$D_n\left|Q_n\right| = \sum_{k=0}^{n} Q_n(k) = \sum_{k=0}^{n}(D_{n-1} + D_{n-2}), n = 3,4, \qquad (12)$$

i. e. the recurrence formula (8) taking into account the initial conditions of the form

$$D_1 = 0,\ D_2 = 1, \qquad (13)$$

at $n \geq 3$ is valid.

System solution (12)–(13). If we divide both sides of the equality (12) by $(n-1)!$, multiply by z^{n-1}, sum up at $n \geq 3$, then taking into account the notation

$$\tilde{D}_n = D_n/n!,\ n \geq 1$$

we obtain the following equation

$$\sum_{n=3}^{\infty}\frac{D_n}{(n-1)!}z^{n-1} = z\sum_{n=3}^{\infty}\frac{D_{n-1}}{(n-2)!}z^{n-1} + z\sum_{n=3}^{\infty}\frac{D_{n-2}}{(n-2)!}z^{n-2}. \qquad (14)$$

Further, from (14), taking into account the initial conditions (13) and the new notation

$$\tilde{D}_n := D_n/n!, n \geq 2, \tilde{D}(z) := \sum_{n=1}^{\infty} z^n\frac{\tilde{D}_n}{n!} = \sum_{n=2}^{\infty} z^n,$$

we obtain

$$\sum_{n=3}^{\infty}\frac{D_n}{(n-1)!}z^{n-1} - z\sum_{n=3}^{\infty}\frac{D_{n-1}}{(n-2)!}z^{n-2} =$$

$$= -z^2 D_2 + (1-z)\sum_{n=3}^{\infty}\frac{D_n}{(n-1)!}z^{n-1} =$$

$$= -z^2 + (1-z)\frac{d}{dz}\{\sum_{n=3}^{\infty}\frac{D_n}{n!}z^n\} =$$

$$= -z^2 + (1-z)\frac{d}{dz}\left\{\tilde{D}(z) - D_2 z^2\right\} = \qquad (15)$$

$$= -z^2 + (1-z)\frac{d}{dz}\left\{\tilde{D}(z)\right\} - (1-z)\frac{1}{2}2z =$$

$$= -z^2 + (1-z)\frac{d}{dz}\left\{\tilde{D}(z) - D_2 z^2\right\} =$$

$$= -z + (1-z)\frac{d}{dz}\left\{\tilde{D}(z)\right\}.$$

It follows from here that

$$z\sum_{n=3}^{\infty}\frac{D_{n-2}}{(n-2)!}z^{n-2} = z\sum_{n=3}^{\infty}\tilde{D}_{n-2}\,z^{n-2} =$$

$$= z\sum_{n=3}^{\infty}\tilde{D}_{n-2}\,z^{n-2} = z\left\{\tilde{D}(z) - z\,\tilde{D}_1\,z\right\} = z\,\tilde{D}(z). \qquad (16)$$

Thus, the solution to the system (12) – (13) by virtue of (14) – (16) reduces to solving the following first order differential equation:

$$(1-z)\frac{d}{dz}\left\{\tilde{D}(z)\right\} - z\,\tilde{D}(z) - z = 0, \tilde{D}(0) = \tilde{D}'(0) = 0. \qquad (17)$$

The equation (17) has the following unambiguous solution

$$\tilde{D}(z) = -1 + e^{-z}\frac{1}{1-z}, \qquad (18)$$

which is verified by direct substitution in (17). The end of the proof is carried out exactly as in Section 4.

6. Notices. From the Maclaurin decomposition for the number e^{-1} the known next important estimate of the number D_n follows immediately:

$$\lim_{n\to\infty}\frac{D_n}{n!} = \frac{1}{e}. \qquad (19)$$

In 1979, M. Aigner found the following unexpected probabilistic interpretation of that asymptotic estimate of the number D_n: «Let us suppose that n pages of a manuscript were mixed up by a gust of wind and then put arbitrarily.

The formula (19) states that for bigger n, the probability that there is not a single page in its place is higher than $1/3$. » [13].

Another, more difficult classical combinatorial problem of the same type is the following: The problem of married couples: in how many ways can couples be arranged around a round table so that women and men alternate, and none of wives is sitting next to her husband?

In 1934, by listing enumerated n-permutations of the corresponding type, Jacques Toucheard found the following formula for the number U_n – ways to place married couples of the above type [14; 15]:

$$U_n = per\left(nJ_n - I_n - P_n\right) = \\ = \sum_{i=0}^{n} -1^i \frac{2n}{2n-1}\binom{n-i}{i}(n-1)!, \quad (20)$$

where the matrix P_n – permutation matrix of the degree n with 1 on the places $(1,2),(2,3),\cdots,...$

Let us note that the formula (20), as well as the formula (6), can also be used to calculate options for the placement of satellites on a given number of orbits with a different set of conditions.

Conclusion. The problem of the possible distribution of satellites over a given number of orbits, depending on the purpose of a satellite, is solved. It is assumed that the number of satellites coincides with the number of orbits on which they can be placed. Several solutions to this problem have been obtained, which make it possible to calculate the number of combinations for distributing satellites over a given number of orbits.

References

1. Dr. Kelso T. S. Basics of the Geostationari Orbit. Available at: http://www.celestrak.com/columns. (accessed 26.03.2020).

2. Treaty on principles governing the activities of States in the exploration and use of outer space, including the moon and other celestial bodies. Available at: http://www.un.org/ru/documents/decl_conv/conventions/outer_space_goveming.html (accessed 26.03.2020)

3. Fateev V. F., Minkov S. [New direction of development of remote sensing of the Earth]. *Izv. vuzov. Instrument making*. 2004, Vol. 47, No. 3, P. 18–22 (In Russ.).

4. Lebedeva A. A., Nesterenko O. P. *Kosmicheskie sistemy nablyudeniya. Sintez i modelirovanie* [Space observation systems. Synthesis and modeling]. Moscow, Mashinostroenie Publ., 1991, 224 p.

5. Pob'ezdkov Yu. A. *Kosmicheskaya s"emka Zemli 2006–2007 gg.* [Space survey of the Earth 2006–2007]. Moscow, Radio engineering Publ., 2008, 275 p.

6. Nevdyaevl L. M., Smirnova A. A. *Personal'naya sputnikovaya svyaz* [Personal satellite communication]. Moscow, Eco-Trends Publ., 1998, 216 p.

7. Fitken A. C. Determinants and Matrices. Edinburgh, 1939, 201 p.

8. Riordan J. An introductions to combinatorial analysis. John Wiley & Sons, Inc., New York, 1982, 288 p.

9. Minc H. Permanents. *Encyclopedia of Mathematics and Its Applications*. 1978, Vol. 6, P. 65–70 p.

10. Egorychev G. P. *Diskretnaya matematika. Permanenty* [Discrete Math. Permanents]. Krasnoyarsk, Siberian Federal University Publ., 2007, 272 p.

11. Egorychev G. P. *Integralnoe predstavlenie i vychislenie kombinatornyh summ* [Integral representation and computation of combinatorial Math.]. Novosibirsk, Nauka Publ., 1977.

12. Kuzmin O. V. Introduction to combinatorial methods of discrete mathematics. Irkutsk, ISU Publishing House, 2012, 113 p.

13. Aigner M. Combinatorial theory, Springer-Verlag, New York, 1979, 90 p.

14. Touchard J. Sur un proble'me de permutations. Ed. C. R. Acad. Sci. Paris, 1934.

15. Kaplansky I. Solution of the proble'me des me'nages. *Bull. Amer. Math. Soc.* 1943, Vol. 49, P. 784–785 p.

Библиографические ссылки

1. Dr. Kelso T. S. Basics of the Geostationari Orbit [Электронный ресурс]. URL: http://www.celestrak.com/columns (дата обращения: 26.03.2020).

2. Договор о принципах деятельности государств по исследованию и использованию космического пространства, включая Луну и другие небесные тела (1967) [Электронный ресурс] / Офиц. сайт ООН. URL: http://www.un.org/ru/documents/decl_conv/conventions/outer_space_goveming.html (дата обращения: 26.03.2020).

3. Фатеев В. Ф., Миньков С. Новое направление развития МКА дистанционного зондирования Земли. // Изв. вузов. Приборостроение. 2004. Т. 47, № 3. С. 18–22.

4. Лебедев А. А., Нестеренко О. П. Космические системы наблюдения. Синтез и моделирование. М. : Машиностроение, 1991. 224 с.

5. Подъездков Ю. А. Космическая съемка Земли 2006–2007 гг. М. : Радиотехника, 2008. 275 с.

6. Невдяев Л. М., Смирнов А. А. Персональная спутниковая связь. М. : Эко-Трендз, 1998. 216 с.

7. Fitken A. C. Determinants and Matrices. Edinburgh, 1939. 201 с.

8. Riordan J. An introductions to combinatorial analysis // John Wiley & Sons, Inc., New York, 1982. 288 p.

9. Minc H. Permanents // Encyclopedia of Mathematics and Its Applications. 1978. Vol. 6. P. 65–70.

10. Егорычев Г. П. Дискретная математика. Перманенты. Красноярск : Изд-во СФУ, 2007. 272 с.

11. Egorychev G. P. Интегральное представление и вычисление комбинаторных сумм. Новосибирск : Наука, 1977.

12. Kuzmin O. V. Introduction to combinatorial methods of discrete mathematics. Irkutsk : ISU Publishing House, 2012. 113 p.

13. Aigner M. Combinatorial theory. Springer-Verlag, New York, 1979. 90 p.

14. Touchard J. Sur un proble'me de permutations / ed. C. R. Acad. Sci. Paris, 1934.

15. Kaplansky I. Solution of the proble'me des me'nages // Bull. Amer. Math. Soc. 1943. Vol. 49. P. 784–785.

Egorychev Georgiy Petrovich – D. Sc., Professor, Siberian Federal University. E-mail: egorychev@sfu-kras.ru.

Shiryaeva Tamara Alekseevna – Cand. of physical and mathematical Sc., Associate Professor, associate Professor of the Department Information technologies and mathematical support of information systems; Krasnoyarsk State Agrarian University. E-mail: info@kgau.ru.

Shlepkin Anatoly Konstantinovich – D. Sc., Professor, Professor of the Department Higher mathematics and computer modeling; Krasnoyarsk State Agrarian University. E-mail: ak_kgau@mail.ru.

Filippov Konstantin Anatolevich – D. Sc., Associate Professor, Professor of the Department Information technologies and mathematical support of information systems; Krasnoyarsk State Agrarian University. E-mail: info@kgau.ru.

Savostyanova Irina Leonidovna – Cand. Sc., Associate Professor of the Department of IES; Siberian State University of Science and Technology. E-mail: savostyanova@sibsau.ru.

Егорычев Георгий Петрович – доктор физико-математических наук, профессор; Сибирский федеральный университет. E-mail: egorychev@sfu-kras.ru.

Ширяева Тамара Алексеевна – кандидат физико-математических наук, доцент; Красноярский государственный аграрный университет. E-mail: tas_sfu@mail.ru.

Шлепкин Анатолий Константинович – доктор физико-математических наук, профессор; Красноярский государственный аграрный университет. E-mail: ak_kgau@mail.ru.

Филиппов Константин Анатольевич – доктор физико-математических наук, доцент; Красноярский государственный аграрный университет. E-mail: filippov_kostya@mail.ru.

Савостьянова Ирина Леонидовна – кандидат педагогических наук, доцент кафедры ИЭС; Сибирский государственный университет науки и технологий имени академика М. Ф. Решетнева. E-mail: savostyanova@sibsau.ru.

UDC 519.711.3
Doi: 10.31772/2587-6066-2020-21-2-176-186

For citation: Kornet M. E., Medvedev A. V., Yareshchenko D. I. Managing a group of objects as a task of system analysis. *Siberian Journal of Science and Technology.* 2020, Vol. 21, No. 2, P. 176–186. Doi: 10.31772/2587-6066-2020-21-2-176-176-186

Для цитирования: Корнет М. Е., Медведев А. В., Ярещенко Д. И. Об управлении группой объектов как о задаче системного анализа // Сибирский журнал науки и технологий. 2020. Т. 21, № 2. С. 176–186. Doi: 10.31772/2587-6066-2020-21-2-176-186

MANAGING A GROUP OF OBJECTS AS A TASK OF SYSTEM ANALYSIS

M. E. Kornet[1], A. V. Medvedev[1], D. I. Yareshchenko[*2]

[1]Reshetnev Siberian State University of Science and Technology
31, Krasnoyarskii rabochii prospekt, Krasnoyarsk, 660037, Russian Federation
[2]Siberian Federal University
26к1, Academician Kirensky St., Krasnoyarsk, 660074, Russian Federation
[*]E-mail: YareshenkoDI@yandex.ru

In this paper, we consider the general statement of the problem of identification and management of a group of objects. A group refers to several objects combined for the manufacture of a product. The main feature is that when managing such systems, it is necessary to change the setting actions for each object.

This is due to the fact that today the technological regulations in many cases are wider than they should be for good operating. This is a consequence of the fact that the current production culture (this, in particular, has been shown by the experience of processing data from the technological process for the production of transistors at Svetlana) is rather low, which leads to some organizational problems. It is clear that it is necessary to have certain models of objects that naturally differ from each other and can be considered under conditions of both parametric and nonparametric uncertainty. Moreover, there may be cases when an object is considered simultaneously under conditions of both parametric and nonparametric uncertainty over various channels. Now, regarding the delay, due to the fact that the measurement of some variables is carried out in a significantly longer time interval than the object constant, it is necessary to distinguish the time of measuring technological variables and, in fact, the delay typical to the process itself, taking into account the difference between the channels.

This leads to the fact that dynamic processes are essentially forced to be considered as inertialess with delay. Another significant feature is that the components of the output variables are stochastically dependent in advance in an unknown manner. The use of correlation or dispersion relations in this case does not lead to success. A special analysis of T-processes and the ability to simulate such processes are required. In particular, this is one of the tasks of this article. It contains: T-processes, T-models and the corresponding heterogeneous control algorithms. The process of hydrodeparaffinization of diesel fuel is considered according to available data, which can be said a priori that they are incomplete, that is they do not reflect the complex behavior of the process. From here it follows that these data require replenishment, which today is not carried out for various reasons. Thus, the process of hydrodewaxing can be taken to the T-process.

Modeling a multidimensional system based on real data has shown that in this problem the presetting effect for different objects should be different. The exception is only the setting actions for the entire complex or group of objects. Modeling was carried out on the basis of T-models considered in the article. It has already been noted that these models should not be taken as complete, giving an idea of reality. They will be subject to algorithmic refinement during further research. The decision is made by the researcher. At this stage that an assessment is given that, under the circumstances, the resulting models and control algorithms can be adopted for use in a production environment. An attempt to use the existing theory of identification and control for the process of hydrodewaxing will inevitably lead to a significant degradation and increase in the cost of a computer system for operating the quality of this process.

Keywords: group of objects, identification, control, setting actions, nonparametric algorithms, T-process, multidimensional objects, adaptation.

ОБ УПРАВЛЕНИИ ГРУППОЙ ОБЪЕКТОВ КАК О ЗАДАЧЕ СИСТЕМНОГО АНАЛИЗА

М. Е. Корнет[1], А. В. Медведев[1], Д. И. Ярещенко[2*]

[1]Сибирский государственный университет науки и технологий имени академика М. Ф. Решетнева
Российская Федерация, 660037, г. Красноярск, просп. им. газ. «Красноярский рабочий», 31
[2]Сибирский федеральный университет
Российская Федерация, 660074, г. Красноярск, ул. Академика Киренского, 26к1
[*]E-mail: YareshenkoDI@yandex.ru

В настоящей работе рассматривается общая постановка задачи идентификации и управления группой объектов. Под группой понимается несколько объектов, объединенных для изготовления того или иного продукта. Главной особенностью является то, что при управлении подобными системами необходимо изменять задающие воздействия для каждого объекта.

Сегодня технологический регламент во многих случаях оказывается более широким, чем следовало бы для качественного управления. А это есть следствие того, что нынешняя культура производства (это, в частности, показал опыт обработки данных технологического процесса производства транзисторов на «Светлане») довольно невысока. Это приводит к некоторым организационным проблемам. Следовательно, необходимо иметь те или иные модели объектов, которые естественно отличаются друг от друга и могут быть рассмотрены в условиях как параметрической, так и непараметрической неопределенности. Более того, могут быть случаи, когда объект рассматривается одновременно в условиях как параметрической, так и непараметрической неопределенности по различным каналам. Измерение некоторых переменных осуществляется в значительно больший интервал времени, чем постоянная объекта, поэтому необходимо отличать время измерения технологических переменных и, собственно, запаздывание, присущее самому технологическому процессу с учетом отличия каналов. Это приводит к тому, что динамические процессы по существу вынуждены рассматриваться как безынерционные с запаздыванием. Другой существенной особенностью является то, что компоненты выходных переменных стохастически зависимы заранее неизвестным образом. Использование в этом случае корреляционных или дисперсионных отношений не приводит к успеху. Необходим специальный анализ Т-процессов и умение моделировать подобные процессы. В частности, это является одной из задач настоящей статьи. В ней приведены: Т-процессы, Т-модели и соответствующие разнотипные алгоритмы управления. Рассмотрен процесс гидродепарафинизации дизельного топлива по имеющимся данным, о которых априори можно сказать, что они неполные, т. е. не отражают комплексное поведение технологического процесса. Отсюда становится ясно, что эти данные требуют пополнения, которое сегодня по разным причинам не осуществляется. Таким образом, процесс гидродепарафинизации может быть отнесен к Т-процессу. Моделирование многомерной системы по реальным данным показало, что в этой задаче задающее воздействие для различных объектов должно быть различным. Исключение составляют только задающие воздействия для всего комплекса или группы объектов.

Моделирование осуществлялось на основании рассмотренных в статье Т-моделей. Уже отмечалось, что эти модели не следует воспринимать как завершенные, дающие представление о действительности. При дальнейших исследованиях они будут подлежать алгоритмическому уточнению. Решение об этом, естественно, принимает исследователь. Именно на этом этапе дается оценка, что в создавшихся условиях полученные модели и алгоритмы управления могут быть приняты для использования в производственных условиях. Попытка использования существующей теории идентификации и управления для процесса гидродепарафинизации неизбежно приведет к значительному ухудшению и увеличению стоимости компьютерной системы управления качеством данного процесса.

Ключевые слова: группа объектов, идентификация, управление, задающие воздействия, непараметрические алгоритмы, Т-процесс, многомерные объекты, адаптация.

Introduction. Modeling of multidimensional inertialess objects continues to be an urgent task of identification. The article emphasizes the case when the vector of the constituents of the output variables stochastically dependents in an unknown manner. In this case, the approach to modeling such objects does not fit within the framework of the existing identification theory. There are plenty of examples of such objects. In particular, they can include processes that occur in the construction industry (cement production), in metallurgy (steel smelting process), in the energy sector (coal burning process), in oil refining (the process of cleaning diesel fuel from sulfur compounds), and also practically all organizational processes, including an educational one [1; 2]. We can consider a multidimensional process at an oil refinery, where there is an installation for hydrotreating diesel fuel from sulfur compounds, combined with the process of hydrodewaxing and increasing the cold flow of diesel fuel [3]. The measurement of the main output stochastically dependent variables of a given process, for example, such as “density at a temperature of 15 ^{o}C” or “boiling point temperature”, takes place once a day. In this case, the process under study is considered as inertialess with time delay [4].

It should be noted that any of these processes corresponds to the statement of different formulations of the

problems, and this difference is due to the presence of various a priori information about the process under study.

The most interesting case is when the nature of the stochastic coupling between the output components is unknown up to parameters. Fig. 1 shows the simplest diagram of series-connected objects. Nevertheless, it demonstrates that in the analysis of such a group of objects specificity arises in modeling, and in the operating similar processes in reality.

In fig. 1, the following notations are agreed: O_q, $q=\overline{1,r}$ – the number of objects (technological devices) included in the group (the group consists of local objects); $-u=(u_1,u_2,...,u_m)$ – input control actions; $\mu=(\mu_1,\mu_2,...,\mu_p)$ – input, unmanaged, but controlled variables (for example, it can be all kinds of additives when working with bulk materials that enter the input of an object); $x=(x_1,x_2,...,x_n)$ – characteristics that determine the composition of the initial product x_1 of semi-finished products $x_2,...,x_n$; z – parameters characterizing the finished product (product). All variables are vectors. The process flow is subject to the technological regulations (GOSTs), which defines the ranges of values of all technological parameters.

The main feature that arises in a group of processes is largely due to its emergence [5] and unreasonably large ranges of technological regulations. Moreover, the compression of technological regulations in real production in most cases cannot be carried out due to emerging organizational problems. Unfortunately, it leads to the production of low-quality products, and often to a large proportion of defective goods. Difficulties are further exacerbated by the fact that defective products cannot always be sent to recycling. A way out can be found using correction of technological regulations in each case. This naturally leads to the problem of automation of a similar process in each local case, at each redistribution of the technological process. In this regard, it is necessary to solve the identification problem and the control task for each technological object, and only then combine them into a group. Thus, there is a need to conduct the process all the time in different ways. This is akin to the well-known idea expressed by the Polish philosopher Ferdinand-Bronislaw Trentovsky in 1843 in the book "The Attitude of Philosophy to Cybernetics as the Art of Managing the People": "The application of the art of control without any serious study of the corresponding theory is like healing without any deep understanding medical science".

He emphasized that truly effective management should take into account all the most important external and internal factors affecting the object of management: "With the same political ideology, cybernet should govern differently in Austria, Russia or Prussia. In the same way, in the same country he must rule tomorrow differently than today".

In such complex multidimensional processes, the output variables of an object are somehow dependent, but this dependence is a priori unknown. Similar processes were called T-processes, and their models – T-models [6]. Identification and management of such processes should be carried out in a non-traditional way [7], because it will not lead to success due to a lack of a priori information about the investigated object. The peculiarity is that the vector of the output constituent, we denote it as $x(t)=(x_1(t),x_2(t),...,x_n(t))$, $j=\overline{1,n}$, is so, that the constituents of this vector are dependent in advance in an unknown manner. Therefore, the mathematical description of the object can be represented as a system of implicit functions:

$$F_j(u(t),\mu(t),x(t))=0,\quad j=\overline{1,n}, \qquad (1)$$

where $u(t)=(u_1(t),u_2(t),...,u_m(t))$, $k=\overline{1,m}$ – input controlled constituent vector; $\mu(t)=(\mu_1(t),\mu_2(t),...,\mu_p(t))$, $\nu=\overline{1,p}$ – vector of input unmanaged but controlled constituents; constituent (t) – means the consideration of input-output variables at a particular point in time. t. The task of identifying the objects under consideration is reduced to the fact that it is necessary to solve the system of implicit nonlinear equations (1) with respect to the constituents of the vector of output variables $x(t)$ with known input $u(t),\mu(t)$. Of course, the task is complicated if there is a group of objects where each local object will have to be considered separately.

The management of such objects is considered in conditions of uncertainty when there is no description of the object accurate to the parameter vector. Moreover, for a group of objects, the preset influences for each individual object will have to be changed.

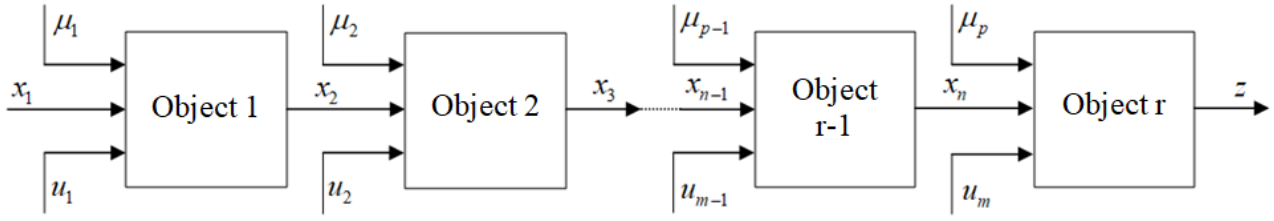

Fig. 1. The group of objects implementing a technological process

Рис. 1. Группа объектов, реализующих технологический процесс

Algorithms identifying local objects. To model a group of objects, the necessary step is to build models of the local objects themselves. In this case, it will be necessary to consider well-known methods, in particular, identification algorithms in a narrow and broad sense. Next, we consider the basic algorithms for modeling local objects. We distinguish two identification classes - parametric and nonparametric.

We consider parametric identification or identification in the narrow sense [8]. In the narrow sense of identification, two main steps are usually considered. The first is the determination of the parametric structure of the object accurate to the coefficients, the second is the determination of the values of the coefficients according to the results of measurements of input-output variables or parameter estimates.

Most often, parameter estimation algorithms are considered in various sources. The most vulnerable stage is the choice of the model structure of the object accurate to the coefficients. It is quite clear that if the structure of the model is chosen inaccurately, this will lead to inaccuracy of the model. It is appropriate to recall the phrase of the ancient Greek philosopher Democritus: “Even a slight departure from truth in the future leads to endless mistakes”.

Thus, at the first stage, a class of equations is selected:

$$F_j\left(u,\mu,x,\alpha\right)=0,\ \ j=\overline{1,n}\,,$$

where u are the input controlled process variables, μ are the input unmanaged, but controlled process variables, x are the output variables, α is the parameter vector.

The parameter estimation algorithms are based on the stochastic approximation method, in particular, they have the following form:

$$\alpha_s^k=\alpha_{s-1}^k+\gamma_s\left(x_s-\sum_{i=1}^{N}\alpha_{s-1}^i\varphi_i\left(u_s\right)\right)\varphi^k\left(u_t\right). \qquad (2)$$

There are many similar algorithms, but we will not dwell on this in detail.

In the case of nonparametric identification or identification in the broad sense, algorithms for simple statement of problems can be based on nonparametric estimates of the Nadarai-Watson regression function [9]. For the multidimensional case, the form of this estimate is as follows:

$$x_s\left(u\right)=\frac{\sum\limits_{i=1}^{s}x_i\prod\limits_{k=1}^{m}\Phi\left(\frac{u_k-u_{ki}}{c_s}\right)}{\sum\limits_{i=1}^{s}\prod\limits_{k=1}^{m}\Phi\left(\frac{u_k-u_{ki}}{c_s}\right)}, \qquad (3)$$

where bell-shaped functions $\Phi\left(\cdot\right)$ and blur parameters c_s satisfy some convergence conditions and satisfy the following properties [9]:

$$0<\Phi\left(c_s^{-1}\left(u_k-u_{ki}\right)\right)<\infty;$$

$$c_s^{-1}\int\limits_{\Omega(u)}\Phi\left(c_s^{-1}\left(u_k-u_{ki}\right)\right)du=1;$$

$$\lim_{s\to\infty}c_s^{-1}\Phi\left(c_s^{-1}\left(u_k-u_{ki}\right)\right)=\delta\left(u_k-u_{ki}\right);\ c_s>0;$$

$$\lim_{s\to\infty}c_s=0;\ \lim_{s\to\infty}sc_s^{\,m}=\infty.$$

In practice, the most common cases are when the vectors of the output variables of the object are stochastically dependent. In this case, the description of the process can be represented as:

$$F_j\left(u,\mu,x\right)=0,\ \ j=\overline{1,n}\,. \qquad (4)$$

And the model of the object in this case, based on the approximation of a local type, can be as follows:

$$\hat{F}_j\left(u,\mu,x,u_s,\mu_s,x_s\right)=0,\ \ j=\overline{1,n},\ \ i=\overline{1,s}\,, \qquad (5)$$

where u_s,μ_s,x_s are time vectors (data set received at the s-th moment of time). Moreover, the functions $\hat{F}_j\left(\cdot\right)$ are unknown because dependencies of the output variables of the process are unknown. As noted above, processes having a stochastic dependence of the output variables were called T-processes.

We consider each individual object in the group as a separate multidimensional object with dependencies of input and output variables, as well as unknown dependencies of output variables among themselves. We show such an object in the following fig. 2.

In fig. 2, the vector of input variables arrives at the input of the object $u=\left(u_1,...,u_m\right)$, the vector of output variables is observed at the output $x=\left(x_1,...,x_n\right)$, $\xi\left(t\right)$ – random jamming acting on the object. When considering such an object, one can notice the dependences of the output variables, which may not always be known.

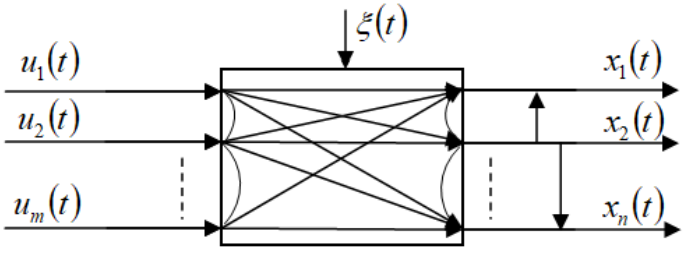

Fig. 2. Multidimensional object

Рис. 2. Многомерный объект

Through various channels of a multidimensional T-object, the dependence of the j constituent of the vector of output variables $\bar{x}$ can be represented as a certain dependence on certain constituents of the vector of input variables $\bar{u}$: $x^{<j>} = f_j\left(u^{<j>}\right),\ j=\overline{1,n}$.

Such functions are determined by the researcher from the available a priori information, and they are called a composite vector. A composite vector is a vector composed of some constituents of the input and output variables, it can also be any set, for example $x^{<2>} = \left(u_3, u_6, x_4\right)$, $x^{<4>} = \left(u_2, u_5, u_6, x_3\right)$. Different channels of a multidimensional system can have a different number of constituents $u(t)$, included in composite vectors $x(t)$.

A model of such a process is considered as a system:

$$\hat{F}_j\left(u^{<j>}, x^{<j>}\right) = 0,\ \ j=\overline{1,n}. \tag{6}$$

where functions $\hat{F}_j(\cdot)$ remain unknown.

As a result of measurements of the input and output variables of the object, a training sample can be obtained $\{u_i, x_i\},\ i=\overline{1,s}$. In this case, for given values of the input variables $u(t)$ it is necessary to solve system (6) with respect to the constituents of the output variables $x(t)$. As a result, it is possible to obtain estimates of the constituents of the output variables from the known input, and this is the main purpose of the desired model.

T-models. It was noted above that if the output variables have unknown stochastic dependencies, then they were called T-objects, and their models are T-models. The description of such a process is specified as follows:

$$F_j\left(u^{<j>}(t), x^{<j>}(t)\right) = 0,\ \ j=\overline{1,n}, \tag{7}$$

where $u^{<j>}(t), x^{<j>}(t)$ is composite vectors, the type of function $F_j(\cdot)$ is unknown. The system of models of the studied object can be represented as follows:

$$\hat{F}_j\left(u^{<j>}(t), x^{<j>}(t), \vec{x}_s, \vec{u}_s\right) = 0,\ \ j=\overline{1,n}, \tag{8}$$

where $\vec{x}_s, \vec{u}_s$ are time vectors, but in this case $\hat{F}_j(\cdot)$ they remain unknown. Therefore, the problem comes down to the fact that for a given value of the vector of input variables $u(t)$ it is necessary to solve system (8) with respect to the vector of output variables $x(t)$. The general scheme for solving such a system is reduced to a nonparametric two-step algorithmic chain, which allows one to find the predicted values of the vector of output variables $x(t)$ from known input $u(t)$.

First, the deficiencies are calculated by the formula:

$$\varepsilon_{ij} = f_j\left(u^{<j>}, x^{<j>}(i), \vec{x}_s, \vec{u}_s\right),\ \ j=\overline{1,n}, \tag{9}$$

where functions $f\left(u^{<j>}, x^{<j>}(i), \vec{x}_s, \vec{u}_s\right)$ are taken in the form of a nonparametric estimate of the Nadarah-Watson regression function [9]:

$$\varepsilon_j(i) = f_{\varepsilon j}\left(u^{<j>}, x_j(i)\right) = x_j(i) - \frac{\sum_{i=1}^{s} x_j[i] \prod_{k=1}^{<n>} \Phi\left(\frac{u'_k - u_k[i]}{c_{su_k}}\right)}{\sum_{i=1}^{s} \prod_{k=1}^{<n>} \Phi\left(\frac{u'_k - u_k[i]}{c_{su_k}}\right)}, \tag{10}$$

where $j=\overline{1,n}$, $,<m>$ is dimension of a composite vector u_k. Bell-shaped functions $\Phi(\cdot)$ and the blur parameter c_{su_k} y some convergence conditions and have the following properties [9]: satisfy $\Phi(\cdot) < \infty$; $\lim_{s\to\infty} sc_s = \infty$; $\lim_{s\to\infty} c_s = 0$; $\int_{\Omega(u)} \Phi\left(c_{su_k}^{-1}\left(u'_k - u_k[i]\right)\right) du = 1$;

$$\lim_{s\to\infty} c_{su_k}^{-1} \Phi\left(c_{su_k}^{-1}\left(u'_k - u_k[i]\right)\right) = \delta\left(u'_k - u_k[i]\right).$$

Next, the conditional expectation is estimated:

$$x_j = M\left\{x \mid u^{<j>}, \varepsilon = 0\right\},\ \ j=\overline{1,n}\ . \tag{11}$$

where the nonparametric estimation of the regression function is taken as the basis. And ultimately, the forecast for each constituent of the vector of the output variable will be as follows:

$$\hat{x}_j = \frac{\sum_{i=1}^{s} x_j[i] \cdot \prod_{k_1=1}^{<n>} \Phi\left(\frac{u_{k_1} - u_{k_1}[i]}{c_{su}}\right) \times \times \prod_{k_2=1}^{<m>} \Phi\left(\frac{\varepsilon_{k_2}[i]}{c_{s\varepsilon}}\right)}{\sum_{i=1}^{s} \prod_{k_1=1}^{<n>} \Phi\left(\frac{u_{k_1} - u_{k_1}[i]}{c_{su}}\right) \times \times \prod_{k_2=1}^{<m>} \Phi\left(\frac{\varepsilon_{k_2}[i]}{c_{s\varepsilon}}\right)},\ \ j=\overline{1,n} \tag{12}$$

where bell-shaped functions $\Phi(\cdot)$ can be taken in the form of a triangular kernel for inputs (13) and residuals (14):

$$\Phi\left(\frac{u_{k_1} - u_{k_1}[i]}{c_{su}}\right) = \begin{cases} 1 - \frac{\left|u_{k_1} - u_{k_1}[i]\right|}{c_{su}}, & \frac{\left|u_{k_1} - u_{k_1}[i]\right|}{c_{su}} < 1, \\ 0, & \frac{\left|u_{k_1} - u_{k_1}[i]\right|}{c_{su}} \geq 1. \end{cases} \tag{13}$$

$$\Phi\left(\frac{\varepsilon_{k_2}[i]}{c_{s\varepsilon}}\right) = \begin{cases} 1 - \frac{\left|0 - \varepsilon_{k_2}[i]\right|}{c_{s\varepsilon}}, & \frac{\left|0 - \varepsilon_{k_2}[i]\right|}{c_{s\varepsilon}} < 1, \\ 0, & \frac{\left|0 - \varepsilon_{k_2}[i]\right|}{c_{s\varepsilon}} \geq 1. \end{cases} \tag{14}$$

Nonparametric algorithm (10) and (12) is a two-step algorithmic chain that allows one to find the predicted values of the constituents of the output vector for the known constituents of the input variables, in the case of stochastic dependence of the output variables [10].

General statement of the problem of identification and management of a group of objects. Modeling and managing a group of objects is significantly different from modeling and managing local objects. And the main difference is that when managing a group, it is necessary to change the defining influences for controlling local objects. Each time, changing the technological regulations, it is requires by reality. Actually, this is shown by the example below at an oil refinery. Otherwise, the technological map requires expansion, but the result of the implementation of this expanded technological regulation is absolutely clear, which will inevitably lead to poor quality products and even to defective product. Thus, the goals that are set in front of a group of objects are significantly different from the goals that are set in front of local objects. It should to be noted that models and control algorithms are not an arithmetic sum of models and algorithms of a group of objects However, the above models and control algorithms can be taken as a basis. Only the contents of the input and output variables of local objects and groups will change. Thus, for good management of the group, a difference in the relevant technological regulations is necessary [11].

At the end of the 70s, one of the authors was able to participate in studies of the technological process for the production of transistors (Svetlana Production Association, Leningrad), due to the fact that the volume of defective products and low-quality products reached 85 %. The studies showed that the range of technological parameters is incredibly wide in all sections of the technological process, although they corresponded to the technological regulations. The research results made it possible to give relevant recommendations, which were included in industry guidance materials [12].

A wide range of values is characteristic of many mining or processing industries. Of course, one can develop, on the basis of studies conducted for each particular enterprise, a more stringent technology regulations and continue to follow it. But it cannot always be used, because strict technological regulations can be implemented only in enterprises with a high level of production culture. This is, first of all, the high quality of technological equipment, local automation, qualifications of workers and their attitude to the subject.

There may be another way, it is necessary to follow the existing technological regulations, but to optimize the process mode in the given technological object taking into account a carried out technological operation at the previous object. This way is more realistic for enterprises, because it does not require expenditures for reconstruction and can significantly improve the quality of products and reduce losses in the production of certain products. For this, it is necessary to develop and introduce computer systems to improve technological conditions. Such computer systems are quite effective.

Let us consider the control scheme of a local object with time delay (fig. 3).

In fig. 3, the following notation is accepted: $u(t)=(u_1(t),...,u_m(t))$ – managed input variables; $\mu(t)=(\mu_1(t),...,\mu_p(t))$ – unmanaged but controlled variables; $x(t+\tau)=(x_1(t+\tau),...,x_n(t+\tau))\in R^n$ – process output variables; $x^*(t+\tau)=(x_1^*(t+\tau),...,x_n^*(t+\tau))\in R^n$ – setting actions; $\xi_t, h_t^{\mu}, h_t^{x}$ – random stationary interference influencing the object and the measurement channels of the input and output variables; τ – known lag on various channels of a multidimensional system.

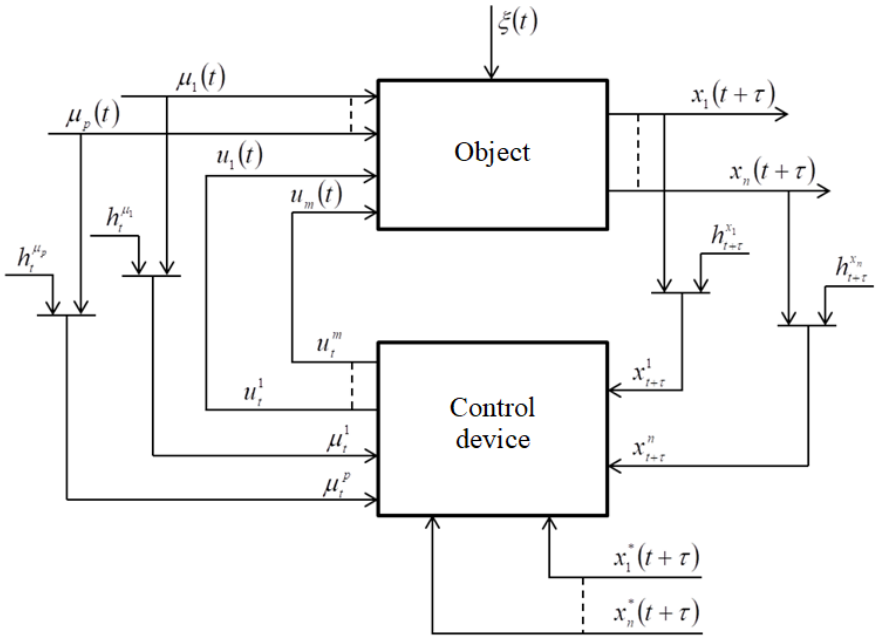

Fig. 3. Multidimensional Object Management Scheme

Рис. 3. Схема управления многомерным объектом

The management of a group of objects should be carried out taking into account the fact that moving from one object to another, it is necessary to change the setting actions.

Multidimensional systems management. The control of multidimensional T-objects is considered under conditions of nonparametric uncertainty, i. e. under conditions when the process model, up to the parameter vector, is completely absent [13]. In this case, well-known techniques are not applicable and other approaches should be used to solve the problem [14–18].

In the problem of controlling a multidimensional process with a stochastic dependence of the output variables, a multistep algorithmic chain is used. It is the following: the input variable $u_1^*(t)$ is taken arbitrarily from the area $\Omega(u_1)$. The following input variable $u_2^*(t)$ is in accordance with the following algorithm:

$$u_2^* = \frac{\sum\limits_{i=1}^{s} u_2^i \Phi\left(\frac{u_1^* - u_1^i}{c_{u_1}}\right) \prod\limits_{j=1}^{<n_q>} \Phi\left(\frac{x_j^* - x_j^i}{c_{x_j}}\right) \times \prod\limits_{\nu=1}^{<p_w>} \Phi\left(\frac{\mu_\nu^* - \mu_\nu^i}{c_{\mu_\nu}}\right)}{\sum\limits_{i=1}^{s} \Phi\left(\frac{u_1^* - u_1^i}{c_{u_1}}\right) \prod\limits_{j=1}^{<n_q>} \Phi\left(\frac{x_j^* - x_j^i}{c_{x_j}}\right) \times \prod\limits_{\nu=1}^{<p_w>} \Phi\left(\frac{\mu_\nu^* - \mu_\nu^i}{c_{\mu_\nu}}\right)}, \quad (15)$$

where $<n_q>$, $<p_w>$ – dimension of the corresponding compound vectors $\bar{x}$ и $\bar{\mu}$, $<n_q> \le n$, $<p_w> \le p$, q, w – the number of constituents included in the composite vector. Compound vectors are determined by the researcher from the available a priori information. If the researcher does not have such information about the object, he uses all the constituents of the input and output variables in a composite vector. Next, the input variable $u_3^*(t)$ is as follows:

$$u_3^* = \frac{\sum\limits_{i=1}^{s} u_3^i \Phi\left(\frac{u_1^* - u_1^i}{c_{u_1}}\right) \Phi\left(\frac{u_2^* - u_2^i}{c_{u_2}}\right) \times \prod\limits_{j=1}^{<n_q>} \Phi\left(\frac{x_j^* - x_j^i}{c_{x_j}}\right) \prod\limits_{\nu=1}^{<p_w>} \Phi\left(\frac{\mu_\nu^* - \mu_\nu^i}{c_{\mu_\nu}}\right)}{\sum\limits_{i=1}^{s} \Phi\left(\frac{u_1^* - u_1^i}{c_{u_1}}\right) \Phi\left(\frac{u_2^* - u_2^i}{c_{u_2}}\right) \times \prod\limits_{j=1}^{<n_q>} \Phi\left(\frac{x_j^* - x_j^i}{c_{x_j}}\right) \prod\limits_{\nu=1}^{<p_w>} \Phi\left(\frac{\mu_\nu^* - \mu_\nu^i}{c_{\mu_\nu}}\right)}, \quad (16)$$

And then the control algorithm continues to find each input constituent of the object, and with each subsequent step, the values of the input variables found at the previous step are added to the algorithm. We write a control algorithm for a multidimensional system that will look like this:

$$u_k^{*s} = \frac{\sum\limits_{i=1}^{s} u_k^i \prod\limits_{k=1}^{k-1} \Phi\left(\frac{u_k^* - u_k^i}{c_{u_k}}\right) \prod\limits_{j=1}^{<n_q>} \Phi\left(\frac{x_j^* - x_j^i}{c_{x_j}}\right) \times \prod\limits_{\nu=1}^{<p_w>} \Phi\left(\frac{\mu_\nu^* - \mu_\nu^i}{c_{\mu_\nu}}\right)}{\sum\limits_{i=1}^{s} \prod\limits_{k=1}^{k-1} \Phi\left(\frac{u_k^* - u_k^i}{c_{u_k}}\right) \prod\limits_{j=1}^{<n_q>} \Phi\left(\frac{x_j^* - x_j^i}{c_{x_j}}\right) \times \prod\limits_{\nu=1}^{<p_w>} \Phi\left(\frac{\mu_\nu^* - \mu_\nu^i}{c_{\mu_\nu}}\right)}, \quad k = \overline{1,m} \quad (17)$$

In the control algorithm (17), the blur parameters for the input and output variables remain the adjustable parameters c_{u_k}, c_{x_j} and c_{μ_ν}, the following formulas can be used for them: $c_{u_k} = \alpha \left| u_k^* - u_k^i \right| + \eta$, $c_{x_j} = \beta \left| x_j^* - x_j^i \right| + \eta$ and $c_{\mu_\nu} = \gamma \left| \mu_\nu^* - \mu_\nu^i \right| + \eta$, where α, β and γ some parameters are more than 1, and parameter $0 < \eta < 1$. It should be noted that the choice of blur parameters c_{u_k}, c_{x_j} и c_{μ_ν} is carried out at each control step. Moreover, if c_{u_k} is determined then the determination of c_{x_j} and c_{μ_ν} is carried out taking into account this fact. The order of determining the blur parameters c_{u_k}, c_{x_j} and c_{μ_ν} is not significant.

Group of objects at a refinery. Installation for hydrotreating diesel fuel from sulfur compounds, combined with the process of hydrodewaxing and improving the cold flow of diesel fuel, operates at a refinery. Imagine the technological scheme of the process (fig. 4).

Fig. 4 shows the reactor block R-301, which combines the processes of hydrotreating and hydrodewaxing; and also shows the cleaning blocks of the circulating hydrogen-containing gas S-301a; stabilization of diesel fuel with the extraction of the side shoulder strap K-301; stabilization of distillation of gasoline; purification of hydrocarbon gases. The input is “Raw materials for installation”, and the output is “SDF”.

The depicted blocks are a group of objects with which combined hydrotreating and hydrodewaxing processes occur.

During the operation of such an installation, information on the progress of the process is collected and accumulated. Therefore, it is necessary to process the accumulated information in order to monitor the entire process and subsequent decision-making on its management [19].

Due to the lack of a priori information about the process in the required volume for the implementation of its modeling and control, it is proposed to use nonparametric systems methods that will help in determining the current state of the process flows at the input and output of the process, identifying inaccurate data, predicting the quality indicators of finished products at the output, correct process control.

Let us depict the general identification scheme for hydrotreating and hydrodewaxing processes in the following form (fig. 5).

The following input and output variables were used for the hydrotreating and hydrodewaxing process: $u_1(t)$ – density at 15 °C, кг/м^3; fractional composition, °C: $u_2(t)$ – boiling point, $u_3(t)$ – full boiling point 50 %, $u_4(t)$ – full boiling point 96 % и $u_5(t)$ – final boiling point; $u_6(t)$ – upstream pressure in P-301, кгс/см^2; $u_7(t)$ – inlet temperature в P-301, °C; $x_1(t)$ – density at 15 °C, кг/м^3, fractional composition, °C: $x_2(t)$ – initial boiling point, $x_3(t)$ – full boiling point 50 %, $x_4(t)$ – full boiling point 96 %, $x_5(t)$ – final boiling point; $x_6(t)$ – cloud point.

Due to the fact that the nature of the dependence of the input and output variables is unknown, as well as the dependences of the output variables on each other, the two-step non-parametric algorithm of the T-model (10) and (12) considered above is used to determine the predicted values of the vector components exit by known input constituents.

The accuracy of the modeling was estimated by the following formula:

$$\delta_j = \frac{\sum_{i=1}^{s} \left| x_i^j - x_s^j(u_i) \right|}{\sum_{i=1}^{s} \left| x_i^j - \hat{x}^j \right|}, \quad j = \overline{1,n}, \tag{18}$$

where x_i^j – observations at the object, $x_s^j(u_i)$ – object exit forecast, $\hat{x}^j$ – average value for each constituent of the vector $\overline{x}$.

For modeling, we carry out the procedure of a rolling exam.

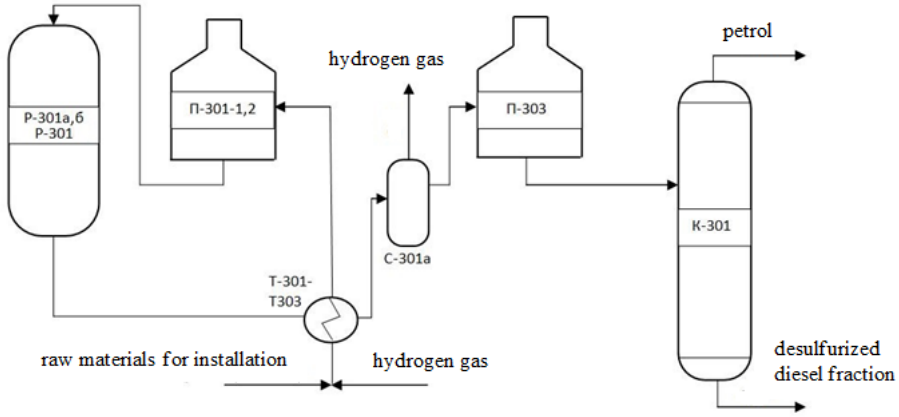

Fig. 4. Fragment of a scheme for hydrotreating diesel fuel and hydrodewaxing

Рис. 4. Фрагмент схемы гидроочистки дизельного топлива и гидродепарафинизации

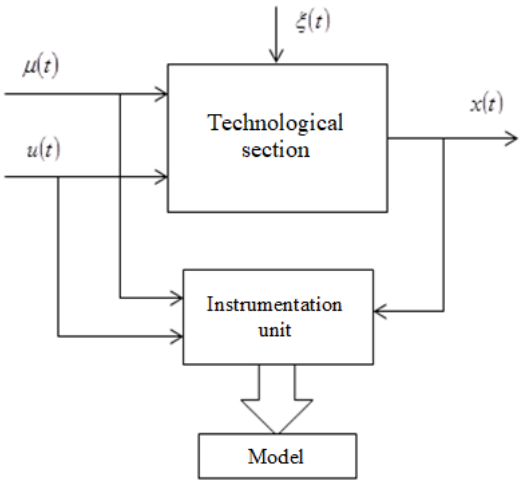

Fig. 5. Fragment of modeling hydrotreating and hydrodewaxing processes

Рис. 5. Фрагмент моделирования процессов гидроочистки и гидродепарафинизации

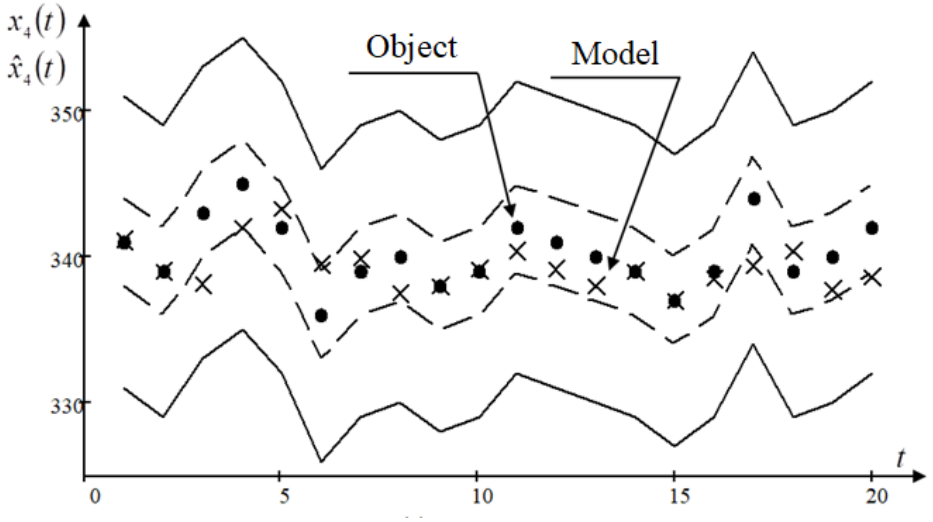

Fig. 6. Prediction of the output constituent $x_4(t)$ for the corresponding input variables $u(t)$

Рис. 6. Прогноз выходной компоненты $x_4(t)$ при соответствующих входных переменных $u(t)$

The adjustable parameters will be the blur parameters c_{su} and $c_{s\varepsilon}$, which in this case we take equal to 0.5 and 0.4, respectively (the values were determined as a result of numerous experiments in order to reduce the quadratic error between the output of the object and model). Sample size $s = 115$. We give the results for the output variable $x_4(t)$ – the boiling point is 96 % (fig. 6).

In fig. 6, the "dot" denotes the outputs of the object, and the "crosses" represent the outputs of the model. For clarity, the presentation of the results on the graph shows 20 sample points. According to GOST R 51069–97 "Oil and oil products. Method for determination of density, relative density and density in degrees by API hydrometer" the accuracy indicators of the method obtained by a statistical study of interlaboratory test results may deviate, for $x_4(t)$ the minimum value is 3 °C, as shown in dashed lines in fig. 6, and the maximum value is 10 °C, as shown in fig. 6 in solid lines. For each constituent of the object output, its own deviation limits are approved. Which of the boundaries to choose, minimum or maximum, are determined by a technologist. According to the schedule, we can say that the forecast was quite satisfactory, the modeling error was $\delta_4 = 0.04$. But it is worth paying attention to the fact that the maximum boundaries of deviations are too wide in all sections of the technological process, and the process itself must take place at the minimum boundaries of deviations. The resulting forecast values sometimes go beyond the minimum boundaries, but lie within the maximum limits, many factors can influence this, such as the small size of the training sample, the inaccuracy of a priori information, random interference affecting the process, etc. But well-tuned models make it possible to increase its accuracy and, in the future, will help in high-quality process control [20].

Conclusion. The article considers nonparametric algorithms for modeling and controlling a group of objects under conditions of both parametric and nonparametric uncertainty. The creation of groups is determined not only by the structure of the enterprise, but also by the nature of the technological process. One feature is emphasized, which manifests itself in the fact that the driving actions for each object are the subject of special consideration at each control step. The paper presents models and algorithms for managing a group of objects, as well as some local and specially emphasized property of emergence. Models of multidimensional inertia-free complexes are presented and, in particular, an example is considered based on the results of measurements of real data of the technological combined process of hydrotreating and hydrodewaxing of diesel fuel occurring at a refinery.

References

1. Medvedev A. V., Yareshchenko D. I. [On modeling the process of acquiring knowledge by students at a university]. *Vysshee obrazovanie*. 2017, No. 1, P. 7–10 (In Russ.).

2. Yareshchenko D. I. [Some notes on the assessment of knowledge of university students]. *Otkrytoe obrazovanie*. 2017, No. 4, P. 66–72 (In Russ.).

3. Agafonov E. D., Medvedev A. V., Orlovskaya N. F., Sinyuta V. R., Yareshchenko D. I. [Predictive model of the process of catalytic hydrodeparaffinization in the absence of a priori information]. *Izv. Tul'skogo gos. un-ta. Tekhn. Nauki*. 2018, No. 9, P. 456–468 (In Russ.).

4. Korneeva A. A., Sergeeva N. A. [On nonparametric identification of inertialess objects with delay]. *Inform. tekhnologii modelirovaniya i upr.* 2012, No. 5, P. 363–370 (In Russ.).

5. Peregudov F. I., Tarasenko F. P. *Vvedenie v sistemnyy analiz* [Introduction to Systems Analysis]. Moscow, Vysshaya shkola Publ., 1989, 367 p.

6. Medvedev A. V. *Osnovy teorii neparametricheskikh sistem. Identifikatsiya, upravlenie, prinyatie resheniy* [Fundamentals of the theory of nonparametric

systems. Identification, management, decision making]. Krasnoyarsk, SibGU im. M. F. Reshetneva Publ., 2018, 732 p.

7. Tsypkin Ya. Z. *Osnovy informatsionnoy teorii identifikatsii* [Fundamentals of the information theory of identification]. Moscow, Nauka Publ., 1984, 320 p.

8. Eykkhoff P. *Osnovy identifikatsii sistem upravleniya* [The basics of identifying control systems]. Moscow, Mir Publ., 1975, 680 p.

9. Nadaraya E. A. *Neparametricheskoe otsenivanie plotnosti veroyatnostey i krivoy regressii* [Nonparametric estimation of probability density and regression curve]. Tbilisi, Izd-vo Tbilisskogo un-ta Publ., 1983, 194 p.

10. Medvedev A. V., Yareshchenko D. I. [Nonparametric modeling of T-processes in conditions of incomplete information]. *Informatsionnye tekhnologii*. 2019, No. 10, P. 579–584 (In Russ.).

11. Medvedev A. V. *Informatizatsiya upravleniya* [Management Informatization]. Krasnoyarsk, SAA Publ., 1995, 80 p.

12. *Tipovaya sistema upravleniya kachestvom* [Typical Quality Management System]. Leningrad, Elektronstandart Publ., 1977, 237 p.

13. Medvedev A. V. [On the theory of nonparametric control systems]. *Vestn. Tom. gos. un-ta. Upr., vychisl. tekhnika i informatika*. 2013, No. 1, P. 6–19 (In Russ.).

14. Pupkov K. A., Egupov N. D. *Metody klassicheskoy i sovremennoy teorii avtomaticheskogo upravleniya. T. 1: Matematicheskie modeli, dinamicheskie kharakteristiki i analiz sistem upravleniya* [Methods of the classical and modern theory of automatic control. Mathematical models, dynamic characteristics and analysis of control systems]. Moscow, MGTU im. N. E. Baumana Publ., 2004, 748 p.

15. Pupkov K. A., Egupov N. D. *Metody klassicheskoy i sovremennoy teorii avtomaticheskogo upravleniya. T. 2: Statisticheskaya dinamika i identifikatsiya sistem avtomaticheskogo upravleniya* [Methods of the classical and modern theory of automatic control. Statistical dynamics and identification of automatic control systems]. Moscow, MGTU im. N. E. Baumana Publ., 2004, 640 p.

16. Pupkov K. A., Egupov N. D. *Metody klassicheskoy i sovremennoy teorii avtomaticheskogo upravleniya. T. 3: Sintez regulyatorov sistem avtomaticheskogo upravleniya* [Methods of the classical and modern theory of automatic control. Synthesis of automatic control system regulators]. Moscow, MGTU im. N. E. Baumana Publ., 2004, 748 p.

17. Pupkov K. A., Egupov N. D. *Metody klassicheskoy i sovremennoy teorii avtomaticheskogo upravleniya. T. 4: Teoriya optimizatsii sistem avtomaticheskogo upravleniya* [Methods of the classical and modern theory of automatic control. Theory of optimization of automatic control systems]. Moscow, MGTU im. N. E. Baumana Publ., 2004, 748 p.

18. Pupkov K. A., Egupov N. D. *Metody klassicheskoy i sovremennoy teorii avtomaticheskogo upravleniya. T. 5: Metody sovremennoy teorii avtomaticheskogo upravleniya* [Methods of the classical and modern theory of automatic control. Methods of the modern theory of automatic control]. Moscow, MGTU im. N. E. Baumana Publ., 2004, 742 p.

19. Faleev S. A., Belinskaya N. S., Ivanchina E. D. [Optimization of the hydrocarbon composition of raw materials in reforming and hydrodewaxing plants using mathematical modeling]. *Neftepererabotka i neftekhimiya. Nauchno-tekhnicheskie dostizheniya i peredovoy opyt*. 2013, No. 10, P. 14–18 (In Russ.).

20. Kostenko A. V., Musaev A. A., Turanosov A. V. [Virtual Raw Flow Analyzer]. *Neftepererabotka i neftekhimiya. Nauchno-tekhnicheskie dostizheniya i peredovoy opyt*. 2006, No. 1, P. 1–13 (In Russ.).

Библиографические ссылки

1. Медведев А. В., Ярещенко Д. И. О моделировании процесса приобретения знаний студентами в университете // Высшее образование. 2017. Вып. 1. С. 7–10.

2. Ярещенко Д. И. Некоторые замечания об оценке знаний студентов университетов // Открытое образование. М., 2017. Вып. 4. С. 66–72.

3. Прогнозная модель процесса каталитической гидродепарафинизации в условиях недостатка априорных сведений / Е. Д. Агафонов, А. В. Медведев, Н. Ф. Орловская и др. // Изв. Тульского гос. ун-та. Техн. науки. 2018. № 9. С. 456–468.

4. Корнеева А. А., Сергеева Н. А. О непараметрической идентификации безынерционных объектов с запаздыванием // Информ. технологии моделирования и упр. 2012. Вып. 5 (77). С. 363–370.

5. Перегудов Ф. И., Тарасенко Ф. П. Введение в системный анализ. М. : Высшая школа, 1989. 367 с.

6. Медведев А. В. Основы теории непараметрических систем. Идентификация, управление, принятие решений : монография / СибГУ им. М. Ф. Решетнева. Красноярск, 2018. 732 с.

7. Цыпкин Я. З. Основы информационной теории идентификации. М. : Наука, 1984. 320 с.

8. Эйкхофф П. Основы идентификации систем управления. М. : Мир, 1975. 680 с.

9. Надарая Э. А. Непараметрическое оценивание плотности вероятностей и кривой регрессии. Тбилиси : Изд-во Тбилисского ун-та, 1983. 194 с.

10. Медведев А. В., Ярещенко Д. И. Непараметрическое моделирование Т-процессов в условиях неполной информации // Информационные технологии. 2019. № 10 (25). С. 579–584.

11. Медведев А. В. Информатизация управления : учеб. пособие / Сиб. аэрокосмич. акад. Красноярск, 1995. 80 с.

12. Типовая система управления качеством. ОРМ. РМ 11 091.146–76. Ленинград : ВНИИ «Электронстандарт», 1977. 237 с.

13. Медведев А. В. О теории непараметрических систем управления // Вестн. Том. гос. ун-та. Упр., вычисл. техника и информатика. 2013. № 1 (22). С. 6–19.

14. Методы классической и современной теории автоматического управления. В 5 т. Т. 1: Математические модели, динамические характеристики и анализ систем управления / под. ред. К. А. Пупкова, Н. Д. Егупова. М. : Изд-во МГТУ им. Н. Э. Баумана, 2004. 748 с.

15. Методы классической и современной теории автоматического управления. В 5 т. Т. 2: Статистиче-

ская динамика и идентификация систем автоматического управления / под. ред. К. А. Пупкова, Н. Д. Егупова. М. : Изд-во МГТУ им. Н. Э. Баумана, 2004. 640 с.

16. Методы классической и современной теории автоматического управления. В 5 т. Т. 3: Синтез регуляторов систем автоматического управления / под. ред. К. А. Пупкова, Н. Д. Егупова. М. : Изд-во МГТУ им. Н. Э. Баумана, 2004. 748 с.

17. Методы классической и современной теории автоматического управления. В 5 т. Т. 4: Теория оптимизации систем автоматического управления / под. ред. К. А. Пупкова, Н. Д. Егупова. М. : Изд-во МГТУ им. Н. Э. Баумана, 2004. 748 с.

18. Методы классической и современной теории автоматического управления. В 5 т. Т. 5: Методы современной теории автоматического управления / под. ред. К. А. Пупкова, Н. Д. Егупова. М. : Изд-во МГТУ им. Н. Э. Баумана, 2004. 742 с.

19. Оптимизация углеводородного состава сырья на установках риформинга и гидродепарафинизации методом математического моделирования / С. А. Фалеев, Н. С. Белинская, Э. Д. Иванчина и др. // Нефтепереработка и нефтехимия. Научно-технические достижения и передовой опыт. 2013. № 10. С. 14–18.

20. Костенко А. В., Мусаев А. А., Тураносов А. В. Виртуальный анализатор сырьевых потоков // Нефтепереработка и нефтехимия. Научно-технические достижения и передовой опыт. 2006. № 1. С. 1–13.

Kornet Maria Evgenievna – candidate; Reshetnev Siberian State University of Science and Technology. E-mail: marya.kornet@gmail.com.

Medvedev Alexander Vasilievich – D. Sc., Professor, Department of System Analysis and Operations Research; Reshetnev Siberian State University of Science and Technology. E-mail: mav2745@mail.ru.

Yareshchenko Darya Igorevna – senior lecturer of the department Intelligent Control Systems of the Institute of Space and Information Technologies; Siberian Federal University. E-mail: YareshenkoDI@yandex.ru.

Корнет Мария Евгеньевна – соискатель; Сибирский государственный университет науки и технологий имени академика М. Ф. Решетнева. E-mail: marya.kornet@gmail.com.

Медведев Александр Васильевич – доктор технических наук, профессор кафедры системного анализа и исследования операций; Сибирский государственный университет науки и технологий имени академика М. Ф. Решетнева. E-mail: mav2745@mail.ru.

Ярещенко Дарья Игоревна – старший преподаватель базовой кафедры Интеллектуальных систем управления Института космических и информационных технологий; Сибирский федеральный университет. E-mail: YareshenkoDI@yandex.ru.

UDC 519.6
Doi: 10.31772/2587-6066-2020-21-2-187-194

For citation: Kuznetsov A. A., Kishkan V. V. A routing algorithm for the Cayley graphs generated by permutation groups. *Siberian Journal of Science and Technology*. 2020, Vol. 21, No. 2, P. 187–194. Doi: 10.31772/2587-6066-2020-21-2-187-194

Для цитирования: Кузнецов А. А., Кишкан В. В. Об одном алгоритме маршрутизации на графах Кэли, порожденных группами подстановок // Сибирский журнал науки и технологий. 2020. Т. 21, № 2. С. 187–194. Doi: 10.31772/2587-6066-2020-21-2-187-194

A ROUTING ALGORITHM FOR THE CAYLEY GRAPHS GENERATED BY PERMUTATION GROUPS

A. A. Kuznetsov*, V. V. Kishkan

Reshetnev Siberian State University of Science and Technology
31, Krasnoyarskii rabochii prospekt, Krasnoyarsk, 660037, Russian Federation
*E-mail: kuznetsov@sibsau.ru

The purpose of this work is to create an effective routing algorithm on the Cayley graphs of permutation groups, superior in its characteristics to an algorithm using an automatic group structure.

In the first section of the article we describe the auxiliary algorithm A–1 which allows numbering elements of a given permutation group.

In the second section we present the algorithm A–2 for calculating the routing table on the Cayley graph and algorithm A–3 for determination the optimal route between two arbitrary vertices of the graph. Estimates of time and space complexity are also obtained for these algorithms.

In the third section we describe the algorithm A–4 for calculation the minimal word of a group element. It is proved that the computational complexity of the algorithm will be proportional to the length of the input word.

The fourth section presents the results of computer experiments for some groups of permutation groups, which compare the time for calculating the minimum words using algorithm A – 4 and an algorithm based on the construction of an automatic group structure. It is shown that A – 4 is much faster than its competitor.

Keywords: Cayley graph, a permutation group.

ОБ ОДНОМ АЛГОРИТМЕ МАРШРУТИЗАЦИИ НА ГРАФАХ КЭЛИ, ПОРОЖДЕННЫХ ГРУППАМИ ПОДСТАНОВОК

А. А. Кузнецов*, В. В. Кишкан

Сибирский государственный университет науки и технологий имени академика М. Ф. Решетнева
Российская Федерация, 660037, г. Красноярск, просп. им. газ. «Красноярский рабочий», 31
*E-mail: alex_kuznetsov80@mail.ru

Целью настоящей работы является создание эффективного алгоритма маршрутизации на графах Кэли групп подстановок, превосходящего по своим характеристикам алгоритм, использующий автоматическую структуру группы.

В первом разделе статьи описан вспомогательный алгоритм А–1, который позволяет нумеровать элементы заданной группы подстановок.

Во втором разделе представлен алгоритм А–2 для вычисления таблицы маршрутизации на графе Кэли и алгоритм А–3, который позволяет определить оптимальный маршрут между двумя произвольными вершинами графа. Для данных алгоритмов также получены оценки временной и пространственной сложности.

В третьем разделе описан алгоритм А–4, при помощи которого можно вычислить минимальное слово элемента группы. Доказано, что вычислительная сложность алгоритма будет пропорциональна длине входящего слова.

В четвертом разделе приведены результаты компьютерных экспериментов для некоторых групп подстановок, в которых сравнивается время вычисления минимальных слов по алгоритму А–4 и алгоритму, основанному на построении автоматической групповой структуры. Показано, что А–4 значительно быстрее своего конкурента.

Ключевые слова: граф Кэли, группа подстановок.

Introduction. Currently, the increasing demand for cloud computing is leading to the growth of large-scale data centers (DPCs).

Modern data centers contain hundreds of thousands of nodes interconnected by a network. The topology of such a network, i.e. the method of connecting nodes is a key link on which speed, fault-tolerance, reliability and other characteristics of the data center depend.

For this reason, network design is a very important task, including the search for graph models that have good topological properties and allow the use of efficient routing algorithms.

These are the qualities of Cayley graphs, which have such attractive topological properties as high symmetry, hierarchical structure, recursive construction, high connectivity, and fault-tolerance [1]. The definition of a Cayley graph implies that the vertices of the graph are elements of some algebraic group. The choice of the group and its generating elements allows us to obtain a graph [2] that meets the necessary requirements for diameter, degree of vertices, number of nodes, etc.

Suppose $G := \langle X \rangle$ is a finite group, generated by an ordered set $X := \{x_1 \prec x_2 \prec \ldots \prec x_m\}$, which is also called the alphabet. The set of all words (strings) over the alphabet X will be denoted by X^*. Let $w := x_1 x_2 \ldots x_l$ be a word over X and $|w| := l$ is its length. On the set X^* we also define the relation of order. Suppose v and w are two arbitrary words in the alphabet X. Then $v \prec w$, if $|v| < |w|$, a and in case of equal word lengths, the smaller word will be determined according to the introduced lexicographic order on generators. If it is necessary to emphasize that the string $v \in X^*$ matches the element $g \in G$, then we write v_g. The string v will be called the minimal word of the element g, if for all others $w \in X^*$, such that $v_g = w_g$, will be conducted $v \prec w$. It's obvious that every $g \in G$, then we will write v_g. It is evident that every $g \in G$ matches the unique minimal word. The length of an element of a group g is the length of its minimal word v, that is $|g| := \min\{|v_g| : v_g \in X^*\}$. It has been noted that in the general case, the task of determining the minimal word is NP-hard [3].

Cayley graph $\Gamma := Cay(G, X)$ of group G with relation to X is called a directed unweighted labeled graph with many vertices $V(\Gamma) := \{g \mid g \in G\}$ and many edges $E(\Gamma) := \{(g, gx) \mid x \in X, g \in G\}$. Suppose $(g, gx) \in E(\Gamma)$, then generator x is called an edge token. If $X = X \cup X^{-1}$, then graph Γ will be non-oriented. We assume that the unit element $e \notin X$, that is in graph Γ there are no loops. As it is known [4], the shortest distance between two arbitrary vertices of the graph g and h, which we denote $d(g,h)$, is equal to the length of the minimum word of the element $g^{-1}h$, i. e. $d(g,h) := |g^{-1}h|$.

Let us dwell on the currently known routing algorithms on Cayley graphs. Traditional methods, such as Dijkstra or Bellman-Ford algorithms, can be used on graphs of any kind, but require significant spatial and temporal resources [5]. For some families of Cayley graphs, there are special routing algorithms that, unlike traditional methods, use the topological characteristics of the graph, while reducing time and/or spatial complexity. These include graph families such as hypercube [6], butterfly [7] and star graph [8], which are Cayley graphs. In work [9], a routing algorithm for creped and star graphs based on sorting permutations is presented. However, this approach does not provide the shortest routing. K. Teng and B. Arden prove [10] that all finite Cayley graphs can be represented by generalized chordal rings, and then offer an iterative routing algorithm based on the lookup table. The space complexity of such an algorithm is $O(|G|^2)$, and temporary is $O(D)$, where $|G|$ and D are size and diameter of the network, respectively. To find the shortest paths on the Borel graph L. Wang and K. Tang offer an algorithm [11], which first calculates in an autonomous mode the routing table from one node to all the others; then, using the transitive property of the Cayley graph, creates a routing table for all nodes. The computational complexity of this algorithm is limited $O(\log_4 |G|)$, and space complexity is $O(D \cdot |G|^2)$. In [12] a distributed fault tolerant routing algorithm on a Borel graph is presented. This two-phase algorithm uses two types of routing tables: static and dynamic.

In the article [13], a routing algorithm for a special class of Cayley graphs used as the topology of a wireless data center network is presented. This algorithm is two-level: for sending messages between servers in the same rack and servers in different racks. Each server is identified by three values: the coordinates of the rack, the tier on which the server is located, and its number on the tier. In addition, each server uses three routing tables to forward packets from the source to the destination along the shortest route.

The monograph [14] is a fundamental work on the relationship of algebraic groups and finite state automaton. In this case, the automaton structure of a special kind is determined on the group $G = \langle X \rangle$, using which it is possible to calculate the minimal word for any element of the group.

According to [14], the group finite state machine reads an arbitrary word $w_g \in X^*$, processes it and produces the minimal word of the element g. Herewith the time T_0 of word processing w will be proportional to the square of its length, i. e. $T_0 = O(|w|^2)$.

Using this result, an algorithm for finding the shortest path on a Cayley graph (denoted by A – 0) was proposed in work [15], while its computational complexity is limited, and space complexity $M_0 = O(|X| \cdot |G| + |\mathcal{A}|)$, where $|\mathcal{A}|$ is the number of states of a group automaton.

It should be noted that all the above routing algorithms can be assigned to one of the following categories:

a) those that are designed for specific Cayley graphs; b) universal with high space and time complexity and c) with low complexity, which do not provide shortest paths.

The purpose of this work is to create an effective routing algorithm on Cayley graphs of permutation groups that surpasses in its characteristics the algorithm from [15].

The first section of the article describes the auxiliary algorithm A – 1, which allows you to number the elements of a given permutation group.

The second section presents the algorithm A – 2 for calculating the routing table on the Cayley graph. Algorithm A – 3 is described below, it allows to determine the optimal route between two arbitrary vertices of the graph. Estimates of time and space complexity are also obtained for these algorithms.

The third section describes the algorithm A – 4, with which you can calculate the minimum word of an element of the group. It is proved that the computational complexity of the algorithm will be proportional to the length of the incoming word.

The fourth section presents the results of computer experiments for some groups of permutations, which compare the time needed to calculate the minimal words using algorithm A – 4 and the procedure from [15].

In conclusion, the prospects for the development of the project are considered.

1. Algorithms on Cayley graphs of permutation groups. Suppose G is finite group of permutations on the set of points $\Omega = \{1,2,\ldots,n\}$. We denote $\alpha^g := g[\alpha]$ element image $\alpha \in \Omega$ under the influence $g \in G$. Orbit point $\alpha \in \Omega$ is called set $\alpha^G := \{\alpha^g |\ g \in G\}$.

Point stabilizer $\alpha \in \Omega$ we will call the set $G_\alpha := \{g \in G |\ \alpha^g = \alpha\}$. For given $\beta_1,\beta_2,\ldots,\beta_i \in \Omega$ we inductively define

$$G_{\beta_1,\beta_2,\ldots,\beta_i} := (G_{\beta_1,\beta_2,\ldots,\beta_{i-1}})_{\beta_i} =$$
$$= \{g \in G |\ \beta_j^g = \beta_j,\ j = 0,1,\ldots,i\}.$$

Sequence of different elements $B := (\beta_1,\beta_2,\ldots,\beta_m)$ we will call the base of the group G, if $G_{\beta_1,\beta_2,\ldots,\beta_m} = e$. Thus, only a single element of the group leaves all the points of the base stationary.

Suppose $G^{(i)} := G_{\beta_1,\beta_2,\ldots,\beta_{i-1}}$. Next, we determine the chain of stabilizers

$$G := G^{(1)} \geq G^{(2)} \geq \ldots \geq G^{(m)} \geq G^{(m+1)} = e.$$

If $G^{(i+1)}$ is its own subgroup $G^{(i)}$ for $i \in [1,m]$, then the base B is called irreducible.

Adjacent group classes $G^{(i)}$ by subgroup $G^{(i+1)}$ have a one-to-one correspondence with the elements of the orbit $\Delta^{(i)} := \beta_i^{G^{(i)}}$. If $a,b \in G^{(i)}$ and $G^{(i+1)}a = G^{(i+1)}b$, then for some $h \in G^{(i+1)}$ will be conducted $a = hb$. Therefore, $\beta_i^a = \beta_i^{hb} = \beta_i^b$.

The above fact makes it possible to calculate a family of representatives of cosets (transversal) $U^{(i)}$ groups $G^{(i)} \mod G^{(i+1)}$. For every $\gamma \in \Delta^{(i)}$ we define $u_i(\gamma) \in G^{(i)}$, which displays β_i in γ, other words $\beta_i^{u_i(\gamma)} = \gamma$. In the particular case if $\beta_i \to \beta_i$, then $u_i(\beta_i) := e$.

According to the notation introduced, we obtain an ordered sequence $U^{(i)} := (u_i(\gamma) |\ \gamma \in \Delta^{(i)})$. It's obvious that $|U^{(i)}| = |\Delta^{(i)}|$.

Putting together all $U^{(i)}$, we get a transversal:

$$U = \bigcup_{i=1}^{m} U^{(i)}.$$

By the Lagrange theorem $|G| = |G^{(1)} : G^{(2)}| \cdot |G^{(2)}| = |U^{(1)}| \cdot |G^{(2)}|$. Similarly, $|G^{(2)}| = |G^{(2)} : G^{(3)}| \cdot |G^{(3)}| = |U^{(2)}| \cdot |G^{(3)}|$. Continuing this process, we get $|G| = |U^{(1)}| \cdot |U^{(2)}| \cdots |U^{(m)}|$.

Suppose $B = (\beta_1,\beta_2,\ldots,\beta_m)$ is the base G, then for any element of the group we can determine its base image $B^g := (\beta_1^g,\beta_2^g,\ldots,\beta_m^g)$.

Lemma 1. *For $\forall g \in G$ base image B^g has a unique view.*

Proof. Suppose $B^g = B^h$, then $B^{gh^{-1}} = B$. Therefore, according to the definition of the base, $gh^{-1} = e$. Consequently, $g = h$.

Lemma 2. *Any element $g \in G$ can be unambiguously written in canonical form*

$$g := (u_m,u_{m-1},\ldots,u_1) = u_m u_{m-1} \ldots u_1,$$

where

$$u_i \in U^{(i)}\ u\ i \in [1,m]. \qquad (1)$$

Proof. As $g \in G$, then it is contained in some coset of the group G by group, th $G^{(2)}$ erefore, we write it in the form $g = h_2 u_1$, where $h_2 \in G^{(2)}$ and $u_1 \in U^{(1)}$. Similarly, $h_2 = h_3 u_2$, where $h_2 \in G^{(2)}$ and $u_2 \in U^{(2)}$.

Continuing this process, we obtain the desired formula.

In the future, we will also need many inverse elements of the transversal

$$\hat{U} = \bigcup_{i=1}^{m} \hat{U}^{(i)},$$

где $\hat{U}^{(i)} := (u_i^{-1}(\gamma) |\ \gamma \in \Delta^{(i)})$

To find items in $U^{(i)}$ and $\hat{U}^{(i)}$ we need an auxiliary array of indices $A_{m \times n}$, whose elements are defined as follows:

$$A_{ij} := \begin{cases} a_{ij} \in [0,|U^{(i)}|-1] - \\ \text{the element number of } u_i(j) \text{ in } U^{(i)}, \text{ if } j \in \Delta^{(i)}; \\ -1 \text{ if } j \notin \Delta^{(i)}. \end{cases}$$

Below is an algorithm that received a word at the input consisting of a product of elements $g_1 g_2 \dots g_l$ of the group G, its base B, the transversal U and its inverse $\hat{U}$, as well as an auxiliary array A, returns canonical representation $u_m u_{m-1} \dots u_1$ of this product.

Algorithm A–1. $u_m u_{m-1} \dots u_1 = \text{Factor}(g_1 g_2 \dots g_l, U, \hat{U}, A, B)$

Input: $g_1 g_2 \dots g_l$, $\hat{U}$, A and B

Output: $u_m u_{m-1} \dots u_1$

1. $h := B$
2. **For all** $i = 1,2,\dots,l$
3. $h := (h_1^{g_i}, h_2^{g_i}, \dots, h_m^{g_i})$
4. **For all** $i = 1,2,\dots,m$
5. $j := h[i]$
6. $u_i := U^{(i)}[a_{ij}]$
7. $u_i^{-1} := \hat{U}^{(i)}[a_{ij}]$
8. $h := (h_1^{u_i^{-1}}, h_2^{u_i^{-1}}, \dots, h_m^{u_i^{-1}})$
9. **Return** $u_m u_{m-1} \dots u_1$

Suppose $T_i = O(f)$ and $M_i = O(f)$ is upper asymptotic estimates of the computational and space complexity of the i algorithm, respectively.

Lemma 3. *Algorithm A–1 is correct and* $T_1 = O(l \cdot m + m^2)$.

Proof. The correctness of the algorithm follows from Lemmas 1 and 2. First we get the base image of the element $g := g_1 g_2 \dots g_l$, and then at each $i \in [1,m]$ stabilize the point $\beta_i \in B$. As a result, we get $B^{g u_1^{-1} \dots u_m^{-1}} = B$. Consequently, $g = u_m u_{m-1} \dots u_1$.

To assess the computational complexity, we note that the number of operations in a cycle of 2–3 is limited $O(l \cdot m)$, and cycle 4–8 – $O(m^2)$. Therefore, $T_1 = O(l \cdot m + m^2)$.

Decomposition (1) makes it possible to effectively number all $g \in G$, using the method of listing tuple elements in a mixed number system [16]. Suppose $c := (c_m, c_{m-1}, \dots, c_1)$ is the basis of a mixed base notation in which $c_1 := 1$ and $c_i = c_{i-1} \cdot |U^{(i-1)}|$ for $i \geq 2$.

Suppose $g := u_m u_{m-1} \dots u_1$. We define a bijective mapping $\mathcal{N} : u_m u_{m-1} \dots u_1 \leftrightarrow (a_m, \dots, a_1)$, where $a_i \in [0,|U^{(i)}|-1]$ is a number of the element u_i in $U^{(i)}$.

We note that the vector $(a_m, \dots, a_1)$ is a number $\mathcal{N}(g) \in [0,|G|-1]$ in the scale of notation with mixed base $(c_m, \dots, c_1)$.

Suppose $k := \mathcal{N}(g)$ is the element number g.

Lemma 4. *Computational complexity* $\mathcal{N}(g)$ *u* $\mathcal{N}^{-1}(k)$ *does not exceed* $O(m)$.

Proof. Suppose $g = u_m u_{m-1} \dots u_1$ and a_i is number u_i in $U^{(i)}$. Then $k = \mathcal{N}(g) = a_m c_m + \dots + a_1 c_1$.

In backward case $g = \mathcal{N}^{-1}(k) = u_m u_{m-1} \dots u_1$, where factors u_i are calculated as follows:

1. **For all** $i = 1,2,\dots,m$
2. $a_i := k \mod |U^{(i)}|$
3. $k := \lfloor k / |U^{(i)}| \rfloor$
4. $u_i := U^{(i)}[a_i]$.

Obviously, the number of operations in these procedures does not exceed $O(m)$.

Comment 1. *For definiteness, we assume that all sequences* $U^{(i)}$ *start with a unity element e. In this case* $\mathcal{N}(e) := 0$.

For numbering the elements of a group, we need to know its base B and the complete family of representatives of adjacent classes U. To calculate them, we will use the well-known Schreyer – Sims algorithm proposed by C. Sims in 1970 [17]. Currently, there is a variety of its modifications [18]. The most efficient versions of the algorithm have low computational complexity and are implemented in computer algebra systems such as GAP, Magma, and Mathematica, as well as in the SymPy library for Python.

2. Cayley graph routing algorithms. To find the shortest paths on Cayley's graph $Cay(G,X)$ we need a routing table $P_{2\times|G|}$, which is also called the parent tree [19]. The following is an algorithm that, having received at the input a generating set of a group X, its base B, the transversal U and its inverse $\hat{U}$, as well as a backing array A, returns the specified table.

Hereinafter, we will be interested in the case $|X| \ll |G|$ and $n \ll |G|$.

Algorithm A–2. $P = \text{BFS}(X, U, \hat{U}A, B)$

Input: X, U, $\hat{U}$, A and B

Output: Routing table P on Cayley's graph $Cay(G,X)$

1. $P_{2\times|G|} := [\infty \ \dots \ \infty]$
2. $k := \mathcal{N}(e) := 0$
3. $P[1][k] := -1$
4. $P[2][k] := -1$
5. $Q := \{k\}$
6. **Until** $Q \neq \varnothing$
7. pop $q \in Q$ from the queue
8. **For all** $x \in X$
9. $s := \text{Factor}(\mathcal{N}^{-1}(q)x, U, \hat{U}, A, B)$
10. $k := \mathcal{N}(s)$

11. **If** $P[1][k] = \infty$
12. add k to the queue Q
13. $P[1][k] := q$
14. $P[2][k] := x$
15. **Return** P

Theorem 1. *Algorithm A–2 is correct and* $T_2 = O(m^2 \cdot |X| \cdot |G|)$.

Proof. This algorithm is a classical method in breadth-first search on a graph [19]. In this case, the vertex with the unit element number *e* (according to comment 1, we have $\mathcal{N}(e) := 0$) will be the root of the parent tree *P*. Suppose $gx = h$, where $\mathcal{N}(g) = k$ and $\mathcal{N}(h) = l$, then $P[1][l] := k$, $P[2][l] = x$. That means the vertex k is the parent of the vertex *l* and *x* is edge tokens (k,l).

We need to check altogether $|X| \cdot |G|$ of elements. The verification time for each element according to Lemmas 3 and 4 is limited $O(m^2)$. Accordingly, $T_2 = O(m^2 \cdot |X| \cdot |G|)$.

The following algorithm using the routing table *P* calculates the shortest route $w := x_1 x_2 \ldots x_s$ between vertexes $a, b \in Cay(G, X)$, where $x_i \in X$. It's obvious that $s \le D$, where *D* is diameter of the graph.

Algorithm A–3. $w = \text{Route}(a, b, U, \hat{U}A, B, P)$

Input: *a*, *b*, U, $\hat{U}$, *A*, *B* and *P*

Output: $w := x_1 x_2 \ldots x_s$ the shortest route from the vertex *a* to the vertex *b*

1. $w :=$ [ ] – empty word
2. $g_1 := \mathcal{N}^{-1}(a)$
3. $g_2 := \mathcal{N}^{-1}(b)$
4. $g := \text{Factor}(g_1^{-1} g_2, U, \hat{U}, A, B)$
5. $k := \mathcal{N}(g)$
6. $l := k$
7. **Until** $P[1][k] \ne -1$
8. $k := P[1][l]$
9. $w := P[2][l] \oplus w$ – string concatenation
10. $l := k$
11. **Return** *w*

Theorem 2. *Algorithm A–3 is correct,* $T_3 = O(m^2 + D)$ *and* $M_3 = O(m \cdot n + |G|)$.

Proof. Cayley's shortest route from the vertex *a* to the vertex *b* will be a minimal word $w := x_1 x_2 \ldots x_s$ of the element $g := g_1^{-1} g_2$, where $g_1 := \mathcal{N}^{-1}(a)$, $g_2 := \mathcal{N}^{-1}(b)$ and $x_i \in X$ [4]. Suppose k is an element vertex number g. Moving through the parent tree *P* from the vertex k to its root, we will get the desired route.

Items 1–6 are limited in time $O(m^2)$, and cycle 7–10 is $O(D)$. As a result, we get $T_3 = O(m^2 + D)$.

Space complexity of variables U, $\hat{U}$, *A*, and *B* is limited $O(m \cdot n)$, and tables *P* – $O(|G|)$. So, $M_3 = O(m \cdot n + |G|)$.

Comment 2. *In many applied problems in the study of Cayley's graph* $\Gamma := Cay(G, X)$ *the order of the generating group G significantly exceeds its degree, i. e.* $m \le n \ll |G|$. *In this case* $M_3 = O(|G|)$.

Example. Let us consider the group $G = \langle X \rangle$, generated by two cycles $x = (1,5,4)$ and $y = (3,4)$. Let us calculate in GAP a base of G and a transversal:

$$B = (1,3,4),$$

$$U^{(1)} = (e,(1,4)(3,5),(1,5)(3,4),(1,3)(4,5)),$$

$$\Delta^{(1)} = (1,4,5,3),$$

$$U^{(2)} = (e,(3,4,5),(3,5,4)),\ \Delta^{(2)} = (3,4,5),$$

$$U^{(3)} = (e,(4,5)),\ \Delta^{(3)} = (4,5).$$

Using Algorithm 2, we get the Cayley graph $\Gamma = Cay(G, X)$ and its parent tree P (fig.1).

To illustrate Algorithm 3, we find the distance from the vertex $a := 15$ to $b := 22$.

$$g_1 := \mathcal{N}^{-1}(a) = U^{(3)}[1]U^{(2)}[0]U^{(1)}[3],$$

$$g_2 := \mathcal{N}^{-1}(b) = U^{(3)}[1]U^{(2)}[2]U^{(1)}[2],$$

$$g := \text{Factor}(g_1^{-1} g_2) = U^{(3)}[0]U^{(2)}[2]U^{(1)}[0],$$

$$k := \mathcal{N}(g) = 8.$$

Moving along the parent tree P from the vertex with the number to its root, we get

$$8 \xrightarrow{y} 20 \xrightarrow{x} 17 \xrightarrow{x} 14 \xrightarrow{y} 6 \xrightarrow{x} 0.$$

Consequently, $w := xyxxy$. On the graph Γ, the route will have the following form:

$$15 \xrightarrow{x} 19 \xrightarrow{y} 1 \xrightarrow{x} 4 \xrightarrow{x} 10 \xrightarrow{y} 22.$$

3. Problem of a minimal word. A small modification of algorithm A – 3 allows us to calculate the minimal word *w* from an arbitrary string $v := x_1 x_2 \ldots x_r$ in the alphabet of generators *X*.

Algorithm A–4. $w = \text{MinimalWord}(v, U, \hat{U}A, B, P)$

Input: *v*, *U*, $\hat{U}$, *A*, *B* и *P*

Output: $w := x_1 x_2 \ldots x_s$ – the minimal word

1. $w :=$ [ ] – the empty word
2. $g := \text{Factor}(v, U, \hat{U}, A, B)$
3. $k := \mathcal{N}(g)$
4. $l := k$
5. **Until** $P[1][k] \ne -1$
6. $k := P[1][l]$

7. $w := P[2][l] \oplus w$ – string concatenation
8. $l := k$
9. **Return** w

Theorem 3. $T_4 = O(|v|)$ and $M_4 = O(m \cdot n + |G|)$.

Proof. According to Lemmas 3 and 4, the execution time of items 1–4 is limited $O(|v| \cdot m + m^2)$. Paragraphs 5–9 of the algorithm represent an upward movement in the parent tree *P*, therefore, the complexity of this section does not exceed $O(D)$. So we get, $T_4 = O(|v| \cdot m + m^2 + D)$. If the word is long, then $T_4 = O(|v|)$.

Space complexity of variables *U*, $\hat{U}$, *A* and *B* is limited $O(m \cdot n)$, and tables *P* – $O(|G|)$. So, $M_4 = O(m \cdot n + |G|)$.

4. Comparative analysis of algorithms. The following table provides estimates of the time and space complexity of algorithms A – 0 and A – 4.

Algorithm	T_i	M_i
A–0	$O(\|v\|^2)$	$O(\|X\| \cdot \|G\| + \|\mathcal{A}\|)$
A–4	$O(\|v\|)$	$O(m \cdot n + \|G\|)$

The table shows that the algorithm A – 4 has lower computational complexity in comparison with the algorithm A – 0.

As for space complexity, according to comment 2, for many interesting topologies $M_0 \sim M_4 \sim |G|$ will be conducted.

A – 4 was implemented by the authors in C ++; in turn, A – 0 was written in C and is a part of the freely distributed KBMAG package. In order to ensure the purity of the experiment, these algorithms were broadcast by the GCC compiler with the same parameters. At the initial stage, two groups were tested.

a) symmetrical group $S_9 = \langle Y \rangle$, where $Y = \{(i, i+1) \mid i \in [1,8]\}$. Caley graph $Cay(S_9, Y)$ is also called a bubble sort graph. It is well known that $S_n = n!$, $m = n - 1$ and $D_Y(S_n) = \dfrac{n(n-1)}{2}$.

б) Matthew's sporadic simple group $M_{22} = \langle X \rangle$, where $X = \{x_1, x_2, x_2^{-1}\}$ and

$$x_1 = (1,13)(2,8)(3,16)(4,12)(6,22)(7,17)(9,10)(11,14);$$

$$x_2 = (1,22,3,21)(2,18,4,13)(5,12)(6,11,7,15)(8,14,20,10)(17,19).$$

Therein $|M_{22}| = 443520$, $m = 5$ and $D_X(M_{22}) = 34$.

Fig. 2 shows graphs of time dependence $T_4(l)$ execution of algorithm A – 4 for groups $S_9 = \langle Y \rangle$ and $M_{22} = \langle X \rangle$ depending on the length of the incoming word.

Fig. 3 shows graphs of the dependence of time $T_0(l)$ and $T_4(l)$ on the length of the input word for the specified groups.

These graphs clearly show that algorithm A – 4 is much faster than A – 0.

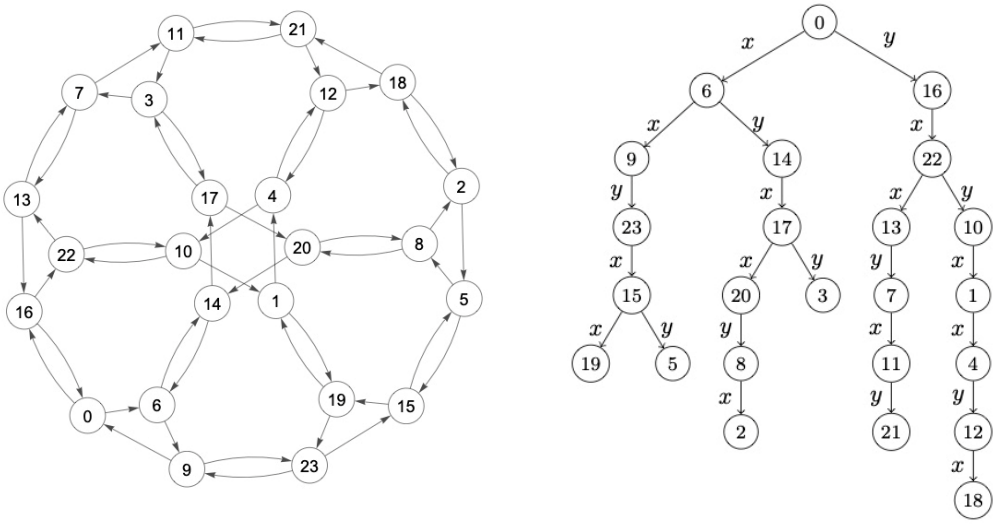

Fig. 1. The Cayley graph Γ = *Cay*(*G*, *X*) and its parent tree.
The edges of the graph Γ with the label *x* are represented as a straight line and *y* as an arc

Рис. 1. Граф Кэли Γ = *Cay*(*G*, *X*) и его родительское дерево *P*.
Ребра графа Γ с меткой *x* представлены в виде прямой линии, а *y* в форме дуги

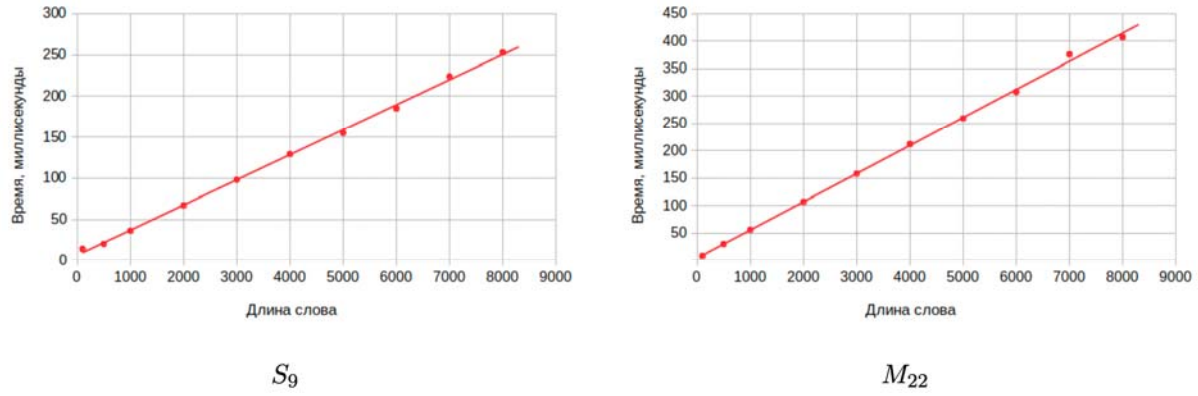

Fig. 2. Graphs of $T_4(l)$ for $S_9 = \langle Y \rangle$ and $M_{22} = \langle X \rangle$

Рис. 2. Графики $T_4(l)$ для групп $S_9 = \langle Y \rangle$ и $M_{22} = \langle X \rangle$

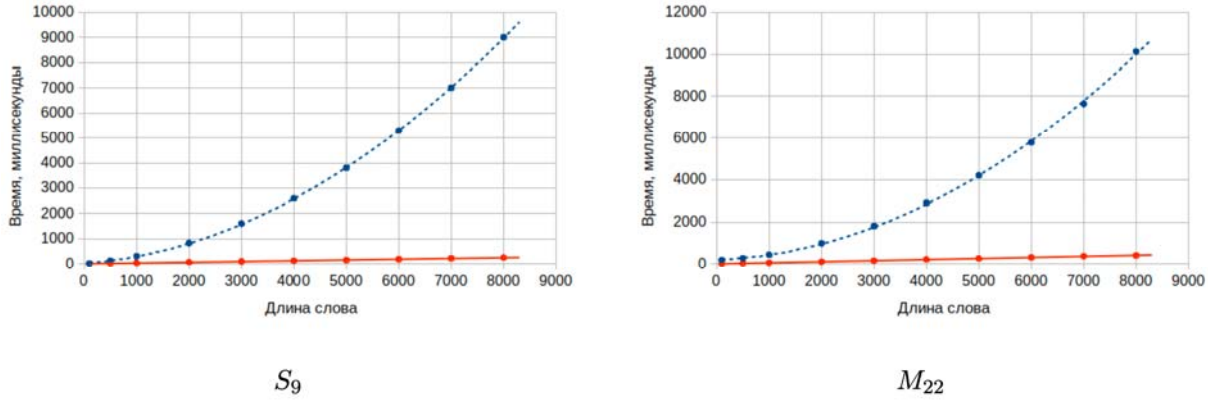

Fig. 3. Graphs of $T_0(l)$ (dotted line) and $T_4(l)$ for groups $S_9 = \langle Y \rangle$ and $M_{22} = \langle X \rangle$

Рис. 3. Графики $T_0(l)$ (пунктир) и $T_4(l)$ для групп $S_9 = \langle Y \rangle$ и $M_{22} = \langle X \rangle$

Conclusion. The algorithms presented in this paper will serve as a starting point for creating new resource-efficient routing algorithms. Two directions can be distinguished. Firstly, it is the creation of algorithms that take into account the network topology. In this case, algorithms will be designed for specific classes of Cayley graphs. Secondly, it is the development of hybrid algorithms that include both static and dynamic routing tables. This will allow to calculate the optimal routes depending on the current state of the network.

References

1. Heydemann M. Cayley graphs and interconnection networks, in Graph symmetry: algebraic methods and applications (Editors: Hahnand Sabidussi). *Dordrecht: Kluwer Academic Publishers*. 1997, P. 167–226.

2. Loz E. New record graphs in the degree-diameter problem. *Australasian Journal of Combinatorics*. 2008, Vol. 41, P. 63–80.

3. Even S., Goldreich O. The Minimum Length Generator Sequence is NP–Hard. *Journal of Algorithms*. 1981, Vol. 2, P. 311–313.

4. Holt D., Eick B., O'Brien E. *Handbook of computational group theory*. Boca Raton: Chapman & Hall/CRC Press, 2005, 514 p.

5. Schibell S., Stafford R. Processor interconnection networks and Cayley graphs. *Discrete Applied Mathematics*. 1992, Vol. 40, P. 337–357.

6. Stamoulis G., Tsitsiklis J. Effcient routing Scheme for Multiple Broadcasts in Hypercubes. *IEEE Trans. on Parallel and Distributed Systems.* 1993, Vol. 4(7), P. 725–739.

7. Stamoulis G., Tsitsiklis J. The Effciency of Greedy Routing in Hypercubes and Butteries. *IEEE Transaction on Communication*. 1994, Vol. 42(11), P. 3051–3061.

8. Kiasari A., Sarbazi-Azad H. Analytic performance comparison of hypercubes and star graphs with implementation constraints. *Journal of Computer and System Sciences*. 2008, No. 6, P. 1000–1012.

9. Akers S., Krishnamurthy B. A group theoretic model for symmetric interconnection networks. *Proceedings of the International Conference on Parallel Processing*. 1986, P. 216–223.

10. Tang K., Arden B. Vertex-transitivity and routing for Cayley graphs in GCR representations. *Proceedings of ACM Symposium on Applied Computing SAC*. 1992, P. 1180–1187.

11. Wang L., Tang K. Topology-Based Routing for Xmesh in Wireless Sensor Networks. *Lecture Notes in Electrical Engineering*. 2009, Vol. 44, P. 229–239.

12. Ryu J., Noel E., and Tang K. Fault-tolerant Routing on Borel Cayley Graph. *IEEE ICC Next Generation Networking Symposium*. 2012, P. 2872–2877.

13. Shin J., Sirer E., Weatherspoon H., Kirovski D. On the feasibility of completely wireless datacenters. *EEE/ACM Transaction On Networking*. 2013, Vol. 21(5), P. 1666–1679.

14. Epstein D., Paterson M., Cannon J., Holt D., Levy S. and Thurston W. *Word Processing in Groups*. Boston: Jones and Barlett Publishers, 1992, 330 p.

15. Camelo M., Papadimitriou D., Fabrega L., Vila P. Efficient Routing in Data Center with Underlying Cayley Graph. *Proceedings of the 5th Workshop on Complex Networks CompleNet*. 2014, P. 189–197.

16. Knuth D. *The Art of Computer Programming, Volume 4A: Combinatorial Algorithms, Part 1*. Boston: Addison-Wesley Professional, 2011, 912 p.

17. Sims C. Computational methods in the study of permutation groups, *Computational problems in abstract algebra (Pergamon Press, Oxford)*. 1970, P.169–183.

18. Seress A. *Permutation Group Algorithms*. Cambridge: Cambridge University Press, 2003, 274 p.

19. Skiena S. *The Algorithm Design Manual*. London: Springer Science+Business Media, 2008, 730 p.

Kuznetsov Alexander Alexeevich – D. Sc., Professor, Head of Institute of Space Research and High Technologies; Reshetnev Siberian State University of Science and Technology. E-mail: alex_kuznetsov80@mail.ru.

Kishkan Vladimir Vladimirovich – Postgraduate student; Reshetnev Siberian State University of Science and Technology. E-mail: kishkan@mail.ru.

Кузнецов Александр Алексеевич – доктор физико-математических наук, профессор, директор НОЦ «Институт космических исследований и высоких технологий»; Сибирский государственный университет науки и технологий имени академика М. Ф. Решетнева. E-mail: alex_kuznetsov80@mail.ru.

Кишкан Владимир Владимирович – аспирант; Сибирский государственный университет науки и технологий имени академика М. Ф. Решетнева. E-mail: kishkan@mail.ru.

UDC 519.87
Doi: 10.31772/2587-6066-2020-21-2-195-200

For citation: Mikhov E. D. Piecewise approximation based on nonparametric modeling algorithms. *Siberian Journal of Science and Technology*. 2020, Vol. 21, No. 2, P. 195–200. Doi: 10.31772/2587-6066-2020-21-2-195-200

Для цитирования: Михов Е. Д. Кусочная аппроксимация, основанная на непараметрических алгоритмах моделирования // Сибирский журнал науки и технологий. 2020. Т. 21, № 2. С. 195–200. Doi: 10.31772/2587-6066-2020-21-2-195-200

PIECEWISE APPROXIMATION BASED ON NONPARAMETRIC MODELING ALGORITHMS

E. D. Mikhov

Siberian Federal University
79, Svobodnii Av., 660041, Krasnoyarsk, Russian Federation
E-mail: edmihov@mail.ru

In this research the issue of inertialess processes modeling is under study. The main modeling algorithm is the nonparametric recovery algorithm of the regression function. The algorithm allows to build a process model under conditions of low a priori information. This feature may be particularly important in modeling processes of large dimensions prevailing in the space industry. One important feature of the algorithm for nonparametric estimation of the regression function is that the accuracy of modeling using this algorithm highly depends on the quality of the observations sample. Due to the fact that in processes with large dimensions of input and output variable vectors observation sampling elements are in most cases unevenly distributed, the development of modifications to improve the quality of modeling is relevant.

The modification of the nonparametric dual algorithm based on piecewise approximations has been developed. According to the proposed modification, the process area is divided into sub-areas and a non-parametric estimate of the regression function for each of these sub-areas is recovered. The proposed modification reduces the impact of some observation sampling features, such as sparseness or voids in observation samples on the quality of the built model.

The computational experiments were carried out, during which a comparison was made between the classical algorithm of non-parametric estimation of regression function and the developed modification. As the computational experiments have shown, with uniform distribution of the sample elements of observations, the developed modification does not lead to the improvement of the quality of modeling. With a substantial uneven distribution of the observations sample elements, the developed modification resulted in a 2-fold improvement in the quality of the simulation. The results suggest that the proposed modification can be used to model complex technological processes, including those in the space industry.

Keywords: identification, nonparametric estimation of the regression function, piecewise approximation.

КУСОЧНАЯ АППРОКСИМАЦИЯ, ОСНОВАННАЯ НА НЕПАРАМЕТРИЧЕСКИХ АЛГОРИТМАХ МОДЕЛИРОВАНИЯ

Е. Д. Михов

Сибирский федеральный университет
Российская Федерация, 660041, г. Красноярск, просп. Свободный, 79
E-mail: edmihov@mail.ru

Рассматривается вопрос моделирования безынерционных процессов. В качестве основного алгоритма моделирования используется алгоритм непараметрического восстановления функции регрессии. Рассматриваемый алгоритм позволяет построить модель технологического процесса в условиях малой априорной информации. Это может быть важно при моделировании процессов больших размерностей, превалирующих в космической отрасли. Одной из важных особенностей алгоритма непараметрической оценки функции регрессии является то, что точность моделирования с использованием этого алгоритма сильно зависит от качества выборки наблюдений. В связи с тем, что в процессах с большой размерностью векторов входных и выходных переменных элементы выборки наблюдений в большинстве случаев распределены неравномерно, разработка модификаций, позволяющих улучшить качество моделирования, является актуальной.

Разработана модификация алгоритма непараметрического дуального на основании кусочно-заданных аппроксимаций. Согласно предложенной модификации, область существования процесса разделяется на подобласти и производится восстановление непараметрической оценки функции регрессии для каждой из этих подобластей. Предложенная модификация позволяет уменьшить влияние некоторых особенностей выборки наблюдения, таких как разрежённости или пустоты в выборках наблюдений, на качество построенной модели.

В ходе вычислительных экспериментов проводилось сравнение между классическим алгоритмом непараметрической оценки функции регрессии и разработанной модификацией. Как показали вычислительные эксперименты, при равномерном распределении элементов выборки наблюдений разработанная модификация не приводит к улучшению качества моделирования. При существенной неравномерности распределения элементов выборки наблюдений, разработанная модификация приводила к улучшению качества моделирования в два раза. Полученные результаты позволяют утверждать, что предложенная модификация может быть использована для моделирования сложных технологических процессов, в том числе и для процессов, имеющих место в космической отрасли.

Ключевые слова: идентификация, непараметрическая оценка функции регрессии, кусочная аппроксимация.

Introduction. The article studies the problem of inertialess technological processes identification.

The scheme of the simulated process is shown in the fig. 1 [1].

The following notations are used in fig. 1: $\vec{u}(t)$ – input variables vector; $\vec{x}(t)$ – output variables vector; $\vec{\xi}(t)$ – interference effect; O – process.

The main modeling algorithm is the nonparametric regression function recovery algorithm [2–5], and piecewise-defined approximations [6–8].

When getting a sample of observations, not only the sample of observations size is important, but also its quality. The quality of a sample of observations is the accuracy of parameters readout, the presence of outliers in it, the uniformity of the distribution of the sample of observations, etc.

Special attention is paid to the problem of modeling the process with an uneven distribution of the sample of observations [9–11].

In some tasks, a sample of observations can be distributed over an area where the process $\Omega(\vec{u},x)$ occurs with sparseness, voids, or concentration of the sample of observations elements. As an example, fig. 2 shows an unevenly distributed sample of observations.

In fig. 2, the area *1* contains the so-called sparseness in the observation samples, number *2* denotes voids in space $\Omega(\vec{u},x)$, and number *3* denotes the elements of the observation sample.

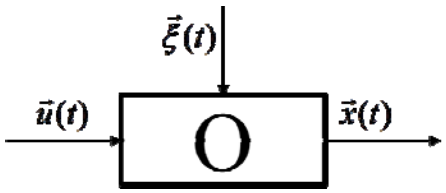

Fig. 1. The simulated process

Рис. 1. Моделируемый процесс

For nonparametric estimation of the regression function, the quality of the sample of observations is of particular importance. With an uneven distribution of the observations sample there arises the difficulty in setting up the blur parameters c_s vector, as some areas are sparse and it is assumed that in such cases c_s should be large, and in some areas there is concentration and it is assumed that for these cases c_s should get a small value. Undoubtedly, all this also affects the quality of the resulting model.

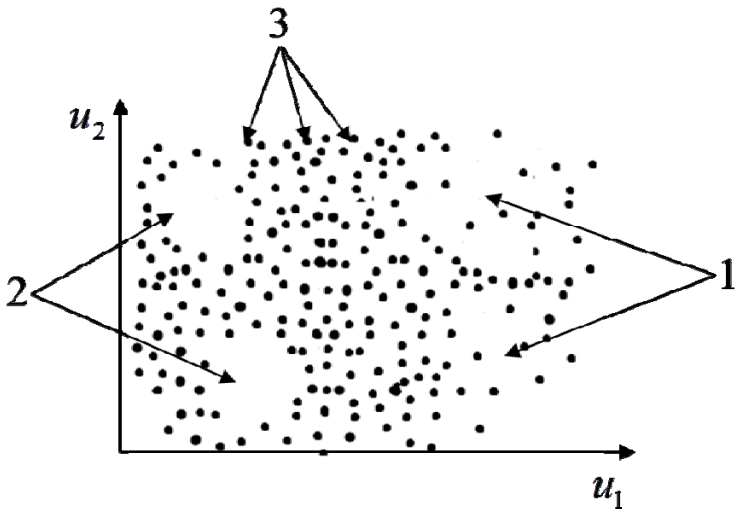

Fig. 2. Uneven sample of observations

Рис. 2. Неравномерно распределенная выборка наблюдений

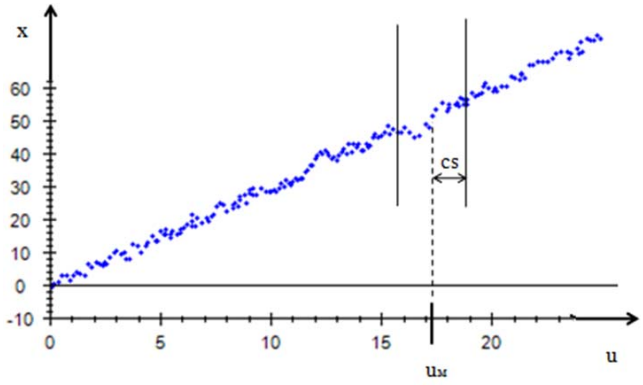

Fig. 3. Determination of blur parameter

Рис. 3. Определение параметра размытости

The process of building a mathematical model of the technological process shown in fig. 1 can be divided into several consecutive stages:

1) getting a priori information about the process;

2) getting a sample of observations;

3) choosing a metod of building a mathematical model;

4) building a mathematical model.

The article focuses on the stage of choosing a method for constructing a mathematical model.

Nonparametric recovery of the regression function. "Parametric approach" implies that the structure of the process or object under study is known, but the parameters of this structure are not known.

The type of algorithm used depends on the level of a priori information. If a priori information is sufficient to select the object structure, then parametric algorithms can be used.

Nonparametric identification is generally implemented using a nonparametric estimation of the regression function.

$$x_s(\vec{u}_s) = \frac{\sum_{i=1}^{s} x_i \prod_{j=1}^{n} \Phi\left(\frac{u_{s,j} - u_{j,i}}{c_s}\right)}{\sum_{i=1}^{s} \prod_{j=1}^{n} \Phi\left(\frac{u_{s,j} - u_{j,i}}{c_s}\right)}. \quad (1)$$

In (1) the following notations are used: Φ(*) – is a bell-shaped smoothing function; c_s – is the blur parameter.

The quality of the built model directly depends on the chosen blur parameter c_j^x. This coefficient determines the degree of participation of the sample elements in the calculation of x_s at the $u_м$ point.

As shown in fig. 3, only those variables that have $|u - u_м| < c_s$ participate in building the model at the $u_м$ point, and the closer $|u - u_м|$ is to zero, the more influence this point has on the results of calculations.

In nonparametric estimation of the regression function, the quality of the sample of observations is of particular importance. Of course, for any model, the quality of the sample of observations also affects the accuracy of the constructed model, but in the case of nonparametric estimation of the regression function, this is of particular importance.

Piecewise-defined approximation One of the options for building a mathematical model of the process the ideas of which will be further used is a piecewise-defined approximation.

The idea of a piecewise-defined approximation is to divide the Omega area into some sub-areas $\Omega_i(\vec{u}), i = \overline{1,m}$ (fig. 4), and to build for each area $\Omega_i(\vec{u})$ its own mathematical model of the process.

One of the most well-known piecewise-defined approximations are spline functions. The advantage of this approach is that unevenness of the sample of observations does not have a big impact on the quality of the model. The weak side of spline functions is that it is quite difficult to select a function and set parameters for each area $\Omega_i(\vec{u})$ for the tasks of large dimensions.

The developed modification of the nonparametric estimation of the regression function. The complexity of nonparametric estimation of the regression function, in contrast to spline functions, increases much more slowly. In this regard, it seems logical to combine the idea of a piecewise-defined approximation and a nonparametric estimation of the regression function.

The following modification of the nonparametric estimation of the regression function has been developed:

The stage of building the model:

1) omega area is divided into sub-areas $\Omega_i(\vec{u})$;

2) for each area $\Omega_i(\vec{u})$, the regression function is recovered using a nonparametric estimation of the regression function;

3) the blur vector is being set for each area $\Omega_i(\vec{u})$ [12].

The stage of making a forecast at point $\vec{u}$:

1) the area $\Omega_i(\vec{u})$ to which the point $\vec{u}$ belongs is defined;

2) the regression function is recovered using the set vector of blur parameters for the area $\Omega_i(\vec{u})$.

Sub-areas $\Omega_i(\vec{u})$ can be split by various methods. It is possible to apply the algorithms for splitting samples into

classes, or choose the classic way for splines and split the entire area of input variables definition into equal parts and set the vector of blur parameters for each of them.

Computational experiments. The numerical experiments were performed comparing the classical nonparametric estimation of the regression function with the proposed modification. Numerical experiments were performed for several cases that differ in the uneven distribution of the components of the observation samples.

First of all, an experiment was conducted to model an object described by the following equation:

$$f(\vec{u}) = f(u_1, u_2, u_3, u_4, u_5, u_6) = \\ = 6\sin(u_1) + 2u_2 + u_3 / 6 + 4\cos(u_4) + u_5 - 8u_6. \quad (2)$$

It should be noted that the algorithm for the regression function recovery does not identify the type of equation. The equation is only used for generating a sample of observations.

The following initial data were taken for the experiment: the size of the sample of observations s = 4000; the amount of interference affecting the object $\xi = 4\,\%$; $\vec{u} \in (0;3)$; the elements of the sample of observations are distributed evenly.

The model will be constructed using an algorithm for nonparametric estimation of the regression function and using the proposed modification of the algorithm.

The simulation results are shown in tab. 1

According to the results of the experiment, the average forecast error in the modified algorithm slightly decreased, as well as the time for setting the blur parameters and the speed of making the forecast increased.

This experiment showed that if the sample of observations is uniformly distributed, it is not necessary to divide the elements of the sample of observations into classes. Here we would like to note that the considered case is quite rare in practice. The sample almost always has concentration or sparseness.

In the next numerical experiment, the sample of observations will have sparseness and concentration of the elements of the sample of observations.

The results of object modeling under these conditions are summarized in tab. 2.

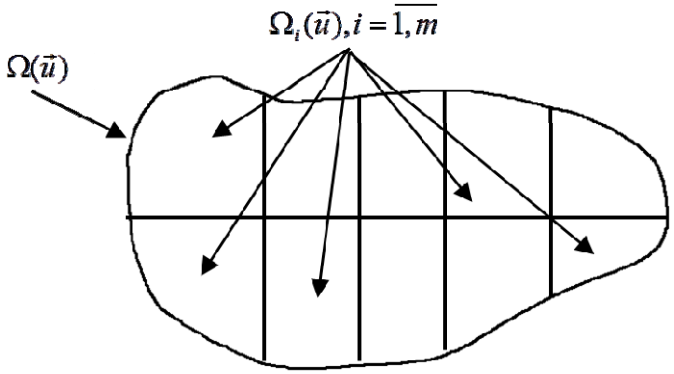

Fig. 4. Split of $\Omega_i(\vec{u})$ into sub-areas $\Omega_i(\vec{u})$

Рис. 4. Разбиение $\Omega_i(\vec{u})$ на подобласти $\Omega_i(\vec{u})$

Table 1

The results of the regression function recovery

	Nonparametric algorithm for the regression function recovery	Modified nonparametric algorithm for the regression function recovery
Average forecast error, %	3	4
Blur paramerers setting time, ms	30	70
Forecasting speed, ms	45	69

Table 2

The results of the regression function recovery

	Nonparametric algorithm for the regression function recovery	Modified nonparametric algorithm for the regression function recovery
Average forecast error, %	14	7
Blur paramerers setting time, ms	35	70
Forecasting speed, ms	52	84

Table 3

The results of the regression function recovery

	Nonparametric algorithm for the regression function recovery	Modified nonparametric algorithm for the regression function recovery
Average forecast error, %	23	8
Blur paramerers setting time, ms	36	69
Forecasting speed, ms	49	78

According to the experiment, the difference between the average simulation error of the classical algorithm for nonparametric estimation of the regression function and the proposed modification is higher than in the experiment shown in tab. 1. Based on this, we can conclude that when heterogeneity appears in the sample of observations, the proposed modification allows us to estimate the regression function more accurately.

To confirm this assumption, another experiment was conducted, which introduced an even greater heterogeneity in the observation sample than in the experiment shown in tab. 2.

The results of this experiment are summarized in tab. 3.

As can be concluded from tab. 3, when the uneven distribution of the sample of observations elements increases, the accuracy of the proposed modification becomes higher than the accuracy of the classical algorithm.

It is important to note that unevenness in the sample of observations is ubiquitous when modeling objects with large input-output dimensions.

Conclusion. The modification of the algorithm for nonparametric recovery of the regression function has been developed. The modification consists in using the idea of piecewise-defined approximations and splitting the modeling area into sub-areas, for each of them the regression function is separately recovered .

During the computational experiments, it was demonstrated that the proposed modification significantly improves the quality of modeling the process when the elements of the sample of observations are distributed unevenly, there are sparseness and voids in the sample of observations. It is important to note that there are other methods for dealing with an unevenly distributed sample of observations [13–15].

Acknowledgment. This work was financially supported by the Ministry of Science and Higher Education of the Russian Federation in the implementation of the integrated project “Creation of a production of earth stations of advanced satellite communications systems to ensure the coherence of hard, northern and Arctic territory of Russian Federation”, implemented with the participation of the Siberian Federal University (agreement number 075-11-2019-078 dated 13.12.2019).

Благодарности. Работа выполнена при финансовой поддержке Министерства науки и высшего образования Российской Федерации в ходе реализации комплексного проекта «Создание высокотехнологичного производства земных станций перспективных систем спутниковой связи для обеспечения связанности труднодоступных, северных и Арктических территорий Российской Федерации», осуществляемого при участии Сибирского федерального университета (соглашение № 075-11-2019-078 от 13.12.2019).

References

1. Medvedev A. V., Mihov E. D., Ivanov N. D. Identification of multidimensional technological processes with dependent input variables. *Journal of the Siberian Federal University. Series: Mathematics and Physics.* 2018, Vol. 11, No. 5, P. 649–658.

2. Kornet M. E., Shishkina A. V. About the identification of dynamic systems under nonparametric uncertainty. *Aspire to Science*. 2018, P. 166–170.

3. Lapko A. V., Lapko V. A. Multilevel nonparametric information processing systems. Krasnoyarsk : SibGAU, 2013. 270 p. (In Russ.)

4. Medvedev A. V. Some remarks on the theory of non-parametric systems. *Applied Methods of Statistical Analysis*. 2017, P. 72–81.

5. Medvedev A. V., Raskina A. V., Chzhan E. A., Korneeva A. A., Videnin C. A. Determination of the order of stochastically linear dynamic systems by using nonparametric estimation of a regression function. *Journal of Physics: Conference Series. Krasnoyarsk Science and Technology City Hall of the Russian Union of Scientific and Engineering Associations; Polytechnical Institute of Siberian Federal University. Bristol, United Kingdom*. 2019, P. 1–8.

6. Reisinger C., Forsyth P. A. Piecewise constant policy approximations to Hamilton–Jacobi–Bellman equations. *Applied Numerical Mathematics.* 2016, Vol. 103, P. 27–47.

7. Gaudioso M., Giallombardo G., Miglionico G., Bagirov A. M. Minimizing nonsmooth DC functions via successive DC piecewise-affine approximations. *Journal of Global Optimization.* 2018, Vol. 71, P 37–55.

8. Liu J., Bynum M., Castillo A., Watsonb J., Lairda C. D. A multitree approach for global solution of ACOPF problems using piecewise outer approximations. *Computers & Chemical Engineering.* 2018, Vol. 114, P. 145–157.

9. Medvedev A. V., Meleh D. A., Sergeeva N. A., Chubarova O. V. [On the problem of classifying objects by data with gaps]. *Information Technology and Mathematical Modeling (ITMM-2019).* P. 146–151 (In Russ.).

10. Chzhan E. A., Medvedev A. V., Kukartsev V. V. Nonparametric modelling of multidimensional technological processes with dependent variables. *IOP Conference Series: Earth and Environmental Science*. 2018, P. 1–5.

11. Paul S., Shankar S. On estimating efficiency effects in a stochastic frontier model. *European Journal*

of Operational Research. 2018, Vol. 271, Iss. 2, P. 769–774.

12. Mikhov E. D. [Core blur coefficient optimization in nonparametric modeling]. *Vestnik SibGAU*. 2015, Vol. 16, No. 2, P. 338–342 (In Russ.).

13. Medvedev A. V., Chzhan E. A. [Modeling of multidimensional H-processes]. *Information and mathematical technologies in science and management*. 2018, No. 1 (9), P. 99–105 (In Russ.).

14. Simar L., Keilegom I., Zelenyuk V. Nonparametric least squares methods for stochastic frontier models. *Journal of Productivity Analysis.* 2017, Vol. 47, P. 189–204.

15. Zhang C., Travis D. Gaps-fill of SLC-off Landsat ETM+ satellite image using a geostatistical approach. *International Journal of Remote Sensing.* 2007, Vol. 28, Iss. 22, P. 5103–5122.

Библиографические ссылки

1. Medvedev A. V., Mihov E. D., Ivanov N. D. Identification of multidimensional technological processes with dependent input variables // Journal of the Siberian Federal University. Series: Mathematics and Physics. 2018. Vol. 11, No. 5. P. 649–658.

2. Kornet M. E., Shishkina A. V. About the identification of dynamic systems under nonparametric uncertainty // Aspire to Science. 2018. P. 166–170.

3. Лапко А. В., Лапко В. А. Многоуровневые непараметрические системы обработки информации : монография / Сиб. гос. аэрокомич. ун-т. Красноярск, 2013. 270 с.

4. Medvedev A. V. Some remarks on the theory of non-parametric systems // Applied Methods of Statistical Analysis. 2017. P. 72–81.

5. Determination of the order of stochastically linear dynamic systems by using non-parametric estimation of a regression function / A. V. Medvedev, A. V. Raskina, E. A. Chzhan et al. // Journal of Physics: Conference Series. Krasnoyarsk Science and Technology City Hall of the Russian Union of Scientific and Engineering Associations; Polytechnical Institute of Siberian Federal University. Bristol, United Kingdom. 2019. P. 1–8.

6. Reisinger C., Forsyth P. A. Piecewise constant policy approximations to Hamilton–Jacobi–Bellman equations // Applied Numerical Mathematics. 2016. Vol. 103. P. 27–47.

7. Gaudioso M., Giallombardo G., Miglionico G., Bagirov A. M. Minimizing nonsmooth DC functions via successive DC piecewise-affine approximations // Journal of Global Optimization 2018. Vol. 71. P. 37–55.

8. A multitree approach for global solution of ACOPF problems using piecewise outer approximations / J. Liu, M. Bynum, A. Castillo et al. // Computers & Chemical Engineering. 2018. Vol. 114. P. 145–157.

9. О задаче классификации объектов по данным с пропусками / А. В. Медведев, Д. А. Мелех, Н. А. Сергеева, О. В. Чубарова // Информационные технологии и математическое моделирование (ИТММ-2019) : материалы XVIII Междунар. конф. им. А. Ф. Терпугова. 2019. С. 146–151.

10. Chzhan E. A., Medvedev A. V., Kukartsev V. V. Nonparametric modelling of multidimensional technological processes with dependent variables // IOP Conference Series: Earth and Environmental Science. 2018. P. 1–5.

11. Paul S., Shankar S. On estimating efficiency effects in a stochastic frontier model // European Journal of Operational Research. 2018. Vol. 271, Iss. 2. P. 769–774.

12. Михов Е. Д. Оптимизация коэффициента размытости ядра в непараметрическом моделировании // Вестник СибГАУ. 2015. Т. 16, № 2. С. 338–342.

13. Медведев А. В., Чжан Е. А. Моделирование многомерных Н-процессов // Информационные и математические технологии в науке и управлении. 2018. № 1 (9). С. 99–105.

14. Simar L., Keilegom I., Zelenyuk V. Nonparametric least squares methods for stochastic frontier models. Journal of Productivity Analysis. 2017. Vol. 47. P. 189–204.

15. Zhang C., Travis D. Gaps-fill of SLC-off Landsat ETM+ satellite image using a geostatistical approach // International Journal of Remote Sensing. 2007. Vol. 28, Iss. 22. P. 5103–5122.

Mikhov Evgeniy Dmitrievich – Cand. Sc., Associate Professor, Department of electronic warfare; Siberian Federal University. E-mail: edmihov@mail.ru.

Михов Евгений Дмитриевич – кандидат технических наук, доцент кафедры радиоэлектронной борьбы; Сибирский федеральный университет. E-mail: edmihov@mail.ru.

UDC 539.374
Doi: 10.31772/2587-6066-2020-21-2-201-205

For citation: Senashov S. I., Savostyanova I. L., Cherepanova O. N. Elastic-plastic problem in the case of inhomogeneous plasticity under complex shear conditions. *Siberian Journal of Science and Technology.* 2020, Vol. 21, No. 2, P. 201–205. Doi: 10.31772/2587-6066-2020-21-2-201-205

Для цитирования: Сенашов С. И., Савостьянова И. Л., Черепанова О. Н. Упругопластическая задача в случае неоднородной пластичности в условиях сложного сдвига // Сибирский журнал науки и технологий. 2020. Т. 21, № 2. С. 201–205. Doi: 10.31772/2587-6066-2020-21-2-201-205

ELASTIC-PLASTIC PROBLEM IN THE CASE OF INHOMOGENEOUS PLASTICITY UNDER COMPLEX SHEAR CONDITIONS

S. I. Senashov[1*], I. L. Savostyanova[1], O. N. Cherepanova[2]

[1] Reshetnev Siberian State University of Science and Technology
31, Krasnoyarskii rabochii prospekt, Krasnoyarsk, 660037, Russian Federation
[2] Siberian Federal University
79, Svobodniy Av., Krasnoyarsk, 660041, Russian Federation
*E-mail: sen@sibsau.ru

In this research, the authors solved a two-dimensional elastic-plastic problem of the stress state under complex shear conditions in the body weakened by a hole that is bounded by a piecewise smooth contour. The stress state of a complex shear occurs in a cylindrical body of infinite length under the action of loads directed along the cylinder generators and constant along the generators. At the same time, with a sufficiently large load, both elastic and plastic zones appear in the body. As in any problem of this kind, it is necessary to find a previously unknown boundary separating the elastic and plastic zones. Finding such a boundary is not an easy task, but the specificity of elastic-plastic problems of complex shear is that solving such problems is easier than solving similar elastic problems. Apparently, for the first time this fact was noted by G. P. Cherepanov.

A lot of research is devoted to elastic-plastic problems of complex shear in the case of homogeneous and isotropic plasticity. All articles that solve complex shear problems essentially use the representation of stresses and displacements in the elastic zone in a complex form. In this research, the problems of complex shear are solved using conservation laws. It is assumed that the yield strength is a function of the coordinates of the point where the stress state is being studied. It is known that the elastic properties of structural materials can be homogeneous and isotropic, while their yield point and strength are inhomogeneous. This situation is observed, for example, in the case of neutron bombardment of structural materials. This research will examine exactly this situation. The article presents conservation laws for equations describing a complex shear. It was assumed that the components of the conserved current depend on the components of the stress tensor and coordinates. The components of the stress tensor are included in them linearly. The problem of finding the components of the conserved current was reduced to the Cauchy-Riemann system. The solution of this system allowed us to reduce the calculations of the stress tensor components to a curvilinear integral along the contour of the hole and thus find the boundary between the elastic and plastic areas.

Keyword: elastic-plastic problem, inhomogeneous plasticity, complex shear, conservation laws.

УПРУГОПЛАСТИЧЕСКАЯ ЗАДАЧА В СЛУЧАЕ НЕОДНОРОДНОЙ ПЛАСТИЧНОСТИ В УСЛОВИЯХ СЛОЖНОГО СДВИГА

С. И. Сенашов[1*], И. Л. Савостьянова[1], О. Н. Черепанова[2]

[1] Сибирский государственный университет науки и технологий имени академика М. Ф. Решетнева
Российская Федерация, 660037, г. Красноярск, просп. им. газ. «Красноярский рабочий», 31
[2] Сибирский федеральный университет
Российская Федерация, 660041, г. Красноярск, просп. Свободный, 79
*E-mail: sen@sibsau.ru

В работе решена плоская упругопластическая задача о напряженном состоянии в условиях сложного сдвига в теле, ослабленном отверстием, которое ограничено кусочно гладким контуром. Напряженное состояние сложного сдвига возникает в цилиндрическом теле бесконечной длины под действием нагрузок, направленных по образующим цилиндра и постоянным вдоль образующих. При этом при достаточно большой нагрузке в теле возникают как упругие, так и пластические зоны. Как и в любой задаче подобного рода, возникает необходимость в нахождении заранее неизвестной границы, разделяющей упругую и пластическую зоны. Отыскание такой границы непростая задача, но специфика упругопластических задач о сложном сдвиге состоит в том,

что решение подобных задач проще, чем решение аналогичных упругих задач. По-видимому, впервые этот факт отметил Г. П. Черепанов.

Упругопластическим задачам о сложном сдвиге в случае однородной и изотропной пластичности посвящена обширная литература. Во всех статьях, в которых решаются задачи о сложном сдвиге, существенно используют представление напряжений и смещений в упругой зоне в комплексном виде. В предлагаемой работе решены задачи о сложном сдвиге с помощью законов сохранения. При этом предполагается, что предел текучести является функцией от координат точки, в которой исследуется напряженное состояние. Известно, что упругие свойства конструкционных материалов могут быть однородными и изотропными, а при этом их предел текучести и прочности – неоднородным. Такая ситуация наблюдается, например, при нейтронной бомбардировке конструкционных материалов. В данной статье будет изучена именно такая ситуация. В статье приведены законы сохранения для уравнений, описывающих сложный сдвиг. При этом предполагалось, что компоненты сохраняющегося тока зависят от компонент тензора напряжений и координат. Компоненты тензора напряжений входят в них линейно. Задача о нахождении компонент сохраняющегося тока свелась к системе Коши–Римана. Решение этой системы позволило свести вычисления компонент тензора напряжений к криволинейному интегралу по контуру отверстия и тем самым найти границу между упругой и пластической областями.

Ключевые слова: упругопластическая задача, неоднородная пластичность, сложный сдвиг, законы сохранения.

Introduction. The stress state of a complex shear occurs in a cylindrical body of infinite length under the action of loads directed along the generators of the cylinder and constant along the generators [1]. At the same time, with a sufficiently large load, both elastic and plastic zones appear in the body. As in any problem of this kind, it is necessary to find a previously unknown boundary separating the elastic and plastic zones. Finding such a boundary is not an easy task, but the specificity of elastic-plastic problems about complex shear is that the solution of such problems is easier than the solution of similar elastic problems. Apparently, this fact was first noted by G. P. Cherepanov [1].

A lot of research is devoted to the elastic-plastic problems of complex shear in the case of homogeneous and isotropic plasticity, and its review can be seen, for example, in [1]. In all articles that solve complex shear problems, the representation of stresses and displacements in the elastic zone in a complex form is significantly used. In this research, we solve the problem of complex shear using conservation laws. For the first time, plasticity problems were solved using conservation laws in [2–6]. In articles [3; 7–12], the method of conservation laws was successfully applied to finding elastic-plastic rods and beams. In this article, this technique is used for the first time to solve elastic-plastic problems. And it is assumed that in the plastic area, the yield strength is a function of the coordinates of the point at which the stress state is studied. It is known that the elastic properties of structural materials can be homogeneous and isotropic, and their yield strength and strength – inhomogeneous. This situation is observed, for example, in the case of neutron bombardment of structural materials [13]. This article will study exactly this situation.

1. Basic ratios. The shear and stress fields in this case are as follows [1]

$$u = v = 0,\ \ w = w(x, y),$$
$$\sigma_x = \sigma_y = \sigma_z = \tau_{xy} = 0, \qquad (1)$$
$$\tau_{xz} = \tau^1(x, y), \tau_{yz} = \tau^2(x, y).$$

Here u, v, w – shear vector components, $\sigma_x, \sigma_y, \sigma_z, \tau_{xy}, \tau_{xz}, \tau_{yz}$ – stress tensor components, x, y, z – cartesian coordinates, the z axis is directed parallel to the generator

$$\frac{\partial \tau^1}{\partial x} + \frac{\partial \tau^2}{\partial y} = 0, \text{ (equilibrium equation);} \qquad (2)$$

$$\tau^1 = G\frac{\partial w}{\partial x},\ \ \tau^2 = G\frac{\partial w}{\partial y}, \text{ (Hooke's law).} \qquad (3)$$

Here G – a constant called the shear modulus.

From (2), (3) follow the ratios in the elastic zone

$$\frac{\partial^2 w}{\partial x^2} - \frac{\partial^2 w}{\partial y^2} = 0; \qquad (4)$$

$$\frac{\partial \tau^1}{\partial y} = \frac{\partial \tau^2}{\partial x}. \qquad (5)$$

From (2) and (5) it follows that τ^1, τ^2 satisfy the Cauchy-Riemann equations

$$F_1 = \frac{\partial \tau^1}{\partial x} + \frac{\partial \tau^2}{\partial y} = 0,\ \ F_2 = \frac{\partial \tau^1}{\partial y} - \frac{\partial \tau^2}{\partial y} = 0. \qquad (6)$$

In the plastic area, there is a ratio (2), and also

$$(\tau^1)^2 + (\tau^2)^2 = k^2 \text{ (the yield condition);} \qquad (7)$$

$$\tau^2 \frac{\partial w}{\partial x} = \tau^1 \frac{\partial w}{\partial y} \text{ (Genki equation).} \qquad (8)$$

Here $k(x, y)$ – some smooth function equal to the yield strength at pure shear [13].

At the boundary of elastic and plastic areas, stresses and shears are assumed to be continuous.

2. Conservation laws. The conservation law for the system of equations (6) is the following ratio

$$\frac{\partial A\left(x, y, \tau^1, \tau^2\right)}{\partial x} + \frac{\partial B\left(x, y, \tau^1, \tau^2\right)}{\partial y} = \omega^1 F_1 + \omega^2 F_2, \qquad (9)$$

where $\omega^i = \omega^i(x, y, \tau^1, \tau^2)$ – some functions that are simultaneously not not equal to zero.

Comment. A more general definition of conservation laws and their use in the mechanics of a deformable solid can be found, for example, in [4; 6; 14]. In [15], you can

read about the application of the group analysis technique for constructing solutions for the equations of inhomogeneous elasticity theory.

For the purposes set out in the article, a simplified formulation in the form of (9) is quite appropriate.

In the case of (9), the values A and B are called the components of the conserved current.

Let us assume that components A And B have the following form

$$A = \alpha^1\tau^1 + \beta^1\tau^2 + \gamma^1, B = \alpha^2\tau^1 + \beta^2\tau^2 + \gamma^2, \qquad (10)$$

where $\alpha^i = \alpha^i(x,y), \beta^i = \beta^i(x,y), \gamma^i = \gamma^i(x,y)$ – some smooth functions to be defined. Substituting (10) in (9), as a result we get

$$\alpha^1_x\tau^1 + \alpha^1\tau^1_x + \beta^1_x\tau^2 + \beta^1\tau^2_x + \gamma^1_x + \alpha^2_y\tau^1 + \alpha^2\tau^1_y + \beta^2_y\tau^2 + \\ + \beta^2\tau^2_y + \gamma^2_y = \omega^1\left(\tau^1_x + \tau^2_y\right) + \omega^2\left(\tau^1_y - \tau^2_x\right) = 0, \qquad (11)$$

where the index at the bottom means the derivative of the corresponding variable.

From (11) we get

$$\alpha^1 = \omega^1, \beta^1 = -\omega^2,\ \alpha^2 = \omega^2,\ \beta^2 = \omega^1, \\ \alpha^1_x + \alpha^2_y = 0, \beta^1_x + \beta^2_y = 0,\ \gamma^1_x + \gamma^2_y = 0. \qquad (12)$$

From (12), excluding ω^i we get

$$\alpha^1_x - \beta^1_y = 0, \beta^1_x + \alpha^1_y = 0, \gamma^1_x + \gamma^2_y = 0. \qquad (13)$$

Due to the ratios (12), the components of the conserved current have the form

$$A = \alpha^1\tau^1 + \beta^1\tau^2 + \gamma^1,\ B = -\beta^1\tau^1 + \alpha^1\tau^2 + \gamma^2. \qquad (14)$$

Since the right part (9) is zero, by Green formula we obtain

$$\iint_S \left(A_x + B_y\right)dxdy = \int_{\partial S} Ady - Bdx = \\ = \int_{\partial S} (\alpha^1\tau^1 + \beta^1\tau^2 + \gamma^1)dy - \left(-\beta^1\tau^1 + \alpha^1\tau^2 + \gamma^2\right)dx = 0. \qquad (15)$$

Where S – area, ∂S – its piecewise smooth border. All functions included in (15) are assumed to be smooth.

Elastic plastic problem for an arbitrary hole in the case when the plastic area covers the entire hole. Let C – a piecewise smooth contour with a load applied to it

$$l^1\tau^1 + l^2\tau^2 = \tau_n, \left|\tau_n\right| \le k, \qquad (16)$$

where (l^1, l^2) – the components of the normal vector to contour C. The contour of the plastic area L completely covers the hole C (see fig. 1).

In this case, in addition to condition (16), the yield condition (7) on the contour C is also satisfied. Thus, there are two conditions on C:

$$l^1\tau^1 + l^2\tau^2 = \tau_n,\ (\tau^1)^2 + (\tau^2)^2 = k^2. \qquad (17)$$

From conditions (17), we find the stress tensor components on the conour C:

$$\tau^1 = \tau_n \pm l^2\sqrt{k^2 - \tau_n^2}, \\ \tau^2 = \tau_n l^2 \mp l^1\sqrt{k^2 - \tau_n^2}. \qquad (18)$$

Further, for certainty in formulas (18), we will choose the upper sign.

4. The use of conservation laws to find the stress tensor component in the area. Let the point $M(x_m, y_m)$ lie outside of contour C. Let us build a radius ε circle centered at point M. We have $\varepsilon : (x - x_m)^2 + (y - y_m)^2 = \varepsilon^2$. Let D be a straight line connecting point M with contour C. We get a closed contour consisting of a circle ε, a straight line D, and contour C (fig. 2).

From (15) we get

$$\oint_C Ady - Bdx + \int_{D^+} Ady - Bdx + \\ + \int_{D^-} Ady - Bdx + \int_{\varepsilon} Ady - Bdx = 0. \qquad (19)$$

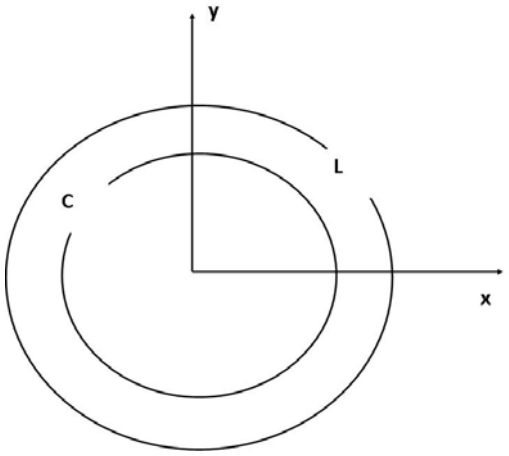

Fig. 1. Elastic-plastic problem for an arbitrary hole in the case when the plastic area covers the entire hole

Рис. 1. Упруго пластическая задача для произвольного отверстия в случае, когда пластическая область охватывает все отверстие

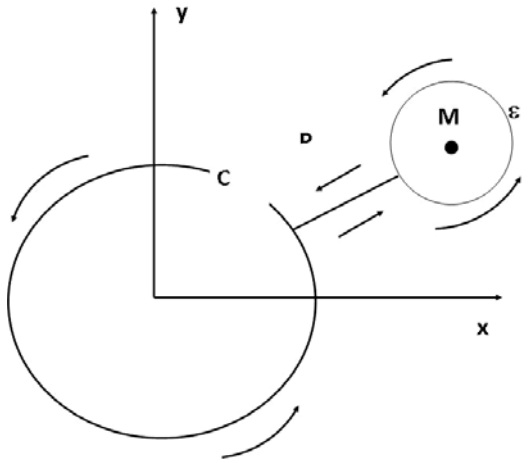

Fig. 2. Closed contour consisting of a circle ε, straight line D, and contour C

Рис. 2. Замкнутый контур, состоящий из окружности ε, прямой D и контура C

The sum of the second and third terms in (19) is zero, since the integrals are calculated in different directions. Finally from (19) we have

$$\int_C Ady - Bdx = -\oint_\varepsilon Ady - Bdx. \qquad (20)$$

We transform the right side of equation (20) by introducing parameterization $x = \varepsilon\cos\cos t$, $y = \varepsilon sint$, $0 \le t \le 2\pi$. As a result, we have

$$\oint_\varepsilon Ady - Bdx = \varepsilon\int_0^{2\pi}\left(Acost + Bsint\right)dt. \qquad (21)$$

Let in (15)

$$\alpha^1 = \frac{x}{x^2+y^2},\ \beta^1 = -\frac{y}{x^2+y^2}. \qquad (22)$$

Then from (21) we get

$$\int_\varepsilon A_1dy - B_1dx = \varepsilon\int_0^{2\pi}\left(A_1cost + B_1sint\right)dt = \\ = \int_0^{2\pi}\tau^1 dt = 2\pi\tau^1\left(x_m, y_m\right). \qquad (23)$$

The last equality in (23) is obtained using the theorem on the mean at ε tending to zero.

Let in (15)

$$\alpha^1 = \frac{y}{x^2+y^2},\ \beta^1 = \frac{x}{x^2+y^2}. \qquad (24)$$

Then from (21) we get

$$\oint_\varepsilon A_2dy - B_2dx = \varepsilon\int_0^{2\pi}\left(A_2cost + B_2sint\right)dt = \\ = \int_0^{2\pi}\tau^2 dt = 2\pi\tau^2\left(x_m, y_m\right). \qquad (25)$$

The last equality in (25) is obtained using the theorem on the mean at ε tending to zero.

The last equality in (25) is obtained using the theorem on the mean at ε tending to zero.

From the formula (20), as well as from (23) and (25), we get

$$\oint_C A_1dy - B_1dx = -2\pi\tau^1\left(x_m, y_m\right), \\ \oint_C A_2dy - B_2dx = -2\pi\tau^2\left(x_m, y_m\right). \qquad (26)$$

Formulas (26) make it possible to find the components of the stress tensor at any point outside the contour C. This allows to set the boundary between the elastic and plastic areass. If the condition of plasticity $(\tau^1)^2 + (\tau^2)^2 = k^2$ is satisfied at a point x_m, y_m, then this point belongs to the plastic area, when the condition $(\tau^1)^2 + (\tau^2)^2 < k^2$ is satisfied , to the elastic.

Comment. The above formulas allow us to solve elastic-plastic problems, even if the plastic contour does not completely cover the contour C, provided that the plasticity condition is satisfied on the contour C (7).

References

1. Annin B. D., CHerepanov G. P. *Uprugo plasticheskaya zadacha*. [Elastic plastic task] Novosibirsk, Nauka Publ., 1983, 239 p.

2. Senashov S. I. [On the laws of conservation of plasticity equations]. *Dokl. AN SSSR.* 1991, Vol. 320, No. 3, P. 606–608 (In Russ.).

3. Senashov S. I., Filyushina E. V. *Uprugoplasticheskie zadachi dlya ortotropnyh sred*. [Elastic-plastic problems for orthotropic environments]. Krasnoyarsk, SibGU im. M. F. Reshetneva Publ., 2017, 116 p.

4. Kiryakov P. P., Senashov S. I., Yahno A. N. *Prilozhenie simmetrij i zakonov sohraneniya k resheniyu differencial'nyh uravneniy.* [Application of symmetries and conservation laws to the solution of differential equations]. Novosibirsk, Nauka Publ., 2001, 192 p.

5. Senashov S. I., Gomonova O. V., Yahno A. N. *Matematicheskie voprosy dvumernyh uravnenij ideal'noj plastichnosti.* [Mathematical problems of two-dimensional equations of ideal plasticity] Sib. gos. aerokosmich. un-t. Krasnoyarsk, 2012. 139 p.

6. Ivlev D. D. et al. *Predel'noe sostoyanie deformirovannyh tel i gornyh porod* [Limit state of deformed bodies and rocks]. Moscow, FIZMTLIT Publ., 2008.

7. Senashov S. I., Filyushina E. V. [Analytical solution of the problem of the load wave in an elastic-plastic rod]. *Dinamika sploshn. sredy*. 2012, No. 127.

8. Senashov S. I., Filyushina E. V., Gomonova O. V. [Building elastic-plastic boundaries using conservation laws]. *Vestnik SibGAU*. 2015, Vol. 16, No. 2, P. 343–359 (In Russ.).

9. Senashov S. I., Kondrin A. V. [Development of an information system for finding the elastic-plastic boundary of rolling profile rods]. *Vestnik SibGAU*. 2014, No. 4(56), P. 119–125 (In Russ.).

10. Senashov S. I., Cherepanova O. N., Kondrin A. V. [About elastic-plastic torsion of a rod]. *Vestnik SibGAU*. 201, No. 3(49), P. 100–103 (In Russ.).

11. Senashov S. I., Cherepanova O. N., Kondrin A. V. Elastoplastic Torsion of a Rod with MultiplyConnected Cross-Section. *J. Siberian Federal Univ. Math. & Physics*. 2015, No. 7(1), P. 343–351.

12. Senashov S. I., Cherepanova O. N., Kondrin A. V. On Elastoplastic Bending of Beam. J. *Siberian Federal Univ. Math. & Physics*. 2014, No. 7(2), P. 203–208.

13. Ol'shak V., Mruz Z., Pezhina P. *Neodnorodnaya teoriya plastichnosti* [Heterogeneous theory of plasticity] Moscow, Mir Publ., 1964, 156 p.

14. Senashov S. I., Vinogradov A. M. Symmetries and conservation laws of 2-dimensional ideal plasticity. *Proc. EdinburgMath. Soc.* 1988, Vol. 3(2), P. 415–439.

15. Annin B. D., Bytev V. O., Senashov S. I. *Gruppovye svojstva uravnenij uprugosti i plastichnosti* [Group properties of elasticity and plasticity equations]. Novosibirsk, Nauka Publ., 1985, 143 p.

Библиографические ссылки

1. Аннин Б. Д., Черепанов Г. П. Упруго пластическая задача. Новосибирск : Наука, 1983. 239 с.

2. Сенашов С. И. О законах сохранения уравнений пластичности // Докл. АН СССР. 1991. Т. 320, № 3. С. 606–608.

3. Сенашов С. И., Филюшина Е. В. Упругопластические задачи для ортотропных сред / СибГУ им. М. Ф. Решетнева. Красноярск, 2017. 116 с.

4. Киряков П. П., Сенашов С. И., Яхно А. Н. Приложение симметрий и законов сохранения к решению дифференциальных уравнений. Новосибирск : Наука, 2001. 192 с.

5. Сенашов С. И., Гомонова О. В., Яхно А. Н. Математические вопросы двумерных уравнений идеальной пластичности / Сиб. гос. аэрокосмич. ун-т. Красноярск, 2012. 139 с.

6. Предельное состояние деформированных тел и горных пород / Д. Д. Ивлев и др. М. : Физмтлит, 2008.

7. Сенашов С. И., Филюшина Е. В. Аналитическое решение задачи о волне нагрузки в упругопластическом стержне // Динамка сплошн. среды. 2012. Вып. 127.

8. Сенашов С. И., Филюшина Е. В., Гомонова О. В. Построение упругопластических границ с помощью законов сохранения // Вестник СибГАУ. 2015. Т. 16, № 2. С. 343–359.

9. Сенашов С. И., Кондрин А. В. Разработка информационной системы для нахождения упругопластической границы стержней прокатного профиля // Вестник СибГАУ. 2014. № 4(56). С. 119–125.

10. Сенашов С. И., Черепанова О. Н., Кондрин А. В. Об упругопластическом кручении стержня // Вестник СибГАУ. 2013. № 3(49). С. 100–103.

11. Сенашов С. И., Черепанова О. Н., Кондрин А. В. Elastoplastic Torsion of a Rod with MultiplyConnected Cross-Section // J. Siberian Federal Univ. Math. & Physics. 2015. No. 7(1). P. 343–51.

12. Сенашов С. И., Черепанова О. Н., Кондрин А. В. On Elastoplastic Bending of Beam // J. Siberian Federal Univ. Math. & Physics. 2014. No. 7(2). P. 203–208.

13. Ольшак В., Мруз З., Пежина П. Неоднородная теория пластичности. М. : Мир, 1964. 156 с.

14. Senashov S. I., Vinogradov A. M. Symmetries and conservation laws of 2-dimensional ideal plasticity // Proc. EdinburgMath. Soc. 1988. Vol. 3(2). P. 415–439.

15. Аннин Б. Д., Бытев В. О., Сенвшов С. И. Групповые свойства уравнений упругости и пластичности. Новосибирск : Наука. Сиб. отделение, 1985. Бытев 143 с.

Senashov Sergei Ivanovich – D. Sc., Professor, Head of the Department of IES; Reshetnev Siberian State University of Science and Technology. E-mail: sen@sibsau.ru.

Savostyanova Irina Leonidovna – Cand. Sc., Associate Professor of the Department of IES, Reshetnev Siberian State University of Science and Technology. E-mail: savostyanova@sibsau.ru.

Cherepanova Olga Nikolaevna – Cand. Sc., associate Professor, acting Director of the Institute of Mathematics and Fundamental Informatics; Siberian Federal University. E-mail: cheronik@mail.ru.

Сенашов Сергей Иванович – доктор физико-математических наук, профессор, заведующий кафедрой ИЭС; Сибирский государственный университет науки и технологий имени академика М. Ф. Решетнева. E-mail: sen@sibsau.ru.

Савостьянова Ирина Леонидовна – кандидат педагогических наук, доцент кафедры ИЭС; Сибирский государственный университет науки и технологий имени академика М. Ф. Решетнева. E-mail: savostyanova@sibsau.ru.

Черепанова Ольга Николаевна – кандидат физико-математических наук, доцент, исполняющая обязанности директора Института математики и фундаментальной информатики; Сибирский федеральный университет. E-mail: cheronik@mail.ru.

UDC 004.896
Doi: 10.31772/2587-6066-2020-21-2-206-214

For citation: Tynchenko V. S., Golovenok I. A., Petrenko V. E., Milov A. V., Murygin A. V. Gradient boosting method application to support process decisions in the electron-beam welding proces. *Siberian Journal of Science and Technology*. 2020, Vol. 21, No. 2, P. 206–214. Doi: 10.31772/2587-6066-2020-21-2-206-214

Для цитирования: Применение метода градиентного бустинга для поддержки принятия технологических решений в процессе электронно-лучевой сварки / В. С. Тынченко, И. А. Головенок, В. Е. Петренко и др. // Сибирский журнал науки и технологий. 2020. Т. 21, № 2. С. 206–214. Doi: 10.31772/2587-6066-2020-21-2-206-214

GRADIENT BOOSTING METHOD APPLICATION TO SUPPORT PROCESS DECISIONS IN THE ELECTRON-BEAM WELDING PROCESS

V. S. Tynchenko, I. A. Golovenok, V. E. Petrenko, A. V. Milov, A. V. Murygin

Reshetnev Siberian State University of Science and Technology
31, Krasnoyarskii rabochii prospekt, Krasnoyarsk, 660037, Russian Federation
E-mail: vadimond@mail.ru

The purpose of the study is to develop a technological process mathematical model of creating permanent joints of dissimilar materials based on electron-beam welding using machine learning algorithms. Each of the connected elements is a responsible unit of the complex device, due to this fact, strict criteria are set for the quality of the welded joint. In essence, the set task is a regression task. There are many algorithms suitable for solving the regression problem. However, often the use of one algorithm does not provide sufficient accuracy of the result. One way to solve this problem is to develop a composition of algorithms to compensate for the problems of each of them. One of the most effective and potent compositional algorithms is the gradient boosting algorithm. This algorithm use will improve the quality of the regression model. The proposed model will allow the technologist to set the process parameters and to get an assessment of the final product quality, as well as by setting input and output values. The use of assessment methods and forecasting will reduce the time and labor costs of searching, developing and adjusting the process. A description of the gradient boosting algorithm is given, as well as an analysis of the applicability of this algorithm to the model and a conclusion regarding the areas of its applicability and the reliability of the forecasts obtained by its direct use. In addition, we consider the process of direct model training based on the data obtained as part of search experiments to improve the quality of final product. The results of the applicability analysis allow us to judge the admissibility of using the proposed method for processes that have similar statistical dependencies. The application of the proposed approach will make it possible to support the adoption of technological decisions by specialists in electron-beam welding during the development of the technological process and when new types of products are put into production.

Keywords: electron-beam welding, technological process, experiments, gradient boosting, machine learning.

ПРИМЕНЕНИЕ МЕТОДА ГРАДИЕНТНОГО БУСТИНГА ДЛЯ ПОДДЕРЖКИ ПРИНЯТИЯ ТЕХНОЛОГИЧЕСКИХ РЕШЕНИЙ В ПРОЦЕССЕ ЭЛЕКТРОННО-ЛУЧЕВОЙ СВАРКИ

В. С. Тынченко, И. А. Головенок, В. Е. Петренко, А. В. Милов, А. В. Мурыгин

Сибирский государственный университет науки и технологий имени академика М. Ф. Решетнева
Российская Федерация, 660037, г. Красноярск, просп. им. газ. «Красноярский рабочий», 31
E-mail: vadimond@mail.ru

Целью исследования является создание математической модели технологического процесса изготовления неразъемных соединений разнородных материалов на основе электронно-лучевой сварки с использованием алгоритмов машинного обучения. Каждый из соединяемых элементов представляет собой ответственный узел комплексного устройства, в связи с чем выставляются жесткие критерии к качеству сварного соединения. В сущности, поставленная задача представляет собой задачу регрессии. Существует множество алгоритмов, подходящих для решения задачи регрессии. Однако зачастую использование одного алгоритма не обеспечивает достаточной точности полученного результата. Одним из способов решения такой проблемы является построение композиции алгоритмов для компенсации проблем каждого из них. Одним из наиболее эффективных и мощных алгоритмов композиции является градиентный бустинг. Использование данного алгоритма повысит качество модели регрессии. Предлагаемая модель позволит технологу задавать параметры технологического процесса и получать оценку качества конечного изделия равно как по заданию входных, так и выходных величин. Использование методов оценки и прогнозирование снизит временные и трудовые затраты на поиск, отработку и наладку технологического процесса. Приводится описание алгоритма градиентного бустинга, а также анализ применимости данного алгоритма к модели, равно как и заключение касательно

областей его применимости и достоверности прогнозов, получаемых при его использовании. Кроме того, рассматривается процесс непосредственного обучения модели на основе данных, полученных в рамках проведения поисковых экспериментов для улучшения качества конечного изделия. Результаты анализа применимости позволяют судить о допустимости использования предложенного метода для процессов, имеющих схожие статистические зависимости. Применение предложенного подхода позволит осуществить поддержку принятия технологических решений специалистов по электронно-лучевой сварке при отработке технологического процесса и при вводе в производство новых видов продукции.

Ключевые слова: электронно-лучевая сварка, технологический процесс, эксперименты, градиентный бустинг, машинное обучение.

Introduction. For a number of technological processes the issue of selecting or conscious choosing optimal parameters that depend on the quality criteria applied to the final product is acute [1–5]. Moreover, this statement is also true for ways to search for improvement or transformation of an already established technological process. For example, when you need to improve one of the parameters that determine the quality of the final product, without changing the others, or without allowing them to deviate by a certain amount. However, some processes, such as electron-beam welding [6; 7] are relatively difficult to adjust or change, due to either insufficient knowledge or integrated complexity, when it is impossible to take into account all factors in a way that would allow us to uniquely determine the potential changes and the impact of parameters on the process as a whole. This leads to the need to search for methods to simplify the process of setting up and converting technological processes.

Considering the technological process as a closed system with different input and output parameters, you can build an appropriate model and then use it as a tool for forecasting and optimization. The purpose of this research was to study one of the machine learning algorithms as a subject for creating a complex mathematical model that would allow forming a conscious view of the choice of process parameters in both local and global search for the optimum determined by the technologist. This approach will significantly reduce the time to set up the technological process, as well as the cost of research, which will ultimately have a positive impact on the cost and quality of products.

In essence, the task is a regression task. One of the most effective and potent composition algorithms is the gradient boosting algorithm [8–13]. The use of the proposed mathematical model will improve the quality of control of the electron-beam welding process by implementing support for technological decision-making using the gradient boosting algorithm. In the future, this approach can be used for technological processes that have similar statistical dependencies.

Description of the training data set. As the initial data, the results of experimental studies conducted to improve the technological process of electron-beam welding of a product, the assembly of which consists of elements consisting of dissimilar material, were used. The electron beam welding unit where the research was conducted is designed for electron-beam welding in high vacuum of assembly units parts made of stainless steels, titanium, aluminum and special alloys. The existing unit of electron beam welding provides repeatability of modes within the capabilities of the implemented control system. Welding operations were performed on simulators corresponding to the technological product. To reduce energy input during welding:

1. The welding current value decreased (IW).
2. The current focus of the electron beam increased (IF).
3. The welding speed increased (VW).
4. The distance from the surface of the samples to the electron-optical system changed (FP).

According to the set of technological modes parameters, the minimum possible sizes of welding seams were provided: the depth of the seam (Depth) and the width of the seam (Width).

During the research, electron-beam welding of 18 samples was performed. The results of metallographic control on the size of the welding seam for each sample were carried out in 4 cross-sections of the welding seam. The accelerating voltage was constant in the range of 19.8–20 kV. The obtained data set is collected as a part of welding modes, sizes of welding seams in cross sections of all samples. Statistical indicators of the training data set are shown in tab. 1.

Mathematical statement of the problem. The formal statement of the supporting technological decision-making problem in the process of electron-beam welding is a regression problem, in which the characteristics of the welded joint must be predicted based on a set of the technological process initial parameters. The mathematical statement of the control problem in this case will be the following. Let there be a set of process parameters: IW – welding current value, IF – electron beam focusing current, VW – welding speed, FP – distance from the sample surface to the electron-optical system, Depth – weld depth, Width – weld width. There is an unknown target mapping dependency: y*: (IW, IF, VW, FP) → (Depth, Width), the value of which is known only in the training sample. You need to develop a mapping algorithm.

As part of this work, we have:

1. Data set: $L = \{x_i, y_i\}$, $i = 1 \ldots n$, where:

– x_{iw} – welding current, mA;

– x_{if} – focusing current, mA;

– x_{vw} – welding speed, r/min;

– x_{fp} – distance to Electron Optical Welding System (EOWS), mm;

– y_{depth} – weld depth;

– y_{width} – weld width;

– x belongs to Q^4, y belongs to Q^2, where Q is the set of positive rational numbers.

2. Model $f(X)$, which predicts the values for each object, where X is the technological process parameters, in this case, the technological parameters of electron

beam-welding. To evaluate the quality of the model $f(X)$, the following metrics are used: mean square error (MSE); mean absolute error (MAE); coefficient of determination R^2 (R2).

In this research, $f(x)$ is an ensemble of «Gradient Boosting» models (Gradient Boosting Regressor).

Gradient Boosting. The Gradient Boosting Regressor model was implemented using the scikit-learn 0.22.2 package in Python 3.8 [14; 15]. Boosting is a technique for constructing ensembles, in which predictors are not built independently, but sequentially. This technique uses the idea that the next model will learn from the mistakes of the previous one. They have an unequal probability of appearing in subsequent models, and those that give the greatest error are more likely to appear [16]. The algorithm is Gradient boosting:

1. Initialize the model with a constant value

$$\hat{f}(x,0) = \hat{f}_0, \hat{f}_0 = y, y \in \mathbb{R}:$$

$$\hat{f}_0 = \arg\min_y \sum_{i=1}^{n} L(y_i, y).$$

2. For each iteration $t = 1 \ldots M$ (M = n_estimators) repeat:

a) count the pseudo-remains r_{it}

$$r_{it} = -\left[\frac{\partial L(y_i, f(x_i))}{\partial f(x_i)}\right]_{f(x)=\hat{f}(x,t-1)}, \; i = 1,...,n;$$

b) build a new algorithm $h_t(x)$ as a regression on pseudo-residues

$$\{(x_i, r_{it})\}_{i=1...n};$$

c) find the optimum ratio of p_t when $h_t(x)$ relative to the original loss function:

$$\rho_t = \arg\min_{\rho} \sum_{i=1}^{n} L(y_i, \hat{f}(x_i, t-1) + \rho \cdot h(x_i, \theta));$$

d) record the model:

$$\hat{f}_t(x) = \rho_t \cdot h_t(x);$$

e) update the current approximation:

$$\hat{f}(x,t) = \hat{f}(x,t-1) + \hat{f}_t(x) = \sum_{i=0}^{t} \hat{f}_i(x)$$

3. Build the final model:

$$f(x) = \sum_{i=0}^{M} \hat{f}_i(x).$$

In this work, gradient boosting is implemented over the decision trees. This implementation of gradient boosting allows you to build a model in the form of a weak predictive models ensemble of decision trees.

In scikit-learn, the Gradient Boosting Regressor model builds the model in stages, which allows you to optimize arbitrary differentiable loss functions. At each stage, the decision tree corresponds to the negative gradient of the specified loss function. The main parameters in Gradient Boosting Regressor that were selected to find the optimal solution:

1) n_estimators – the number of steps to increase the gradient (the number of weak decision trees used);

2) loss – loss function for optimization. (MSE, MAE);

3) max_depth – maximum depth of each decision tree;

4) max_features – the number of features by which the split is searched;

5) min_samples_split – the minimum number of objects required to split the internal node of the tree;

6) min_samples_leaf — the minimum number of objects in the leaf.

Selection of optimal parameters for the model. The GridSearchCV function, which is part of the scikit-learn module, was used to select the optimal parameters in the model. The GridSearchCV function implements an exhaustive search for the specified parameter values for the model. This function implements the „selection" and „assessment" methods.

Model parameters are optimized by cross – validation over the parameter grid.

Main parameters of the GridSearchCV function:

1) estimator – the model in which the selection happens;

2) param_grid – sets of hyper-parameters that need to be checked;

3) scoring – the metric that will be used for assessment;

4) cv – the number of blocks in cross-validation.

Experimental research.

Experiment setup. The model was set up and trained separately for each: y_{depth} and y_{width}, on a set of X parameters. Training a model with optimal parameters on a full dataset is designated as train_score. To check the accuracy of the model prediction (cv_score), the cross-validation was used. To get an estimate by cross-validation, the cross_val_score function from the scikit-learn module is used.

Table 1

Statistical indicators of the training data set

Indicator	IW	IF	VW	FP	Depth	Width
Number	72	72	72	72	72	72
Sample mean	45.666	141.333	8.639	78.333	1.196	1.970
Mean square deviation	1.678	5.146	2.061	21.494	0.225	0.279
Minimum	43	131	4,5	50	0.80	1.68
25 %	44	139	8	60	1.08	1.76
50 %	45	141	9	80	1.20	1.84
75 %	47	146	10	80	1.29	2.05
Maximum	49	150	12	125	1.76	2.60

Table 2

The best results of selection of model parameters for the depth of the seam

n_estimators	loss	max depth	max features	min samples leaf	min samples split	mean_test_score
100	MSE	3	2	1	5	0.050862
90	MSE	3	2	1	5	0.050887
80	MSE	3	3	1	5	0.050893
80	MSE	3	2	1	5	0.050893
80	MSE	3	4	1	4	0.050893
100	MSE	3	3	1	5	0.050896
90	MSE	3	3	1	2	0.050898
80	MSE	3	4	1	2	0.050899
80	MSE	3	4	1	3	0.050899
100	MSE	3	3	1	2	0.050900

The number of blocks in cross-validation is 4. To improve the accuracy of the check, the algorithm is performed:

For each $i = 1, \ldots, K$:

1. Randomly shuffle the *dataset*– DS_i.
2. Get the score using *cross_val_score* on $DS_i - S_i$.
3. The final score is the average:

$$cv\_score_K = \frac{1}{K}\sum_{i=1}^{K} S_i$$

The number of K is selected in this way until:

$$cv\_score_K - cv\_score_{K-1} \le 0.1.$$

Selection of parameters for the Gradient Boosting Regressor (GBR) model.

The model for the seam depth. Model hyper-parameters were selected among the following values:

1. n_estimators: 10, 20, 30, 40, 50, 60, 70, 80, 90, 100;
2. loss: MSE, MAE;
3. max_depth: 1, 2, 3, 4;
4. max_features:1, 2, 3, 4;
5. min_samples_leaf: 1, 2, 3, 4;
6. min_samples_split: 2, 3, 4, 5.

The search for optimal hyper-parameters was carried out using *GridSearchCV*, where the average absolute error (MAE) was used as a metric for evaluating each test, and the number of blocks in the cross-validation is 5.

The best ten results, in descending order, are shown in tab. 2.

In tab. 2 the following notations are used: mean_test_score – the average value of the test score.

When fixing the values (loss = MSE, max_depth = 3, max_features = 2, min_samples_leaf = 1, min_samples_split = 5), n_estimators change graphs were built (fig. 1).

When fixing values (n_estimators = 100, loss = MSE, max_features = 2, min_samples_leaf = 1, min_samples_split = 5), the max_depth change graphs were built (fig. 2).

When fixing values (n_estimators = 100, loss = MSE, max_depth = 3, max_features = 2, min_samples_leaf = 1), the graphs of min_samples_split were changes built (fig. 3).

As shown in fig. 3, the best score on the test was min_samples_split = 7.

Best hyper-parameters: n_estimators = 100, loss = MSE, max_depth = 3, max_features = 2, min_samples_leaf = 1, min_samples_split = 7.

The importance of technical parameters is distributed as follows: x_{iw} – 6 %; x_{if} – 26 %; x_{vw} – 44 %; x_{fp} – 24 %.

Tab. 3 presents the scores of the mathematical model for the depth of the weld.

Table 3

The scores of a mathematical model for the depth of the welding seam

Scores	R2	MAE
train_score	0.932651	0.042958
cv_score	0.896255	0.044262

The search for optimal hyper-parameters was carried out using *GridSearchCV,* where the metric is the MAE used to assess each test, and the number of blocks in cross-validation is 5.

The top ten results, in descending order, are shown in tab. 4.

The following notations are used in tab. 4: mean_test_score – the average value of the test score.

When fixing the values (loss = MSE, max_depth = 3, max_features = 3, min_samples_leaf = 1, min_samples_split = 4), the n_estimators change graphs were built (fig. 4).

When fixing values (n_estimators = 100, loss = MAE, max_features = 3, min_samples_leaf = 1, min_samples_split = 4), the max_depth change graphs were built (fig. 5).

When fixing values (n_estimators = 100, loss = MAE, max_depth = 3, max_features = 3, min_samples_leaf = 1), the graphs of min_samples_split changes were built (fig. 6).

Best hyper-parameters: n_estimators = 100, loss = MAE, max_depth = 3, max_features = 3, min_samples_leaf = 1, min_samples_split = 4.

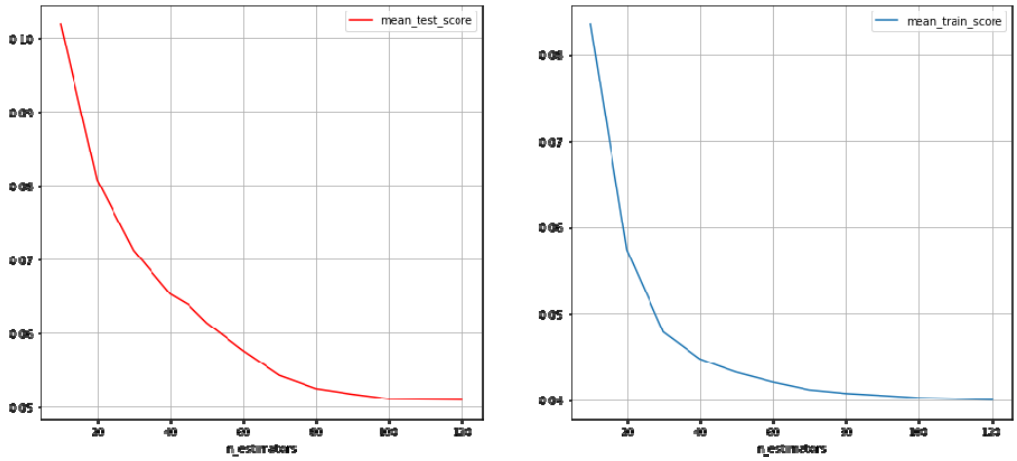

Fig. 1. The changes of n_estimators parameter

Рис. 1. Изменения параметра n_estimators

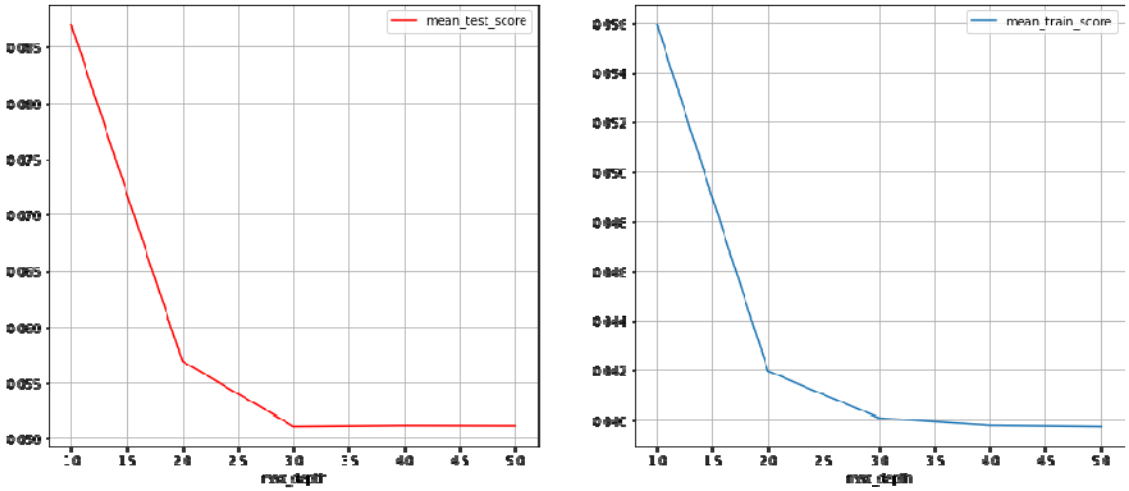

Fig. 2. The changes of max_depth parameter

Рис. 2. Изменения параметра max_depth

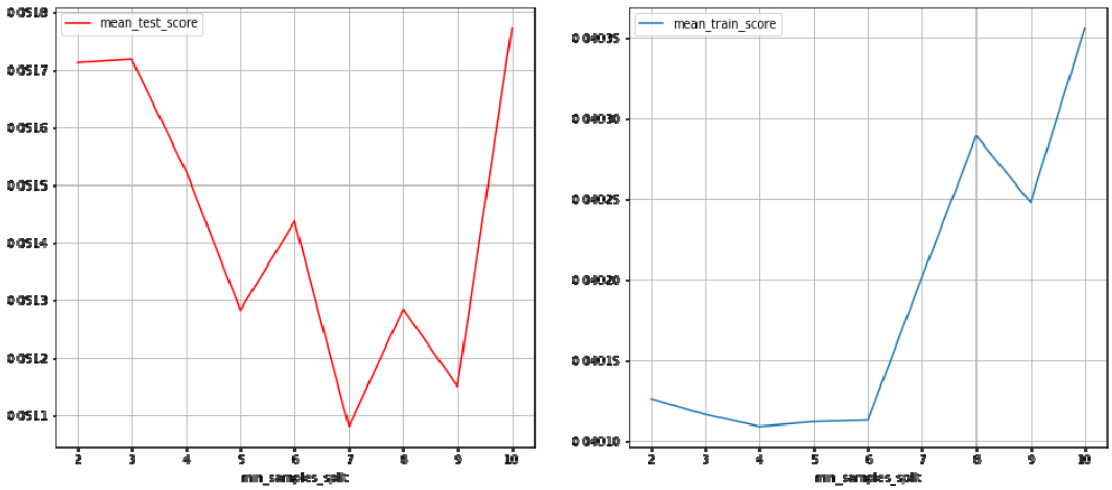

Fig. 3. The changes of min_samples_split parameter

Рис. 3. Изменения параметра min_samples_split

Table 4

The best results of selection of model parameters for the width of the seam

n_estimators	loss	max depth	max features	min samples leaf	min samples split	mean_test_score
100	MAE	3	3	1	4	0.030108
80	MAE	3	3	1	4	0.030112
90	MAE	3	3	1	4	0.030166
70	MAE	3	3	1	4	0.030391
100	MAE	3	3	1	5	0.030459
80	MAE	3	3	1	5	0.030475
90	MAE	3	3	1	5	0.030509
80	MAE	3	3	1	3	0.030615
80	MAE	3	3	1	2	0.030615
60	MAE	3	3	1	4	0.030649

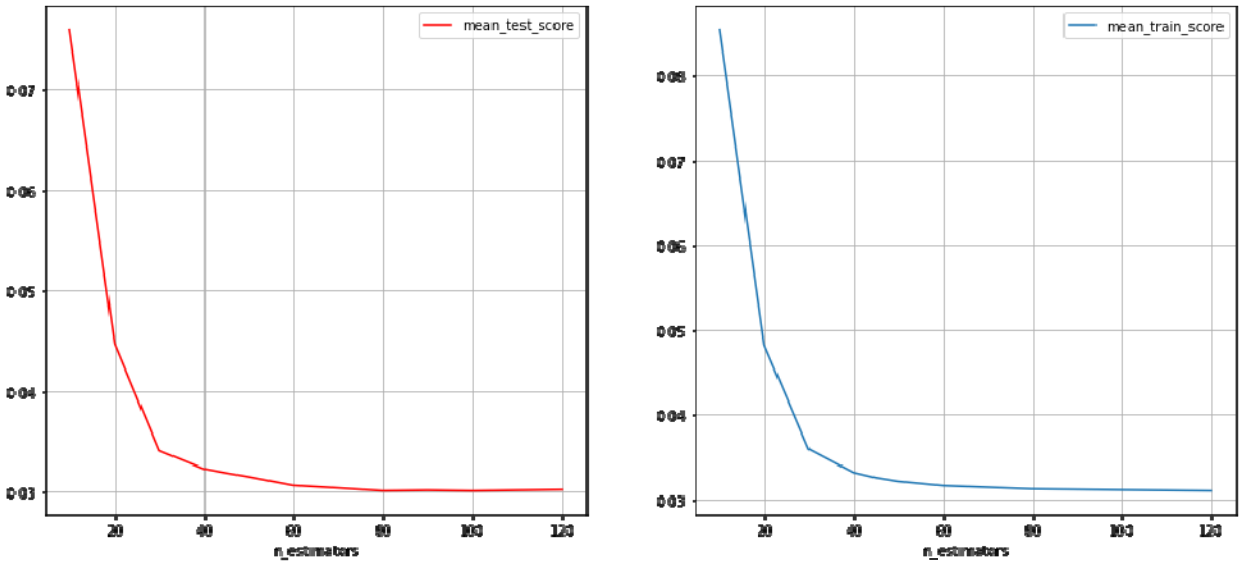

Fig. 4. The changes of n_estimators parameter

Рис. 4. Изменения параметра n_estimators

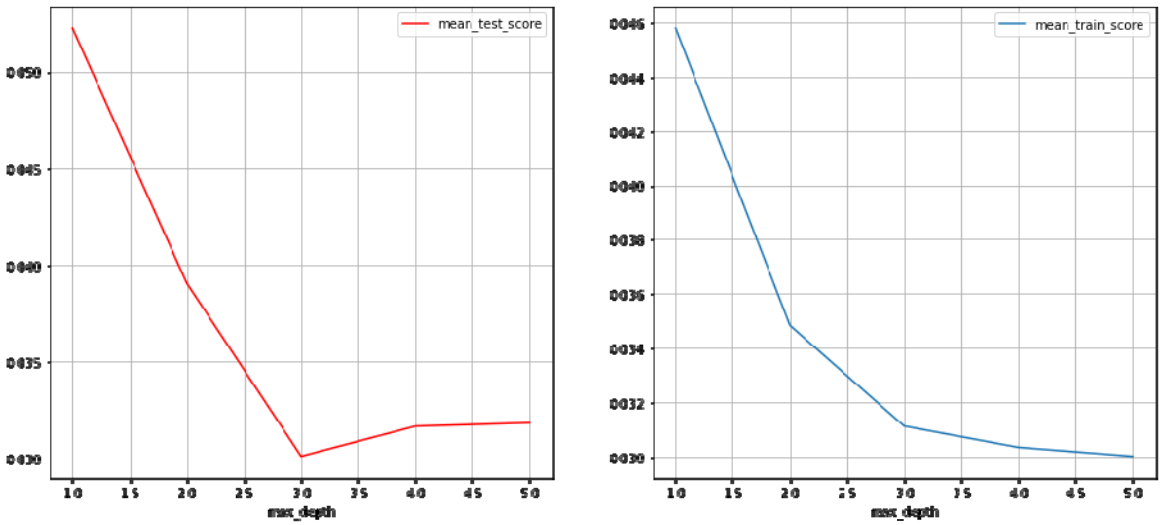

Fig. 5. The changes of max_depth parameter

Рис. 5. Изменения параметра max_depth

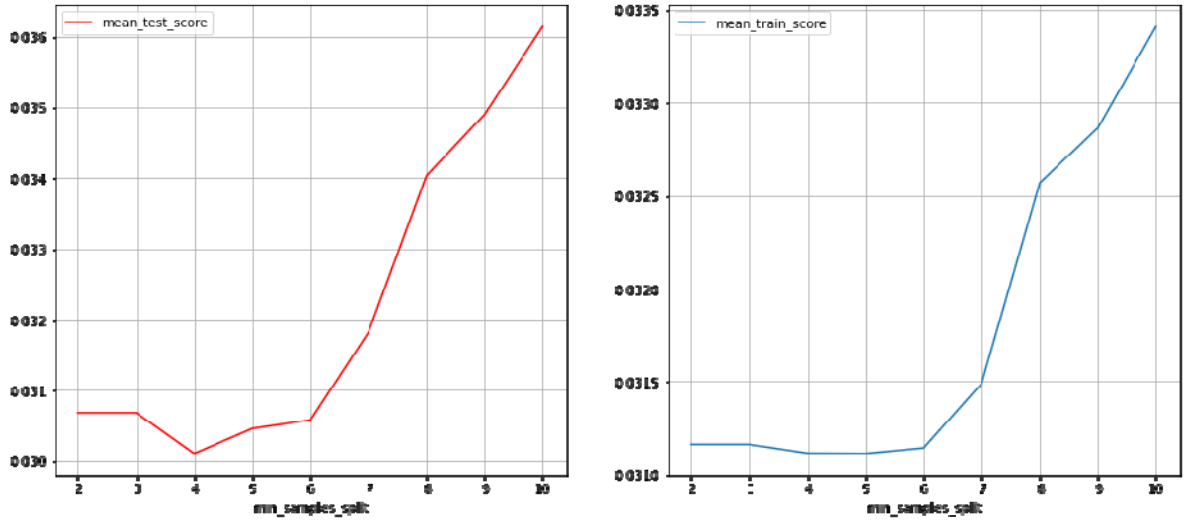

Fig. 6. The changes of min_samples_split parameter

Рис. 6. Изменения параметра min_samples_split

The importance of technical parameters is distributed as follows: x_{iw} – 13 %; x_{if} – 41 %; x_{vw} – 33 %; x_{fp} – 13 %.

Tab. 5 shows the results of evaluations.

Table 5

Model scores by the width of the weld

Scores	R2	MAE
train_score	0.970136	0.030648
cv_score	0.960603	0.040242

Results. In this research the mathematical models based on gradient boosting according to the training set data (dataset) were considered.

The following best parameters of the mathematical model are obtained:

1. For the seam depth: n_estimators = 100, loss = MSE, max_depth = 3, max_features = 2, min_samples_leaf = 1, min_samples_split = 7.

2. For the seam width: n_estimators = 100, loss = MSE, max_depth = 3, max_features = 3, min_samples_leaf = 1, min_samples_split = 4.

The scores of the finished models are shown in tab. 6.

Table 6

Model scores when testing cv_score

Model	R2	MAE
Depth	0.896255	0.044262
Width	0.960603	0.040242

As can be seen from the scores of the mathematical model based on gradient boosting, the proposed model is able to solve the problem of supporting technological decision-making based on gradient boosting with a fairly low value of the average absolute error and a high value of the coefficient of determination.

Conclusion. As a result of the research, the analysis of the applicability of the Gradient Boosting Regressor method as a basis for creating a mathematical model for optimizing and forecasting the process of electron-beam welding was performed. Based on the obtained model scores we can judge the feasibility of using the proposed approach to support technological decision-making in the technological processes control that have similar statistical dependencies.

The obtained model allows us to support technological decision-making in the process of electron-beam welding of dissimilar materials with high accuracy. The use of the technique will improve the quality of the electron-beam welding process control. The results of this study are planned to be used in further research designed to support decision-making in relation to other technological processes that have similar statistical dependencies.

Acknowledgment. The reported study was funded by RFBR, Government of the Krasnoyarsk Territory and the Regional Science Foundation, project number 19-48-240007 “Mathematical and algorithmic support of the electron-beam welding of thin-walled aerospace structures”.

Благодарности. Исследование выполнено при финансовой поддержке РФФИ, Правительства Красноярского края и Краевого фонда науки в рамках научного проекта № 19-48-240007 «Математическое и алгоритмическое обеспечение процесса электронно-лучевой сварки тонкостенных конструкций аэрокосмического назначения».

References

1. Braverman V. Ya., Belozertsev V. S., Litvinov V. P., Rozanov O. V. [Issues of managing weld formation in electron beam welding]. *Sibirskiy zhurnal nauki i tekhnologiy*. 2008,. Vol. 2 (19), P. 148–152 (In Russ.).

2. Weglowski M. S., Blacha S., Phillips A. Electron beam welding – Techniques and trends – Review. Vacuum. 2016, Vol. 130, P. 72–92.

3. Zlobin S. K., Mikhnev M. M., Laptenok V. D., Seregin Yu. N., Bocharov A. N., Tynchenko V. S.,

Dolgopolov B. B. [Automated equipment and technology for soldering waveguide paths of spacecraft]. *Sibirskiy zhurnal nauki i tekhnologiy*. 2014, No. 4 (56), P. 219–229 (In Russ.).

4. Murygin A. V., Tynchenko V. S., Laptenok V. D., Emilova O. A., Seregin Y. N. Modeling of thermal processes in waveguide tracts induction soldering. *IOP Conference Series: Materials Science and Engineering*. 2017, Vol. 173, No. 1, P. 012026.

5. Aydin K., Kaya Y., Kahraman N. Experimental study of diffusion welding/bonding of titanium to copper. *Materials & Design*. 2012, Vol. 37, P. 356–368.

6. Kurashkin S. O., Tynchenko V. S., Seregin Y. N., Petrenko V. E., Milov A. V., Murygin A. V. Mathematical models of beam input and output in the process of electron beam welding of thin-walled structures. *Journal of Physics: Conference Series.* 2020, Vol. 1515, P. 052048.

7. Tynchenko V. S., Milov A. V., Bukhtoyarov V. V., Kukartsev V. V., Tynchenko V. V., Bashmur K. A. The concept of an electron beam I/O control system to optimize the weld formation in the process of electron beam welding. *Journal of Physics: Conference Series.* 2019, Vol. 1399, No. 4, P. 044092.

8. Duffy N., Helmbold D. Boosting methods for regression. *Machine Learning.* 2002, Vol. 47, No. 2–3, P. 153–200.

9. Goodfellow I., Bengio Y., Courville A. Deep learning. Cambridge, MA, MIT press, 2016, 318 p.

10. Son J., Jung I., Park K., Han B. Tracking-by-segmentation with online gradient boosting decision tree. *Proceedings of the IEEE International Conference on Computer Vision*. 2015, P. 3056–3064.

11. Peter S., Diego F., Hamprecht F. A., Nadler B. Cost efficient gradient boosting. Advances in Neural Information Processing Systems. 2017, P. 1551–1561.

12. Salakhutdinova K. I., Lebedev I. S., Krivtsova I. Ye. [Gradient boosting algorithm for decision trees in the software identification problem]. *Nauchno-tekhnicheskiy vestnik informatsionnykh tekhnologiy, mekhaniki i optiki.* 2018, Vol. 18, No. 6, P. 1016–1022 (In Russ.).

13. Dyakonov I. D., Novikova S. V. [Solution of the forecasting problem with the help of gradient boosting over decision trees]. *Nauchnyy forum: Tekhnicheskiye i fiziko-matematicheskiye nauki.* 2018, P. 9–12.

14. Pedregosa F., Varoquaux G., Gramfort A., Michel V., Thirion B., Grisel O., Vanderplas J. Scikit-learn: Machine learning in Python. *The Journal of Machine Learning research.* 2011, Vol. 12, P. 2825–2830.

15. VanRossum G., Drake F. L. The python language reference. Amsterdam, Netherlands, Python software foundation. 2010, 162 p.

16. Schapire R. E., Freund Y. Boosting: Foundations and algorithms. *Kybernetes.* 2013, Vol. 42, No. 1, P. 164–166.

Библиографические ссылки

1. Вопросы управления формированием сварного шва при электронно-лучевой сварке / В. Я. Браверман, В. С. Белозерцев, В. П. Литвинов и др. // Сибирский журнал науки и технологий. 2008. № 2 (19). С. 148–152.

2. Weglowski M. S., Blacha S., Phillips A. Electron beam welding – Techniques and trends –Review // Vacuum. 2016. Vol. 130. P. 72–92.

3. Автоматизированное оборудование и технология для пайки волноводных трактов космических аппаратов / С. К. Злобин, М. М. Михнев, В. Д. Лаптенок и др. //Сибирский журнал науки и технологий. 2014. №. 4 (56). С. 219–229.

4. Modeling of thermal processes in waveguide tracts induction soldering / A. V. Murygin, V. S. Tynchenko, V. D. Laptenok et al. // IOP Conference Series: Materials Science and Engineering, 2017. Vol. 173, No. 1. P. 012026.

5. Aydin K., Kaya Y., Kahraman N. Experimental study of diffusion welding/bonding of titanium to copper // Materials & Design. 2012. Vol. 37. P. 356–368.

6. Mathematical models of beam input and output in the process of electron beam welding of thin-walled structures / S. O. Kurashkin, V. S. Tynchenko, Y. N. Seregin et al. // Journal of Physics: Conference Series. 2020. Vol. 1515. P. 052048.

7. The concept of an electron beam I/O control system to optimize the weld formation in the process of electron beam welding / V. S. Tynchenko, A. V. Milov, V. V. Bukhtoyarov et al. // Journal of Physics: Conference Series. 2019. Vol. 1399, No. 4. P. 044092.

8. Duffy N., Helmbold D. Boosting methods for regression // Machine Learning. 2002. Vol. 47, No. 2–3. P. 153–200.

9. Goodfellow I., Bengio Y., Courville A. Deep learning. Cambridge, MA: MIT press, 2016. 318 p.

10. Tracking-by-segmentation with online gradient boosting decision tree / J. Son, I. Jung, K. Park et al. // Proceedings of the IEEE International Conference on Computer Vision. 2015. P. 3056–3064.

11. Cost efficient gradient boosting / S. Peter, F. Diego, F. A. Hamprecht et al. // Advances in Neural Information Processing Systems. 2017. P. 1551–1561.

12. Салахутдинова К. И., Лебедев И. С., Кривцова И. Е. Алгоритм градиентного бустинга деревьев решений в задаче идентификации программного обеспечения // Научно-технический вестник информационных технологий, механики и оптики. 2018. Т. 18, №. 6. С. 1016–1022.

13. Дьяконов И. Д., Новикова С. В. Решение задачи прогнозирования при помощи градиентного бустинга над решающими деревьями // Научный форум: технические и физико-математические науки. 2018. С. 9–12.

14. Scikit-learn: Machine learning in Python / F. Pedregosa, G. Varoquaux, A. Gramfort et al. // The Journal of Machine Learning research, 2011. Vol. 12. P. 2825–2830.

15. VanRossum G., Drake F. L. The python language reference. Amsterdam, Netherlands : Python software foundation. 2010. 162 p.

16. Schapire R. E., Freund Y. Boosting: Foundations and algorithms // Kybernetes. 2013. Vol. 42, No. 1. P. 164–166.

Tynchenko Vadim Sergeevich – Cand. Sc., docent, associate professor of Information-control Systems department; Reshetnev Siberian State University of Science and Technology. E-mail: vadimond@mail.ru.

Golovenok Igor Aleksandrovich – master student of Information-control Systems department; Reshetnev Siberian State University of Science and Technology. E-mail: golovonokia@mail.ru.

Petrenko Vyacheslav Evgenievich – post-graduate student of Information-control Systems department; Reshetnev Siberian State University of Science and Technology. E-mail: dpblra@inbox.ru.

Milov Anton Vladimirovich – post-graduate student of Information-control Systems department; Reshetnev Siberian State University of Science and Technology. E-mail: helehad@gmail.com.

Murygin Aleksandr Vladimirovich – Dr. Sc., professor, head of Information-control Systems department; Reshetnev Siberian State University of Science and Technology. E-mail: avm514@mail.ru.

Тынченко Вадим Сергеевич – кандидат технических наук, доцент, доцент кафедры информационно-управляющих систем; Сибирский государственный университет науки и технологий имени академика М. Ф. Решетнева. E-mail: vadimond@mail.ru.

Головенок Игорь Александрович – магистрант кафедры информационно-управляющих систем; Сибирский государственный университет науки и технологий имени академика М. Ф. Решетнева. E-mail: golovonokia@mail.ru.

Петренко Вячеслав Евгеньевич – аспирант кафедры информационно-управляющих систем; Сибирский государственный университет науки и технологий имени академика М. Ф. Решетнева. E-mail: dpblra@inbox.ru.

Милов Антон Владимирович – аспирант кафедры информационно-управляющих систем; Сибирский государственный университет науки и технологий имени академика М. Ф. Решетнева. E-mail: helehad@gmail.com.

Мурыгин Александр Владимирович – доктор технических наук, профессор, заведующий кафедрой информационно-управляющих систем; Сибирский государственный университет науки и технологий имени академика М. Ф. Решетнева. E-mail: avm514@mail.ru.

UDC 519.711.3
Doi: 10.31772/2587-6066-2020-21-2-215-223

For citation: Yareshchenko D. I. Non-parametric multi-step algorithms for modeling and control of multi-dimensional inertia-free systems. *Siberian Journal of Science and Technology.* 2020, Vol. 21, No. 2, P. 215–223. Doi: 10.31772/2587-6066-2020-21-2-215-223

Для цитирования: Ярещенко Д. И. Непараметрические многошаговые алгоритмы моделирования и управления многомерными безынерционными системами // Сибирский журнал науки и технологий. 2020. Т. 21, № 2. С. 215–223. Doi: 10.31772/2587-6066-2020-21-2-215-223

NON-PARAMETRIC MULTI-STEP ALGORITHMS FOR MODELING AND CONTROL OF MULTI-DIMENSIONAL INERTIA-FREE SYSTEMS

D. I. Yareshchenko

Siberian Federal University
26к1, Academician Kirensky St., Krasnoyarsk, 660074, Russian Federation
E-mail: YareshenkoDI@yandex.ru

The paper discusses new classes of models of multidimensional inertia-free systems with a delay in the conditions of a lack of a priori information. The subject is multidimensional discrete-continuous processes, the components of the vector of output variables of which are stochastically dependent in an unknown way. There are also processes, through some channels of which aprior information corresponds simultaneously to both the parametric and nonparametric type of source data about the studied process. The mathematical description of such processes leads to a system of implicit nonlinear equations, some of which will be unknown, while others will be known with accuracy to the parameter vector. The main purpose of a model of an object having stochastic dependencies of output variables is to find a forecast of output variables with known input variables.

To find the predicted values of the output variables from known inputs, it is necessary to solve a system of implicit nonlinear equations. The problem is to solve a system that is actually unknown, when only equations for some channels of a multidimensional system are known. Thus, a rather nontrivial situation arises when solving a system of implicit nonlinear equations under conditions when, in one channel of a multidimensional system, the equations themselves are not in the usual sense, and in others they are known accurate to parameters. Therefore, an object model cannot be constructed using the methods of the existing identification theory because of a lack of aprior information. The purpose of this work is the solution of the identification problem in the presence of a partially-parameterized discrete-continuous process, and despite the fact that the parameterization stage cannot be overcome without additional priori information about the process under study.

The control algorithm for multidimensional processes with dependencies of output variables is a sequential multi-step algorithmic chain that allows finding the control action and bring the object to the desired state.

Computational experiments to study the proposed models and to control multidimensional discrete-continuous processes have shown quite satisfactory results. The article presents the results of computational experiments illustrating the effectiveness of the proposed technology for predicting the values of output variables from known input variables, as well as for managing these processes.

Keywords: multidimensional discrete-continuous process, identification, control, T-models, KT-models.

НЕПАРАМЕТРИЧЕСКИЕ МНОГОШАГОВЫЕ АЛГОРИТМЫ МОДЕЛИРОВАНИЯ И УПРАВЛЕНИЯ МНОГОМЕРНЫМИ БЕЗЫНЕРЦИОННЫМИ СИСТЕМАМИ

Д. И. Ярещенко

Сибирский федеральный университет
Российская Федерация, 660074, г. Красноярск, ул. Академика Киренского, 26к1
E-mail: YareshenkoDI@yandex.ru

В настоящей статье рассматриваются новые классы моделей многомерных безынерционных систем с запаздыванием в условиях недостатка априорной информации. Речь идет о многомерных дискретно-непрерывных процессах, компоненты вектора выходных переменных которых стохастически зависимы заранее неизвестным образом. Но также существуют процессы, по некоторым каналам которых априорная информация соответствует одновременно как параметрическому, так и непараметрическому типу исходных данных об исследуемом процессе. Математическое описание подобных процессов приводит к системе неявных нелинейных уравнений, одни из которых будут неизвестны, а другие известны с точностью до вектора пара-

метров. Основное назначение модели объекта, имеющего стохастические зависимости выходных переменных, состоит в нахождении прогноза выходных переменных при известных входных.

Для нахождения прогнозных значений выходных переменных по известным входным необходимо решить систему неявных нелинейных уравнений. И тут возникает странная ситуация, так как необходимо решить систему, которая на самом деле неизвестна, но могут быть лишь известны уравнения по некоторым каналам многомерной системы. Таким образом, возникает довольно нетривиальная ситуация решения системы неявных нелинейных уравнений в условиях, когда по одним каналам многомерной системы самих уравнений в обычном смысле нет, а по другим они известны с точностью до параметров. Поэтому модель объекта не может быть построена с помощью методов существующей теории идентификации в результате недостатка априорной информации. Основным содержанием настоящей работы является решение задачи идентификации при наличии частично-параметризованного дискретно-непрерывного процесса и при том, что этап параметризации не может быть преодолен без дополнительной априорной информации об исследуемом процессе.

Алгоритм управления многомерными процессами с зависимыми выходными переменными представляет собой последовательную многошаговую алгоритмическую цепочку, позволяющую найти управляющее воздействие и привести объект в желаемое состояние.

Вычислительные эксперименты по исследованию предлагаемых моделей и по управлению многомерными дискретно-непрерывными процессами показали достаточно удовлетворительные результаты. В статье приводятся результаты вычислительных экспериментов, иллюстрирующих эффективность предлагаемой технологии прогноза значений выходных переменных по известным входным, а также по управлению данными процессами.

Ключевые слова: многомерный дискретно-непрерывный процесс, идентификация, управление, Т-модели, КТ-модели.

Introduction. Consideration and study of multidimensional inertial processes with a delay, which have a stochastic dependence of output variables, is a relatively urgent task. Since such processes are typical for many popular industries, such as metallurgy (steel melting), construction industry (cement production), energy (coal burning), oil refining (increasing the cold flow of diesel fuel) [1], as well as in active systems, such as the educational process (acquisition of knowledge by University students) [2]. Such processes are characterized by the lack of necessary aprior information. The researcher, in such circumstances, should model and manage such multidimensional discrete-continuous processes. These processes are dynamic in nature, but controlled at discrete time intervals, including various ones. Inertia-free systems are considered with known delays, for example, when the object's time constant is 5–10 minutes, and the control of the output variable is measured once every two hours. This leads to the dependence of output variables, for example, in the production of cement, the main output indicator – the activity of cement (compressive strength) depends on another output indicator – the fineness of grinding.

Processes with stochastic dependence of output variables refer to T-processes [3]. The main point here is that the identification of such objects should be carried out in a way that is not traditional for the existing identification theory [4]. There are also cases when aprior information corresponds simultaneously to both nonparametric and parametric types of source data about the studied. Such processes refer to KT-processes [3].

The main feature of T-processes and KT-processes is that the mathematical description of an object is represented as some analog of a system with partially parameterized functions $F_j\left(u,x,\alpha\right)=0,\ \ j=\overline{1,n}$ and unknown functions $F_j\left(u,x\right)=0,\ \ j=\overline{1,n}$. Thus, the identification problem is reduced to the problem of solving a system of nonlinear equations of a partially parameterized discrete-continuous process relative to the components of vector $x=\left(x_1,x_2,...,x_n\right)$, with known values of input variables $u=\left(u_1,u_2,...,u_m\right)$. Specific identification tasks will differ in different volumes of aprior information through various channels of the multidimensional process, and in their specific flow.

Researchers have to deal with a system of different types of equations from the point of view of mathematics, the solution of which requires the development of special methods [5]. In this case, it is advisable to use the theory of nonparametric systems [6; 7].

Processes with the stochastic dependence of output variables. As noted earlier, T-processes are multidimensional inertia-free processes with stochastic dependence of output variables. In fig. 1, we consider a multidimensional system that implements the T-process.

In fig. 1 the following notation is used: $u=\left(u_1,...,u_m\right)$ – m-dimensional vector of input variables, $x=\left(x_1,...,x_n\right)$ – n-dimensional vector of output variables, $\xi\left(t\right)$ – random interferences effecting the process. The vertical arrows on the output variables show their dependencies. Through various channels of the multidimensional process, the dependence of the j-th component of the vector can be represented as a certain dependence on certain components of the vector $\overline{u}$: $x^{<j>}=f_j\left(u^{<j>}\right),\ \ j=\overline{1,n}$.

Such functions are determined basing on the available aprior information. Such correlations are called a composite vector. A composite vector is a vector composed of some components of input and output variables, in particular, it can be any set, for example $x^{<5>}=\left(u_2,u_5,u_7,u_8\right)$, $x^{<6>}=\left(u_3,u_4,u_7,x_2\right)$ [8].

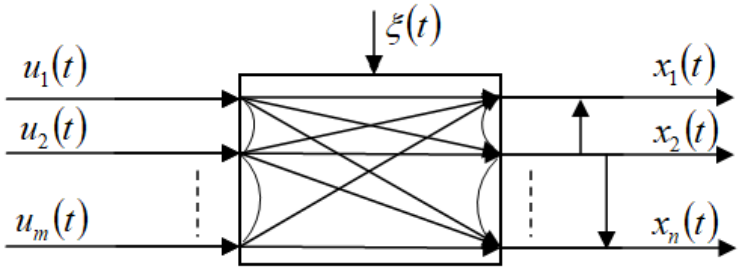

Fig. 1. The multidimensional system that implements the *T*-process

Рис. 1. Многомерная система, реализующая *T*-процесс

The mathematical description of an object is represented as a system of implicit functions of the next form $F_j\left(\bar{u}(t),\bar{x}(t)\right)=0,\ \ j=\overline{1,n}$. The identification problem is reduced to the problem of solving a system of nonlinear equations:

$$F_j\left(\bar{u}(t),\bar{x}(t)\right)=0,\ \ j=\overline{1,n} \qquad (1)$$

relative to the vector components $\bar{x}$, with known values of the input variables u .

Note that the type of equations $F_j(\cdot)$, $j=\overline{1,n}$ remains unknown and cannot be interpreted as a model of the process under study. The task is to model such processes, i.e. T-processes.

Partially-parameterized multidimensional processes. Partially-parameterized multidimensional KT-processes differ from T-processes because their aprior information may correspond to a parametric type in some channels, and nonparametric in others.

A feature of identifying a multidimensional object is that the process under study is described by a system of implicit stochastic equations of the form:

$$F_j\left(u(t),\ x(t+\tau),\ \xi(t)\right)=0,\ \ j=\overline{1,n}, \qquad (2)$$

where for some channels the functions $F_j(\cdot)$ are not known, and for other channels they are known, τ – a delay over various channels of a multidimensional system [3]. In the future, for reasons of simplicity, τ will be omitted by shifting the values in the observation matrix by a value τ .

In this case, the system of equations will take the form:

$$\begin{cases} F_1\left(u^{<j>},x^{<j>},\alpha\right)=0,\\ F_2\left(u^{<j>},x^{<j>},\alpha\right)=0,\\ \ldots \qquad\qquad j=\overline{1,n},\\ F_{n-1}\left(u^{<j>},x^{<j>}\right)=0,\\ F_n\left(u^{<j>},x^{<j>}\right)=0. \end{cases} \qquad (3)$$

where $\hat{F}_j(\cdot)$ are partially parameterized or unknown, α is the parameter vector.

Modeling of multidimensional inertia-free processes. Multidimensional KT-models combine T-models and K-models and represent a model in which there is a set of relationships between input and output variables, and they are known through some channels, for example, based on known laws of physics, and such dependencies are unknown through other channels. I. e., the presence of aprior information on various channels of a multidimensional object corresponds to both parametric and nonparametric types of source data. Therefore, we present the model system in the following form:

$$\begin{cases} \hat{F}_1\left(u^{<j>},x^{<j>},\hat{\alpha}\right)=0;\\ \hat{F}_2\left(u^{<j>},x^{<j>},\hat{\alpha}\right)=0;\\ \ldots \qquad\qquad j=\overline{1,n},\\ \hat{F}_{n-1}\left(u^{<j>},x^{<j>},\vec{x}_s,\vec{u}_s\right)=0;\\ \hat{F}_n\left(u^{<j>},x^{<j>},\vec{x}_s,\vec{u}_s\right)=0. \end{cases} \qquad (4)$$

where $\vec{x}_s,\vec{u}_s$ – the time vectors (the data set received by the s-th moment of time), and $u^{<j>},x^{<j>}$ – the composite vectors. However, even in this case, some functions $\hat{F}_j(\cdot),\ \ j=\overline{1,n}$ remain unknown. Therefore, the problem of constructing KT-models is considered in conditions of nonparametric uncertainty, i.e. in conditions when the system (4) is known only through some channels and is not known to the accuracy of parameters through others.

The identification problem comes to the fact that for given values of the vector of input variables, it is necessary to solve system (4) with connection to the vector of output variables. For some channels of a multidimensional system, for which equations are known up to parameters, the coefficients are found, for example, by stochastic approximations or the least-squares method [9; 10]. For the other channels, where the equations with accuracy up to the parameter vector are unknown, the following two-step algorithmic chain [3] must be applied, which allows to find the predicted values of the vector of output variables from the known input ones. In the first step, the residuals are calculated using the following formula:

$$\varepsilon_{ij}=F_j\left(u^{<j>},x^{<j>}(i),\vec{x}_s,\vec{u}_s\right),\ \ j=\overline{1,n}, \qquad (5)$$

where $F\left(u^{<j>}, x^{<j>}(i), \vec{x}_s, \vec{u}_s\right)$ accepted in the form of a nonparametric estimate of the regression function Nadaraya-Watson [11]:

$$\varepsilon_j(i) = F_{\varepsilon j}\left(u^{<j>}, x_j(i)\right) = \\ = x_j(i) - \frac{\sum_{i=1}^{s} x_j[i] \prod_{k=1}^{<m>} \Phi\left(\frac{u'_k - u_k[i]}{c_{su_k}}\right)}{\sum_{i=1}^{s} \prod_{k=1}^{<m>} \Phi\left(\frac{u'_k - u_k[i]}{c_{su_k}}\right)}, \quad (6)$$

where $j = \overline{1,n}$, $< m >$ – the dimension of the composite vector u_k, then this notation is used for other variables. Moreover, the dimension of the composite vector may be different for different channels. Bell-shaped functions $\Phi(\cdot)$ and the blur parameter c_{su_k} satisfy certain convergence conditions and have the following properties [12]:

$$\Phi(\cdot) < \infty;\ \lim_{s\to\infty} c_s = 0; \\ \int_{\Omega(u)} \Phi\left(c_{su_k}^{-1}\left(u'_k - u_k[i]\right)\right) du = 1; \quad (7)$$

$$\lim_{s\to\infty} c_{su_k}^{-1} \Phi\left(c_{su_k}^{-1}\left(u'_k - u_k[i]\right)\right) = \delta\left(u'_k - u_k[i]\right); \\ \lim_{s\to\infty} s c_s = \infty. \quad (8)$$

The second step is to evaluate the conditional mathematical expectation:

$$x_j = M\left\{x \mid u^{<j>}, \varepsilon = 0\right\},\ j = \overline{1,n}. \quad (9)$$

As a result the forecast for each component of the output variable vector will be as follows:

$$\hat{x}_j = \frac{\sum_{i=1}^{s} x_j[i] \cdot \prod_{k_1=1}^{<m>} \Phi\left(\frac{u_{k_1} - u_{k_1}[i]}{c_{su}}\right) \prod_{k_2=1}^{<n>} \Phi\left(\frac{\varepsilon_{k_2}[i]}{c_{s\varepsilon}}\right)}{\sum_{i=1}^{s} \prod_{k_1=1}^{<m>} \Phi\left(\frac{u_{k_1} - u_{k_1}[i]}{c_{su}}\right) \prod_{k_2=1}^{<n>} \Phi\left(\frac{\varepsilon_{k_2}[i]}{c_{s\varepsilon}}\right)}, \quad (10)$$
$$j = \overline{1,n},$$

where the bell-shaped functions can be taken as a triangular core (11) and (12), and satisfy the conditions presented above.

$$\Phi\left(\frac{u_{k_1} - u_{k_1}[i]}{c_{su}}\right) = \begin{cases} 1 - \frac{\left|u_{k_1} - u_{k_1}[i]\right|}{c_{su}}, & \frac{\left|u_{k_1} - u_{k_1}[i]\right|}{c_{su}} < 1, \\ 0, & \frac{\left|u_{k_1} - u_{k_1}[i]\right|}{c_{su}} \geq 1. \end{cases} \quad (11)$$

$$\Phi\left(\frac{\varepsilon_{k_2}[i]}{c_{s\varepsilon}}\right) = \begin{cases} 1 - \frac{\left|0 - \varepsilon_{k_2}[i]\right|}{c_{s\varepsilon}}, & \frac{\left|0 - \varepsilon_{k_2}[i]\right|}{c_{s\varepsilon}} < 1, \\ 0, & \frac{\left|0 - \varepsilon_{k_2}[i]\right|}{c_{s\varepsilon}} \geq 1. \end{cases} \quad (12)$$

The nonparametric algorithm (6), (10) is a two-step algorithmic chain that allows to find the predicted values of the components of the output vector for known components of input variables, in the case of stochastic dependence of output variables.

The relative standard deviation is taken as the error function:

$$\delta_j = \frac{1}{s} \sqrt{\frac{\sum_{i=1}^{s}\left(x_j^i(t) - \hat{x}_j^i\left(u^{<j>}(t)\right)\right)^2}{\sum_{i=1}^{s}\left(x_j^i(t) - M_{x_j}\right)^2}},\ j = \overline{1,n}, \quad (13)$$

where $x_j^i(t)$ – observation on the object, $\hat{x}_j^i\left(u^{<j>}(t)\right)$ – forecast values of the object's output variables, M_{x_j} – the average value for each component of the vector.

The problem of managing multidimensional discrete-continuous processes. Consider the scheme of a multi-dimensional object control system (fig. 2).

In fig. 2 the following notations are used: $u(t) = \left(u_1(t), u_2(t), ..., u_m(t)\right)$ – input controlled variables of the process; – input free, but controllable variables of the process; $x(t) = \left(x_1(t), x_2(t), ..., x_n(t)\right)$ – output variables of the process; $x^* = \left(x_1, ..., x_n^*\right) \in \Omega\left(x^*\right) \subset R^n$ – setting action, $\xi(t)$ – random interferences affecting the process.

Control of T-objects is considered in conditions of nonparametric uncertainty, i. e. in conditions when the process model with accuracy up to the parameter vector is completely absent.

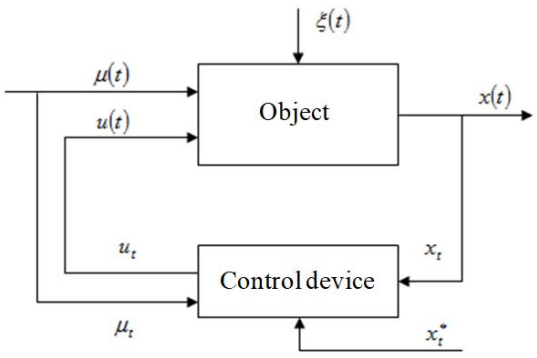

Fig. 2. Diagram of a nonparametric control system of an inertia-free object

Рис. 2. Схема непараметрической системы управления безынерционным объектом

In this case, the known techniques are not applicable and you should use other approaches to solve the problem.

In the problem of controlling a multidimensional process with stochastic dependence of output variables, the following multi-step algorithmic chain must be used: we take the input variable $u_1^*(t)$ arbitrarily from the area $\Omega(u_1)$. Any other input variable can be taken from the specified area at any time. The next input variable $u_2^*(t)$ is found in accordance with the following algorithm:

$$u_2^* = \frac{\sum_{i=1}^{s} u_2^i \Phi\left(\frac{u_1^* - u_1^i}{c_{u_1}}\right) \prod_{j=1}^{<n>} \Phi\left(\frac{x_j^* - x_j^i}{c_{x_j}}\right) \times \times \prod_{\nu=1}^{<p>} \Phi\left(\frac{\mu_\nu^* - \mu_\nu^i}{c_{\mu_\nu}}\right)}{\sum_{i=1}^{s} \Phi\left(\frac{u_1^* - u_1^i}{c_{u_1}}\right) \prod_{j=1}^{<n>} \Phi\left(\frac{x_j^* - x_j^i}{c_{x_j}}\right) \times \times \prod_{\nu=1}^{<p>} \Phi\left(\frac{\mu_\nu^* - \mu_\nu^i}{c_{\mu_\nu}}\right)}, \quad (14)$$

where $<n>$, $<p>$ – dimension of the corresponding composite vectors $\bar{x}$ and $\bar{\mu}$, $<n> \le n$, $<p> \le p$. Then we find the input variable $u_3^*(t)$ as follows:

$$u_3^* = \frac{\sum_{i=1}^{s} u_3^i \Phi\left(\frac{u_1^* - u_1^i}{c_{u_1}}\right) \Phi\left(\frac{u_2^* - u_2^i}{c_{u_2}}\right) \prod_{j=1}^{<n>} \Phi\left(\frac{x_j^* - x_j^i}{c_{x_j}}\right) \times \times \prod_{\nu=1}^{<p>} \Phi\left(\frac{\mu_\nu^* - \mu_\nu^i}{c_{\mu_\nu}}\right)}{\sum_{i=1}^{s} \Phi\left(\frac{u_1^* - u_1^i}{c_{u_1}}\right) \Phi\left(\frac{u_2^* - u_2^i}{c_{u_2}}\right) \prod_{j=1}^{<n>} \Phi\left(\frac{x_j^* - x_j^i}{c_{x_j}}\right) \times \times \prod_{\nu=1}^{<p>} \Phi\left(\frac{\mu_\nu^* - \mu_\nu^i}{c_{\mu_\nu}}\right)}, \quad (15)$$

And then the control algorithm continues to find each component of the object's input, and with each subsequent step, the values of the input variables found in the previous step are added to the formula. The control algorithm for a multidimensional system:

$$u_k^{*s} = \frac{\sum_{i=1}^{s} u_k^i \prod_{k=1}^{k-1} \Phi\left(\frac{u_k^* - u_k^i}{c_{u_k}}\right) \prod_{j=1}^{<n>} \Phi\left(\frac{x_j^* - x_j^i}{c_{x_j}}\right) \times \times \prod_{\nu=1}^{<p>} \Phi\left(\frac{\mu_\nu^* - \mu_\nu^i}{c_{\mu_\nu}}\right)}{\sum_{i=1}^{s} \prod_{k=1}^{k-1} \Phi\left(\frac{u_k^* - u_k^i}{c_{u_k}}\right) \prod_{j=1}^{<n>} \Phi\left(\frac{x_j^* - x_j^i}{c_{x_j}}\right) \times \times \prod_{\nu=1}^{<p>} \Phi\left(\frac{\mu_\nu^* - \mu_\nu^i}{c_{\mu_\nu}}\right)}, \quad k = \overline{1,m}. \quad (16)$$

In the control algorithm (16), the blurring parameters for input and output variables remain configurable c_{u_k}, c_{x_j} and c_{μ_ν}, the following formulas can be used for them: $c_{u_k} = \alpha\left|u_k^* - u_k^i\right| + \eta$, $c_{x_j} = \beta\left|x_j^* - x_j^i\right| + \eta$ and $c_{\mu_\nu} = \gamma\left|\mu_\nu^* - \mu_\nu^i\right| + \eta$, where α, β and γ some parameters greater than 1, and the parameter $0 < \eta < 1$. Note that the selection of blur parameters c_{u_k}, c_{x_j} and c_{μ_ν} is performed at each control cycle. In this case, if c_{u_k} is defined first, then the definition c_{x_j} and c_{μ_ν} is carried out according to this fact. The order in which the blurring parameters c_{u_k}, c_{x_j} and c_{μ_ν} are defined is not important.

Often in real process control tasks, the number of component vector $\bar{u}$ is greater than the number of component vector $\bar{x}$. If the dimension of the vector $\bar{u}$ exceeds the dimension of the vector $\bar{x}$, i. e. $m > n$, it is usually done as follows. To the number of component vector $\bar{\mu}$ some (non-essential) components of the vector $\bar{u}$ are included, so that the dimension of the vector $\bar{u}$ and $\bar{x}$ to be equal.

Computational identification experiment. A multidimensional object with input variables $u = (u_1, u_2, u_3, u_4)$ and output variables $x = (x_1, x_2, x_3)$ was used for the computational experiment. A training sample of input and output variables was formed for the object under consideration, based on a system of equations consisting of two parametric and one nonparametric channels. As a result, a training sample was obtained $\vec{u}_s, \vec{x}_s$, where $\vec{u}_s, \vec{x}_s$ are the time vectors. In case we had a real object, the training sample would be obtained in the process of measurements performed by the available controls.

After receiving a sample of observations $\vec{u}_s, \vec{x}_s$, you can start the task under study – finding the predicted values of output variables x based on known input variables u. The forecast for each component of the output variable vector is made according to the formula (10).

The configurable parameters are the blur parameters c_{su} and $c_{s\varepsilon}$, which in this case are equal to 0.4 and 0.3, respectively (the values were determined as a result of numerous experiments to reduce the quadratic error between the output of the object and the model). Sample volume $s = 1000$, uniform interference that affects the components of the vector of output variables $\xi = 0,07$. Graphs for the outputs of the object x_1, x_2 and x_3 (fig. 3–5).

In fig. 3–5 "point" denotes the output value of the object, and "x" are values of the patterns found by the algorithm (5), (9). For clarity of the results in the figures, there are 20 sample points. The model describes the object fairly well with 7 % interference affecting the components of output variables.

Computational control experiment. The results of computational experiments for a multidimensional object with input variables $u = (u_1, u_2, u_3, u_4)$ and output variables $x = (x_1, x_2, x_3)$ using a multistep control algorithm

(13). For the object under consideration, the number of component vector $\bar{u}$ is greater than the number of component vector $\bar{x}$. So replace $u_4(t) = \mu(t)$ to make the dimension of the vector $\bar{u}$ equal to $\bar{x}$. The input variable is free but controlled $\mu(t) \in [0,\ 3]$.

We underline that the researcher is not familiar with the type of system of equations that describes a controlled multidimensional object. Measurements of input and output variables are used as information about the object under study.

First, we present the results of the multistep control algorithm (16) with a variable step setting effect $x_1^*(t)$ (fig. 6).

As you can see from fig. 6, the output of the object $x_1(t)$ is quite close to the setting effect $x_1^*(t)$. Here are the results of the algorithm with a soft changing setting effect $x_2^*(t)$ (fig. 7).

Here are the results of the algorithm when the task $x_3^*(t)$ is random (fig. 8).

Fig. 8 shows that the output of the object $x_3(t)$ is also quite close to the setting effect $x_3^*(t)$. None of the known regulators can cope with such a task when the setting effect is random [14].

Still, this case is interesting from a theoretical point of view.

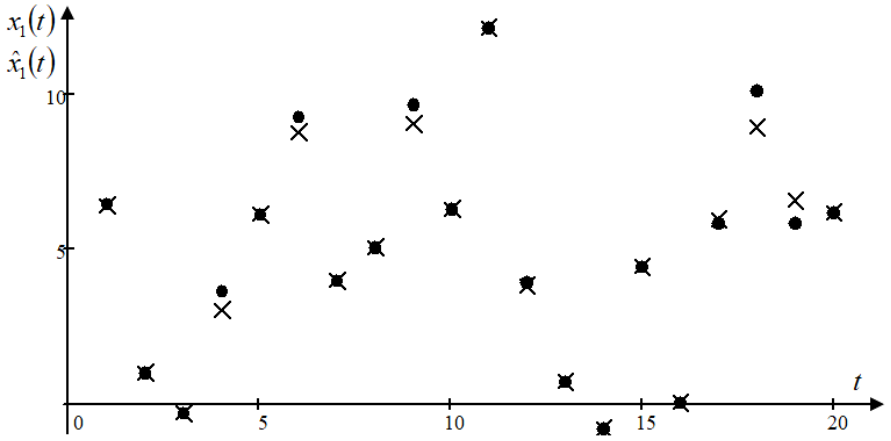

Fig. 3. The predicted values of the output variable x_1 with an interference of 7 %

Рис. 3. Прогнозные значения выходной переменной x_1 при помехе 7 %

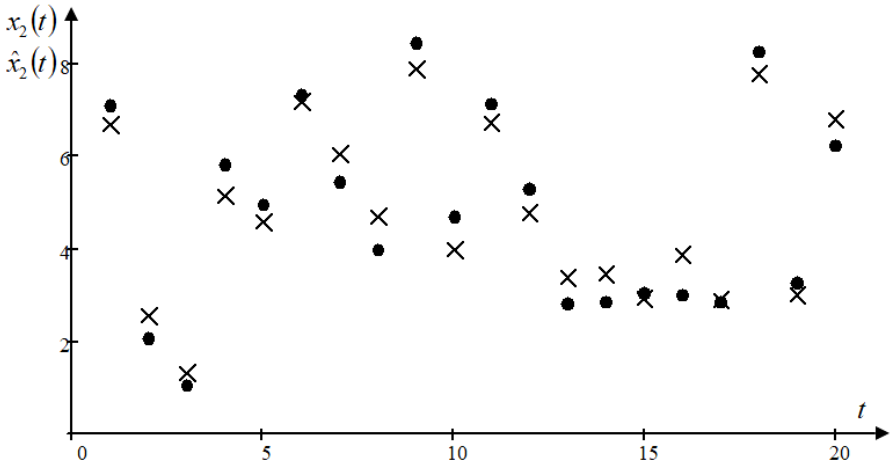

Fig. 4. The predicted values of the output variable x_2 with an interference of 7 %

Рис. 4. Прогнозные значения выходной переменной x_2 при помехе 7 %

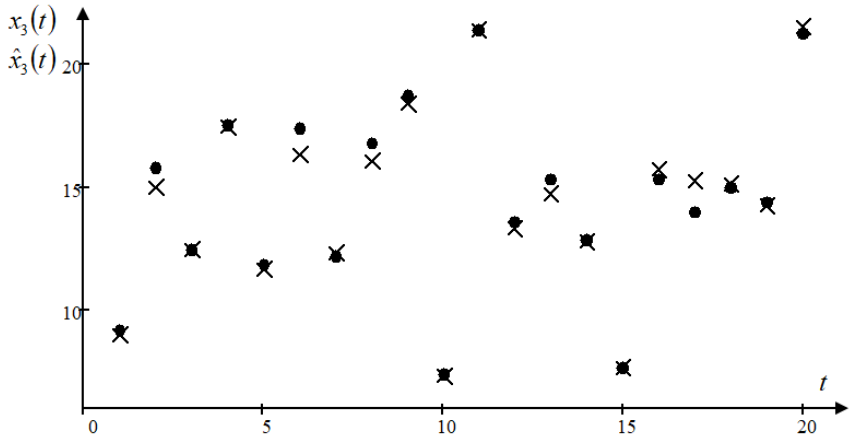

Fig. 5. The predicted values of the output variable x_3 with an interference of 7 %

Рис. 5. Прогнозные значения выходной переменной x_3 при помехе 7 %

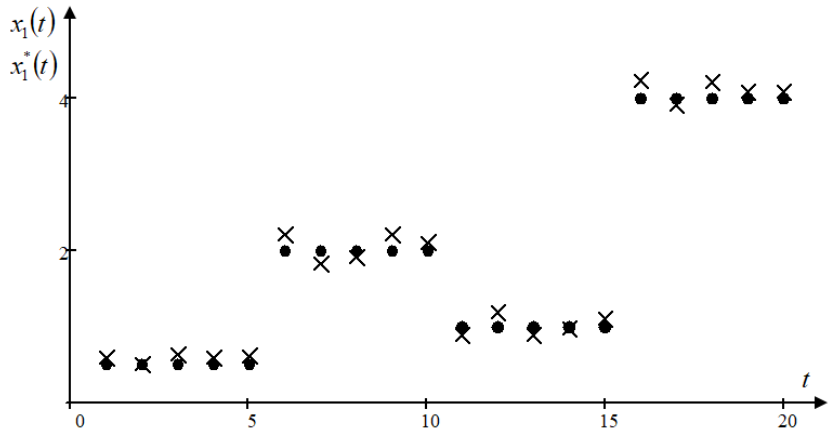

Fig. 6. Control under the setting action $x_1^*(t)$ in the form of a step function

Рис. 6. Управление при задающем воздействии $x_1^*(t)$ в виде ступенчатой функции

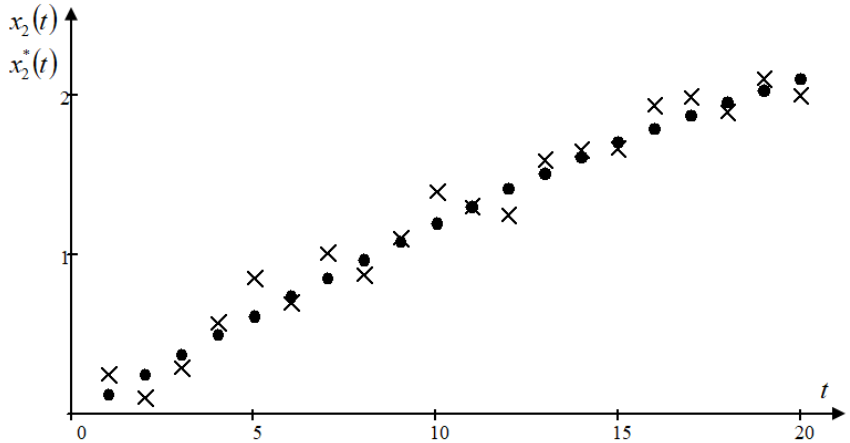

Fig. 7. Control under the set action $x_2^*(t)$ in the form of a soft changing function

Рис. 7. Управление при задающем воздействии $x_2^*(t)$ в виде плавно изменяющейся функции

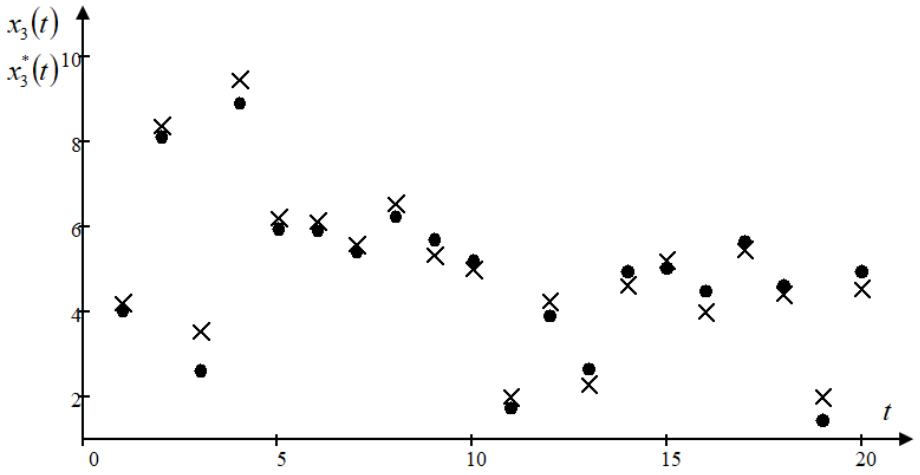

Fig. 8. The dependence of the output of the object $x_3(t)$ on the setting effect $x_3^*(t)$, which is of random nature

Рис. 8. Зависимость выхода объекта $x_3(t)$ от задающего воздействия $x_3^*(t)$, носящего случайный характер

Conclusion. In this paper, the problem of identification and control of multidimensional inertia-free systems with a delay in the conditions of a lack of aprior information considered. We note the fact that identification and control problems are considered under conditions of nonparametric uncertainty and, as a result, can not be presented with accuracy to a set of parameters. Well-configured modeling and control algorithms can be successfully applied in real control systems, diagnostics, decision-making, etc. [15].

These computational experiments on identification and control have shown satisfactory results of modeling multidimensional processes. At the same time, we investigated issues related to the introduction of various interference, different volumes of training samples, but also objects of different dimensions.

References

1. Sinyuta V. R., Yareshchenko D. I. [On nonparametric modeling of the process of catalytic hydrodeparaffinization]. *Materialy XXII Mezhdunar. nauch. konf. "Reshetnevskie chteniya"* [Materials XXII Intern. Scientific. Conf "Reshetnev reading"]. Krasnoyarsk, 2018, P. 160–162 (In Russ.).

2. Yareshchenko D. I. [Some notes on the assessment of knowledge of university students]. *Otkrytoe obrazovanie*. 2017, No. 4, P. 66–72 (In Russ.).

3. Medvedev A. V. *Osnovy teorii neparametricheskikh sistem. Identifikatsiya, upravlenie, prinyatie resheniy* [Fundamentals of the theory of nonparametric systems. Identification, management, decision making]. Krasnoyarsk, SibGU im. M. F. Reshetneva Publ., 2018, 732 p.

4. Tereshina A. V., Yareshchenko D. I. [On nonparametric modeling of inertialess systems with delay]. *Sibirskiy zhurnal nauki i tekhnologiy*. 2018, Vol. 19, No. 1, P. 37–44 (In Russ.).

5. Moiseev N. N. *Matematika stavit eksperiment* [Mathematics is an experiment]. Moscow, Nauka Publ., 1979, 224 p.

6. Medvedev A. V. *Neparametricheskie sistemy adaptacii* [Nonparametric adaptation systems]. Novosibirsk, Nauka Publ., 1983. 174 p.

7. Vasil'ev V. A., Dobrovidov A. V., Koshkin G. M. *Neparametricheskoe ocenivanie funkcionalov ot raspredelenij stacionarnyh posledovatel'nostej* [Nonparametric estimation of functionals of stationary sequences distributions]. Moscow, Nauka Publ., 2004, 508 p.

8. Cypkin Ya. Z., *Osnovy informacionnoj teorii identifikacii* [Fundamentals of information theory of identification]. Moscow, Nauka Publ., 1984, 320 p.

9. Zarubin, V. S. *Matematicheskaya statistika* [Mathematical statistics]. Moscow, MGTU im. Baumana Publ., 2008, 424 p.

10. Linnik Yu. V. *Metod naimen'shikh kvadratov i osnovy teorii obrabotki nablyudeniy* [Least Squares Method and the Basics of Observation Processing Theory]. Moscow, FIZMATLIT Publ., 1958, 336 p.

11. Nadaraya Eh. A. *Neparametricheskoe ocenivanie plotnosti veroyatnostej i krivoj regressii* [Nonparametric estimation of probability density and regression curve]. Tbilisi, Tbilisskiy universitet Publ., 1983, 194 p.

12. Zhivoglyadov V. P., Medvedev A. V. *Neparametricheskie algoritmy adaptatsii* [Nonparametric adaptation algorithms]. Frunze, Ilim Publ., 1974, 135 p.

13. EHjkhoff P. *Osnovy identifikacii sistem upravleniya* [Basics of identification of control systems]. Moscow, Mir Publ., 1975, 7 p.

14. Fel'dbaum A.A. *Elektricheskie sistemy avtomaticheskogo regulirovaniya* [Electric automatic control systems]. Moscow, Gos. izd-vo oboronnoy promyshlennosti Publ., 1957, 808 p.

15. Antomonov Yu. G., Harlamov V. I. *Kibernetika i zhizn'* [Cybernetics and life]. Moscow, Sov. Rossiya Publ., 1968, 327 p.

Библиографические ссылки

1. Синюта В. Р., Ярещенко Д. И. О непараметрическом моделировании процесса каталитической гидродепарафинизации // Решетневские чтения : материалы XXII Междунар. науч.-практ. конф., посвящ. памяти генерального конструктора ракетно-космических систем академика М. Ф. Решетнева. Красноярск, 2018. С. 160–162.

2. Ярещенко Д. И. Некоторые замечания об оценке знаний студентов университетов // Открытое образование. 2017. Вып. 4. С. 66–72.

3. Медведев А. В. Основы теории непараметрических систем. Идентификация, управление, принятие решений : монография / СибГУ им. М. Ф. Решетнева. Красноярск, 2018. 732 с.

4. Терешина А. В., Ярещенко Д. И. О непараметрическом моделировании безынерционных систем с запаздыванием // Сибирский журнал науки и технологий. 2018. Т. 19, № 3. С. 452–461.

5. Моисеев Н. Н. Математика ставит эксперимент. М. : Наука, 1979. 224 с.

6. Медведев А. В. Непараметрические системы адаптации. Новосибирск : Наука, 1983. 174 с.

7. Васильев В. А., Добровидов А. В., Кошкин Г. М. Непараметрическое оценивание функционалов от распределений стационарных последовательностей / отв. ред. Н. А. Кузнецов. М. : Наука, 2004. 508 с.

8. Цыпкин Я. З., Основы информационной теории идентификации. М. : Наука, 1984. 320 с.

9. Зарубин В. С. Математическая статистика / под ред. В. С. Зарубина, А. П. Крищенко. М. : Изд-во МГТУ им. Баумана, 2008. 424 с.

10. Линник Ю. В. Метод наименьших квадратов и основы теории обработки наблюдений. М. : Физматлит, 1958. 336 с.

11. Надарая Э. А. Непараметрические оценки плотности вероятности и кривой регрессии. Тбилиси : изд-во Тбил. ун-та, 1983. 194 с.

12. Медведев А. В., Живоглядов В. П. Непараметрические алгоритмы адаптации. Фрунзе : Илим, 1974. 135 с.

13. Эйкхофф П., Основы идентификации систем управления : пер. с англ. В. А. Лотоцкого, А. С. Манделя. М. : Мир, 1975. 7 с.

14. Фельдбаум А. А. Электрические системы автоматического регулирования. М. : Гос. изд-во оборонной промыш-ти 1957. 808 с.

15. Антомонов Ю. Г., Харламов В. И. Кибернетика и жизнь. М. : Сов. Россия, 1968. 327 с.

Yareshchenko Darya Igorevna – senior lecturer of the department Intelligent Control Systems of the Institute of Space and Information Technologies; Siberian Federal University. E-mail: YareshenkoDI@yandex.ru.

Ярещенко Дарья Игоревна – старший преподаватель базовой кафедры интеллектуальных систем управления Института космических и информационных технологий; Сибирский федеральный университет. E-mail: YareshenkoDI@yandex.ru.

Раздел
Part
2

АВИАЦИОННАЯ И РАКЕТНО-КОСМИЧЕСКАЯ ТЕХНИКА

AVIATION AND SPACECRAFT ENGINEERING

UDC 536.2
Doi: 10.31772/2587-6066-2020-21-2-226-232

For citation: Vasil'ev E. N. Calculation of heat transfer characteristics of a finned wall. *Siberian Journal of Science and Technology.* 2020, Vol. 21, No. 2, P. 226–232. Doi: 10.31772/2587-6066-2020-21-2-226-232

Для цитирования: Васильев Е. Н. Расчет характеристик теплообмена оребренной стенки // Сибирский журнал науки и технологий. 2020. Т. 21, № 2. С. 226–232. Doi: 10.31772/2587-6066-2020-21-2-226-232

CALCULATION OF HEAT TRANSFER CHARACTERISTICS OF A FINNED WALL

E. N. Vasil'ev

Institute of Computational Modelling SB RAS
50/44, Akademgorodok, Krasnoyarsk, 660036, Russian Federation
E-mail: ven@icm.krasn.ru

The reliability and resource of the radio-electronic equipment of the spacecraft is increased by ensuring optimal temperature conditions. Thermal control systems maintain the set temperature mode and heat removal from the on-board equipment to the surrounding space. Finned heat exchangers are an important element of the design of thermal control systems, which allows intensifying the heat transfer process. The calculation of the characteristics of finned heat exchangers must be carried out taking into account their parameters and the physical properties of the heat transfer agent. The organic liquid LZ-TK-2, which has a very low freezing point and other useful performance characteristics, is considered as a heat transfer agent. The dependences of the local heat transfer coefficient of the LZ-TK-2 heat transfer agent on the wall temperature are calculated using criteria equations. Based on the numerical solution of the two-dimensional problem of thermal conductivity, the temperature fields in finned walls of various configurations are determined. Calculations of the heat transfer coefficient of the finned wall of the heat exchanger were made in two model approximations, the error of using a simplified approximation that does not take into account the temperature dependence of the local heat transfer coefficient was determined.

Keywords: thermal control system, heat transfer coefficient, finned wall, heat exchanger, heat transfer agent LZ-TK-2.

РАСЧЕТ ХАРАКТЕРИСТИК ТЕПЛООБМЕНА ОРЕБРЕННОЙ СТЕНКИ

Е. Н. Васильев

Институт вычислительного моделирования СО РАН
Российская Федерация, 660036, г. Красноярск, Академгородок, 50/44
E-mail: ven@icm.krasn.ru

Надежность и ресурс радиоэлектронной аппаратуры космических аппаратов повышается при обеспечении оптимального температурного режима. Системы терморегулирования поддерживают заданный температурный режим и отвод теплоты от бортовой аппаратуры в окружающее пространство. Ребристые теплообменники являются важным элементом конструкции систем терморегулирования, позволяющим интенсифицировать процесс теплопередачи. Расчет характеристик ребристых теплообменников необходимо проводить с учетом их параметров и физических свойств теплоносителя. В качестве теплоносителя рассмотрена органическая жидкость ЛЗ-ТК-2, имеющая очень низкую температуру замерзания и другие полезные эксплуатационные характеристики. В работе с помощью критериальных уравнений рассчитаны зависимости локального коэффициента теплоотдачи теплоносителя ЛЗ-ТК-2 от температуры стенки. На основе численного решения двумерной задачи теплопроводности определены температурные поля в оребренных стенках различной конфигурации. Проведены расчеты коэффициента теплопередачи оребренной стенки теплообменника в двух модельных приближениях, определена погрешность применения упрощенного приближения, не учитывающего температурную зависимость локального коэффициента теплоотдачи.

Ключевые слова: система терморегулирования, коэффициент теплоотдачи, оребренная стенка, теплообменник, теплоноситель ЛЗ-ТК-2.

Introduction. The thermal control system (TCS) of a spacecraft performs the most important function for ensuring optimal temperature conditions for all units and subsystems in real operating conditions [1–5]. In TCS finned surfaces that are in contact with a liquid or gaseous heat transfer agent are widely used to intensify heat trans-

fer and reduce dimensions in heat exchangers. The characteristics of the TCS depend on the parameters of the finned surfaces and the thermophysical properties of the heat transfer agent; therefore, the development of the TCS requires solving a number of problems, such as determining the local heat transfer coefficient on the contact surface of the wall and the heat transfer agent, calculating the heat transfer characteristics of the finned wall and optimizing its parameters.

The heat transfer characteristics are calculated by the temperature field in the volume of the finned wall obtained from the solution of the heat conduction problem. As a rule, when solving the heat conduction problem various simplifying assumptions are made: temperature gradients over the thickness of the fin are neglected (approximation of a thin fin), a uniform temperature distribution is taken at the base of the finned wall, a constant value of the heat transfer coefficient over the finned surface is set, etc. [6]. So that such simplifying assumptions do not lead to significant calculation errors, it is necessary to verify the validity of their application for each task.

The characteristics of the heat transfer process of the finned wall and a heat transfer agent depend, on the one hand, on the heat transfer coefficient of the heat transfer agent on the surface of the heat exchanger, and on the other hand, on the conditions of heat transfer in the wall volume by the heat conduction mechanism. In this paper, we present the results of calculations of the wall heat transfer characteristics based on determining the dependence of the heat transfer coefficient LZ-TK-2 on the temperature of a finned surface and modeling the heat transfer process in a finned heat exchanger by numerically solving the two-dimensional heat equation without using the simplifying assumptions mentioned above.

Heat transfer coefficient of the heat transfer agent LZ-TK-2. According to the requirements of the TCS operation, the heat transfer agent must have a freezing point not higher than –80 °C, corrosion inertness to the TCS materials, fireproof, and have a number of other specific properties [7; 8]. As a working substance for the circuit, we consider the heat transfer agent LZ-TK-2, the basis of which is isooctane, which has a freezing temperature of –107 °C and includes anti-wear additives to reduce bearing wear of electric pump units. Description and temperature dependences of the physical properties of the heat transfer agent LZ-TK-2 are given in [8].

The calculation of the heat transfer coefficient was carried out taking into account the mode of motion and physical properties of the heat transfer agent, the geometric parameters of the finned surface. Depending on the Reynolds number $\mathrm{Re} = uD/\nu$, there are stable laminar ($\mathrm{Re} < 2\cdot10^3$), transitional ($2\cdot10^3 < \mathrm{Re} < 10^4$), and developed turbulent ($\mathrm{Re} > 10^4$) modes, here u – is the coolant velocity, ν – is coefficient of kinematic viscosity. For a rectangular channel having a height a and a width b, the equivalent hydraulic diameter $D = 2ab/(a+b)$ is usually used as a characteristic dimension. The value of the local heat transfer coefficient α at the "heat transfer agent-finned surface" interface was determined using criteria equations based on the results of experimental studies and similarity theory [9]. For the developed turbulent regime, an equation is used that determines the value of Nusselt number

$$\mathrm{Nu} = 0.021\,\mathrm{Re}^{0.8}\,\mathrm{Pr}_\mathrm{h}^{0.43}(\mathrm{Pr}_\mathrm{h}/\mathrm{Pr}_\mathrm{s})^{0.25}\varepsilon\,.$$

Prandtl number $\mathrm{Pr} = \nu c\rho/\lambda$ is determined by the values of the kinematic viscosity coefficient ν, the heat capacity c, the density ρ and the thermal conductivity coefficient λ, corresponding to the average temperature of the heat transfer agent ($\mathrm{Pr_h}$) and the wall surface temperature ($\mathrm{Pr_s}$). If the channel length is more than $50D$, the coefficient value is $\varepsilon = 1$. The value of the local heat transfer coefficient LZ-TK-2 is calculated from the value of Nusselt number using the formula

$$\alpha = \frac{\mathrm{Nu}\lambda}{D}\,.$$

Calculations were performed for a = 2.5 mm, b = 1.3 mm and the coolant velocity u = 2.9 м/с, the value $\mathrm{Re} = 1.1\cdot10^4$ was obtained with a characteristic value $\mathrm{V} = \nu = 0.45$ mm^2/s. The obtained dependences of the heat transfer coefficient α on the temperature of the wall surface T_s are shown in fig. 1 for the heat transfer agent temperature values of 20, 40 and 60 °C. The figure shows that the value of α increases with an increase in both the wall surface temperature and the temperature of the heat transfer agent. The dependences $\alpha(T_\mathrm{s})$ are the initial data for calculating the temperature field of the finned wall.

Calculation of the temperature field in the finned wall. The task of thermal calculation is to determine the temperature field and heat transfer coefficient, which reflects the ratio of the transmitted heat power to the temperature difference between the heat carrier and the wall. We consider the process of heat transfer of a heat transfer agent LZ-TK-2 with a finned wall, the cross section of which is shown in fig. 2.

The calculation of the temperature field in the wall of the heat exchanger was carried out on the basis of solving the non-stationary problem of thermal conductivity. In the case of a thick fin in which the temperature gradients are comparable in width and height, a two-dimensional thermal conductivity equation of the form is numerically solved

$$c\rho\frac{\partial T}{\partial t} = \lambda\left(\frac{\partial^2 T}{\partial x^2} + \frac{\partial^2 T}{\partial y^2}\right). \qquad (1)$$

The calculation area of the problem, which is half of a periodically repeated fragment of the finned wall, is highlighted in fig. 2 with a dashed outline. On the internal boundaries of the wall the symmetry conditions for the heat flow $\partial T/\partial \mathrm{x} = 0$ are set, and on the contact surfaces with the heat transfer agent (including the end surface of the fin), the boundary conditions of the third kind are set

$$\left[\lambda\frac{\partial T}{\partial l} + \alpha T\right]_{l=0,L} = q\big|_{l=0,L}\,, \qquad (2)$$

here T – is the temperature, x, y – are the spatial coordinates, $l = x, y$ and L – are the size corresponding to these coordinates, q – is the heat flux density. It was assumed that the temperature of the heat transfer agent in contact with the finned surface has a constant value.

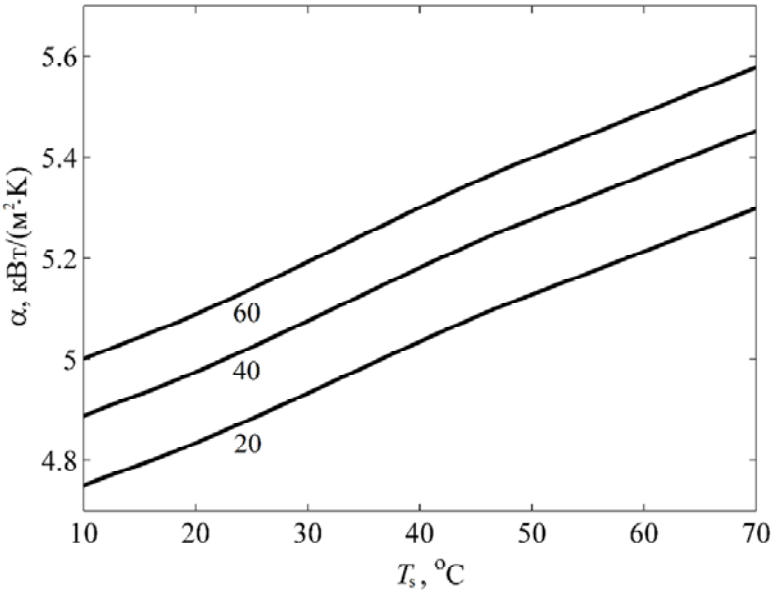

Fig. 1. Dependence of the local heat transfer coefficient LZ-TK-2 on the wall temperature

Рис. 1. Зависимости локального коэффициента теплоотдачи ЛЗ-ТК-2 от температуры стенки

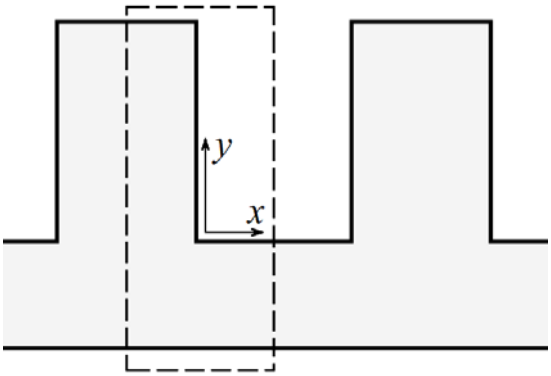

Fig. 1. Diagram of the finned wall and the boundary of the calculation area

Рис. 2. Схема оребренной стенки и границы расчетной области

To solve equations (1) and (2), we used the method of total approximation with splitting the problem by spatial coordinates [10–15]. The temperature field in the volume of the wall $\Delta T(x, y)$ and with distribution $\alpha(T_s)$ has a mutual influence on each other, since $\alpha(T_s)$ determines the amount of heat flow at the border of the finned surface with the heat transfer agent. Coordination of these distributions occurs in the process of obtaining a steady solution to a non-stationary problem.

The wall material was considered to be steel 12X18N10T, which has a thermal conductivity coefficient λ =19 Вт/(м·К). The temperature of the heat transfer agent in contact with the upper finned surface was set constant and equal to 50 °C, on the lower surface of the base its value was 60 °C. The value of the local heat transfer coefficient α was determined in accordance with the values of temperatures on the surface of the wall and the heat transfer agent. Fig. 3 shows the temperature field for the following geometric parameters of the finned walls: fin thickness 1.5 mm, fin height 2.5 mm, wall thickness 1.6 mm, the distance between the fins b = 1.3 мм. The calculation was performed for half of a periodically repeated fragment of the finned wall, so the size of the base in the x direction is 1.4 mm in the figure. The temperature values for the corresponding isolines are given in degrees Celsius. At the base of the wall, the temperature gradient is observed in the y direction, and there are practically no temperature gradients in the x direction.

The fin has a temperature gradient in both directions. In this case, the temperature distributions of the lower surfaces of the base and fin are close to uniform, so it is legitimate to use simplified calculation models that assume uniformity of temperature.

A change in geometric parameters affects the nature of the temperature field. Fig. 4 shows the calculation results with decreasing thickness of the fin (0.7 mm) and the wall (0.5 mm), while the height of the fin and the width of the base did not change.

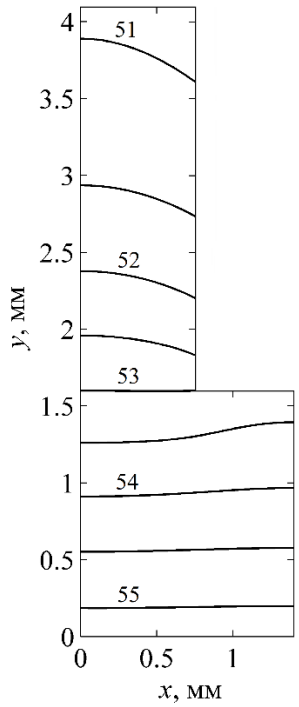

Fig. 3. Temperature field of the finned wall with the thickness of the fin 1.5 mm and the wall 1.6 mm

Рис. 3. Температурное поле оребренной стенки при толщинах ребра 1,5 мм и стенки 1,6 мм

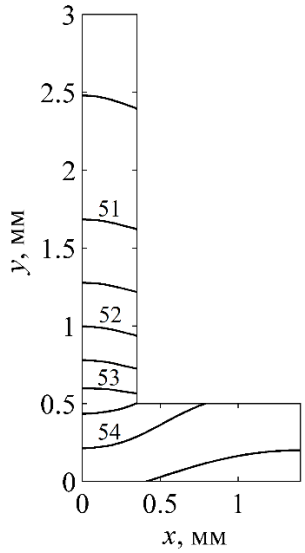

Fig. 4. Temperature field of the finned wall with the thickness of the fin 0.7 mm and the wall 0.5 mm

Рис. 4. Температурное поле оребренной стенки при толщинах ребра 0,7 мм и стенки 0,5 мм

At the base of the wall, the temperature field is substantially inhomogeneous already in both directions; in a thinner fin, an increase in the temperature difference in height is accompanied by a decrease in the transverse direction.

The heat transfer coefficient of the finned wall. The heat transfer coefficient k is an important integral characteristic of the heat transfer process of a finned wall with a heat transfer agent. Of greatest interest are the heat transfer characteristics in the volume of the wall and on the upper finned surface, therefore, we define the value of k as the ratio of the transmitted heat power to the temperature difference of the heat transfer agent T_h and the lower smooth surface of the wall, as well as to the area of this surface. The total heat flux transferred by the wall to the heat transfer agent was calculated on the basis of solving the heat conduction problem from the temperature distributions of the upper finned surface T_s and the local heat transfer coefficient α using the formula $\alpha(T_s - T_h)$. The heat flux was calculated in two model approximations. In the first case, the local heat transfer coefficient was determined taking into account its dependences on T_s and T_h, which are shown in Fig. 1, in the second, the value of α had a constant value corresponding to the surface temperature, i.e. the value α was set at $T_s = T_h$. Comparison of the calculation results allows us to estimate the error in applying the simplified mathematical model, which does not take into account the heterogeneity of the distribution of the heat transfer coefficient α over the finned surface.

When solving the problem of heat conduction on the lower surface of the wall base, an ideal heat supply was assumed, therefore, here the temperature was set with a uniform distribution and a value of T_0. In the calculations, the value of T_0 varied in the range of 30–70 °C; the temperature of the heat transfer agent in contact with the upper finned surface was fixed and equal to T_h = 20 °C. Fig. 5 shows the dependences $k(T_0)$ obtained using both considered model approximations. Lines 1 correspond to the wall configuration shown in fig. 3, lines 2 refer to the wall shown in Fig. 4. The horizontal lines were obtained as a result of calculations with a fixed local heat transfer coefficient α, which leads to the constancy of the values of k. Growing graphs were obtained in the calculations taking into account the temperature dependence $\alpha(T_s, T_h)$.

From the calculations of two model approximations, the dependences $k(T_0)$ were obtained, the difference between which increases with the growth of T_0 (fig. 5). The relative magnitude of this difference is shown in fig. 6. The largest discrepancy is expected to correspond to configuration 2, since higher temperature differences are set in the fin of smaller thickness, which ultimately leads to greater heterogeneity of the local heat transfer coefficient α over the finned surface.

In general, for the considered wall configurations, the maximum deviation, which is the error of the simplified model, does not exceed 5 %. Such an error value for many practical calculations is quite acceptable and the use of a simplified model for the considered configurations of the finned walls is justified. However, for other wall parameters and heat transfer agent properties, the discrepancy may be higher, therefore, in each case, the admissibility of the use of a simplified model requires justification and confirmation by evaluating the calculation error.

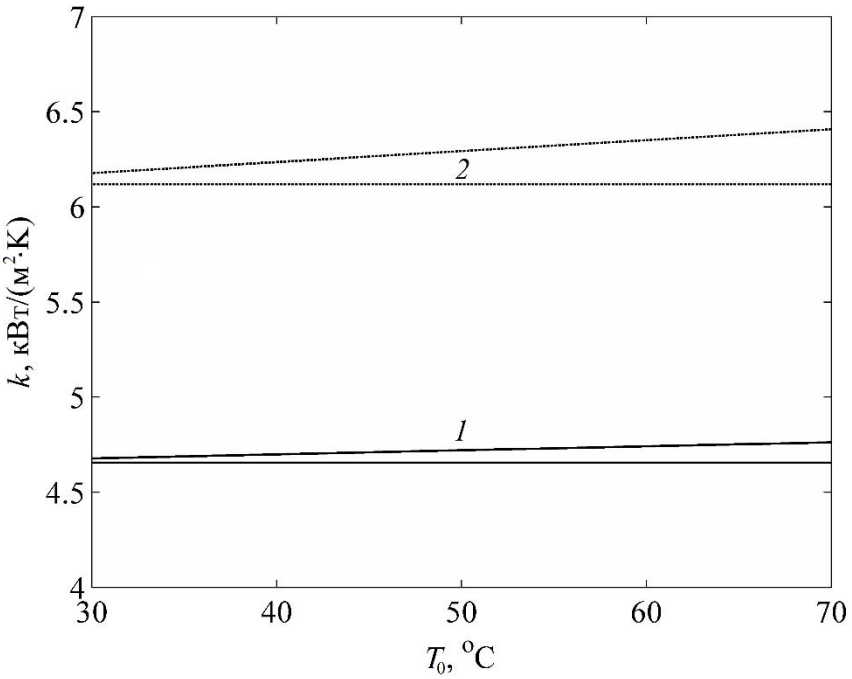

Fig. 5. Dependence of the heat transfer coefficient on the wall base temperature

Рис. 5. Зависимости коэффициента теплопередачи от температуры основания стенки

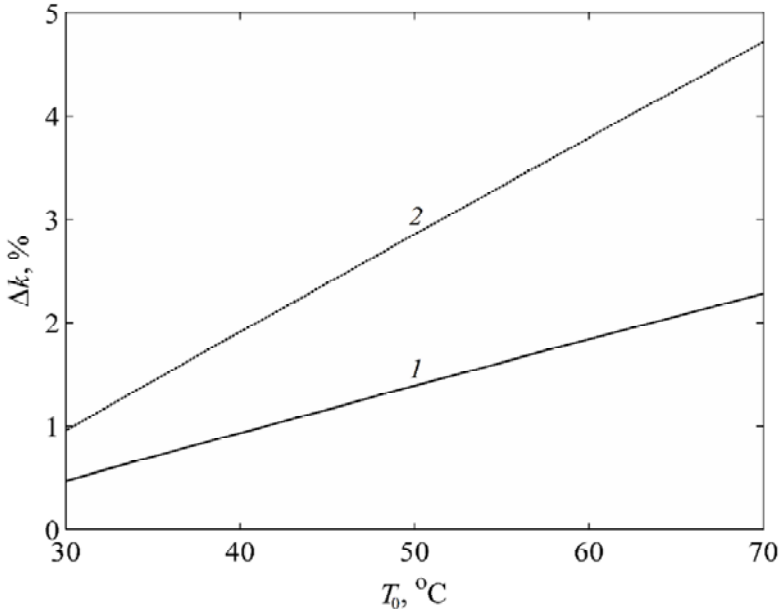

Fig. 6. Relative error in calculating the heat transfer coefficient in a simplified approximation

Рис. 6. Относительная погрешность расчета коэффициента теплопередачи в упрощенном приближении

Conclusion. Thus, the paper analyzes the heat transfer process in the finned wall of the heat exchanger. Based on the criteria relations, the temperature dependences of the local heat transfer coefficient α on a finned surface are obtained. The temperature field was calculated for two configurations of the finned wall, and the influence of the geometric parameters of the wall on the heterogeneity of the temperature distribution was estimated. The temperature dependences of the heat transfer coefficient are obtained using two model approximations that differ in taking into account α, the relative error of the simplified approximation is determined, which does not take into account the temperature dependence of the local heat transfer coefficient.

Acknowledgments. The reported study was funded by the Russian Foundation for Basic Research, the Government of the Krasnoyarsk Territory, the Krasnoyarsk Regional Fund of Science to the research project: "Theoretical and experimental investigation of heat and mass transfer processes in the two-phase systems of thermal control" (project № 18-41-242005).

Благодарности. Исследование выполнено при финансовой поддержке Российского фонда фундаментальных исследований, Правительства Красноярского края, Красноярского краевого фонда науки в рамках научного проекта: «Теоретическое и экспериментальное исследование процессов тепломассобмена в двухфазных системах термического контроля» (код проекта 18-41-242005).

References

1. Chebotarev V. E., Kosenko V. E. *Osnovy proyektirovaniya kosmicheskikh apparatov informatsionnogo obespecheniya* [Foundation of information satellites design]. Krasnoyarsk, Sib. gos. aerokosmich. un-t Publ., 2011, 488 p.

2. Kraev M. V., Zagar O. V., Kraev V. M., Golikovskaja K. F. *Nestatsionarnye teplovye rezhimy kosmicheskikh apparatov sputnikovykh system* [Unsteady thermal conditions of spacecrafts of satellite system]. Krasnoyarsk, Sib. gos. aerokosmich. un-t Publ., 2004, 282 p.

3. Vasil'ev E. N., Derevyanko V. A., Kosenko V. E. et al. *Vychislitel'nye tekhnologii*. [Computational modeling of heat exchange in thermoregulation systems of space vehicle]. 2009, Vol. 14, No. 6, P. 19–28 (In Russ.).

4. Vasil'ev E. N., Dekterev A. A. [Mathematical modeling of heat and mass transfer processes in the two-phase thermal control loop with the capillary pump]. *Vestnik SibGAU*. 2008, No. 4 (21), P. 12–16 (In Russ.).

5. Vasil'ev E. N. Optimization of Thermoelectric Cooling Regimes for Heat-Loaded Elements Taking into Account the Thermal Resistance of the Heat-Spreading System. Technical Physics. 2017, Vol. 62, No. 9, P. 1300–1306.

6. Roizen L. I., Dulkin I. N. *Teplovoy raschet orebrennykh poverkhnostey* [Thermal design of finned surfaces]. Moscow, Energiya Publ., 1977, 256 p.

7. Morkovin A. V., Plotnikov A. D., Borisenko T. B. [Heat transfer medium for heat pipes and external hydraulic circuits of thermal control systems of unmanned and manned spacecraft]. *Kosmicheskaya teknika i tekhnologii*. 2015, No. 3, P. 89–99 (In Russ.).

8. Morkovin A. V., Plotnikov A. D., Borisenko T. B. [Heat-transfer media for internal loops of thermal control systems for manned spacecraft]. *Kosmicheskaya tekhnika i tekhnologii.* 2013, No. 1, P. 79–87 (In Russ.).

9. Karminsky V. D. *Tekhnicheskaya termodinamika* [Technical thermodynamics and heat transfer]. Moscow, Marshrout Publ., 224 p.

10. Samarskii A. A. *Teoriya raznostnykh skhem* [The theory of difference schemes]. Moscow, Nauka Publ., 1989, 616 p.

11. Dulnev G. N. et al. *Primenenie EVM dlya resheniya zadach teploobmena* [Application of computer to solving heat transfer problems]. Moscow, Vysshaya Shkola Publ., 1990, 207 p.

12. Vasilyev E. N., Derevyanko V. V. [Mathematical model of heat exchange processes in honeycomb panels with heat pipes]. *Vestnik SibGAU*. 2010, No. 2 (28), P. 4–7 (In Russ.).

13. Vasil'ev E. N., Nikiforova E. S. [Mathematical model of heat exchange processes in honeycomb panels with heat pipes]. *Vestnik SibGAU*. 2005, No. 3, P. 23–26 (In Russ.).

14. Vasil'ev E. N. Calculation and Optimization of Thermoelectric Cooling Modes of Thermally Loaded Elements. *Technical Physics.* 2017, Vol. 62, No. 1, P. 90–96.

15. Vasil'ev E. N. Calculation of characteristics of thermoelectric cooling system of heat-loaded elements of radio electronic equipment. *Siberian Journal of Science and Technology*. 2018, Vol. 19, No. 1, P. 17–21.

Библиографические ссылки

1. Чеботарев В. Е., Косенко В. Е. Основы проектирования космических аппаратов информационного обеспечения / Сиб. гос. аэрокосмич. ун-т. Красноярск, 2011. 488 с.

2. Нестационарные тепловые режимы космических аппаратов спутниковых систем / М. В. Краев, О. В. Загар, В. М. Краев и др. ; Сиб. гос. аэрокосмич. ун-т. Красноярск, 2004. 282 с.

3. Вычислительное моделирование процессов теплообмена в системах терморегулирования космических аппаратов / Е. Н. Васильев, В. А. Деревянко, В. Е. Косенко и др. // Вычислительные технологии. 2009. Т. 14, вып. 6. С. 19–28.

4. Васильев Е. Н., Дектерев А. А. Математическое моделирование процессов тепломассообмена в двухфазном контуре терморегулирования с капиллярным насосом // Вестник СибГАУ. 2008. №. 4 (21). С. 12–16.

5. Васильев Е. Н. Оптимизация режимов термоэлектрического охлаждения теплонагруженных элементов с учетом термического сопротивления теплоотводящей системы // Журнал технической физики. 2017. Т. 87, № 9. С. 1290–1296.

6. Ройзен Л. И., Дулькин И. Н. Тепловой расчет оребренных поверхностей. М. : Энергия, 1977. 256 с.

7. Морковин А. В., Плотников А. Д., Борисенко Т. Б. Теплоносители для тепловых труб и наружных гидравлических контуров систем терморегулирования автоматических и пилотируемых космических аппаратов // Космическая техника и технологии. 2015. № 3. С. 89–99.

8. Морковин А. В., Плотников А. Д., Борисенко Т. Б. Теплоносители для внутренних контуров систем терморегулирования пилотируемых космических аппаратов // Космическая техника и технологии. 2013. № 1. С. 79–87.

9. Карминский В. Д. Техническая термодинамика и теплопередача. М. : Маршрут. 224 с.

10. Самарский А. А. Теория разностных схем. М. : Наука, 1989. 616 с.

11. Дульнев Г. Н., Парфенов В. Г., Сигалов А. В. Применение ЭВМ для решения задач теплообмена. М. : Высшая школа, 1990. 207 с.

12. Васильев Е. Н., Деревянко В. В. Математическая модель процессов теплообмена в сотовой панели с тепловыми трубами // Вестник СибГАУ. 2010. № 2 (28). С. 4–7.

13. Васильев Е. Н., Никифорова Е. С. Математическое моделирование теплового режима гипертеплопроводного радиатора мощного радиоэлемента // Вестник СибГАУ. 2005. № 3. С. 23–26.

14. Васильев Е. Н. Расчет и оптимизация режимов термоэлектрического охлаждения теплонагруженных элементов // Журнал технической физики. 2017. Т. 87, № 1. С. 80–86.

15. Vasil'ev E. N. Calculation of characteristics of thermoelectric cooling system of heat-loaded elements of radio electronic equipment // Сибирский журнал науки и технологий, 2018. Т. 19, №. 1. С. 17–21.

Vasil'ev Evgenii Nikolaevich – Cand. Sc., Senior Researcher; Federal research center "Krasnoyarsk Science Centre of the Siberian Branch of Russian Academy of Science", Institute of Computational Modelling of the Siberian Branch of Russian Academy of Science. E-mail: ven@icm.krasn.ru.

Васильев Евгений Николаевич – кандидат физико-математических наук, старший научный сотрудник; Федеральный исследовательский центр «Красноярский научный центр Сибирского отделения Российской академии наук», Институт вычислительного моделирования Сибирского отделения Российской академии наук. E-mail: ven@icm.krasn.ru.

UDC 621.455
Doi: 10.31772/2587-6066-2020-21-2-233-243

For citation: Ermoshkin Yu. M., Kochev Yu. V., Volkov D. V., Yakimov E. N., Ostapushchenko A. A. Design of a multifunctional electric propulsion subsystem of the spacecraft. *Siberian Journal of Science and Technology.* 2020, Vol. 21, No. 2, P. 233–243. Doi: 10.31772/2587-6066-2020-21-2-233-243

Для цитирования: Построение многофункциональной электрореактивной двигательной подсистемы космического аппарата / Ю. М. Ермошкин, Ю. В. Кочев, Д. В. Волков и др. // Сибирский журнал науки и технологий. 2020. Т. 21, № 2. С. 233–243. Doi: 10.31772/2587-6066-2020-21-2-233-243

DESIGN OF A MULTIFUNCTIONAL ELECTRIC PROPULSION SUBSYSTEM OF THE SPACECRAFT

Yu. M. Ermoshkin[1*], Yu. V. Kochev[1], D. V. Volkov[1], E. N. Yakimov[1], A. A. Ostapushchenko[2]

[1]JSC Academician M. F. Reshetnev Information Satellite Systems
52, Lenin Str., Zheleznogorsk, Krasnoyarsk region, 662972, Russian Federation
[2]JSC "Scientific & Industrial Centre "Polyus"
56v, Kirov Av., Tomsk, 634050, Russian Federation
[*]E-mail: erm@iss-reshetnev.ru

A common way to form an electric propulsion subsystem of the spacecraft is to create specialized equipment or to select the most suitable one from the ready-made ones. However, there are cases when the use of existing equipment is not optimal enough and leads to an unjustified increase of the subsystem mass. Therefore, the question of creating a minimum equipment set possibility from which it would be possible to form propulsion subsystems in optimal way is of interest. The set of tasks, variants of use and possible schemes of placing orbital correcting propulsion on the spacecraft are presented. The list of necessary propulsion subsystem elements is presented as follows: a thruster block, a tank, a xenon feed unit, a power processing unit consisting of a power unit and switching units, the complete set of cables and pipelines, the software and mechanical devices for control of the thrust vector (as an option). The necessary capacity of propellant tanks for the tasks of correction and raising of the satellite to GEO with a high-pulse Hall thruster is defined: for orbit correction tasks – up to100 kg, for orbit correction and raising to GEO tasks – up to200 kg. Necessary angle rates of mechanical devices for control of the thrust vector are defined taking into account possible schemes of placing thrusters on the spacecraft. It is shown that in cases when it is required to apply two or more thrusters to increase overall thrust, it is more preferable in the weight aspect to apply a combination of power and switching units instead of monoblock type of power processing units, and advantage can reach tens of kilograms. Provided the listed set of functional units is created, the offered concept will make it easy to form propulsion subsystems of the spacecraft for solving a wide range of tasks. It will reduce the time and money spent on creation of propulsion subsystem for new spacecrafts.

Keywords: thruster, spacecraft, power processing unit, tank, propellant feed unit, orbit correction.

ПОСТРОЕНИЕ МНОГОФУНКЦИОНАЛЬНОЙ ЭЛЕКТРОРЕАКТИВНОЙ ДВИГАТЕЛЬНОЙ ПОДСИСТЕМЫ КОСМИЧЕСКОГО АППАРАТА

Ю. М. Ермошкин[1*], Ю. В. Кочев[1], Д. В. Волков[1], Е. Н. Якимов[1], А. А. Остапущенко[2]

[1]АО «Информационные спутниковые системы» имени академика М. Ф. Решетнева»
Российская Федерация, 662972, г. Железногорск Красноярского края, ул. Ленина, 52
[2]АО «Научно-производственный центр «Полюс»
Российская Федерация, 634050, г. Томск, просп. Кирова, 56в
[*]E-mail: erm@iss-reshetnev.ru

Распространенным способом формирования электрореактивной двигательной подсистемы космического аппарата является создание специализированного оборудования или подбор наиболее подходящего из уже готового. Однако нередки случаи, когда применение имеющегося оборудования недостаточно оптимально и приводит к неоправданному увеличению массы подсистемы. Поэтому представляет интерес вопрос о возможности создания некоторого минимального набора оборудования, из которого можно было бы оптимальным образом формировать двигательные подсистемы. Представлен набор задач, варианты использования и возможные схемы размещения двигателей коррекции орбиты на космическом аппарате. Перечень необходимых элементов электрореактивной двигательной подсистемы представлен следующим образом: блок коррекции, бак, блок подачи рабочего тела, система преобразования и управления, состоящая из отдельно выполненного силового блока и коммутационных блоков, комплект кабелей и трубопроводов, программное обеспечение

и приводные механизмы для управления вектором тяги двигателей (как опция). Определена необходимая вместимость баков рабочего тела для задачи коррекции и довыведения спутника на геостационарную орбиту при использовании высокоимпульсного холловского двигателя: до 100 кг для задач коррекции орбиты, до 200 кг для задач довыведения и коррекции. С учетом схемы размещения двигателей на корпусе космического аппарата определены требуемые углы прокачки для механизмов управления вектором тяги двигателей. Показано, что в случаях, когда для увеличения суммарной тяги требуется применять два и более двигателя, в весовом отношении выгоднее применять вместо моноблочных систем преобразования и управления комбинацию из силовых и коммутационных блоков, причем преимущество может достигать десятков килограммов. При условии создания перечисленного набора функциональных блоков предложенная концепция позволит легко формировать двигательные подсистемы космических аппаратов для решения достаточно широкого круга задач. Это позволит снизить затраты времени и средств на создание двигательных подсистем для новых космических аппаратов.

Ключевые слова: двигатель, космический аппарат, система преобразования и управления, бак, блок подачи рабочего тела, коррекция орбиты.

Inroduction. A considerable part of automatic spacecraft (SC) contains propulsion subsystems that perform the tasks of correcting the orbit and controlling the angular position of the spacecraft. These subsystems can be built on the basis of chemical fuel thrusters or on the basis of electric propulsion (EP). Of the many types of EP, the most widespread are ion and plasma thrusters [1]. They are mainly used for tasks requiring high total pulse costs (from 3000 kNs and more). Their advantage over thrusters using chemical fuels lies in significantly greater propellant savings. However, to use EP it is necessary to apply special on-board electronic devices (in the domestic literature – conversion and control systems (SPU), in the foreign literature – Power Processing Unit (PPU)), which convert the on-board supply voltage to the voltage necessary for the thruster to work.

The choice of thruster size and the construction of the propulsion subsystem including the PPU architecture, depends on the size and type of the spacecraft and the amount of tasks assigned to the propulsion subsystem. This volume, characterized by the magnitude of the total momentum and thrust, can vary by several times. Accordingly, the concept of the propulsion subsystem that solves these problems should be significantly different. Obviously, the best solution in terms of minimum total mass is to build a propulsion subsystem based on specially designed blocks for each individual task. However, the creation of new blocks of the subsystem (thrusters, tanks, PPU) is associated with significant cost and time. Therefore, in practice, a different approach is often used - the formation of the propulsion subsystem based on a ready-made one, that is experimentally tested or flight-qualified units. This raises the question of what should be the set and concept of these blocks, from which it would be possible to build the propulsion subsystems of different SC, easily adapting to various tasks. This article is devoted to consideration of this issue. The concept of building a multifunctional electric propulsion subsystem based on a limited number of types of constituent elements is presented.

The list of tasks for the multifunctional electric propulsion subsystem. The following tasks for the multifunctional propulsion subsystem used on automatic SC can be formulated:

1) correction of the orbit of the geostationary SC;

2) raising a spacecraft to GSO and correcting its orbit;

3) raising a spacecraft to GSO and correcting its orbit with the simultaneous creation of control moments;

4) correction of the spacecraft orbit in the HEO (highly elliptical orbit);

5) finding main stage solutions for placing the interorbital transfer of payloads or the scientific spacecraft to the bodies of the solar system, service unmanned spacecraft flight support (servicing the spacecraft in the GSO, towing spent satellites into disposal orbit, etc.);

The composition of the multifunctional propulsion subsystem and the architecture of power processing units can be different depending on the tasks to be solved and the selected configuration of thrusters. These differences are a consequence of optimization of the propulsion subsystem in terms of mass characteristics.

The composition of the electric propulsion subsystem. According to the tasks, the full composition of the electric propulsion subsystem can be determined in the following way.

1) A propulsion unit or a correction unit, consisting, as a rule, of a gas distribution unit (BGR) and a thruster itself, containing an anode block and two cathodes. Note that the domestic school traditionally prefers the use of two cathodes in order to reserve this rather complex and loaded element, but in foreign practice, cathode reservation has not been used recently, based on operating experience and calculated cathode reliability indicators.

The number of propulsion units in the system can be different depending on the tasks being solved – from 1 to 8.

Both an ion and a plasma thruster can be used as an thruster for a multifunctional electric propulsion subsystem. In this article, we consider the use of a high-pulse plasma thruster, for example, from a number of thrusters developed at the Keldysh Center [2] or at the Fakel Design Bureau [3]. This type of thruster has a number of advantages over an ionic one: smaller mass and dimensions, relative cheapness with comparable efficient performance.

2) Power Processing Unit (PPU). It is necessary to power one, two, three or four thruster units as selected from a specific set. Various possible approaches will be discussed below. The importance of the search for optimal solutions for the construction of the PPU is due to the following factors specific to this device:

– significant mass;

– a large number of electronic elements, high complexity of the device as a whole;

– the high cost of flight samples;

– significant cost and time when developing new designs.

3) The propellant tank (xenon storage unit). The mass of the propellant tank is important due to large refueling. When designing a subsystem, various approaches are possible: an individual tank for each required refueling or a set of standard tanks of relatively small dimension or one large tank that allows various refuels. Obviously, the chosen concept should provide the minimum mass of the tank design or set of tanks for each typical task or groups of tasks with similar requirements.

4) Xenon feed unit. This device is necessary to lower the inlet (tank) pressure to the pressure required by the operating conditions of the thruster. The range of gas flow rates provided by such a device can be very large – from milligrams (for powering the plasma thruster) to grams per second (for powering gas-jet nozzles, if a gas-reactive system is used instead of a separate mono-fuel attitude propulsion subsystem).

5) A set of pipelines and cables connecting gas and electricity sources with recipients.

6) On-board software (OBSW) for controlling the subsystem blocks.

7) Mechanical drives for controlling the thrust vector of thrusters (as an additional option). If such devices are available, it is necessary to provide an auxiliary gas-reactive system to create control moments in the initial modes and modes of ensuring the survivability of the spacecraft.

The number of thrusters can be different depending on the tasks to be solved. This issue should be considered in more detail, since the thrusters and their number are determining factors in specifying the appearance of the propulsion subsystem. So, for task 1 (correction of the geostationary spacecraft orbit) with rigid fixing of the thrusters, the number of thrusters can vary from 4 to 8 (for example, 4, 6, 8). There are examples of spacecraft with 8 thrusters (4 for longitude correction, 4 for inclination correction, fig. 1) with cold reserve, that is, 4 thrusters are the main, 4 are the reserve. There are examples of applying the scheme with a reduced number of thrusters: 6 (2 for longitude correction, 4 for inclination correction, fig. 2) or 4 universal thrusters used both for longitude correction and inclination correction with functional redundancy (fig. 3).

Correcting the orbit of a geostationary spacecraft with a mass of 3–4 tons, thrust up to 80–100 mN is sufficient, which can be provided by one thruster [4]. Therefore, to solve the above problems, one redundant power supply and control device with the ability to power one thruster out of 8 or one of 4 is enough. A variant with 6 thrusters can be provided with some redundancy by a PPU with powering one thruster out of 8.

For task 2 (raising a spacecraft to GSO and correcting its orbit), it is necessary to provide increased thrust at the raising stage to reduce the time of raising. For this purpose special thrusters of increased thrust and power (for example, type SPD-140) can be used. However, from a structural and operational point of view, it is more convenient to use thrusters of the same type on board, and to increase thrust at the raising stage make thrusters run together or in a large number, if the available power of the power supply system (PSS) of the spacecraft allows.

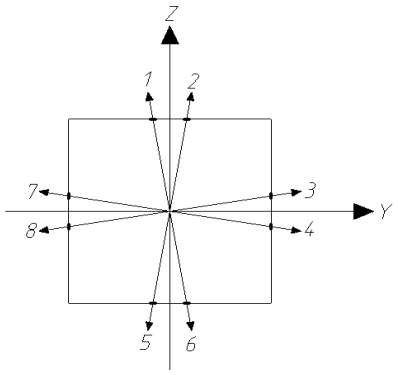

Fig. 1. Eight orbit correction thrusters placing in ±Y, ±Z directions (4 main, 4 reserve)

Рис. 1. Размещение 8 двигателей коррекции для коррекции орбиты в направлениях ±Y, ±Z (4 основных, 4 резервных)

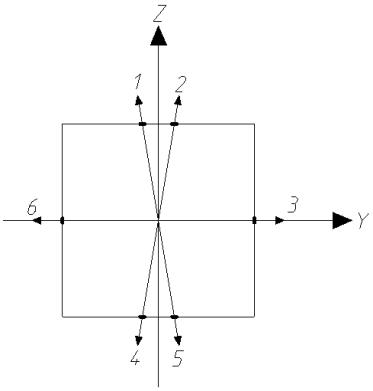

Fig. 2. Six orbit correction thrusters placing in ±Y, ±Z directions

Рис. 2. Размещение 6 двигателей коррекции для коррекции орбиты в направлениях ±Y, ±Z

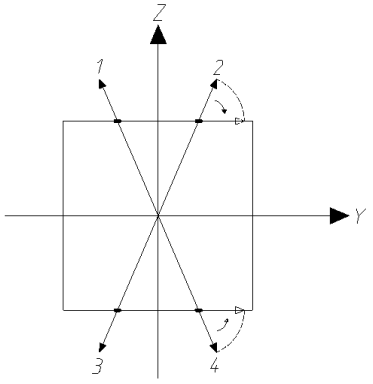

Fig. 3. Four orbit correction thrusters placing in ±Y, ±Z directions. Functional reserve

Рис. 3. Размещение 4 двигателей коррекции для коррекции орбиты в направлениях ±Y, ±Z. Резервирование – функциональное

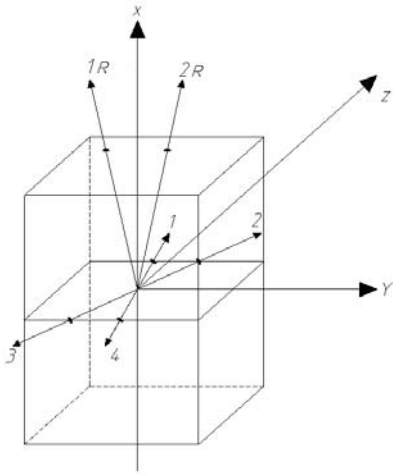

Fig. 4. Four orbit correction thrusters placing and two orbit raising thrusters (R) placing

Рис. 4. Размещение четырех двигателей коррекции для коррекции орбиты и двух двигателей для довыведения

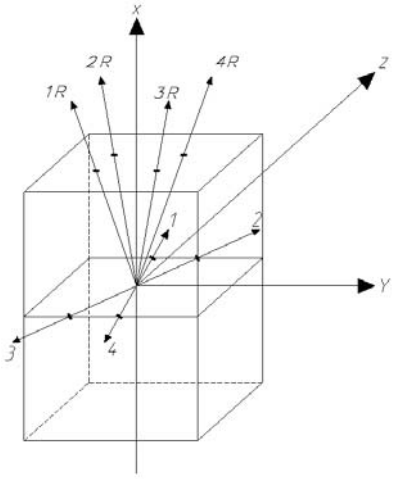

Fig. 5. Four orbit correction thrusters placing and four orbit raising thrusters (R) placing

Рис. 5. Размещение четырех двигателей коррекции для коррекции орбиты и четырех двигателей для довыведения

When there is a rigid fixing on the body of the spacecraft, it is advisable to use at least 2 separate thrusters at the same time; that is, the usual scheme of 4 or 6 correction thrusters should be supplemented with two more extension thrusters (fig. 4). It is advisable to place them along the + X axis, directing a jet stream into an area free of spacecraft structural elements. For the thrust impulse to be produced by these thrusters in the ± Y direction, that is, along the velocity vector, the satellite must be turned around the Z axis by 90°. It is also necessary to provide the ability to power 2 thrusters at the same time from a choice of 6 or 8. It should be noted that at the raising stage due to its limited time (no more than six months with a service life of 15 years or more), it is possible to do without reservation of power converters in the PPU, and use 2 thrusters.

If the thrust of 2 thrusters at the raising stage is not enough, then one or two thrusters can be additionally used (within the available power of the PSS), (fig. 5). It means that facilities should be provided to power them.

When installing thrusters on drives similar to European ones developed for the EUROSTAR 3000 spacecraft [5] for example, there is a possibility in principle to obtain the thrust of two thrusters at the same time in the same direction in addition to creating control moments along at least two axes (see. fig. 3). In this case, it is necessary to power two thrusters out of 4.

Construction of a power processing unit of thrusters. An important issue is the formation of the construction concept of the PPU to provide power to the thrusters. The traditional approach is to create a specialized device for the most common applications of thrusters, that is, to ensure the operation of one thruster from as selected 2, 4 or 8 [6; 7].

However, to solve the whole spectrum of problems, especially where simultaneous operation of two or more thrusters is required, the use of such control systems is not rational enough, since it requires the use of two or more control systems, or the development of special modifications of the device for simultaneously powering several thrusters, which is irrational, as it leads either to additional mass costs, or requires a new development with the corresponding costs of time and money. It is possible to propose another approach, which will minimize both the mass costs for solving various problems, and the costs of developing PPU. According to this concept, it is necessary to separate the tasks, that is, to create an unreserved power block that allows directly (without switching) powering one thruster and two switching blocks - to power one of two thrusters (we will designate it conventionally SU-2) and one thruster of four (SU-4). It is shown below, in tab. 1 and fig. 6–14 that a combination of these three blocks can provide, with the necessary level of redundancy, the supply of one, two, three, four thrusters from a certain set. Possible options for powering the PU using power and switching units are presented graphically in fig. 6–14.

Evaluations based on the current level of commutation technology excellence show that when solving tasks involving only one thruster during the entire mission (powering one of four, six, or eight thrusters), the option of using monoblock PPUs is more preferable. However, if it is necessary to power two or more thrusters, the use of the above mentioned combination of power and switching units can achieve significant mass savings while maintaining the required level of redundancy. Moreover, the advantage can reach tens of kilograms, which is a very significant amount, which may justify the costs of the development of power and switching units.

For the case when simultaneous operation of two thrusters at the same time for a limited period of time is required (for example, when raising a spacecraft to GSO), the cold reserve in the power unit can be abandoned, and then only two power units are used, in this case the weight advantage of the options based on combinations of power and switching units is increasing even more.

Table 1

Options for constructing a thruster power circuit

Task	Number of thrusters	Powering option	Number of units					ΔM_{Σ} [kg]***
			Monoblock PPU version		Version based on a power unit and switching units			
			PPU for powering 1 out of 4 thrusters	PPU for powering 1 out of 8 thrusters	Power unit	SU-2	SU-4	
Geostationary and highly elliptical SC								
1. Correction of GSO	8	1 out of 8	–	1	2	–	2*	Minus 13
2. Correction of GSO	6	1 out of 6	–	1	2	1*	1*	Minus 8
3. Correction of GSO	4	1 out of 4	1	–	2	–	1	Minus 8
4. Correction of HEO	4	2 out of 4 constant	2	–	3**	–	1*	11
5. Correction of HEO	6	2 out of 6 constant	–	2	3**	1*	1*	18.5
6. Final ascent and correction of GSO	4	2 out of 4 temporary, 1 out of 4 constant	2	–	2	–	1	25.5
7. Final ascent and correction of GSO	6	2 out of 6 temporary, 1 out of 6 constant	0	2	2	1*	1*	33
8. Final ascent and correction of GSO	8	2 out of 8 temporarily, 1 out of 8 constant	0	2	2	–	2*	28
9. Accelerated final ascent and correction of GSO	8	4 out of 8 temporary, 1 out of 4 constant	4	–	4	1*	1*	56
Sustainer task								
10. Long continuous operation (acceleration, braking)	2	2 out of 2	2	–	3**	1	–	16
					2	–	–	38
11. Long continuous operation (acceleration, braking)	3	3 out of 3	3	–	4**	–	1	30
					3	–	–	57
12. Long continuous operation (acceleration, braking)	4	4 out of 4	4	–	5**	–	1	49
					4	–	–	76

* if using splitter cables;
** one power unit in cold reserve;
*** the difference in the total mass of the monoblock PPU version and the variant based on the power unit and switching units.

Thus, the concept of dividing the PPU into power and switching units is more flexible and allows solving various problems that require the operation of several thrusters in a more optimal way compared to the option of monoblock PPU. There are also options with direct power supply of thrusters without switching blocks. In this case, each thruster has its own power unit. The number of such sets of thruster-PPU can be from one to four in a reasonable range of available power of the PSS. Another important advantage of the concept of constructing a conversion and control system on the basis of individual blocks is the absence of the need to develop new variants of monoblock PPU for each new task, which makes it possible to significantly reduce the time and money spent on creating a propulsion subsystem.

Estimation of required tank capacity. For the typical task of raising and correcting the orbit of a geostationary spacecraft with a mass of 3000 kg for a service life of 15 years, about 4100 kNs (≈420 t·s) of the total pulse is required. It is advisable to choose a thruster with a power of about 2 kW with a specific impulse of up to 2700 s as a thruster for a promising propulsion subsystem. With this specific impulse, 156 kg of xenon will be required to produce this total impulse.

Taking into account 10 % of the reserve for leaks, non-produced balance and guarantee stock, refueling should be 170 kg.

Taking into account an additional 10–15 kg to ensure the operation of the pneumatic system on cold gas, which is necessary for passing the initial orientation modes and survivability modes in the version of the system with drives, the total stock will be up to 187 kg. Thus, a tank capacity of 200 kg of xenon is sufficient to ensure the listed tasks.

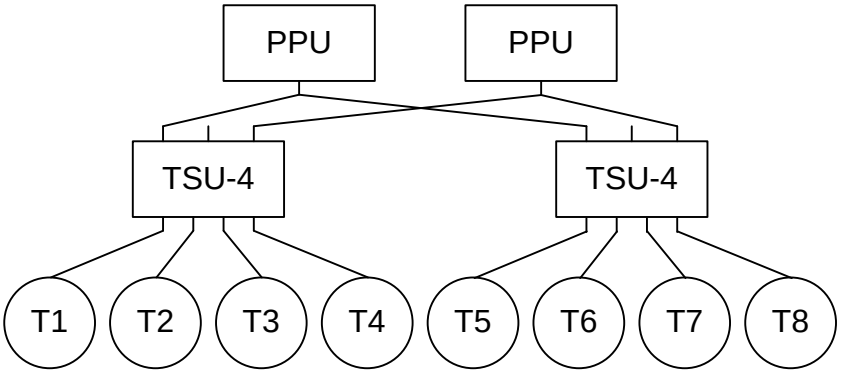

Fig. 6. The powering of one out of eight thrusters or temporary powering
of two out of eight thrusters and constant powering of one out of eight thrusters

Рис. 6. Запитка одного двигателя из восьми или двух из восьми временно
и одного из восьми постоянно

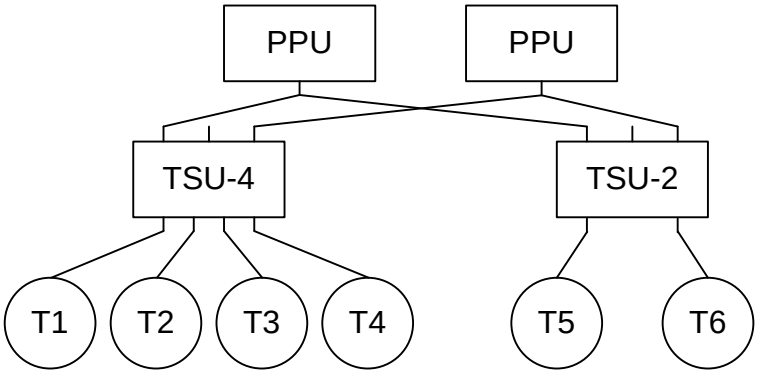

Fig. 7. The powering of one out of six thrusters or temporary powering
of two out of six thrusters and constant powering of one out of six thrusters

Рис. 7. Запитка одного двигателя из шести или двух из шести временно
и одного из шести постоянно

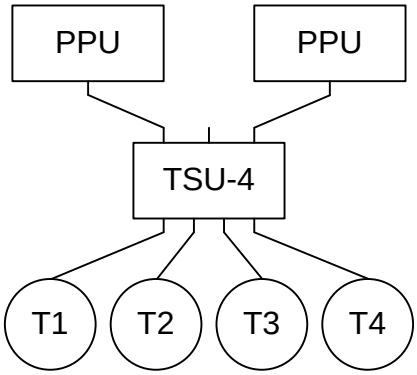

Fig. 8. The powering of one out of four thruster or temporary powering
of two out of four thrusters and constant powering of one out of four thrusters

Рис. 8. Запитка одного двигателя из четырех или двух из четырех временно
и одного из четырех постоянно

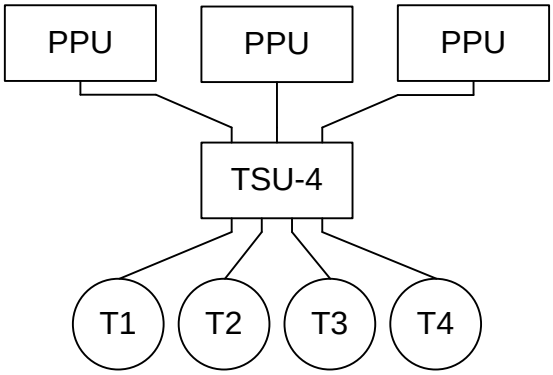

Fig. 9. Constant powering of two out of four thrusters

Рис. 9. Запитка двух из четырех двигателей постоянно

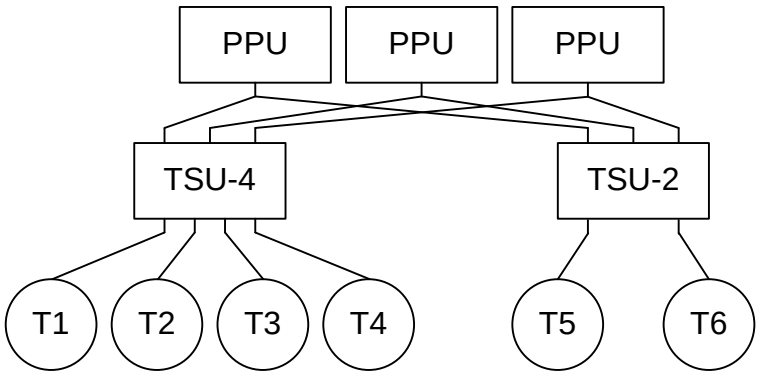

Fig. 10. Constant powering of two out of six thrusters

Рис. 10. Запитка двух из шести двигателей постоянно

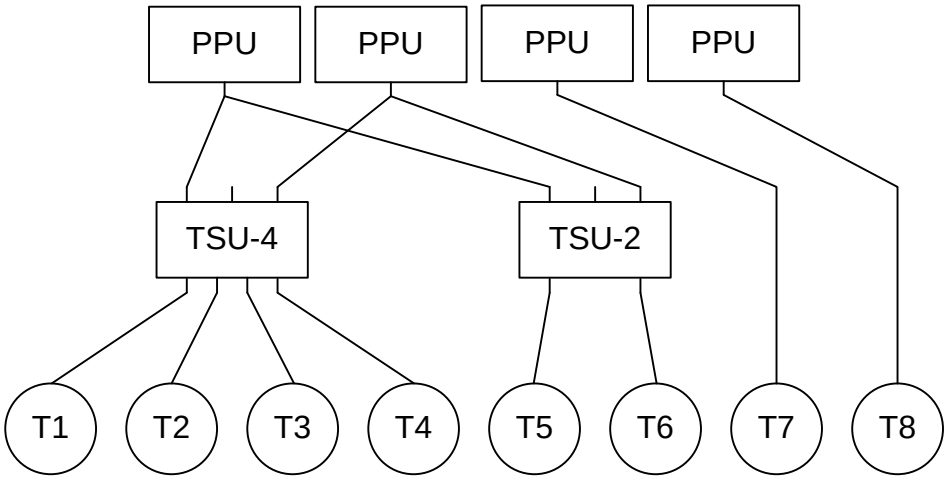

Fig. 11. Temporary powering of four out of eight thrusters and constant powering of one out of four thrusters

Рис. 11. Запитка четырех из восьми двигателей временно и одного из четырех постоянно

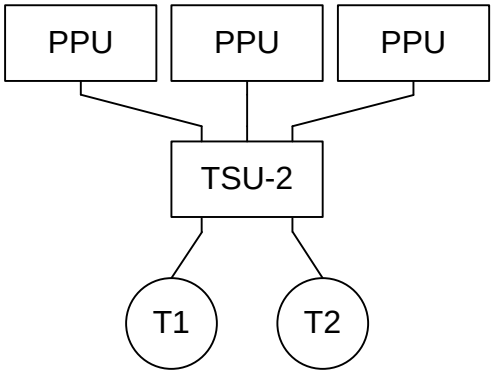

Fig. 12. Constant powering of two out of two thrusters with PPU reservation

Рис. 12. Запитка двух из двух двигателей постоянно с резервированием по силовому блоку

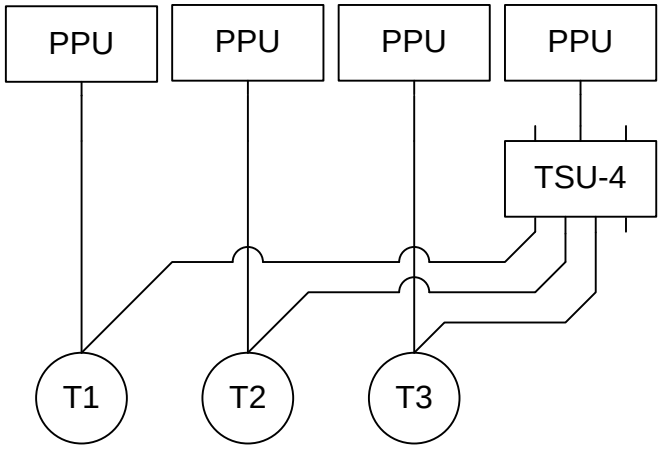

Fig. 13. Constant powering of three out of three thrusters with PPU reservation

Рис. 13. Запитка трех из трех двигателей постоянно с резервированием по силовому блоку

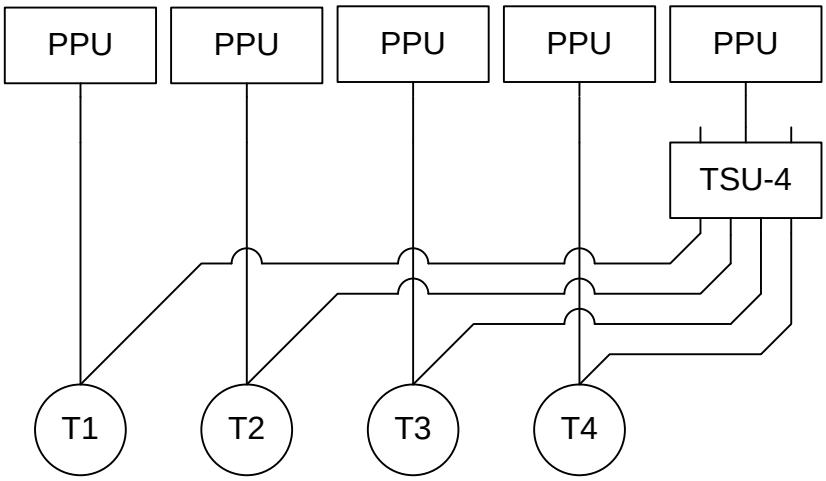

Fig. 14. Constant powering of four out of four thrusters with PPU reservation

Рис. 14. Запитка четырех из четырех двигателей постоянно с резервированием по силовому блоку

Table 2

The quantitative composition of the constituent elements of the propulsion subsystem for the solution of various tasks

Unit	Possible number in the propulsion subsystem
PU (thruster)	up to 8
PPU (power unit)	up to 5
SU-2 (switching unit with output to 2 thrusters)	up to 2
SU-4 (switching unit with output to 4 thrusters)	up to 2
XFU (high flow rate xenon feed unit)	1
T-100 (100 kg tank)	1
T-200 (200 kg tank)	1
Cable set	1
Pipeline set	1
On-board software (OBSW), set	1
Gas-jet nozzles (for version with actuators)	up to 8
Additionally	
Two-stage drive with flow angles ± 90°	4
Orientation device with two-stage drives and rods	2

It should be noted that in the presence of a monofuel propulsion subsystem, it is possible to abandon a pneumatic system using cold gas and drives to create control moments.

If the task of final ascent is not set, then about 200 t·s from the total impulse will be enough to ensure orbit correction. Consequently, a tank capacity of 100 kg is sufficient, taking into account the reserve for leaks, non-produced balance, guarantee balance and reserve to ensure the operation of the pneumatic system on cold gas (if any). Thus, for the operation of the propulsion subsystem, it is enough to have tanks with a capacity of 100 and 200 kg. It is desirable that the tanks have identical dimensions and design, different only in the thickness of the pressure restraint layer and weight, for example, on the basis of the tank developed at ISS JSC [8]. If it is necessary the combination of such tanks can easily obtain a total capacity of 300 and 400 kg. Taking into account the actually achieved perfection of the design of the tanks, characterized by the value of the tank coefficient (the ratio of the mass of the tank to the maximum refueling) of about 0.1, the mass savings in the case of creating a tank with a capacity of 200 kg can reach about 10 kg, for a tank with a capacity of 100 kg – up to 20 kg compared to the option of placing the stock of the propellant in a tank with a capacity of 300 kg.

Xenon feed unit requirements. When xenon consumption in one thruster is about 4 mg/s and there is a simultaneous operation of up to 4 thrusters, then it is necessary to ensure consumption up to 16 mg/s. When maximum 4 nozzles operate simultaneously it is necessary to ensure a flow rate of about 1.6 g/s for the pneumatic system to work on cold gas. Thus, when there is a pneumatic system, a xenon feed unit with a very large flow range from 4 mg/s to 1.6 g/s is needed.

Basic requirements for the drive (orientation mechanism) of thrusters. a cross-shaped arrangement of 4 thrusters (fig. 3) is taken as a basis with an optimal deviation of the thrust line from the Z direction of 20–25 °, then to create thrust in the Y direction (for a final ascent) it is necessary to deploy two thrusters at an angle of about 70°. To provide pitch control torque (around the Z axis), one or two thrusters must be turned towards ± X at an angle of about 90°. Thus, it is desirable to have a two-stage drive for one thruster with pumping angles up to ± 90°. If rods are also provided for changing the position of the thrusters, drives of this type can be placed in their root and end parts.

In view of the foregoing, the quantitative composition of the constituent elements of the propulsion subsystem for the solution of the tasks enumerated in tab. 1 is presented in tab. 2.

Conclusion. It is shown that if a high-pulse plasma thruster with a power of 2 kW, a power converter unit, switching units with access to two and four thrusters, a xenon feed unit with a wide flow range, tanks for 100 and 200 kg of xenon, and also, as an additional options, two-stage drives or combinations of drives with rods are created, then it is possible to form an electric propulsion subsystem for solving a wide range of tasks – from orbital correction in the simplest version of four motionless mounted thrusters to a multifunctional system that provides raising a spacecraft to the GSO, orbit correction and creation of control moments. The presence of these blocks will also allow the formation of propulsion subsystems for solving various sustainer tasks in a fairly wide range of available power of the onboard power supply system. The construction of a conversion and control system in the form of separate power and switching units will allow in many cases to reduce weight, simplify the formation of the propulsion subsystem as a whole, and reduce the cost of its development. Thus, if the presented concept is implemented, it will create conditions for expanding, in justified cases, the scope of application of electric propulsion subsystems and increasing on this basis the overall efficiency of a spacecraft by reducing the mass of the propulsion subsystem compared to alternative types, in particular subsystems based on chemical thrusters.

References

1. Lev D., Myers R. V., Lemmer K. M. et al. The Technological and Commercial Expansion of Electric

Propulsion in the Past 24 Years. *35th Electric Propulsion Conference*. IEPC-2017-242. Georgia Institute of Technology. USA, October 8–12, 2017, 18 p.

2. Lovtsov A. S., Tomilin D. A., Muravlev V. A. Development of the high-voltage Hall-effect thrusters in the Keldish Research Centre. *68th International Astronautical Congress*. IAC-17-C4.4.4, Adelaide, Australia, 25–29 September 2017, 5 p.

3. Gnizdor R., Komarov A., Mitrofanova O., Saevets P., Semenenko D. High-impulse SPT-100D Thruster with discharge power of 1.0…3.0 kW. *The 35th International Electric Propulsion Conference, Georgia Institute of Technology*. USA, October 8–12, 2017, 8 p.

4. Ermoshkin Yu. M., Bulynin Yu. L. [Assessment of the minimum permissible thrust of engines for correcting the orbit of geostationary satellites]. *Upravlenie dvizheniem i navigaciya letatelnykh apparatov*. *Chast 1. Sbornik trudov XIII Vserossiiskogo nauchno-tekhnicheskogo seminara po upravleniyu dvizheniem i navigacii letatelnykh apparatov*. Samara, 13–15 june 2007. P. 109–111 (In Russ.).

5. Falkner M., Nitschko T., Zemann J., Mitterbauer G., Traxler G. Electric Propulsion Thruster Pointing Mechanism (TPM) For EUROSTAR 3000: Design & Development Test Results. *The 29th International Electric Propulsion Conference*. IEPC-2005-001. Princeton University, Okt. 31 – Nov. 4, 2005, 10 p.

6. Gollor M., Schwab U., Boss M., Bourguignon E. et al. Power Processing Units – activities in Europe 2015. *34th International Electric Propulsion Conference*. IEPC-2015-225, Kobe-Hyogo, Japan, July 4–10, 2015, 13 p.

7. Gladuchenko V. N., Galaiko V. N., Gordeev K. G., Ermoshkin Yu. M., Mikhailov M. V., Yakimov E. N. Modern status and future directions of evolution of power processing units for electric plasma thrusters. *Electronic and electromechanical systems and devices*. Scientific papers, JSC “NPC “Polus”. Tomsk Polytechnic University Press, 2016, p. 59–65.

8. Kravchenko I. A., Mikheev A. V., Borodin L. M. Application features of metal composite tanks on board of SC. *Proceedings of XYII International conference “Reshetnevskie chteniya”*. 12–14 November, Krasnoyarsk, 2013, P. 71–72.

9. Ermoshkin Yu. M., Yakimov E. N On the concepts of the station keeping and geostationary orbit injection thruster’s application. *Proceedings of XVI International conf. “Aviation and Space”*. Moscow, 2017, Nov. 20–24, P. 92–93.

10. Ermoshkin Yu. M. [Electric propulsion’s rational application range on the applied spacecrafts]. *Vestnik SibGAU*. 2011, No. 2 (35), P. 109–113 (In Russ.).

11. Yermoshkin Yu. M., Volkov D. V., Yakimov E. N. On the concept of “all electric propulsion spacecraft”. *Siberian Journal of Science and Technology*. 2018, Vol. 19, No. 3, P. 489–496. Doi: 10.31772/2587-6066-2018-19-3-489-496.

12. Ostrovsky V. G., Sukhov Yu. I. [Development and operation of electric thrusters and electric propulsion systems at OKB-1 – TsKBEM – NPO “Energia” – RSC “Energia” named S.P.Korolev (1958-2011)]. *Raketno-kosmicheskaya tekhnika. Trudy*. 2011. Ser. XII., Iss. 3–4, P. 122–127 (in Russ.).

13. Khodnenko V. P. Activities of VNIIEM in EPT field. History, our days and prospects. *33rd International Electric Propulsion Conference.* IEPC-2013-65. The George Washington University. D.C. US. October 6–10, 2013.

14. De Tata M., Frigor P., Beekmans S. et al. SGEO Electric Propulsion Subsystem Development Status and Future Opportunities. *33rd International Electric Propulsion Conference*. IEPC-2013-144. The George Washington University, USA, October, 6–10, 2013, 11 p.

15. Ferreira J. L., Martins A. A., Miranda R. A. et al. Development of a Solar Electric Propulsion System for the First Brazilian Deep Space Mission. *35th Electric Propulsion Conference*. IEPC-2017-166. Georgia Institute of Technology. USA, October 8–12, 2017, 14 p.

Библиографические ссылки

1. The Technological and Commercial Expansion of Electric Propulsion in the Past 24 Years / D. Lev, R. V. Myers, K. M. Lemmer et al. // 35th Electric Propulsion Conference. IEPC-2017-242. Georgia Institute of Technology. USA, October 8–12, 2017. 18 p.

2. Ловцов А. С., Томилин Д. А., Муравлев В. А. Разработка высоковольтных холловских двигателей в Центре Келдыша // 68th International Astronautical Congress. IAC-17-C4.4.4, Adelaide, Australia, 25–29 September 2017. 5 p.

3. High-impulse SPT-100D Thruster with discharge power of 1.0…3.0 kW / R. Gnizdor, A. Komarov, O. Mitrofanova et al. // The 35th International Electric Propulsion Conference, Georgia Institute of Technology. USA, October 8–12, 2017. 8 p.

4. Ермошкин Ю. М., Булынин Ю. Л. Оценка минимально допустимой тяги двигателей коррекции орбиты геостационарных спутников // Управление движением и навигация летательных аппаратов : сб. тр. XIII Всеросс. науч.-технич. семинара по управлению движением и навигации летательных аппаратов / Самар. гос. аэрокосмич. ун-т им. акад. С. П. Королева. Самара, 13–15 июня 2007 г. Ч. I. С. 109–111.

5. Electric Propulsion Thruster Pointing Mechanism (TPM) For EUROSTAR 3000: Design & Development Test Results / M. Falkner, T. Nitschko, J. Zemann et al. // The 29th International Electric Propulsion Conference. IEPC-2005-001. Princeton University, Okt. 31-Nov. 4, 2005. 10 p.

6. Power Processing Units – activities in Europe 2015 / M. Gollor, U. Schwab, M. Boss et al. // 34th International Electric Propulsion Conference. IEPC-2015-225, Kobe-Hyogo, Japan, July 4–10, 2015. 13 p.

7. Современное состояние и перспективы развития систем преобразования и управления электрореактивными плазменными двигателями / В. Н. Гладущенко, В. Н. Галайко, К. Г. Гордеев и др. // Электронные и электромеханические системы и устройства : сб. науч. тр. Томск : АО НПЦ «Полюс» ; Изд. Томского политехнич. ун-та. 2016. С. 59–65.

8. Кравченко И. А., Михеев А. В., Бородин Л. М. Особенности применения металлокомпозитных баков на борту КА // Решетневские чтения : материалы XVII междунар. науч.-технич. конф. Красноярск, 12–14 ноября 2013. Ч. 1. С. 71–72.

9. Ермошкин Ю. М., Якимов Е. Н. О концепциях применения двигателей коррекции и довыведения // Авиация и космонавтика – 2017 : тез. доклада 16-й Междунар. конф. Москва, МАИ, 20–24 ноября 2017. С. 92–93.

10. Ермошкин Ю. М. Области рационального применения электрореактивных двигательных установок на космических аппаратах прикладного назначения // Вестник СибГАУ. 2011. № 2 (35). С. 109–113.

11. Ермошкин Ю. М., Волков Д. В., Якимов Е. Н. О концепции «полностью электрического космического аппарата» // Сибирский журнал науки и технологий. 2018. Т. 19, № 3. С. 489–496. Doi: 10.31772/2587-6066-2018-19-3-489-496.

12. Островский В. Г., Сухов Ю. И. Разработка, создание и эксплуатация электроракетных двигателей и электроракетных двигательных установок в ОКБ-1-ЦКБЭМ-НПО «Энергия»-РКК «Энергия» им. С. П. Королева (1958-2011 г.) // Ракетно-космическая техника. Труды. Сер. XII. Вып. 3–4. С. 122–127.

13. Khodnenko V. P. Activities of VNIIEM in EPT field. History, our days and prospects // 33rd International Electric Propulsion Conference. IEPC-2013-65. The George Washington University. D.C. US. October 6–10, 2013. 19 p.

14. SGEO Electric Propulsion Subsystem Development Status and Future Opportunities / M. De Tata, P. Frigor, S. Beekmans et al. // 33rd International Electric Propulsion Conference. IEPC-2013-144. The George Washington University, USA, October, 6–10, 2013. 11 p.

15. Development of a Solar Electric Propulsion System for the First Brazilian Deep Space Mission / J.L.Ferreira, A.A.Martins, R.A.Miranda et al. // 35th Electric Propulsion Conference. IEPC-2017-166. Georgia Institute of Technology. USA, October 8–12, 2017. 14 p.

Ermoshkin Yuriy Mikhailovich – D. Sc. (tech.), head of propulsion department; JSC “Academician M. F. Reshetnev Information Satellite Systems”. E-mail: erm@iss-reshetnev.ru.

Kochev Yuriy Vladimirovich – Cand. Sc. (tech.), head of propulsion subsystem electric design group; JSC “Academician M. F. Reshetnev Information Satellite Systems”. E-mail: koch@iss-reshetnev.ru.

Volkov Dmitry Viktorovich – head of propulsion subsystem design sector; JSC “Academician M. F. Reshetnev Information Satellite Systems”. E-mail: dmitri@iss-reshetnev.ru.

Yakimov Evgeniy Nikolaevich – head of attitude control and propulsion division; JSC “Academician M. F. Reshetnev Information Satellite Systems”. E-mail: yen@iss-reshetnev.ru.

Ostapushchenko Alexander Anatolyevich – leading design thrusterer; JSC “Scientific & Industrial Centre “Polyus”.

Ермошкин Юрий Михайлович – доктор технических наук, доцент, начальник лаборатории; АО «Информационные спутниковые системы» имени академика М. Ф. Решетнева». E-mail: erm@iss-reshetnev.ru.

Кочев Юрий Владимирович – кандидат технических наук, начальник группы; АО «Информационные спутниковые системы» имени академика М. Ф. Решетнева». E-mail: koch@iss-reshetnev.ru.

Волков Дмитрий Викторович – начальник сектора; АО «Информационные спутниковые системы» имени академика М. Ф. Решетнева». E-mail: dmitri@iss-reshetnev.ru.

Якимов Евгений Николаевич – начальник отделения; АО «Информационные спутниковые системы» имени академика М. Ф. Решетнева». E-mail: yen@iss-reshetnev.ru.

Остапущенко Александр Анатольевич – ведущий инженер-конструктор; АО «Научно-производственный центр «Полюс».

UDC 621.396.69:629.76/.78
Doi: 10.31772/2587-6066-2020-21-2-244-251

For citation: Kochev Yu. V., Ermoshkin Yu. M., Ostapushchenko A. A. The use of sealed gas-filled EEE-parts in units intended for long operation under vacuum and increased voltage environment. *Siberian Journal of Science and Technology.* 2020, Vol. 21, No. 2, P. 244–251. Doi: 10.31772/2587-6066-2020-21-2-244-251

Для цитирования: Кочев Ю. В., Ермошкин Ю. М., Остапущенко А. А. О применении герметичных газонаполненных электрорадиоизделий в приборах, длительно работающих в условиях вакуума и повышенного напряжения // Сибирский журнал науки и технологий. 2020. Т. 21, № 2. С. 244–251. Doi: 10.31772/2587-6066-2020-21-2-244-251

THE USE OF SEALED GAS-FILLED EEE-PARTS IN UNITS INTENDED FOR LONG OPERATION UNDER VACUUM AND INCREASED VOLTAGE ENVIRONMENT

Yu. V. Kochev[1], Yu. M. Ermoshkin[1*], A. A. Ostapushchenko[2]

[1]JSC Academician M. F. Reshetnev Information Satellite Systems
52, Lenin St., Zheleznogorsk, Krasnoyarsk region, 662972, Russian Federation
[2]JSC "Scientific & Industrial Centre "Polyus"
56v, Kirov Av., Tomsk, 634050, Russian Federation
[*]E-mail: erm@iss-reshetnev.ru

Today, the scope of application of electric propulsion systems for orbit correction and spacecraft's attitude control is rapidly expanding due to their high efficiency compared to liquid jet systems. The main elements of electric jet systems are plasma or ion thrusters. To ensure power supply of such thrusters, complex electronic power processing systems – power processing units (PPU) – are used. These units are capable to operate for a long time (up to 15 years or more) in a high vacuum environment and generate sufficiently high accelerating voltages – from 300 V and higher. PPU's comprise various EEE-parts, mainly in the case design. As a rule, the technology of their production is such that air or nitrogen is initially located inside the housing at atmospheric pressure. During the operation of the unit, the non-absolute hermeticity causes pressure decrease inside EEE housings. Due to high voltages applied, this can lead to electrical breakdowns between current-carrying elements inside the parts, their failure with the subsequent failure of the functional blocks of the unit. The paper considers the physical principles of the breakdown occurrence inside EEE-parts cases. The results of non-hermiticity measurements of several types of HV EEE-parts are presented. The dynamics of the pressure drop to the values dangerous from the point of view of breakdown event and the relevant occurrence duration are estimated. It is shown that duration of being exposed to the pressure-dangerous conditions can be as long as spacecraft service lifetime. It can make difficult to use packaged gas-filled EEE-parts at the level of units intended to operate in non-pressurized compartments of spacecraft. Recommendations are provided for selecting the design of EEE parts with an operating voltage of about 300 V or more, as well as circuit solutions used to develop high-voltage equipment intended to operate in vacuum environment.

Keywords: Paschen law, breakdown, vacuum, non-hermeticity, EEE-parts, power processing unit, spacecraft.

О ПРИМЕНЕНИИ ГЕРМЕТИЧНЫХ ГАЗОНАПОЛНЕННЫХ ЭЛЕКТРОРАДИОИЗДЕЛИЙ В ПРИБОРАХ, ДЛИТЕЛЬНО РАБОТАЮЩИХ В УСЛОВИЯХ ВАКУУМА И ПОВЫШЕННОГО НАПРЯЖЕНИЯ

Ю. В. Кочев[1], Ю. М. Ермошкин[1*], А. А. Остапущенко[2]

[1]АО «Информационные спутниковые системы» имени академика М. Ф. Решетнева»
Российская Федерация, 662972, г. Железногорск Красноярского края, ул. Ленина, 52
[2]АО «Научно-производственный центр «Полюс»
Российская Федерация, 634050, г. Томск, просп. Кирова, 56в
[*]E-mail: erm@iss-reshetnev.ru

В настоящее время динамично расширяется сфера применения электрореактивных двигательных систем для коррекции орбиты и управления положением космических аппаратов. Это вызвано их высокой экономичностью по сравнению с системами на базе жидкостных реактивных двигателей. Основными элементами электрореактивных систем являются плазменные или ионные двигатели. Для электропитания таких двигателей применяются сложные энергопреобразующие электронные приборы – системы преобразования и управле-

ния (СПУ). Такие приборы должны длительно (до 15 лет и более) работать в условиях глубокого вакуума и при этом вырабатывать достаточно высокие ускоряющие напряжения – от 300 В и выше. В составе приборов СПУ применяются различные электрорадиоизделия (ЭРИ), преимущественно в корпусном исполнении. Как правило, технология их изготовления такова, что внутри корпуса изначально находится воздух или азот при атмосферном давлении. Однако в процессе эксплуатации прибора вследствие неабсолютной герметичности корпусов ЭРИ давление внутри них снижается. В условиях приложения повышенных напряжений это может приводить к возникновению электрических пробоев между токоведущими частями внутри элементов, выходу их из строя с последующим отказом функциональных блоков прибора. В статье рассматриваются физические принципы возникновения пробоя в подкорпусном пространстве электрорадиоизделий. Приведены результаты измерения негерметичности некоторых типов высоковольтных ЭРИ. Дается оценка динамики спада давления до опасной с точки зрения пробоя зоны и длительности нахождения в ней. Показано, что длительность нахождения в опасной зоне по давлению может быть сопоставимой со сроком службы космического аппарата. Данное обстоятельство может затруднить применение корпусных газонаполненных ЭРИ в составе приборов, предназначенных для работы в негерметичных отсеках космических аппаратов. Сформулированы рекомендации по выбору конструкции электрорадиоизделий с рабочим напряжением порядка 300 В и более, а также схемных решений при разработке высоковольтного оборудования, предназначенного для работы в вакууме.

Ключевые слова: закон Пашена, пробой, вакуум, негерметичность, электрорадиоизделие, система преобразования и управления, космический аппарат

Introduction. As a part of the propulsion subsystems of modern spacecrafts (SC), electric propulsion engines (EPE) are increasingly used [1]. This is primarily due to their better efficiency compared to engines running on chemical fuel. Various types of engines and devices for controlling and powering such engines are being developed all over the world. [2–5]. Further improvement in the characteristics of electric propulsion engines is directly related to the increase in the accelerating voltage generated by the power processing unit (PPU). If the voltage of a widely used domestic engine of the SPT-100 type is about 300 V [6], then in more economical models it is already about 800 V and higher [7; 8]. In this regard, the need to use high-voltage element base in PPU devices is obvious. The reliability of electrical components and their correct application determines the final reliability of the onboard equipment, subsystem, and spacecraft itself. Therefore, the issues of reliability and conditions of use of EEE-parts are very important and relevant.

It should be pointed that current Russian spacecrafts are non-hermetic and designed for 15 or more years of active existence [9]. This means that the EEE-parts used in the spacecraft equipment, including high-voltage ones, must also ensure normal operation in vacuum conditions during this period.

Usually, the design of high-voltage EEE assumes the presence of a sealed housing, inside of which the active element is located (fig. 1).

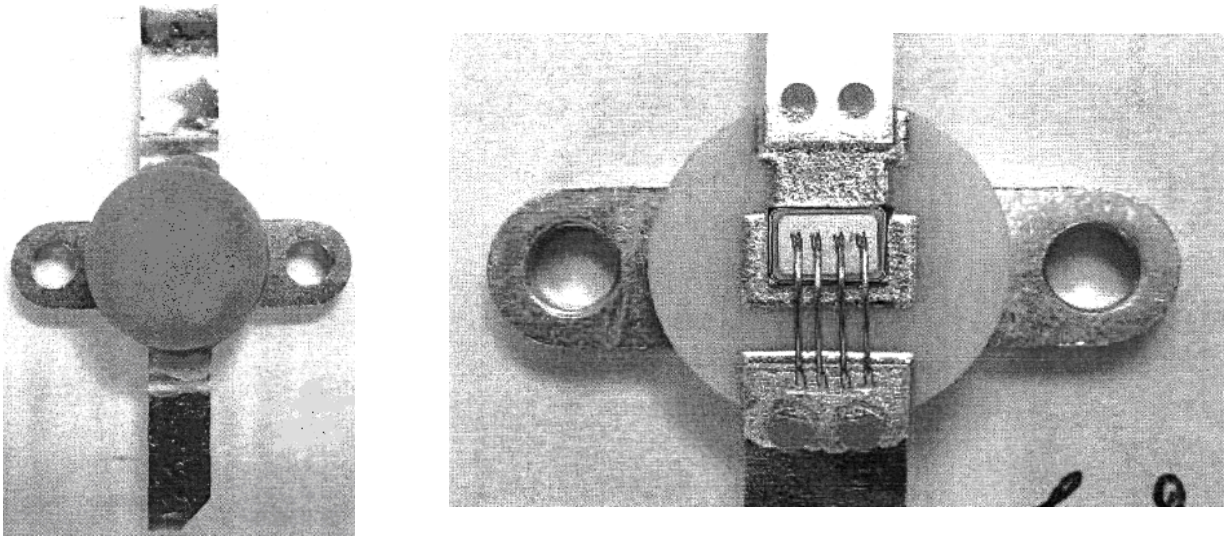

а *б*

Fig.1. Standard hermetic EEE housing design:
a – external view; *b* – view with the case cover removed

Рис. 1. Конструкция корпуса типового герметичного ЭРИ:
а – внешний вид; *б* – вид со снятой крышкой корпуса

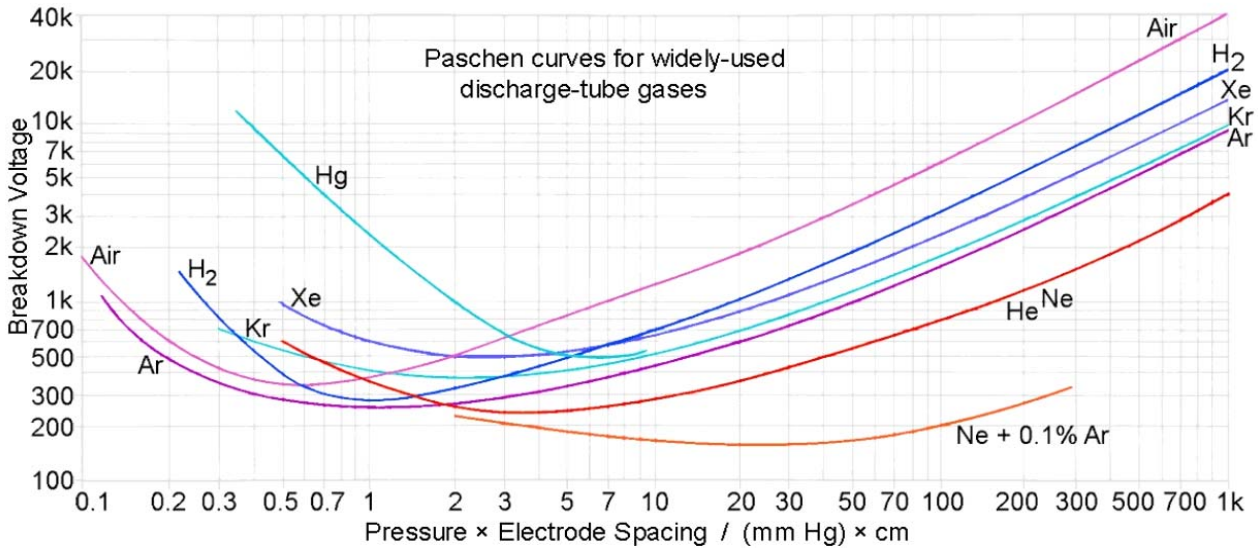

Fig. 2. Paschen curves for different gases

Рис. 2. Кривые Пашена для различных газов

The case is designed to protect active elements during storage and ground operation from mechanical damage and from ingress of foreign pollutants or chemically aggressive substances, primarily moisture, which can cause corrosion. As a rule, air or nitrogen at atmospheric pressure is located inside the case of a manufactured hermetic EEE. However, it is obvious that the tightness of the EEE case can not be absolute. During the operation of the EEE in a vacuum, due to leaks at the place where the cover is attached to the base of the housing and diffusion directly through the housing material, the pressure inside the EEE case inevitably decreases. In accordance with Paschen law, in the presence of high voltage between the inner electrodes of EEE and at the value of inner pressure falls within a certain range (hereinafter "Paschen zone"), you may experience breakdown, leading to electronics failure. It is obvious that the consequence of the EEE failure, depending on the adopted circuit solutions of the device, may be a decrease in its performance up to a complete failure. Note that the level of hermeticity of EEE housings is regulated in the technical specifications (TU) for them and confirmed in the process of qualification and periodic tests of electrical products. It can be $5 \cdot 10^{-5} – 5 \cdot 10^{-4}$ cm^3·mmHg/s in order of value. Confirmation of the hermeticity parameter during the acceptance tests of the EEE is usually not carried out. It is also obvious that the actual hermeticity of a particular type of EEE may vary, as it depends on many technological factors: the actual size of the case and base of the EEE, the quality of the cover connection, the amount of glue applied, external conditions during the sealing process, etc.

Taking into account the importance of ensuring the normal operation of EEE as a part of high-voltage devices designed to operate in a vacuum it seems appropriate to consider the problem in more detail and outline possible ways to solve it. This article is devoted to the analysis of the causes and conditions of breakdowns in the cases of hermetic EEE, the forecast of the time when the EEE proceeds to the "Paschen zone" and the time spent in it, and the consideration of possible ways to resist this phenomenon to improve the reliability of high-voltage onboard devices of non-hermetic SC.

Physical principles of occurrence of electric discharges within the design of EEE-parts. The effects of electrical breakdowns in high-voltage onboard equipment are well known and studied. In particular, the fact that plasma formed by the spacecraft engines that penetrates into the internal cavities of high-voltage equipment can create conditions for the occurrence of arc discharges [10]. There are recommendations for reducing the probability of electric discharges, for example, minimizing pointed and curved surfaces of conductors and electrodes that lead to strong electric field inhomogeneities [11]. However, these recommendations apply to the device design, EEE and conductors installation. The issues of electrical breakdowns at the level of the EEE structure are currently insufficiently studied.

According to generally accepted concepts, an independent electric discharge in gas occurs because of an electrical breakdown when an ignition voltage is applied between the electrodes. In the case of a homogenous field, the ignition potential depends on the type of gas and on the multiplying the gas pressure P by the distance between the electrodes d. The Paschen law established experimentally says that the lowest ignition voltage of a gas discharge (breakdown voltage) between two flat electrodes is a constant value for the same values of the multiplication $P \cdot d$ (fig. 2) [12].

The theory of the occurrence of a breakdown (electronic avalanche) in gas was proposed by Townsend [13]. According to this theory the breakdown voltage depends as follows on multiplying the pressure by the electrode spacing:

$$U_{\text{пр}} = \frac{B \cdot P \cdot d}{\ln[\frac{A \cdot P \cdot d}{\ln(1+\gamma^{-1})}]}, \quad (1)$$

where γ is the coefficient that characterizes surface ionization (the number of electrons knocked out of the cathode by a single incident ion), $B = A\varphi i$, $A = (P\lambda)^{-1}$, P is the pressure, λ is the free path of electrons under these conditions, and φ_i is the ionization potential of the gas molecule (volts).

The diagrams and formulae demonstrate that at a fixed distance between the electrodes there is a pressure range ("Paschen zone"), where the conditions for the breakdown of the interelectrode gap can be created within a certain electric field. It also follows that the greater the applied voltage, the wider "Paschen zone".

On the right side of the Paschen curve, that is, when the pressure increases, the breakdown voltage increases due to a decrease in the free path of the electrons and a corresponding decrease in the kinetic energy they gain when moving in an external electric field. On the left side of the curve, that is, when the pressure decreases, the breakdown voltage also increases, but due to the decrease in the number of newly appeared electrons because of the frequency collisions fall due to the decrease in the concentration of gas molecules.

The graphs (fig. 2) show that the minimum breakdown voltage for air is 325–330 V at the parameter value $P{\cdot}d \approx 0.5$–0.6 mm Hg·cm. It is obvious that for a particular EEE the constant values are the distance between the electrodes and the maximum applied voltage, and the variable value is the air pressure inside the case. It is also clear that the time of reaching the Paschen zone from the moment of placing the element in a vacuum and the duration of its stay in it depends on the volume of the inside space of the EEE case and the value of the hermeticity index.

The volume of inner space of some typical EEE, as shown below (tab. 1), is in a limited range, about 120–1500 mm^3. Therefore, the actual value of the hermeticity index is the decisive factor determining the time of reaching the Paschen zone and the duration of staying in it.

Dynamics of pressure changes inside the EEE case. When considering the change in pressure inside the EEE case, we can use an analogy with the problem of changing the pressure in a vessel when air flows out of it into a vacuum through a small hole. In vacuum technology, this task is interpreted as pumping air out of a vessel using a so-called ideal vacuum pump, which is taken as an environment with zero pressure. The following basic concepts are applied in the theory of vacuum technology [14–16]:

By definition, $Q = d\,(PV)/dt$ – gas flow (leak, flow rate, or leak indicator) – the amount of gas pumped out of the vessel per unit of time. This parameter has a dimension of PA·м^3/sec (W) or l·mm Hg/s – for microtubules. It can be measured and depends on the pressure in the vessel.

S – speed (velocity) of pumping out of the vacuum pump or conductivity of the conditional opening – the volume of gas pumped out by the pump per unit of time. Dimension – m^3/sec, l/sec. The pumping speed characterizes the pump performance and is determined at a specific pressure, so it is a fixed value.

The following relation connects the parameters Q and S:

$$Q = S \cdot P, \tag{2}$$

where P is the current pressure in the vessel.

Hence, for known initial values P_0 and Q_0:

$$S = \frac{Q_0}{P_0}. \tag{3}$$

Based on the definition of the flow, taking into account the constant value of the volume of the inner case space V and the negative value of the pressure change rate (the pressure inside the case of the EEE falls due to micro-leakage), we can write:

$$Q = S \cdot P = \frac{Q_0}{P_0} \cdot P = -V \cdot \frac{dP}{dt} \tag{4}$$

or

$$\frac{Q_0}{V \cdot P_0} \cdot dt = -\frac{dP}{P}. \tag{5}$$

After integrating (5) from 0 to t and from P_0 to P, we get the time of pressure reduction inside the case from P_0 to P:

$$t = \frac{V \cdot P_0}{Q_0} \cdot \ln\left(\frac{P_0}{P}\right). \tag{6}$$

Accordingly, the value of the pressure inside the case in time t after placing the EEE in a vacuum is:

$$P = P_0 \cdot e^{-\frac{Q_0}{P_0 \cdot V} \cdot t}. \tag{7}$$

It should be noted that the standard conditions for determining leaks are pressure difference between the inner and outer sides of the product $\Delta P = 10^5\ PA$ (1 *atm*), test gas – air, temperature –298 K. The flow of a leak in standard conditions is indicated by the symbol B. However, in practice, the leak value is determined not by air, but by the test gas, (in most cases – helium). For the molecular flow regime, the ratio between the flow in standard B and test Q conditions is valid [16]:

$$B = Q_0 \cdot \sqrt{\frac{M_\Gamma}{M_\text{B}}}. \tag{8}$$

where $M_\Gamma \approx 4$ – is the molecular weight of the sample gas (helium), $M_\text{B} \approx 29$ – is the molecular weight of the air.

Since in this example we consider the outflow of air from the EEE case, and the flow Q is determined experimentally by helium, in formulas (6), (7), the parameter Q_0 should be multiplied by the value $(M_\Gamma/M_\text{B})^{-1/2} = 0.375$. Then the formula (6) is refined:

$$t = 2{,}67 \cdot \frac{V \cdot P_0}{Q_0} \cdot \ln\left(\frac{P_0}{P}\right). \tag{9}$$

If t_1 is the time of pressure reduction from the initial P_0 to the upper border of the Paschen zone P_1, and t_2 is the time of reduction to the lower border P_2, then the interval of time spent in the Paschen zone:

$$\Delta t = t_2 - t_1 = 2{,}67 \cdot \frac{V \cdot P_0}{Q_0} \cdot \ln\left(\frac{P_1}{P_2}\right). \tag{10}$$

To estimate the time of pressure reduction from atmospheric to the upper and lower limits of the dangerous range, it is necessary to know the level of actual non-hermeticity of the EEE case, that is, the value of the leak Q_0. The main factor affecting this indicator is the design of the element and the method of sealing the housing. Depending on the design and manufacturing method, elements can be distinguished: a) with ceramic housings, the hermeticity of which is provided by an adhesive connection; b) with metal-glass housings, the hermeticity of which is provided by welding; c) metal-ceramic housings, the hermeticity of which is provided by seam-roller welding. At JSC "SPC "Polyus", samples of some high-voltage EEE manufactured using various technologies were tested. They showed that the actual value of the hermeticity index is 1–2 orders less than in the technical specifications (TS) per element, that is, the actual leak is significantly less than indicated in the TS. The test results for various types of EEE are shown in tab. 1.

Using the formula (10), we estimate the time required for the pressure in the inside the housing to decrease from the initial value of 1 atm to the Paschen zone, as well as the time spent in this zone (fig. 3), based on the norm of the hermeticity index for the TS and the measured values (see tab. 1). Since the actual value of the leak has a spread, the maximum possible duration of stay in the danger zone for this type of EEE is equal to the difference between the time of exit from the zone at the minimum leak and the time of entry at the maximum leak.

The calculated data on pressure drop times for various levels of hermeticity index, operating voltages and types of EEE, shown in tab. 1, are presented in tab. 2. The considered types of EEE do not have protection of the electrodes with an insulating compound, with the exception of type 2.

Analysis of the results obtained. From tab. 1, 2 and fig. 3, we can conclude the following:

1. The actual level of the hermeticity index is usually 1–2 orders lower than the level recorded in the TS per element.

2. The actual level of the hermeticity index depends on the design of the EEE and has the highest values (maximum leak) for EEE with ceramic housings, the hermeticity of which is provided by an adhesive connection.

3. There is a significant variation in the actual values of the hermeticity index of a particular type of EEE (up to 40 times), due to various technological factors.

4. The time to reach the upper border of the Paschen zone from the start of operation in full-scale conditions, as well as the duration of stay in this zone depends on the actual level of the EEE hermeticity index, the value of the subcase volume and the maximum operating voltage between the internal electrodes. The duration of being in a dangerous zone can range from two weeks to several tens or even hundreds of years.

These conclusions, at least, call into question the possibility of normal operation of gas-filled high-voltage housing EEE in vacuum, since during the long-term operation of the product (15 years or more), elements of this type must necessarily fall into the Paschen zone with an increased risk of breakdown.

In addition, the analysis of existing domestic standards regulating the methodology of qualification and acceptance tests of EEE was carried out. It showed that tests of high-voltage EEE for the occurrence of electrical breakdowns in the sub-housing space are not currently provided.

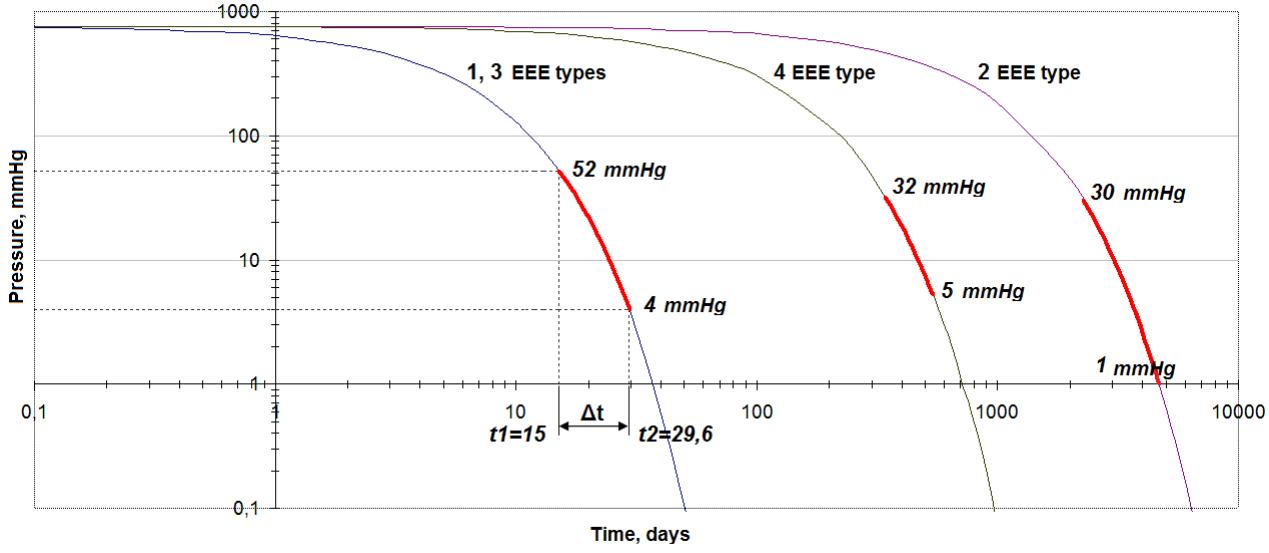

Fig. 3. Graph of pressure drop at the rate of hermeticity index for TS with indication of the Paschen zone for each type of EEE
(pressure, mmHg; types of EEE; time, full day)

Рис. 3. График спада давления при норме показателя герметичности по ТУ с указанием зоны Пашена для каждого типа ЭРИ
(давление, мм рт.ст.; типы ЭРИ; время, сут.)

Table 1

Design, parameters, regulated and actual levels of the EEE hermeticiry index of various types

Type	Design	Operational voltage (TS)	Inner volume	Min distance between electrodes	Hermeticity index Q_0 (TS),	Q_0 (measured valume)	Quantity
		V	mm^3	mm	$cm^3 \cdot mmHg \cdot s^{-1}$	$cm^3 \cdot mmHg \cdot s^{-1}$	item
1	Ceramic housings, hermeticity provided by an adhesive connection	600	120	0.5	$5 \cdot 10^{-4}$	$7.6 \cdot 10^{-6}$ – $9.8 \cdot 10^{-5}$	97
2	Metal-glass housings, hermeticity provided by welding	800	1500	1.5	$5 \cdot 10^{-5}$	$1.9 \cdot 10^{-6}$ – $7.5 \cdot 10^{-5}$	15
3	Metal-ceramic housings, hermeticity provided by seam-roller welding	600	120	0.5	$5 \cdot 10^{-4}$	$2.6 \cdot 10^{-6}$ – $9.5 \cdot 10^{-6}$	15
4	Metal-ceramic housings, hermeticity provided by seam-roller welding	450	230	0.5	$5 \cdot 10^{-5}$	$2 \cdot 10^{-6}$ – $5.5 \cdot 10^{-6}$	15

Table 2

Time of pressure decline to the Paschen zone, duration of stay in it for the EEE of different types and different hermeticity indexes

Type of EEE	Paschen zone, mmHg	Hermeticity index, $cm^3 \cdot mmHg \cdot s^{-1}$	Time of decline to the upper border of the Paschen zone, days	Time of decline to the lower border of the Paschen zone, days	The duration of stay in the Paschen zone, days
1	4–52	TS	15	29	14
		act., max	77	–	1869
		act., min	–	1946	
2	1–30	TS	2277	4674	2397
		act., max	1518	–	121475
		act., min	–	122993	
3	4–52	TS	15	29	14
		act., max	796	–	4892
		act., min	–	5688	
4	5–32	TS	342	543	201
		act., max	3111	–	10458
		act., min	–	13569	

From the above, we concluded that the use of high-voltage gas-filled EEE as part of devices that operate for a long time in vacuum without additional measures that reduce the probability of breakdown is associated with high risk.

Possible ways to solve the problem of ensuring long-term operation of high-voltage devices in vacuum conditions. We can offer developers of high-voltage devices with a long service life, designed to work in a vacuum the following logic for designing devices using high voltage EEE:

1. If possible, build the device circuitry in such a way that the maximum voltage between the internal EEE electrodes does not exceed the breakdown voltage according to Paschen law (with some extra), for example, not more than 250 V.

2. If it is impossible to avoid operating modes of high-voltage EEE with a voltage of about 300 V or higher, then you should use a special version of EEE, which would exclude the possibility of a breakdown according to the Paschen law. In particular, JSC "SPC "Polyus" considered the following options for modification of EEE housing: a) coating the internal electrodes and the crystal with insulating compounds; b) partial filling of the inner cavity with an insulating compound; c) total filling of the inner cavity with an insulating compound.

Experimental studies have shown that the best solution in terms of ensuring the resistance of the EEE to electrical breakdowns is option b), that is, a continuous filling of the inner space with an insulating compound. Other methods enhanced the resistance of the sub-housing space to electrical breakdowns, but did not completely exclude them.

3. Replacing the "small leak" with the "large leak" by performing special holes in the EEE housing to remove the internal atmosphere of the EEE during the initial period of operation of the device in vacuum. Switching on the device should be carried out after guaranteed removal of air from the sub-housing space of the EEE, that is, when the pressure decreases below the lower border of the Paschen zone.

Conclusion. An analysis of the operating conditions of hermetic EEE with gas-filled housing as part of long-term vacuum-operated devices of non-hermetic design

shows that EEE of this type due to natural leaks can fall into a dangerous zone from the point of view of electrical breakdown by internal pressure. At the same time, the time of getting into this zone and, more importantly, the duration of being in it have a significant spread – from two weeks to several decades, that is, the element can be in the danger zone for almost the entire life of the SC. This circumstance bring into question the possibility of using EEE of this type in accordance with the technical specifications as a part of long-life devices of non-hermetic design without special measures to exclude the possibility of breakdowns due to the Paschen effect. These measures include reducing the operating and maximum voltage between the EEE electrodes to the level below the breakdown level, carried out by special circuit solutions, modifying the EEE by filling the inside housing space with an insulating compound, or using specially designed EEE for working in vacuum (ventilated or in a non-housing version).

References

1. Lev D., Myers R. V., Lemmer K. M. et al. [The Technological and Commercial Expansion of Electric Propulsion in the Past 24 Years]. 35th Electric Propulsion Conference. IEPC-2017-242. Georgia Institute of Technology. USA, October 8–12, 2017, 18 p.

2. Boniface C., Castanet F., Giesen G. et al. [An overview of French electric propulsion activities at CNES]. 36th International Electric Propulsion Conference. IEPC-2019-253. University of Vienna, Vienna, Austria, Sept. 15–20, 2019, 22 p.

3. Lev D., Zimmerman R., Shoor B. et al. [Electric Propulsion Activities at Rafael in 2019]. 36th International Electric Propulsion Conference. IEPC-2019-600. University of Vienna, Vienna, Austria, Sept. 15–20, 2019, 9 p.

4. Bourguignon E., Fraselle S. [Power Processing Unit Activities at Thales Alenia Space in Belgium]. 36th International Electric Propulsion Conference. IEPC-2019-584. University of Vienna, Vienna, Austria, Sept. 15–20, 2019, 8 p.

5. A. Mallman, F. Forrisi, E. Mache et al. [High Voltage Power Supply for Gridden Ion Thruster]. 36th International Electric Propulsion Conference. IEPC-2019-A512. University of Vienna, Vienna, Austria, Sept. 15–20, 2019, 7 p.

6. Mitrofanova O. A., Gnzdor R. Yu., Murashko V. M., Koryakin A. I., Ntsterenko A. N.. [New Generation of SPT-100]. 32nd Inernational Electric Propulsion Conference, IEPEC-2011-041, Wiesbaden, Germany, Sept. 11–15, 2011, 7 p.

7. Kostin A. N., Lovtsov A. S., Vasin A. I., Vorontsov V. V. [Development and qualification of Hall thruster KM-60 and the flow control unit]. 33st International Electric Propulsion Conference, IEPC-2013-055, the George Washingtin University, USA, Okt. 6–10, 2013, 11 p.

8. Lovtsov A. S., Tomilin D. A., Muravlev V. A. [High-voltage Hall's thrusters development in Keldysh Centre]. 68th Astronautical Congress, Adelaide, Australia, IAC-17-C4.4.4, 25–29 September 2017, 5 p.

9. *Kosmicheskie vekhi: sb. nauch. tr.* [Space landmarks: papers collection]. OAO "Informacionnye sputnikovye sistemy" im. Akad. M. Ph. Reshetneva". Krasnoyarsk, 2009, 704 p.

10. Ivanov V. V., Maksimov I. A., Balashov S. V., Pervukhin A. V., Nadiradze A. B. [The methodology to ensure immunity of the satellite equipment of plasma from the stationary plasma thrusters]. *Aviacionnaya i kosmicheskaya tekhnika. VestnicSibGAU*. 2006, No. 1, P. 76–80 (In Russ.).

11. ESCC-E-HB-20-05A Space engineering. High voltage engineering and design handbook, 2012. 219 p.

12. Wittenberg H. H. [Gas Tube Design]. From: Electron Tube Design, RCA Electron Tube Division, 1962. P. 792–817.

13. Raizner Yu. P. *Phizika gazovogo razryada* [Gas discharge physic]. Moscow, Nauka Publ., 1992, 535 p.

14. Korolev B. I. *Osnovy vakuumnoi tekhniki* [Vacuum technique basis]. Moscow, Energiya Publ., 1975, 416 p.

15. Vinigradov M. L., Karganov M. V., Kostrin D. K. [The analysis of sensitivity of leak detection methods and a technique for its improvement]. *Control. Diagnostika.* 2016, No. 5, P. 36–42 (In Russ.).

16. Rot A. *Vacuumnye uplotneniya* [Vacuum Sealing Techniques]. 1971, Moscow, Energiya Publ., 464 p.

Библиографические ссылки

1. The Technological and Commercial Expansion of Electric Propulsion in the Past 24 Years / D. Lev, R. V. Myers, K. M. Lemmer et al. // 35th Electric Propulsion Conference. IEPC-2017-242. Georgia Institute of Technology. USA, October 8–12, 2017. 18 p.

2. An overview of French electric propulsion activities at CNES / C. Boniface, F. Castanet, G. Giesen et al. // 36th International Electric Propulsion Conference. IEPC-2019-253. University of Vienna, Vienna, Austria, Sept. 15–20, 2019. 22 p.

3. Electric Propulsion Activities at Rafael in 2019 / D. Lev, R. Zimmerman, B. Shoor et al. // 36th International Electric Propulsion Conference. IEPC-2019-600. University of Vienna, Vienna, Austria, Sept. 15–20, 2019. 9 p.

4. Power Processing Unit Activities at Thales Alenia Space in Belgium / E. Bourguignon, S. Fraselle // 36th International Electric Propulsion Conference. IEPC-2019-584. University of Vienna, Vienna, Austria, Sept. 15–20, 2019. 8 p.

5. High Voltage Power Supply for Gridden Ion Thruster / A. Mallman, F. Forrisi, E. Mache et al. // 36th International Electric Propulsion Conference. IEPC-2019-A512. University of Vienna, Vienna, Austria, Sept. 15–20, 2019. 7 p.

6. New Generation of SPT-100 / O. A. Mitrofanova, R. Yu. Gnzdor, V. M. Murashko, A. I. Koryakin, A. N. Ntsterenko // 32nd Inernational Electric Propulsion Conference, IEPEC-2011-041, Wiesbaden, Germany, September 11–15, 2011. 7 p.

7. Development and qualification of Hall thruster KM-60 and the flow control unit / A. N. Kostin, A. S. Lovtsov, A. I. Vasin, V. V. Vorontsov // 33st International Electric Propulsion Conference, IEPC-2013-055, the George Washingtin University, USA, Okt. 6–10, 2013. 11 p.

8. Разработка высоковольтных холловских двигателей в Центре Келдыша / А. С. Ловцов, Д. А. Томилин, В. А. Муравлев // 68th Astronautical Congress, Adelaide, Australia, IAC-17-C4.4.4, 25–29 September 2017. 5 p.

9. Космические вехи : сб. науч. тр. / под ред. проф. Н. А. Тестоедова ; ОАО «Информационные спутниковые системы» им. акад. М. Ф. Решетнева». Красноярск, 2009. 704 с.

10. Методология обеспечения стойкости космического аппарата в условиях плазмы, формируемой стационарными плазменными двигателями / В. В. Иванов, И. А. Максимов, С. В. Балашов и др. // Вестник СибГАУ. 2006. № 1. С. 76–80.

11. ESCC-E-HB-20-05A Space engineering. High voltage engineering and design handbook, 2012. 219 p.

12. Gas Tube Design / H.H. Wittenberg // From: Electron Tube Design, RCA Electron Tube Division, 1962. P. 792–817.

13. Райзнер Ю. П. Физика газового разрядаю М. : Наука, 1992. 535 с.

14. Королев Б. И. Основы вакуумной техники. М. : Энергия, 1975. 416 с.

15. Виноградов М. Л., Карганов М. В., Кострин Д. К. Анализ чувствительности методов течеискания и способ ее повышения // Контроль. Диагностика. 2016. № 5. С. 36–42.

16. Рот А. Вакуумные уплотнения : пер. с англ. М. : Энергия, 1971. 464 с.

Kochev Yuriy Vladimirovich – Cand. Sc. (tech.), head of propulsion subsystem electric design group; JSC “Academician M. F. Reshetnev Information Satellite Systems”. E-mail: koch@iss-reshetnev.ru.

Ermoshkin Yuriy Mikhailovich – D. Sc. (tech.), head of propulsion department; JSC “Academician M. F. Reshetnev Information Satellite Systems”. E-mail: erm@iss-reshetnev.ru.

Ostapushchenko Alexander Anatolyevich – leading design thrusterer; JSC “Scientific & Industrial Centre “Polyus”.

Кочев Юрий Владимирович – кандидат технических наук, начальник группы; АО «Информационные спутниковые системы» имени академика М. Ф. Решетнева». E-mail: koch@iss-reshetnev.ru.

Ермошкин Юрий Михайлович – доктор технических наук, доцент, начальник лаборатории; АО «Информационные спутниковые системы» имени академика М. Ф. Решетнева». E-mail: erm@iss-reshetnev.ru.

Остапущенко Александр Анатольевич – ведущий инженер-конструктор; АО «Научно-производственный центр «Полюс».

Раздел
Part
3

ТЕХНОЛОГИЧЕСКИЕ ПРОЦЕССЫ И МАТЕРИАЛЫ

TECHNOLOGICAL PROCESSES AND MATERIALS SCIENCE

UDC 539.21:537.86
Doi: 10.31772/2587-6066-2020-21-2-254-265

For citation: Aplesnin S. S., Yanushkivich K. I. Change in magnetoresistance in manganese chalcogenides $MnSe_{1-X}Te_X$ from bulk to thin-film samples. *Siberian Journal of Science and Technology*. 2020, Vol. 21, No. 2, P. 254–265. Doi: 10.31772/2587-6066-2020-21-2-254-265

Для цитирования: Аплеснин С. С., Янушкевич К. И. Изменение магнитосопротивления в халькогенидах марганца $MnSe_{1-X}Te_X$ при переходе от объемных образцов к тонкопленочным // Сибирский журнал науки и технологий. 2020. Т. 21, № 2. С. 254–265. Doi: 10.31772/2587-6066-2020-21-2-254-265

CHANGE IN MAGNETORESISTANCE IN MANGANESE CHALCOGENIDES $MnSe_{1-X}Te_X$ FROM BULK TO THIN-FILM SAMPLES

S. S. Aplesnin[1*], K. I. Yanushkivich [2]

[1]Reshetnev Siberian State University of Science and Technology
31, Krasnoyarskii rabochii prospekt, Krasnoyarsk, 660037, Russian Federation
[2]Scientific-Practical Materials Research Center NAS of Belarus
19, Brovki St., Minsk, 220072, Belarus
[*]E-mail aplesnin@sibsau.ru

The electrical and optical properties of anion-substituted antiferromagnetic semiconductors MnSe1-XTeX ($0.1 \le X \le 0.4$) in the temperature range 77-300 K and magnetic fields up to 13 kOe in bulk samples and in polycrystalline thin films are investigated. Negative magnetoresistance was found in the MnSe1-XTeX solution in the neighbourhood with a Néel temperature for X = 0.1 and for a composition with X = 0.2 in the paramagnetic region up to 270 K. A correlation was established between the spin-glass state and magnetoresistance for X = 0, 1 and 0.2. The optical absorption spectra were measured in the frequency range 2000 cm-1 < ω < 12000 cm-1. A decrease in the gap in the spectrum of electronic excitations and a several of absorption peaks near the bottom of the conduction band were found. Coexistence of two crystalline phases was found in polycrystalline films of the MnSe1-XTeX system by X-ray diffraction analysis. Resistance maxima were established in the region of polymorphic and magnetic transitions. A model of localized spin-polarized electrons with a localization radius varying in a magnetic field as a result of competition between ferromagnetic and antiferromagnetic interactions is proposed. In the paramagnetic region, negative magnetoresistance is caused by tunneling of spin-polarized electrons during orbital ordering.

Keywords: manganese chalcogenides, magnetoresistance, conductivity, thin films, current-voltage curve.

ИЗМЕНЕНИЕ МАГНИТОСОПРОТИВЛЕНИЯ В ХАЛЬКОГЕНИДАХ МАРГАНЦА $MnSe_{1-X}Te_X$ ПРИ ПЕРЕХОДЕ ОТ ОБЪЕМНЫХ ОБРАЗЦОВ К ТОНКОПЛЕНОЧНЫМ

С. С. Аплеснин[1*], К. И. Янушкевич[2]

[1]Сибирский государственный университет науки и технологий имени академика М. Ф. Решетнева
Российская Федерация, 660037, г. Красноярск, просп. им. газеты «Красноярский рабочий», 31
[2]ГО «НПЦ НАН Беларуси по материаловедению»
Беларусь, 220072, г. Минск, ул. П. Бровки, 19
[*]E-mail aplesnin@sibsau.ru

Исследованы электрические и оптические свойства анион-замещенных антиферромагнитных полупроводников MnSe1-XTeX ($0,1 \le X \le 0,4$) в области температур 77–300 К и магнитных полей до 13 кЭ в объемных образцах и поликристаллических тонких пленках. В твердых растворах MnSe1-XTeX обнаружено отрицательное магнитосопротивление в окрестности температуры Нееля для X = 0,1 и для состава с X = 0,2 в парамагнитной области до 270 К. Установлена корреляция спин-стекольного состояния и магнитосопротивления для X = 0,1 и 0,2. Измерены спектры оптического поглощения в интервале частот 2000 см-1 < ω < 12000 см-1. Обнаружено уменьшение щели в спектре электронных возбуждений и ряд пиков поглощения вблизи дна зоны проводимости. В поликристаллических пленках системы MnSe1-XTeX найдено сосуществование двух кристаллических фаз методом рентгеноструктурного анализа. Обнаружены максимумы сопротивления в области полиморфного и магнитного переходов. Предложена модель локализованных спин-поляризованных электронов с радиусом локализации, меняющимся в магнитном поле в результате конкуренции ферромагнитных и антиферромагнитных взаимодействий. В парамагнитной области отрицательное магнитосопротивление вызвано туннелированием спин-поляризованных электронов при орбитальном упорядочении.

Ключевые слова: халькогениды марганца, магнитосопротивление, проводимость, тонкие пленки, ВАХ.

Introduction. To control spacecraft in extreme conditions with a temperature difference of two hundred or three hundred degrees, it is necessary to create elemental electronic microelectronics that operates in these conditions. Traditional electronics operates on silicon and germanium semiconductors operating with an electron charge. But the electron has a spin and orbital angular momentum, which is used in spintronics, which takes advantage of both non-volatile magnetic memory and high-speed electrical information processing systems. In spintronics [1; 2], to convert an electric signal, not only the charge degree of freedom of an electron is used, but also a spin, which allows creating fundamentally new spintronic devices. The electron has orbital degrees of freedom, acting on which it is also possible to regulate the transport and dielectric characteristics in a magnetic field

In chalcogenides, there is a relationship between the parameters of the magnetic and electrical subsystems [3–7] and the effect of magnetoresistance [8–12]. To date, manganese oxide compounds (manganites of the $LaMnO_3$ type) [13–17], europium chalcogenides, $CdCr_2Se_4$, and $HgCr_2Se_4$ selenides [18–20] are being intensively studied. In the MeXMn1-XS sulfide systems (Me = 3d metal) synthesized on the basis of α-MnS monosulfide and undergoing the metal – insulator transition [21–24], the CMR effect was found to be comparable with its value in manganites [25–28].

Manganese chalcogenides MnSe and MnTe are antiferromagnets (AFM) and undergo structural and magnetic transitions with an increase in the degree of hybridization of manganese cations with Se and Te anions [29; 30]. The change of the transport properties from the semiconductor to metal at the temperature near the room one. MnTe crystallizes in a hexagonal structure of the NiAs type [29]. Mn manganese monoselenide MnSe exhibits a structural phase transition from the cubic phase to the NiAs structure in the temperature range 248 K < T < 266 K [30], and below this temperature phase coexistence is observed in the sample.

The antiferromagnet MnTe consists of ferromagnetically ordered spins in the plane that are oriented antiferromagnetically along the hexagonal axis. The spins are located in the base plane and have anisotropy of the light plane type with a Néel temperature T = 340 K [31]. For MnSe, the Néel temperature in the cubic modification is TN = 135 K, and in the hexagonal NiAs phase it coincides with the structural transition temperature TS = 272 K. Manganese chalcogenides are semiconductors with p – type conductivity, which have an energy gap in the spectrum of single particle electronic excitations for MnSe (2.0–2.5) eV and MnTe (0.9–1.3) eV with polaron type charge carriers [32]. The effect of magnetoresistance in a magnetically ordered cubic phase was detected on MnSe samples when approaching the Néel temperature with the electrical resistivity ρ = 104 – 103 Ohm · cm [33]. A decrease in the metal – anion Mn–Te bond length, according to theoretical calculations of the band structure [34], induces a change in the crystal structure from hexagonal to cubic with antiferromagnetic ordering with a binding energy of one Mn–Te pair EZB, H = −0.31 eV/bond with bond length RAF = 2.70 Å, and with ferromagnetic ordering EZB, H = −0.51 eV/bond with RF = 2.71 Å. In the NiAs structure, the bond length is R(Mn–Te) = 0.273 Å. The lattice constant a = 5.44 Å in MnSe with a NaCl structure is somewhere in the middle between 2RF and 2RH; therefore, when selenium is replaced by tellurium at low concentrations, the formation of Mn-Te-Mn ferromagnetic bonds with anisotropy of the light plane type is possible. As a result, the formation of the angular phase and enhancement of the magnetoresistive effect in anion-substituted $MnSe_{1-X}Te_X$ solid solutions are possible. Substitution of selenium with tellurium leads to suppression of the hexagonal phase and to the single-phase state of the $MnSe_{1-X}Te_X$ system with a face-centred cubic structure with space group (225) [35] in the temperature range 120 K < T < 300 K and in the concentration range $0.1 \le X \le 0, 4$ [36]. Local non-correlated lattice deformations are possible, which will cause a change in the electronic structure and a change in resistance during the hopping type of conductivity along with changes in the magnetic properties [37–38].

The aim of this work is to detect the magnetoresistive effect and to elucidate the microscopic mechanism of the influence of the magnetic field on the transport properties of MnSe1-XTeX solid solutions ($0.1 \le X \le 0.4$) based on a comprehensive study, electrical resistivity, current-voltage characteristics and optical absorption spectra depending on temperature and magnitude of the magnetic field.

Materials and research methods. The electrical resistivity is measured by a standard four-probe compensation method using direct current in the temperature range 77–300 K in a magnetic field of up to 13 kOe. Fig. 1 shows a temperature dependence of the resistance of $MnSe_{1-X}Te_X$ solutions for all compositions ($0.1 \le X \le 0.4$). At $T < T_N$, a deviation from the linear dependence $\ln\rho = \ln\rho_0 + \Delta E/T$ is observed. The activation energy $\Delta E \approx$ (0.07–0.09) eV is practically independent of the composition in these samples.

The effect of a magnetic field on transport properties was investigated in two ways. First, the change in resistance was measured by the temperature of $MnSe_{1-X}Te_X$ solid solutions located both in a magnetic field and in its absence. Secondly, at a fixed temperature, the current-voltage characteristics were studied in a zero magnetic field and in a field H = 13 kOe. Fig. 2 shows the current-voltage characteristics of manganese chalcogenides $MnSe_{1-X}Te_X$ for composition X = 0.1 at temperatures (100, 140 and 190 K). The $U(I)$ dependences are linear and independent of the magnitude of the magnetic field at T < 100 K. It was established that the resistance of the samples decreases in the magnetic field and the greatest change (about 100 %) was found in the neighbourhood of the Néel temperature for a composition with X = 0.1 (fig. 3, *a*). For a concentration with X = 0.2, a decrease in resistance was found in the paramagnetic region at a temperature above the Néel temperature and in the temperature range 160 K < T < 270 K is 5 % (fig. 3, *b*). For high concentrations, magnetoresistance (MR) was not detected.

The magnetic moment of the samples was measured in a magnetic field of 0.8 T in the temperature range 80 K < T < 700 K in two modes: cooling in a zero magnetic field and in a magnetic field of 0.8 T.

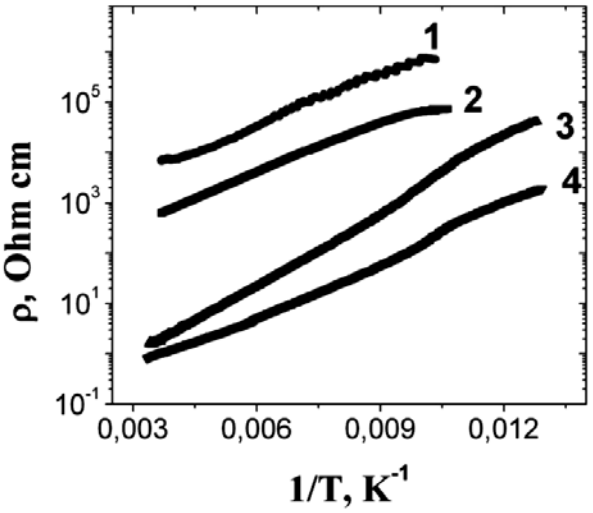

Fig. 1. Temperature dependence of the electrical resistivity $MnSe_{1-X}Te_X$ solutions with concentration of $X = 0.1$ (1), 0.2 (2), 0.3 (3), 0.4 (*b*)

Рис. 1. Температурные зависимости удельного электросопротивления для твердых растворов $MnSe_{1-X}Te_X$ с концентрацией замещения $X = 0{,}1$ (1), 0,2 (2), 0,3 (3), 0,4 (*b*)

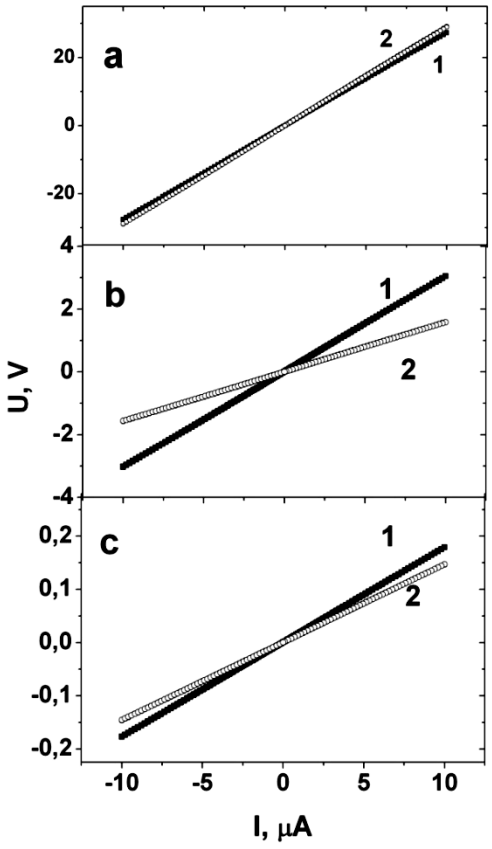

Fig. 2. The current-voltage characteristic of the $MnSe_{1-X}Te_X$ solid solution ($X = 0.1$) in a magnetic field $H = 1$ T (2) and in a zero magnetic field (1) at different temperatures T: 100K (*a*), 140K (*b*), 190K (*c*)

Рис. 2. Вольт-амперная характеристика твердого раствора $MnSe_{1-X}Te_X$ ($X = 0{,}1$) в магнитном поле $H = 1$ Т (2) и в нулевом магнитном поле (1) при разных температурах T: 100 К (*a*), 140 К (*b*), 190 К (*c*)

The dependence of the susceptibility on the history of the sample was found. Thus, the susceptibility of a sample cooled in a magnetic field is lower compared to a sample in a zero field. The relative change in the magnetic moment $(\sigma(H)-\sigma(0))/\sigma(0)$ is shown in fig. 3 (curves 3 and 4) and is in qualitative agreement with the temperature behavior of the magnetoresistance.

For $X = 0.1$, the relative change in the magnetic moment sharply increases in the neighbourhood of the Néel temperature and decreases in absolute value at $T = 220$ K, where the magnetoresistance disappears. For a composition with $X = 0.2$, a quantitative agreement is observed between the change in the magnetic moment and magnetoresistance as a function of temperature. The paramagnetic Curie temperature (θ), determined from the high-temperature inverse susceptibility, gradually decreases with increasing concentration of tellurium. In the molecular field approximation, $\theta = 2/3S(S + 1)zJSe$ for MnSe and for low concentrations, the paramagnetic Curie temperature of the $MnSe_{1-X}Te_X$ solid solution can be represented as $\theta = 2/3S(S + 1)(zJSe(1 - x) + JTex)$ or the normalized dependence $\theta(x)/\theta(MnSe) = 1 + x(\lambda - 1)$ is used to determine the sign of the exchange J(Mn-Te-Mn). The fitting functions with the ratio of the exchange parameters λ = J(Mn-Te-Mn)/J(Mn-Se-Mn) = –1.25 and –0.25 describe the experimental results well. For concentrations X <0.3, the sign of the exchange interaction changes to ferromagnetic with a decrease in the exchange value with increasing bond length, according to the theoretical prediction [34].

The formation of polarons or regions with a high concentration of electron density can be traced from the optical absorption spectra shown in fig. 4 for compositions $X = 0.2$ and 0.4 in the energy range 2000–12 000 cm^{-1}. Electromagnetic radiation can be absorbed by charge carriers during interband transitions, free charge carriers within the same energy zone and crystal lattice vibrations. The low-energy absorption spectrum provides information on phonon spectra and plasmon vibrations in semiconductors, in the high-energy region, on the band gap, on the structure of the valence band and the conduction band near their extrema. For frequencies $\omega < 5000$ cm^{-1}, an increase in the absorption of electromagnetic radiation is observed, caused by an increase in the electron concentration and metallization of the samples. However, these compositions of $MnSe_{1-X}Te_X$ solid solutions retain the activation type of conductivity. A sharp decrease in the absorption intensity below the maximum with energy $\omega = 9700$ cm^{-1} for $X = 0.4$ corresponds to the band gap of MnTe $\omega = 9100$ cm^{-1}. Those. at this concentration, Mn-Te-Mn bonds flow along the lattice. Near the bottom of the conduction band, additional absorption maxima are observed with $\omega_1 = 6300$ cm^{-1} and with $\omega_2 = 8700$ cm^{-1}, located in energy below the bottom of the conduction band by $\Delta E_1 = 3400$ cm^{-1} and $\Delta E_2 = 1000$ cm^{-1}. Possibly, these lines correspond to bound states of an electron and a hole, which form a hydrogen-like spectrum of excitons. The spectral line energies are described by the formula $E_n = 1.2–0.42/n^2$ eV with exciton binding energy $E_b = 0.42$ eV. We estimate the exciton radius from the formula $Rn = n^2\varepsilon m a_B/\mu$, where m is the mass of a free electron, a_B is the Bohr radius of the hydrogen atom, ε is the high-frequency permittivity for a small-radius exciton ε = 8 for MnSe [39], μ is the reduced electron and hole mass. For $\mu = 0.5m$, the exciton radius is $R_1 = 0.8$ nm = = 1.4 Å. Small-radius excitons move through the Mn-Te system and, at different effective masses of the electron and hole, contribute to the conductivity.

Magnetoresistance model. When anionic substitution occurs, chemical pressure and a change in the crystal field of the octahedron arise as a result of the difference in the ionic radii of selenium and tellurium. At low concentrations, when the octahedron consists of five selenium atoms and one tellurium atom, the bond lengths in the octahedron become not equivalent, which leads to a local increase in the crystal field and a change in the electron density between t_{2g} and e_g orbitals, i. e. to the formation of an electron on the t_{2g} orbital and a hole on the e_g orbital and to a change in the spin state of manganese ions in the neighbourhood of tellurium ions. The sign of the exchange interaction will also change as a result of the double exchange of electrons in e_g orbitals and the kinetic exchange in the t_{2g} subsystem. Distortion of the octahedron induces the splitting of t_{2g} and e_g orbitals with different projections of the $+–L^z$ orbital momentum onto the selected axis. The energy of the deformed octahedron decreases as a result of the rotation of the octahedra in the temperature range 200–250 K depending on the tellurium concentration and with a further decrease in temperature, it is possible that the manganese ions shift with a local change in the lattice symmetry, for example, of the orthorhombic type.

The microscopic model can be represented as ferromagnetic clusters in the neighbourhood of tellurium ions with a random orientation of the anisotropy axes and with orbital moments. In the $MnSe_{1-X}Te_X$ solid solution, we distinguish two temperature ranges, for $X = 0.1$ in the vicinity of the Néel temperature and for $X = 0.2$ in the paramagnetic region above the Néel temperature. For a composition with $X = 0.1$, the magnitude of the ferromagnetic exchange in the clusters exceeds the antiferromagnetic exchange in the MnSe matrix and an angular phase forms with a random orientation of the weak magnetic moment in the cluster in the antiferromagnetic region. When heated, the interaction between the clusters decreases, and the magnetic moments are oriented in the direction of the magnetic field, as a result, the ferromagnetic spin-spin correlation function along the transverse components of the spin increases, and the correlation radius increases. Above the Néel temperature, spin-spin correlations and the correlation radius decrease as a result of thermal fluctuations of the spin moment. In the off-diagonal Anderson model, this corresponds to a change in the width of the potential well and is associated with the temperature dependence of the electron localization radius in the form $\xi = A\left|1 - T/T_N\right|$. The magnetoresistance in semiconductors, the conductivity of which is described in a model with a variable jump length, has an exponential dependence

$$\left(\rho(H) - \rho(0)\right)/\rho(0) = \exp\left(-BH\xi\right) - 1 = \\ = \exp\left(-BH/\left|(1 - T/T_N)\right|\right) - 1, \quad (1)$$

where B is the parameter, H is the external magnetic field, ξ is the electron localization radius [40, 41]. The experimental data on magnetoresistance are satisfactorily described in the framework of this model with a field H = 0.8 T and a parameter B = 0.13 T^{-1} for $T > T_N$, and B = 0.05 T^{-1} in the magnetically ordered region. The fitting functions are shown in fig. 3, *a*, curve 5.

For the composition X = 0.2, the magnitude of the ferromagnetic exchange is much smaller than the antiferromagnetic interaction and the electrons are localized within the lattice constant, in potential wells, the width of which is fixed and the potential barrier varies with temperature. Here, one can use the model of tunneling of spin polarized electrons between potential wells in the form

$$\left(\rho(H)-\rho(0)\right)/\rho(0) = 1/\left(1+xP_1P_2\cos\theta\right)-1, \quad (2)$$

where x is the concentration of the wells, $P_{1,2}$ is the degree of polarization of the electrons, the angle θ between the axes of polarization of the electrons. The spin polarization of electrons is due to orbital ordering. Suppose that the polarization value $P_{1,2}$ is the same for all clusters and disappears at a temperature of orbital ordering T_0 according to a power law $P_{1,2} = P_0(1-T/T_0)^{1/4}$. To qualitatively understand the processes of electron tunneling between clusters with polarization axes are in the range of angles from $0 < \theta < \pi$, we consider a simple model when the anisotropy field H_A is parallel to and orthogonal to the external magnetic field. As a result of competition between the Zeeman interaction and the anisotropy field, the electron spin (polarization direction) will rotate in the direction of the external magnetic field with increasing temperature.

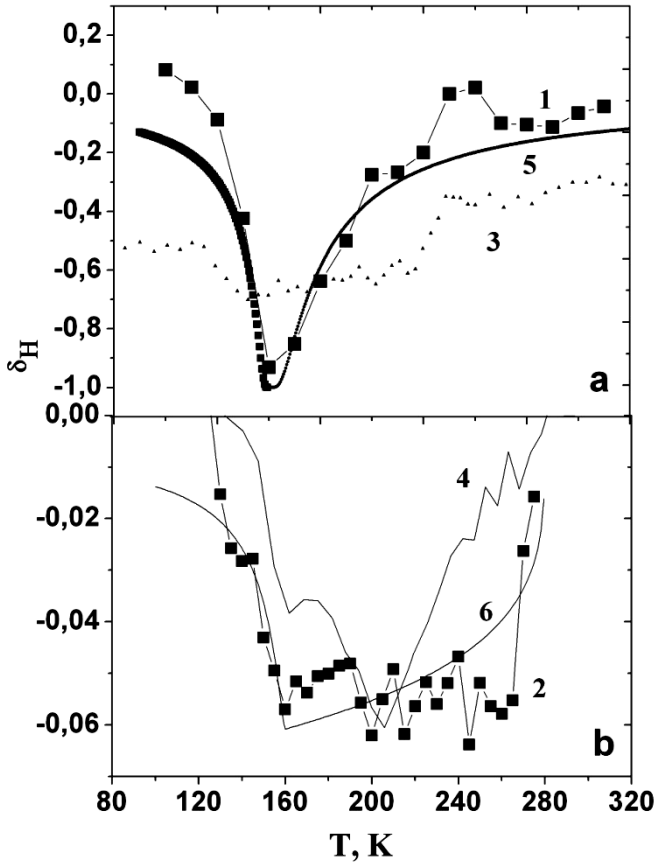

Fig. 3. Temperature dependences of the magnetoresistance of $MnSe_{1-X}Te_X$ chalcogenide with X = 0.1 (1) (*a*) and 0.2 (2) (*b*) at H = 13 kOe. The relative change in the magnetic moment σ (H) – σ (0) / σ (0) for X = 0.1 (3) and X = 0.2 (4). Fitting functions: for a concentration of X = 0.1 (5) from equation (1) at H = 0.8 T, B = 0.13 T^{-1} in the region of $T > T_N$, and B = 0.05 T–1 in $T < T_N$; for X = 0.2 (6) from equation (5) with parameters T_0 = 280 K, T^* = 160 K, n = 2/3, λ = 0.1, cluster concentration x = 0.08

Рис. 3. Температурные зависимости магнитосопротивления халькогенида $MnSe_{1-X}Te_X$ с X = 0,1 (1) (*a*) и 0,2 (2) (*b*) при H = 13 кЭ. Относительное изменение магнитного момента σ (H) – σ(0)/σ(0) для X = 0,1 (3) и X = 0,2 (4). Подгоночные функции: для концентрации X = 0,1 (5) из уравнения (1) при H = 0,8 Т, B = 0,13 Т – 1 в области $T > T_N$, и B = 0,05 Т–1 в $T < T_N$; для X = 0,2 (6) из уравнения (5) с параметрами T_0 = 280 K, T^* = 160 K, n = 2/3, λ = 0,1, концентрация кластеров x = 0,08

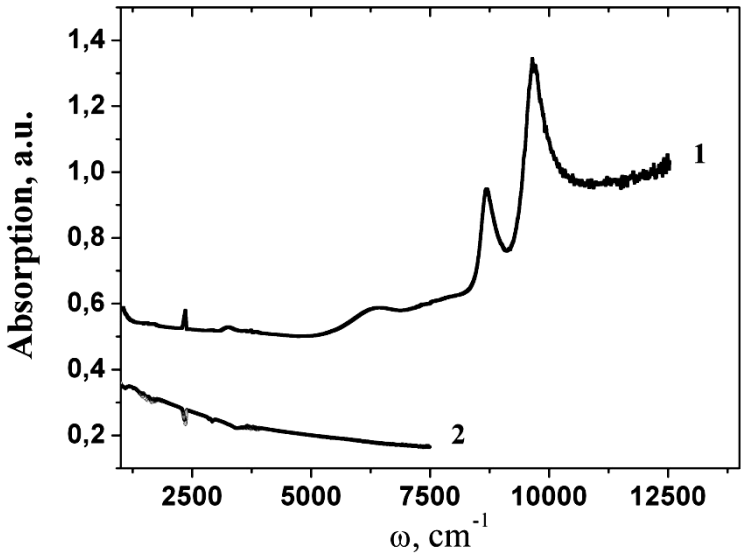

Fig. 4. Optical absorption spectra for $MnSe_{1-X}Te_X$ solid solutions with $X = 0.2$ (1), 0.4 (2) at $T = 300$ K

Рис. 4. Спектры оптического поглощения для твердых растворов $MnSe_{1-X}Te_X$ с $X = 0{,}2$ (1), 0,4 (2) при $T = 300$ К

The correlation between the spins is determined by orbital ordering. The energy of the magnetic system has the form

$$E = -SH\cos\theta - SH_A\cos(\gamma - \theta), \qquad (3)$$

where H_A is the anisotropy field, γ is the angle between the external magnetic field and the anisotropy field. The minimum energy value is achieved at an angle of:

$$\cos\theta = 1/\sqrt{\left(1 + H_A^2\sin^2\gamma/\left(H + H_A\cos\gamma\right)^2\right)}. \qquad (4)$$

The anisotropy field decreases with increasing temperature according to a power law in the form $H_A = K(1 - T/T^*)^n$, where T^* is the temperature at which the anisotropy field caused by rhombic distortion disappears. The ratio of the magnetic field to the anisotropy constant is denoted by $\lambda = H/K$. Then the temperature dependence of the magnetoresistance is presented in the form

$$\left(\rho(H) - \rho(0)\right)/\rho(0) =$$
$$= 1/\left(1 + xP_0^2\left(1 - T/T_0\right)^{1/2}/\sqrt{\left(1 + \left(1 - T/T^*\right)^{2n}/\lambda^2\right)}\right). \qquad (5)$$

In fig. 3, *b*, function (5) describes the experimental results with parameters $T_0 = 280$ K, $T^* = 160$ K, $n = 2/3$, $\lambda = 0.1$, cluster concentration $x = 0.08$. The tunneling model of spin-polarized electrons with orbital ordering explains the experimental results on magnetic properties and magnetoresistance.

The structure and electrical properties of thin films. With a change in the dimension of the system, the physical properties of materials change. In bulk samples of manganese telluride, the resistance is independent of the magnetic field; however, magnetoresistance with a maximum in the region of 200 K was found in thin-film MnTe compounds [42].

Positive magnetoresistance was found in topological insulators [43]. In a bulk Bi_2Te_3 sample, magnetoresistance (MR) is about 15 % at room temperature, and in Bi_2Te_3 thin films the giant MR effect reaches 600 % at room temperature [44; 45]. The observed large MR values at room temperature are directly related to a decrease in the dimension of the topological insulator. The magnetoresistance on 200 nm Bi_2Se_3 films has a linear temperature dependence and is retained in strong magnetic fields, including the high temperature region [46]. The MR effect is explained by the presence of two channels with high carrier mobility, which coexists with the usual bulk channel with a mobility of 60 $cm^2V^{-1}S^{-1}$ at high temperatures in thin Bi_2Se_3 films [47]. With decreasing temperature, the carrier density in the channel with high mobility decreases significantly and free carriers freeze below 85 K, leaving only a conducting bulk channel in the film.

A positive MR may be caused by the competition between the degenerate orbital states of the electron and strong electron correlations [48]. In the vicinity of the transition temperature of the orbitally ordered phase to the paraphase, the "spectral weight" shifts to the Fermi level. In this temperature range, the magnetic field again leads to an increase in the gap width and to stabilization of the orbital order. For narrow-gap semiconductors with a width of $W = 1$ eV, the corresponding temperature for the magnetoresistive effect is $T \approx 600$ K [48].

An increase in the magnetic field resistance in thin films of Sr_2CrWO_6 antiferromagnets is associated with the suppression of the long-range antiferromagnetic order and the formation of a short-range fluctuation region that enhance electron scattering [49].

When passing from bulk to thin-film samples in the MnSe and MnTe chalcogenides, the Néel temperature and activation energy decrease several times [50]. In the MnSe and MnTe films, the cubic structure of NaCl [51]

and the hexagonal NiAs structure [52] stabilize respectively. It is possible to detect an increase in the magnetoelectric effect in polycrystalline thin-film compounds in comparison with bulk samples of the $MnSe_{1-X}Te_X$ system.

Thin film polycrystalline compounds of manganese chalcogenides $MnSe_{1-X}Te_X$ were obtained by flash method deposition of previously synthesized solid solutions on glass slides. The precursors were powders with a grain size of 0.1 to 0.3 mm. Deposition was carried out in a vacuum installation for films deposition of type UVN-71R-2.

The pressure in the reaction chamber during deposition was 10^{-2}–10^{-3} Pa. The temperature of the tantalum evaporator was maintained at ~ 2000 °C. The substrates were located at a distance of 10 cm from the evaporator. The temperature of the substrates was 250–300 °C.

The evaporator temperature was significantly higher than the melting point of the solid solutions. Therefore, when a small mass of material enters the evaporator, it evaporates instantly, which ensures, after crystallization on a substrate located at a considerable distance from the evaporator, the composition and structure corresponding to bulk substances. A device based on shock vibration supplied the precursor to the evaporator. The film thickness ranged from 157 nm to 960 nm. The substrates consisted of quartz.

The X-ray diffraction analysis of the thin-film chalcogenide compounds $MnSe_{1-X}Te_X$ was carried out on a DRON-3 apparatus in CuKα radiation at a temperature of 300 K after they were obtained and after measurements of the magnetic and electrical properties. The structure of thin-film compounds differs from the face-centered cubic structure of bulk polycrystalline $MnSe_{1-X}Te_X$ of the same concentration [51]. According to X-ray diffraction analysis, the substitution of selenium by tellurium in thin-film chalcogenide compounds of the $MnSe_{1-X}Te_X$ system leads to a decrease in the peak intensities characteristic of the cubic structure and leads to the appearance of a nickel – arsenide (NiAs) hexagonal structure. The lattice parameter increases with increasing concentration of the substituting element, and the ratio c/a ~ 1.4 is less than 1.63 characteristic of bulk MnTe with a hexagonal NiAs type structure, which indicates a compression of the hexagonal densely packed structure.

In the temperature dependence of the resistance for $X = 0.1$, a maximum is observed due to the polymorphic transition (fig. 5). With an increase in the concentration of substitution, the maximum is smoothed out. Carrier transfer can occur as a result of electron hopping between domain walls, or due to diffusion of walls. These are activation processes where the electron mobility is determined by the expression $\mu = \mu_0 \exp(-E_a / k_0 T)$, where $\mu_0 = \frac{ba^2\nu}{k_0 T}$, ν is the hopping frequency equal to the phonon frequency (~10^{13} Hz), and a is the distance between domain walls [53]. A process of wall diffusion as a result of interaction with acoustic spin waves is possible. The wall flux is proportional to the diffusion coefficient $j \sim D \sim v\lambda$, where v is the spin wave velocity, λ is the mean free path, which is proportional to the spin correlation radius $\lambda \sim \xi = B/(1 - T/T_N)$.

The more spins deviate from the antiferromagnetic arrangement, the less is the energy loss when moving the wall. The diffusion of domain walls in an antiferromagnetic matrix increases with increasing temperature as $D \sim 1/(1 - T/T_N)$.

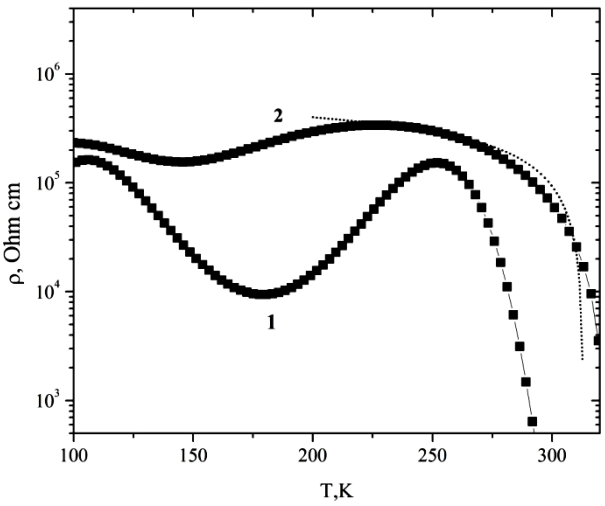

Fig. 5. The temperature dependence of the electrical resistivity for films MnSe0.9Te0.1 (1) and MnSe0.8Te0.2 (2). The dotted line indicates that the temperature dependence of the resistance is described by a power function (6)

Рис. 5. Зависимость электросопротивления от температуры для пленок MnSe0,9Te0,1 (1) и MnSe0,8Te0,2 (2). Пунктирная линия указывает, что зависимость сопротивления от температуры описывается степенной функцией (6)

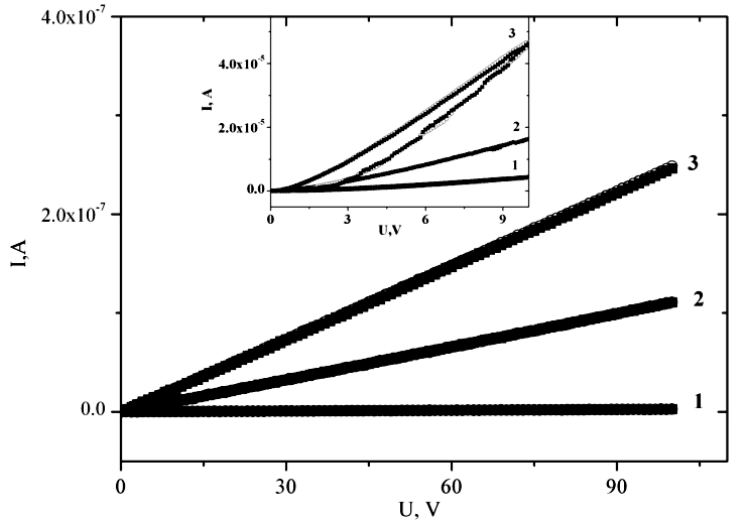

Fig. 6. The current-voltage characteristics measured in a zero magnetic field (empty circles) and field 12 kOe (black circles). MnSe0.9Te0.1 at T = 80 K(1), 180 K(2) and 220 K(3).
Insert: MnSe0.8Te0.2 at T = 80 K(1), 180 K(2) and 280 K(3)

Рис. 6. Вольт-амперные характеристики, измеренные в нулевом магнитном поле (светлые кружки) и поле 12 кЭ (черные кружки). MnSe0,9Te0,1 при T = 80 K (1), 180 K (2) и 220 K (3).
Вставка: MnSe0,8Te0,2 при T = 80K (1), 180K (2) и 280K (3)

The functional dependence of conductivity on temperature is presented in the form

$$\sigma = \frac{A}{T\exp\left(-E_a / kT\right)} + \frac{B}{\left(1-\frac{T}{T_N}\right)}, \qquad (6)$$

where A and B are adjustable parameters. For the composition with X = 0.2, function (1) describes the experimental results with A = 1 10^{-3}, B = 0.4 10^{-6}, E_a = 0.021eV. Above 200 K, the diffusion contribution prevails, and below the hopping carrier tunneling mechanism does.

The existence of domain walls above the polymorphic transition is confirmed from the current–voltage (I–V) characteristics measured at fixed temperatures in a zero magnetic field and in a field of 12 kOe. Fig. 6 shows the I–V characteristics for polycrystalline films of the $MnSe_{1-X}Te_X$ system (X = 0.1 and 0.2). For samples with a low substitution concentration, X = 0.1, the I–V characteristics are linear and independent of the applied field over the entire temperature range. With an increase in the concentration above the polymorphic transition temperature, the I–V characteristic hysteresis is detected, the width of which decreases in a magnetic field and, at voltages above 6 V, the hysteresis width changes by 10–20 %. With an increase in the magnetic field, the density of domain walls decreases and their mobility decreases.

Conclusion. In antiferromagnetic samples of $MnSe_{1-X}Te_X$ with a cubic structure, the effect of magnetoresistance in the neighbourhood of the Néel temperature of about 100 % was found for a composition with a substitution concentration of X = 0.1. The decrease in resistance in a magnetic field is due to an increase in the electron localization radius in potential wells as a result of competition between ferromagnetic and antiferromagnetic interactions and a reduction in the width of the potential barrier. For a composition with X = 0.2, a negative magnetoresistance in the paramagnetic state was discovered, which is caused by the tunneling of spin polarized electrons with orbital ordering and a change in the angle between the directions of polarization of electrons in potential wells as a result of competition between the spin interaction with an external magnetic field and anisotropy field. A correlation was found between the spin-glass behavior of the magnetization of samples cooled in and without a magnetic field and the temperature dependence of the magnetoresistance.

Peaks were found in the optical absorption spectra of $MnSe_{1-X}Te_X$ for a composition with X = 0.4. Near the bottom of the conduction band, there are additional absorption maxima located in energy below the bottom of the conduction band. It is possible that these lines correspond to bound states of an electron and a hole, which form a hydrogen-like spectrum of excitons.

In $MnSe_{1-X}Te_X$ thin polycrystalline films for x < 0.2, magnetoresistance is absent. The existence of domains and domain walls from the hysteresis of the I–V characteristic, which decreases in a magnetic field and is caused by a decrease in the density of domain walls in a magnetic field, is found.

References

1. Borukhovich A. S. *Fizika materialov i struktur sverkhprovodyashchey i poluprovodnikovoy spinovoy elektroniki* [Physics of materials and structures of super-

conducting and semiconductor spin electronics]. Yekaterinburg, 2004, 175 p.

2. Aplesnin S. S. *Osnovy spintroniki* [Spintronics]. Sankt-Peterburg, Lan' Publ., 2010, 288 p.

3. Aplesnin S. S., Sitnikov M. N., Zhivul'ko A. M. Change in the Magnetocapacity in the Paramagnetic Region in a Cation-Substituted Manganese Selenide. *Physics of the Solid State.* 2018, Vol. 60, No. 4, P. 673–680.

4. Romanova O. B., Aplesnin S. S., Sitnikov M. N., Kharkov A. M., Masyugin A. N., Yanushkevich K. I. Polymorphism in MnSe1-XTeX thin-films. *Solid State Communications*. 2019, Vol. 287, P. 72–76.

5. Aplesnin S. S., Romanova O. B., Korolev V. V., Sitnikov M. N., Yanushkevich K. I. Magnetoimpedance and magnetocapacitance of anion-substituted manganese. *J. Appl. Phys*. 2017, Vol. 121, P. 075701–7.

6. Romanova O. B., Aplesnin S. S., Khar'kov A.M., Masyugin A. N., Yanushkevich K. I. Galvanomagnetic properties of polycrystalline manganese selenide Gd0.2Mn0.8Se. *Physics of the Solid State*. 2017, Vol. 59, Iss. 7, P. 1290–1294.

7. Aplesnin S. S. *Magnitnye i elektricheskie svoystva sil'nokorrelirovannykh magnitnykh poluprovodnikov s chetyrekhspinovym vzaimodeystviem i s orbital'nym uporyadocheniem* [Magnetic and electrical properties of strongly correlated magnetic semiconductors with four-spin interaction and orbital ordering]. Moscow, Fizmatlit Publ., 2013, 176 p.

8. Aplesnin S. S. Anomalies of transport properties in a magnetically ordered region on a condo lattice. *JETP Letters.* 2005, Vol. 81, P. 74–79.

9. Aplesnin S. S., Sitnikov M. N. Magnetotransport effects in the paramagnetic state in GDXMN1− XS. *JETP Letters.* 2014, Vol. 100, Iss. 1–2, P. 104–110.

10. Aplesnin S. S., Petrakovskii G. A., Ryabinkina L. I., Abramova G. M., Kiselev N. I., Romanova O .B. Influence of magnetic ordering on the resistivity anisotropy of α-MNS single crystal. *Solid State Communications.* 2004, Vol. 129, Iss. 3, P. 195–197.

11. Aplesnin S. S., Ryabinkina L. I., Abramova G. M. et al. Spin-dependent transport in alpha-MNS single crystal. *Physics of the Solid State.* 2004, Vol. 46, Iss. 11, P. 2000–2005.

12. Aplesnin S. S., Ryabinkina L. I., Romanova O. B. et al. Magnetic and electrical properties of cationically substituted MeXMn1-XS sulfides (Me = Co, Gd). *Physics of the Solid State*. 2009, Vol. 51, Iss. 4, P. 661–664.

13. Nagaev E. L. Lanthanum manganites and other magnetic conductors with giant magnetoresistance. *Phisics Uspekhi*. 1996, Vol. 176, Iss. 8, P. 832–858.

14. Demin R. V., Gorbenko Y. Y., Kaul' A. R. et al. Colossal magnetoresistance at room temperature in La1-xAgyMnO3 epitaxial thin films. *Physics of the Solid State.* 2005, Vol. 56, Iss. 7, P. 2195–2199.

15. Kagan M. Yu., Kugel' K. I. Inhomogeneous charge states and phase separation in manganites. *Phisics Uspekhi.* 2001, Iss. 171, P. 577–596.

16. Kugel K. I., Rakhmanov A. L., Sboychakov A. O. et al. Characteristics of the phase-layered state of manganites and their relationship with the transport and magnetic properties. *JETP*. 2004, Vol. 125, P. 648.

17. Kagan M. Yu., Klapcov A. V., Brodskij I. V. et al. Small-scale phase separation and electron transport in manganites. *Phisics Uspekhi,* 2003, Iss. 173, P. 877.

18. Boruhovich A. S., Ignat'eva N. I., Galyas A. I. et al. Thin-film ferromagnetic composite for spintronics. *JETP Letters.* 2006, Vol. 84, Iss. 9, P. 592–595.

19. Koroleva L. I., Demin R. V., Varchevskij D. et al. Normal spinel CuCr1.6Sb0.4S4 is a new material with giant magnetoresistance. *JETP Letters.* 2000, Vol.72, Iss. 11, P. 813–818.

20. Zhaorong Y., Shun T., Zhiwen C. et. al. Magnetic polaron conductivity in FeCr2S4 with the colossal magnetoresistance effect. *Phys.Rev. B*, 2000. Vol. 62, Iss 21, P. 13872.

21. Aplesnin S., Romanova O., Har'kov A., Balaev D., Gorev M., Vorotinov A., Sokolov V., Pichugin A. Metall-semiconductors transition in SmXMn1-XS solid solutions. *Physica Status Solidi (B): Basic Solid State Physics*. 2012, Vol. 249, Iss. 4, P. 812–817.

22. Aplesnin S. S., Kharkov A. M., Eremin E. V., Romanova O. B., Balaev D. A., Sokolov V. V., Pichugin A. Yu. Nonuniform Magnetic States and Electrical Properties of Solid Solutions. *IEEE Transactions on magnetics.* 2011, Vol. 47, P. 4413–4416.

23. Ryabinkina L. I., Romanova O. B., Aplesnin S. S. Sulfide compounds MeXMn1-XS (Me = Cr, Fe, V, Co): technology, transport properties and magnetic ordering. *Bulletin of the Russian Academy of Sciences. Physics*. 2008, Vol. 72, Iss. 8, P. 1115–1117.

24. Ryabinkina L. I., Petrakovskii G. A., Loseva G. V., Aplesnin S. S. Metal-insulator transition and magnetic properties in disordered systems of solid solutions MEXMN1-XS. *Journal of Magnetism and Magnetic Materials*. 1995, Vol. 140–144, Iss. 1, P. 147–148.

25. Aplesnin S. S., Ryabinkina L. I., Abramova G. M. et al. Spin-dependent transport in an alpha-MnS single crystal. *Physics of the Solid State.* 2000, Vol. 46, Iss. 11, P. 2004.

26. Petrakovskij G. A., Ryabinkina L. I., Velikanov D. A. et al. Low-temperature electronic and magnetic transitions in the antiferromagnetic semiconductor Cr0.5Mn0.5S. *Physics of the Solid State*. 1999, Vol. 41, Iss. 9, P. 1660–1664.

27. Petrakovskij G. A., Ryabinkina L. I., Abramova G. M. et al. The phenomenon of colossal magnetoresistance in MexMn1-xS sulfides (Me = Fe, Cr). *JETP Letters.* 2000, Vol. 72, Iss. 2, P. 99–102.

28. Ryabinkina L. I., Abramova G. M., Romanova O. B. et al. Hall effect in magnetic semiconductors FexMn1-xS. *Physics of the Solid State.* 2004, Vol. 46, Iss. 6, P. 1038–1042.

29. Efrem J. B. C., D'Sa, Bhobe P. A. et. al. Low temperature magnetic structure of MnSe. *J. Phys*. 2004, Vol. 63, P. 227–232.

30. Yanushkevich K. I. Solid solutions of 3d metal monochalcogenides, *Varaksin AN*. 2009, P. 256.

31. Decker D. L., Wild R. L. Optical Properties of a-MnSe. *Physical Review*. 1971, Vol. 4, P. 3425.

32. Szuszkiewicz B., Hennion B., Witkowska B. et al. Neutron scattering study of structural and magnetic properties of hexagonal MnTe. *Physica status solidi*. 2005, Vol. 2, Iss. 3, P. 1141.

33. Aplesnin S. S., Ryabinkina L. I., Romanova O. B. et. al. The effect of orbital ordering on the transport and magnetic properties of MnSe and MnTe. *Phisics of the solid state*. 2007, Vol. 49, Iss. 11, P. 1984–1989.

34. Su-Huai Wei, Zunger A. Total-energy and band – structure calculations for the semimagnetic $Cd_{1-x}Mn_xTe$ semiconductor alloy and its binary consistuens. *Physical Review B*. 1987, Vol. 35, P. 2340.

35. Penkalya T. *Ocherki kristallokhimii. Khimiya* [Essays on Crystal Chemistry. Chemistry]. Leningrad, 1974, 496 p.

36. Aplesnin S. S., Romanova O. B., Gorev M. V. et. al. Synthesis, structural and magnetic properties of anion-substituted manganese chalcogenides. *Phisics of the solid state*. 2012, Vol. 54, Iss. 7, P. 1296–1301.

37. Aplesnin S. S. Nonadiabatic interaction of acoustic phonons with spins $S = 1/2$ in the two-dimensional Heisenberg model. *Journal of Experimental and Theoretical Physics*. 2003, Vol. 124, B. 5, P. 1080–1089.

38. Petrakovskiĭ G. A., Sablina K. A., Vorotynov A. M., Kruglik A. I., Klimenko A. G., Balaev A. D., Aplesnin S. S. The magnetic and resonance properties of the crystal and amorphous $CuGeO_3$. *Journal of Experimental and Theoretical Physics*. 1990, Vol. 71, P. 772–780.

39. Kitel' Ch. *Vvedenie v fiziku tverdogo tela* [Introduction to Solid State Physics]. Moscow, Nauka Publ., 1978, 791 p.

40. Nguen V. L., Spivak B. Z., Shklovskiy B. I. [Aharonov-Bohm Oscillation with normal and superconducting flux quanta in jump conductivity]. *JETP Letters*. 1985, Vol. 41, P. 35–38.

41. Nguen V. L., Spivak B. Z., Shklovskiy B. I. [Tunnel jumps in disordered systems]. *JETP Letters*. 1985, Vol. 89, P. 1770–1784.

42. Kriegner D., Výborný K., Olejník K., Reichlová H., Novák V., Marti X., Gazquez J., Saidl V., Nêmec P., Volobuev V. V., Springholz G., Holý V., Jungwirth T. Multiple-stable anistropic magneto resistance memory in antiferromagnetic MnTe. *Nature Communications*. 2016, Vol. 7, P. 11623.

43. Yuan Li, Mansoor B. A. Jalil, Seng Ghee Tan, Zhou G., Qian Z. Magnetoresistive effect of a topological-insulator waveguide in the presence of a magnetic field. *Applied Physics Letters*. 2012, Vol. 101, P. 262403–4.

44. Qu D. X., Hor Y. S., Xiong J., Cava R. J., Ong N. P. Quantum Oscillations and Hall Anomaly of Surface States in the Topological Insulator Bi_2Te_3. *Science*. 2010, Vol. 329, P. 821284.

45. Hsieh D., Xia Y., Qian D., Wray L., Meier F., Dil J.H., [et. al.] Observation of Time-Reversal-Protected Single-Dirac-Cone Topological-Insulator States in Bi_2Te_2 and Sb_2Te_3. *Physical Review Letters.* 2009, Vol. 103. P. 146401.

46. Xu Z. J., Guo X., Yao M. Y., He H. T., Miao L., Jiao L., Liu H. C., Wang J. N., Qian D., Jia J. F., Ho W. K., Xie M. H. Molecular-beam epitaxy of topological insulator Bi_2Se_3 (111) and (221) thin films. *Adv. Mater*. 2013, Vol. 25, P. 1557–1562.

47. He H. T., Liu H. C., Li B. K., Guo X., Xu Z. J., Xie M. H. Disorder-induced liner magnetoresistance in (221) topological insulator Bi_2Se_3 films. *Applied Physics Letters*. 2013, Vol. 103, P. 031606–4.

48. Peters R., Kawakami N., Pruschke T. Orbital Order, Metal Insulator Transition, and Magnetoresistance-Effect in the two-orbital Hubbard model. *Physical Review B*. 2011, Vol. 83, No. 12, P. 125110.

49. Ji Zhang, Wei-Jing Ji, Jie Xu, Xiao-Yu Geng, Jian Zhou, Zheng-Bin Gu, Shu-Hua Yao, Shan-Tao Zhang Giant positive magnetoresistance in half-metallic double-perovskite Sr_2CrWO_6 thin films. *Science Advances*. 2017, Vol. 3, No 11, P. 1–7.

50. John Q., Samuel Jiang, Chien C. L., Xiao J. Q. Giant magnetoresistance in nonmultilayer magnetic systems. *Physical Review Letters*. 1992, Vol. 68, Iss. 25, P. 3749.

51. Mahalingam T., Thanikaikarasan S., Dhanasekaran V., Kathalingam A., Velumani S., Rhee Jin-Koo Preparation and characterization of MnSe thin films. *Materials Science and Engineering*. 2010, Vol. 174, P. 257–262.

52. Szuszkiewicz W., Hennion B., Witkowska B., Łusakowska E., Mycielski A. A Neutron skattering study of structural and magnetic properties of hexagonal MnTe. *Physica Status Solidi C*. 2005, No. 2, P. 1141–1146.

53. Kagan M. Yu., Kugel K. I. *Popravki k stat'e. Neodnorodnye zaryadovye sostoyaniya i fazovoe rassloenie v magnitakh* [Amendment to article. Inhomogeneous charge States and phase stratification in magnets]. *Physics-Uspekhi*. 2001, Vol. 171, P. 577–596.

Библиографические ссылки

1. Борухович А. С. Физика материалов и структур сверхпроводящей и полупроводниковой спиновой электроники. Екатеринбург : УрО РАН, 2004. 175 с.

2. Аплеснин С. С. Основы спинтроники. СПб. : Лань, 2010. 288 с.

3. Aplesnin S. S., Sitnikov M. N., Zhivul'ko A. M. Change in the Magnetocapacity in the Paramagnetic Region in a Cation-Substituted Manganese Selenide // Physics of the Solid State. 2018. Vol. 60, No. 4. P. 673–680.

4. Polymorphism in MnSe1-XTeX thin-films / O. B. Romanova, S. S. Aplesnin, M. N. Sitnikov et al. // Solid State Communications. 2019. Vol. 287. P. 72–76.

5. Magnetoimpedance and magnetocapacitance of anion-substituted manganese / S. S. Aplesnin, O. B. Romanova, V. V. Korolev et al. // J. Appl. Phys. 2017. Vol. 121. P. 075701–7.

6. Гальваномагнитные свойства поликристаллического селенида марганца Gd0.2Mn0.8Se / О. Б. Романова, С. С. Аплеснин, А. М. Харьков и др. // Физика твердого тела. 2017. Т. 59, В. 7. С. 1290–1294.

7. Аплеснин С. С. Магнитные и электрические свойства сильнокоррелированных магнитных полупроводников с четырехспиновым взаимодействием и с орбитальным упорядочением. М. : Физматлит, 2013. 176 с.

8. Аплеснин С. С. Аномалии транспортных свойств в магнитоупорядоченной области на кондорешетке // Письма в ЖЭТФ. 2005. Т. 81. С. 74–79.

9. Аплеснин С. С., Ситников М. Н. Магнитотранспортные эффекты в парамагнитном состоянии в GDXMN1− XS. // Письма в ЖЭТФ. 2014. Т. 100, В. 1-2. С. 104–110.

10. Influence of magnetic ordering on the resistivity anisotropy of α-MNS single crystal / S. S. Aplesnin,

G. A. Petrakovskii, L. I. Ryabinkina et al. // Solid State Communications. 2004. Vol. 129, Iss. 3. P. 195–197.

11. Спин-зависимый транспорт в монокристалле alpha-MNS / С. С. Аплеснин, Л. И. Рябинкина, Г. М. Абрамова и др. // Физика твердого тела. 2004. Т. 46, В. 11. С. 2000–2005.

12. Магнитные и электрические свойства катион-замещенных сульфидов MeXMn1-XS(Me = Co, Gd) / С. С. Аплеснин, Л. И. Рябинкина, О. Б. Романова и др. // ФТТ. 2009. Т. 51, В. 4. С. 661–664.

13. Нагаев Э. Л. Манганиты лантана и другие магнитные проводники с гигантским магнитосопротивлением // Успехи физических наук. 1996. Т. 166, В. 8. С. 832–858.

14. Колоссальное магнитосопротивление при комнатных температурах в эпитаксиальных тонких пленках La1-xAgyMnO$_3$ / Р. В. Демин, Ю. О. Горбенко, А. Р. Кауль и др. // ФТТ. 2005. Т. 47, В. 12. С. 2195–2199.

15. Каган М. Ю., Кугель К. И. Неоднородные зарядовые состояния и фазовое расслоение в манганитах // УФН. 2001. В. 171. С. 577–596.

16. Характеристики фазово-расслоенного состояния манганитов и их связь с транспортными и магнитными свойствами / К. И. Кугель, А. Л. Рахманов, А. О. Сбойчаков и др. // ЖЭТФ. 2004. Т. 125. С. 648.

17. Мелкомасштабное фазовое расслоение и электронный транспорт в манганитах / М. Ю. Каган, А. В. Клапцов, И. В. Бродский и др. // УФН. 2003. В. 173. С. 877.

18. Тонкопленочный ферромагнитный композит для спинтроники / А. С. Борухович, Н. И. Игнатьева, А. И. Галяс и др. // Письма в ЖЭТФ. 2006. Т. 84, В. 9. С. 592–595.

19. Нормальная шпинель CuCr$_{1.6}$Sb$_{0.4}$S$_4$-новый материал с гигантским магнитосопротивление / Л. И. Королева, Р. В. Демин, Д. Варчевский и др. // Письма в ЖЭТФ. 2000. Т. 72, В. 11. С. 813–818.

20. Magnetic polaron conductivity in FeCr$_2$S$_4$ with the colossal magnetoresistance effect / Y. Zhaorong, T. Shun, C. Zhiwen et al. // Phys.Rev. B. 2000. Vol. 62, Iss. 21. P. 13872.

21. Metall-semiconductors transition in SmXMn1-XS solid solutions / S Aplesnin., O. Romanova, A. Har'kov et al. // Physica Status Solidi (B): Basic Solid State Physics. 2012. Vol. 249, Iss. 4. P. 812–817.

22. Aplesnin S. S., Kharkov A. M., Eremin E. V., Romanova O. B., Balaev D. A., Sokolov V. V., Pichugin A. Yu. Nonuniform Magnetic States and Electrical Properties of Solid Solutions // IEEE Transactions on magnetics. 2011, Vol. 47, P. 4413–4416.

23. Рябинкина Л. И., Романова О. Б., Аплеснин С. С. Сульфидные соединения MeXMn1-XS(Me = Cr, Fe, V, Co): технология, транспортные свойства и магнитное упорядочение // Известия российской академии наук. Серия физическая. 2008. Т. 72, В. 8. С. 1115–1117.

24. Ryabinkina L. I., Petrakovskii G. A., Loseva G. V., Aplesnin S. S. Metal-insulator transition and magnetic properties in disordered systems of solid solutions MEXMN1-XS // Journal of Magnetism and Magnetic Materials. 1995. Vol. 140–144, Iss. 1. P. 147–148.

25. Спин-зависимый транспорт в монокристалле alpha-MnS / С. С. Аплеснин, Л. И. Рябинкина, Г. М. Абрамова и др. // ФТТ. 2000. Т. 46, В. 11. С. 2004.

26. Низкотемпературные электронные и магнитные переходы в антиферромагнитном полупроводнике Cr$_{0.5}$Mn$_{0.5}$S / Г. А. Петраковский, Л. И. Рябинкина, Д. А. Великанов и др. // ФТТ. 1999. Т. 41, В. 9. С. 1660–1664.

27. Явление колоссального магнитосопротивления в сульфидах Me$_x$Mn$_{1-x}$S (Me=Fe, Cr) / Г. А. Петраковский, Л. И. Рябинкина, Г. М. Абрамова и др. // Письма в ЖЭТФ. 2000. Т. 72, В. 2. С. 99–102.

28. Эффект Холла в магнитных полупроводниках Fe$_x$Mn$_{1-x}$S / Л. И. Рябинкина, Г. М. Абрамова, О. Б. Романова и др. // ФТТ. 2004. Т. 46, В. 6. С. 1038–1042.

29. Low temperature magnetic structure of MnSe / J. B. C. Efrem, D'Sa, P. A. Bhobe et al. // J. Phys. 2004. Vol. 63. P. 227–232.

30. Янушкевич К. И., Вараксин А. Н. Твердые растворы монохалькогенидов 3d-металлов. Минск, 2009. С. 256.

31. Decker D. L., Wild R. L. Optical Properties of a-MnSe // Phys. Rev. 1971. Vol. 4. P. 3425.

32. Neutron scattering study of structural and magnetic properties of hexagonal MnTe / B. Szuszkiewicz, B. Hennion, B. Witkowska et. al. // Physica status solidi. 2005, Vol. 2, Iss 3. P. 1141.

33. Влияние орбитального упорядочения на транспортные и магнитные свойства MnSe и MnTe / С. С. Аплеснин, Л. И. Рябинкина, О. Б. Романова и др. // ФТТ. 2007. Т. 49, В. 11. С. 1984–1989.

34. Su-Huai Wei, Zunger A. Total-energy and band – structure calculations for the semimagnetic Cd$_{1-x}$Mn$_x$Te semiconductor alloy and its binary consistuens // Phys. Rev. B. 1987. Vol. 35. P. 2340.

35. Пенкаля Т. Очерки кристаллохимии. Химия. Ленинград, 1974. 496 с.

36. Синтез, структурные и магнитные свойства анион-замещенных халькогенидов марганца / С. С. Аплеснин, О. Б. Романова, М. В. Горев и др. // ФТТ. 2012. Т. 54, В.7. С. 1296–1301.

37. Аплеснин С. С. Неадиабатическое взаимодействие акустических фононов со спинами S = 1/2 в двумерной модели гейзенберга // Журнал экспериментальной и теоретической физики. 2003. Т. 124, В. 5. С. 1080–1089.

38. The magnetic and resonance properties of the crystal and amorphous CuGeO$_3$ / G. A. Petrakovskiĭ, K. A. Sablina, A. M. Vorotynov et al. // Soviet Physics – JETP. 1990. Vol. 71. P. 772–780.

39. Китель Ч. Введение в физику твердого тела. М. : Наука, 1978. 791 с.

40. Нгуен В. Л., Спивак Б. З., Шкловский Б. И. Осциляция Ааронова – Бома с нормальным и сверхпроводящим квантами потока в прыжковой проводимости // Письма в ЖЭТФ. 1985. Т. 41. С. 35–38.

41. Нгуен В. Л., Спивак Б. З., Шкловский Б. И. Туннельные прыжки в неупорядоченных системах // ЖЭТФ. 1985. Т. 89. С. 1770–1784.

42. Multiple-stable anistropic magneto resistance memory in antiferromagnetic MnTe / D. Kriegner, K. Výborný, K. Olejník et al. // Nature Communications. 2016, Vol. 7. P. 11623.

43. Magnetoresistive effect of a topological-insulator waveguide in the presence of a magnetic field / Yuan Li, B. A. Mansoor Jalil, Seng Ghee Tan et al. // Appl. Phys. Lett. 2012, Vol. 101. P. 262403–4.

44. Quantum Oscillations and Hall Anomaly of Surface States in the Topological Insulator Bi2Te3 / D. X. Qu, Y. S. Hor, J. Xiong et al. // Science. 2010. Vol. 329. P. 821284.

45. Observation of Time-Reversal-Protected Single-Dirac-Cone Topological-Insulator States in Bi_2Te_2 and Sb_2Te_3 / D. Hsieh, Y. Xia, D. Qian et. al. // Phys. Rev. Lett. 2009. Vol. 103. P. 146401.

46. Molecular-beam epitaxy of topological insulator Bi_2Se_3 (111) and (221) thin films / Z. J. Xu, X. Guo, M. Y. Yao et al. // Adv. Mater. 2013. Vol. 25. P. 1557–1562.

47. Disorder-induced liner magnetoresistance in (221) topological insulator Bi_2Se_3 films / H. T. He, H. C. Liu, B. K. Li et al. // Appl. Phys. Lett. 2013. Vol. 103. P. 031606–4.

48. Peters R., Kawakami N., Pruschke T. Orbital Order, Metal Insulator Transition, and Magnetoresistance-Effect in the two-orbital Hubbard model // Phys. Rev. B. 2011. Vol. 83, No. 12. P. 125110.

49. Giant positive magnetoresistance in half-metallic double-perovskite Sr_2CrWO_6 thin films / Ji Zhang, Wei-Jing Ji, Jie Xu et al. // Sci. Adv. 2017. Vol. 3, No. 11. P. 1–7.

50. Giant magnetoresistance in nonmultilayer magnetic systems / Q. John, Jiang Samuel, C. L. Chien, J. Q. Xiao // Phys. Rev. Lett. 1992. Vol. 68, Iss. 25. P. 3749.

51. Preparation and characterization of MnSe thin films / T. Mahalingam, S. Thanikaikarasan, V. Dhanasekaran et al. // Mat.Sci. Eng. 2010. Vol. 174. P. 257–262.

52. A Neutron skattering study of structural and magnetic properties of hexagonal MnTe / W. Szuszkiewicz, B. Hennion, B. Witkowska et al. // Phys. Stat. Sol. C. 2005. Vol. 2. P. 1141–1146.

53. Kagan M. Yu., Kugel K. I. Поправки к статье. Неоднородные зарядовые состояния и фазовое расслоение в магнитах // UFN. 2001. Vol. 171. P. 577–596.

Aplesnin Sergey Stepanovich – D. Sc., Professor; Reshetnev Siberian State University of Science and Technology. E-mail: aplesnin@sibsau.ru.

Yanushkevich Kazimir Iosifovich – D. Sc., Head of the Lab Magnetic Materials, GO "SPC NAS of Belarus on Material Science". E-mail: kazimir@mail.ru.

Аплеснин Сергей Степанович – доктор физико-математических наук, профессор, заведующий кафедрой; Сибирский государственный университет науки и технологий имени академика М. Ф. Решетнева. E-mail: aplesnin@sibsau.ru.

Янушкевич Казимир Иосифович – доктор физико-математических наук, заведующий лаборатории магнитных материалов; ГО «НПЦ НАН Беларуси по материаловедению». E-mail: kazimir@mail.ru.

UDC 621.791.722
Doi: 10.31772/2587-6066-2020-21-2-266-273

For citation: Kurashkin S. O., Seregin Yu. N., Murygin A. V., Petrenko V. E. Features of modeling the electron beam distribution energy for the electron-beam welding process. *Siberian Journal of Science and Technology.* 2020, Vol. 21, No. 2, P. 266–273. Doi: 10.31772/2587-6066-2020-21-2-266-273

Для цитирования: Особенности моделирования распределения энергии электронного пучка для процесса электронно-лучевой сварки / С. О. Курашкин, Ю. Н. Серегин, А. В. Мурыгин, В. Е. Петренко // Сибирский журнал науки и технологий. 2020. Т. 21, № 2. С. 266–273. Doi: 10.31772/2587-6066-2020-21-2-266-273

FEATURES OF MODELING THE ELECTRON BEAM DISTRIBUTION ENERGY FOR THE ELECTRON-BEAM WELDING PROCESS

S. O. Kurashkin*, Yu. N. Seregin, A. V. Murygin, V. E. Petrenko

Reshetnev Siberian State University of Science and Technology
31, Krasnoyarskii rabochii prospekt, Krasnoyarsk, 660037, Russian Federation
*E-mail: scorpion_ser@mail.ru

The energy distribution of the electron beam by means of application of various scanning paths, affects formation of the weld, which relates to the quality of the welded joints. Experimental studies, conducted by the authors of the article showed that scanning the electron beam in the form of a raster shape gives the best quality of welded joints; therefore, the trajectories of a classical raster and a truncated raster are proposed for the electron beam welding process. When conducting research in this direction, the authors discovered the following regularity: with an increase in the scanning amplitude along the junction, the vapour-gas penetration channel transforms into a stable cavity, along the front wall of which the metal melts, and along the side walls it is transferred to the tail of the weld pool.

The discovered effect of the formation of a penetration cavity is to be investigated in electron beam welding of various materials and thicknesses. For this the necessary equipment is to be created, allowing to make scanning in the form of various rasters. To improve the quality of the electron beam welding process, trajectories of a classical raster and a truncated raster across the joint are proposed. For these scanning trajectories, analytical expressions and families of calculated characteristics of the electron beam energy density distribution over the heating spot are obtained. Modulation of the electron beam oscillation in the form of a truncated raster across the junction makes it possible to obtain a two-humped distribution of the beam energy on the surface of the part along the heating spot. The obtained characteristics allow a more meaningful approach to optimizing the process of electron beam welding of various materials.

Keywords: electron-beam welding, modelling, technological parameters, electron beam, optimisation, normal distribution law.

ОСОБЕННОСТИ МОДЕЛИРОВАНИЯ РАСПРЕДЕЛЕНИЯ ЭНЕРГИИ ЭЛЕКТРОННОГО ПУЧКА ДЛЯ ПРОЦЕССА ЭЛЕКТРОННО-ЛУЧЕВОЙ СВАРКИ

С. О. Курашкин*, Ю. Н. Серегин, А. В. Мурыгин, В. Е. Петренко

Сибирский государственный университет науки и технологий имени академика М. Ф. Решетнева
Российская Федерация, 660037, Красноярск, просп. им. газ. «Красноярский рабочий», 31
*E-mail: scorpion_ser@mail.ru

Распределение энергии электронного пучка путем использования различных траекторий сканирования влияет на формирование сварного шва, что связано с качеством сварного соединения. Экспериментальные исследования авторов статьи показали, что наилучшее качество сварных соединений дает сканирование электронного пучка в виде растровой формы; поэтому для процесса электронно-лучевой сварки предложены траектории классического растра и усеченного растра. При исследовании в этом направлении авторами обнаружена следующая закономерность: при увеличении амплитуды сканирования вдоль стыка парогазовый канал проплавления трансформируется в устойчивую полость, по передней стенке которой происходит плавление металла, а по боковым стенкам – его перенос в хвостовую часть сварочной ванны.

Обнаруженный эффект образования полости проплавления необходимо исследовать при электронно-лучевой сварке различных материалов и толщин. Для этого должна быть создана аппаратура, реализующая сканирование в виде различных растров. Для повышения качества процесса электронно-лучевой сварки предложены траектории классического и усеченного растра поперек стыка. Для этих траекторий сканирования получены аналитические выражения и семейства расчетных характеристик плотности распределения энергии электронного пучка по пятну нагрева. Моделирование форм осцилляции электронного пучка в виде усеченного растра поперёк стыка даёт возможность получить двугорбое распределение энергии пучка на по-

верхности детали по пятну нагрева. Полученные характеристики позволяют более осмысленно подходить к оптимизации процесса электронно-лучевой сварки различных материалов.

Ключевые слова: электронно-лучевая сварка, моделирование, технологические параметры, электронный пучок, оптимизация, распределение энергии.

Introduction. The combination of energy and technological parameters of the process determines the quality of the weld in electron beam welding (EBW). The electron beam is a source of highly concentrated energy. The formation of deep penetration by a focused electron beam is achieved by means of formation of a vapor-gas channel in which the beam energy is transported. In this case, the welding seam gets a dagger shape with a characteristic mushroom formation in the upper part. The process of forming a weld in this case is oscillatory in nature with a periodic unstable melting channel. The mushroom-shaped expansion of the weld in its upper part is connected with periodic beam scattering on the metal vapor. Such a welding process is rarely used in practice except cases of through penetration. The pointed shape of the weld in the root part leads to the formation of root defects – voids arising from the displacement of liquid metal by the penetration channel. In order to avoid such defects, it is necessary to form a wider root part of the seam. The simplest way to form the radius at the root of the seam is to defocus the electron beam, which is used in practice mainly at installations with an accelerating voltage of 30÷60 kV.

The beam defocusing does not completely eliminate the root defects, in addition, the seam takes a shape close to a triangular one, the penetration depth decreases, deformation and tension occurs. Therefore, the defocusing of the electron beam is used only for EBW products of small thickness [1].

To prevent root defects, it is necessary to form a parodynamic channel with a sufficiently wide lower part. From the technical side, the most effective way of influencing the formation of a penetration channel is to oscillate an electron beam on the surface of the welded product. The current trend in the development of welding technology is to use complex reamers to form welds with a given cross-sectional shape. Illustration of an example of such a development, executed by Steirgerwald Strahltechnik company, is shown in fig. 1. Application of digital signal generators allows to create rasters of any shape with a fairly high resolution of up to 24 bits, which opens up great opportunities in the field of heat treatment, welding and soldering, and also plays a key role in solving the problem of pointing to the joint [2].

The technique for choosing the shape of the electron beam scan has not yet been developed. At the same time, a rather large amount of experimental data has been gathered [3]. The following beam scans are most widely used: longitudinal [4], x-shaped [4–6], circular and elliptical [6–9], arc and staple [10–13]. Sweep amplitudes usually vary between 1–3 mm.

Electron beam welding with the rotation of the electron beam along a circular path allows to gain a significant reduction in root defects and peak formation, however, since the power density in the central part of the heating zone is small, application of circular scanning leads to a decrease in the penetration depth compared to a fixed beam electron beam welding.

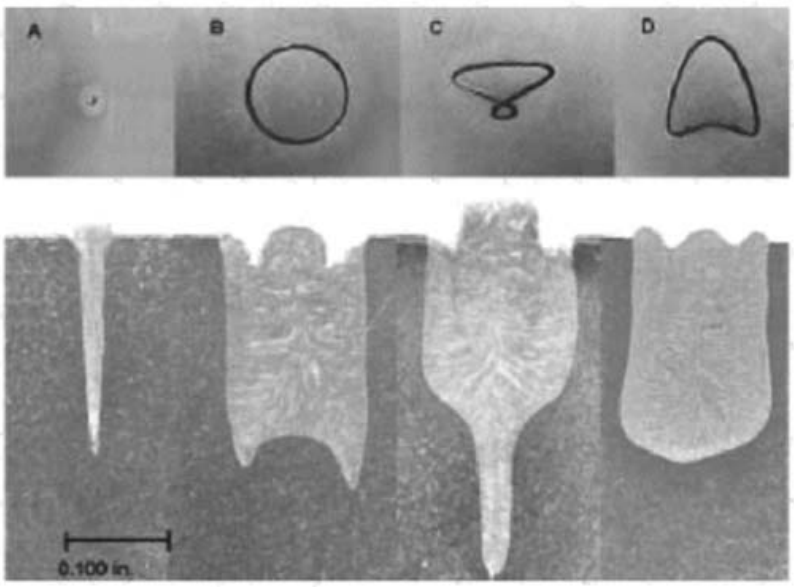

Fig. 1. Influence of the beam scanning trajectory on the weld cross-section:
A – without scanning; B – circle; C – eight; D – arrowhead

Рис. 1. Влияние траектории развертки пучка на поперечное сечение сварного шва:
A – отсутствие развертки; B – окружность; C – восьмерка; D – наконечник стрелы

The disadvantage of a circular sweep of the electron beam is also the difference in the directions of the beam at opposite edges of the weld. At the same time, on one of the edges, the direction of the beam motion coincides with the direction of the welding speed, and on the other side, it is opposite to it, which can lead to uneven formation of the weld.

In [14], the authors developed a new scanning path based on energy input. The study suggests applying trajectory instead of a contour to the beam control module along which the beam follows. As a result, the nominal energy density and modulation function are experimentally obtained, what makes it possible to determine the optimal input energy. However, this method of determining energy, proposed by the authors, is energy and resource consuming. Illustration of such a development is shown in fig. 2.

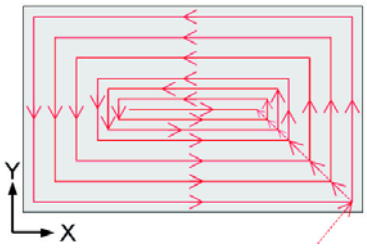

Fig. 2. New trajectories for melting a rectangular area

Рис. 2. Новые траектории для плавления прямоугольной области

In [15], experimental studies on the application of various electron beam scans with the aim of the qualitative formation of welded joints are presented. The influence of the following scans was studied: circular and elliptical, x-shaped, zigzag, gimlet, raster, triangle, rowing with oars along isotherms. Studies have shown that the best scan for the quality of the formation of the weld is a raster in which the beam is scanned in the coordinate combined with the junction of the welded product according to a unilateral saw tooth law, while the beam moves from the front of the bath to the tail according to a linear law with subsequent instant return to the front. Such a scan facilitates the transfer of molted metal to the tail section of the weld pool. During one scanning along the joint, 16, 32 or 64 scans across the joint along a bilateral sawtooth path are performed. The scan period along the junction is 1–2 ms. More detailed studies with scanning in the form of a raster revealed that with an increase in the scanning amplitude along the joint from 5 mm when welding small thicknesses to 15 mm when welding medium thicknesses, the gas-vapor channel transforms into a stable cavity over the entire penetration depth [16]. The shape of the cavity was fixed by abrupt discontinuing the welding process by switching off the accelerating voltage.

Mathematical modeling of the electron beam energy distribution. In fig. 3 a diagram of electron beam welding during scanning as a raster is presented. The form of the weld obtained has almost parallel walls and a significant radius in the root, what allows root defects to be eliminated, and instability of the penetration depth is reduced by 3–4 times. The openness and stability of the penetration cavity leads to degassing of the welding pool and a decrease in porosity. By reducing the proportion of energy, spent on the evaporation of the material, the penetrating ability of the EBW process increases [1].

It is advisable to study the effect of the formation of a penetration cavity when welding various materials and different thicknesses. For this, equipment should be created, which realizes scanning in the form of various rasters. In this paper, three types of scanning are considered: a classical raster, a sinusoidal raster, and a truncated raster. The objective of this study is to obtain the density of the energy distribution of the scanning electron beam on the surface of the part along the heating spot. It characterizes the distribution of energy in the weld pool.

The energy distribution in an electron beam is usually described by a normal law, which is characterized by a density probability in the form [17]:

$$f(x) = \frac{1}{\sigma \cdot \sqrt{2 \cdot \pi}} \cdot \exp\left(-\frac{(x-m)^2}{2 \cdot \sigma^2} \right), \quad (1)$$

where x is the coordinate along the abscissa axis, m is the mathematical expectation, and σ is the standard deviation, characterizing the diameter of the electron beam, and the concentration of the energy in it. This value is determined by the electron-optical system of the gun and its focusing system. It depends on the welding current and is usually determined in the range of σ = 0.05–0.5 mm. The smaller the diameter of the electron beam, the more high-quality beam the gun forms.

In order not to take into consideration the specific value of the standard deviation in the construction of the characteristics of the density of energy distribution over the heating spot, we introduce the dimensionless coordinates and amplitudes of the beam scanning along these coordinates:

$$\bar{y} = \frac{y}{\sigma}, \quad (2)$$

where y is the coordinate along the joint, σ standard deviation, $\bar{y}$ is the dimensionless coordinate along the joint. In the system of dimensionless coordinates σ = 1

$$\bar{x} = \frac{x}{\sigma}, \quad (3)$$

where x is the coordinate across the joint, $\bar{x}$ – is the dimensionless coordinate across the joint.

$$\bar{A} = \frac{A}{\sigma}, \quad (4)$$

where A is the amplitude, $\bar{A}$ – is the dimensionless amplitude.

It is known that the maximum ordinate of the normal distribution (1), is equal, corresponds to the point $x = m$; as the distance from point m increases, the distribution density decreases. The centre of symmetry of the distribution is the scattering centre m. This is clear from the fact that when the sign of the difference (x–m) is reversed, expression (1) does not change. If the scattering centre m is changed, the distribution curve will shift along the ab-

scissa without changing its shape. The scattering centre characterizes the distribution position on the coordinate axis [9]. Therefore, by changing the scattering centre according to the corresponding law, one can obtain the energy distribution density along the corresponding coordinate.

Energy of an electron beam [18]:

$$W(x,y) = U \cdot I \cdot \int_{-\infty}^{\infty} \int_{-\infty}^{\infty} W(x)W(y)dxdy\,, \qquad (5)$$

where U is the accelerating voltage, I is the beam current, $W(x)$ and $W(y)$ are the normalized energy distribution functions along the corresponding coordinates,

$$\int_{-\infty}^{\infty} W(x)dx = 1\,,\ \int_{-\infty}^{\infty} W(y)dy = 1\,.$$

Next, let us consider each scan in more detail. Scanning is conducted in the form of a classic raster, while the movement along the coordinate across the joint is carried out on a two-sided saw, described by a piecewise linear function:

$$x = k \cdot t + m, \qquad (6)$$

where t is an independent variable, k and m are some numbers, and in case, when, $k = 1$, for a time $t = [-1; 1]$ for a period T, this graph will be presented in the form of a triangular function (fig. 4).

It is known that when changing the mathematical expectation in formula (1), the graph shifts relative to its center. Consequently, instead of mathematical expectation, it is possible to substitute the necessary expression, for a raster it is a linear function. It is also necessary to integrate the resulting expression.

The following formula is obtained [18]:

$$W(\bar{x}) = \int_{-1}^{1} \frac{1}{\sigma \cdot \sqrt{2 \cdot \pi}} \cdot \exp\left(-\frac{\left(\bar{x} - \left(\bar{A}_x \cdot k \cdot t + m\right)\right)^2}{2 \cdot \sigma^2} \right) dt\,, \qquad (7)$$

where, $\bar{A}_x \in [1;10]$, $\bar{x} \in [-15;15]$, $k = 1$, $m = 0$, $\bar{x}$ is the dimensionless coordinate along the joint, $\bar{A}_x$ is the dimensionless amplitude across the joint, and σ is the standard deviation.

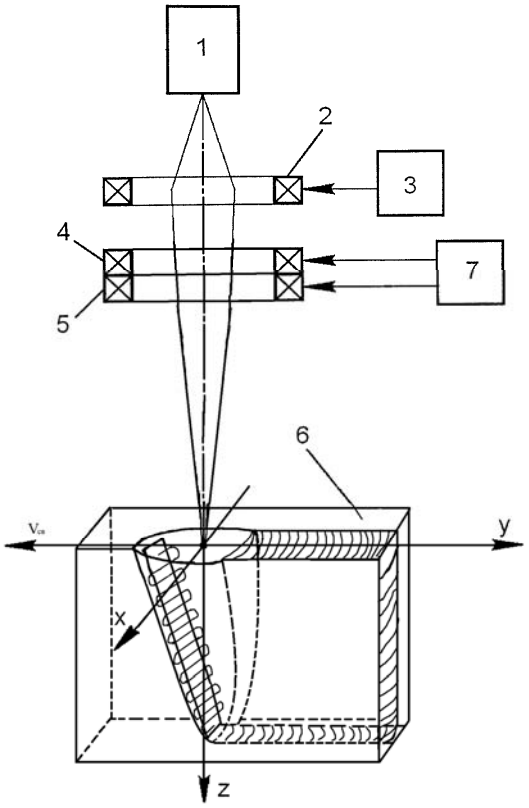

Fig. 3. A scheme of electron-beam welding when scanning in the form of a raster:
1 – electron beam gun; *2* – focusing system; *3* – focus current source; *4* – deflection coil; *5* – deflection coil; *6* – product surface; *7* – beam scan generator

Рис. 3. Схема электронно-лучевой сварки при сканировании в виде растра:
1 – электронно-лучевая пушка; *2* – фокусирующая система; *3* – источник тока фокусировки; *4* – отклоняющая катушка; *5* – отклоняющая катушка; *6* – поверхность изделия; *7* – генератор сканирования пучка

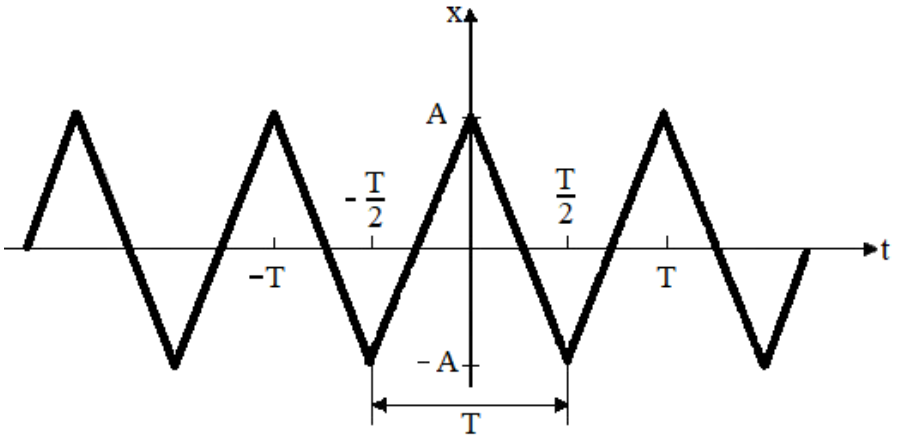

Fig. 4. Graph of successive triangular pulses

Рис. 4. График последовательных треугольных импульсов

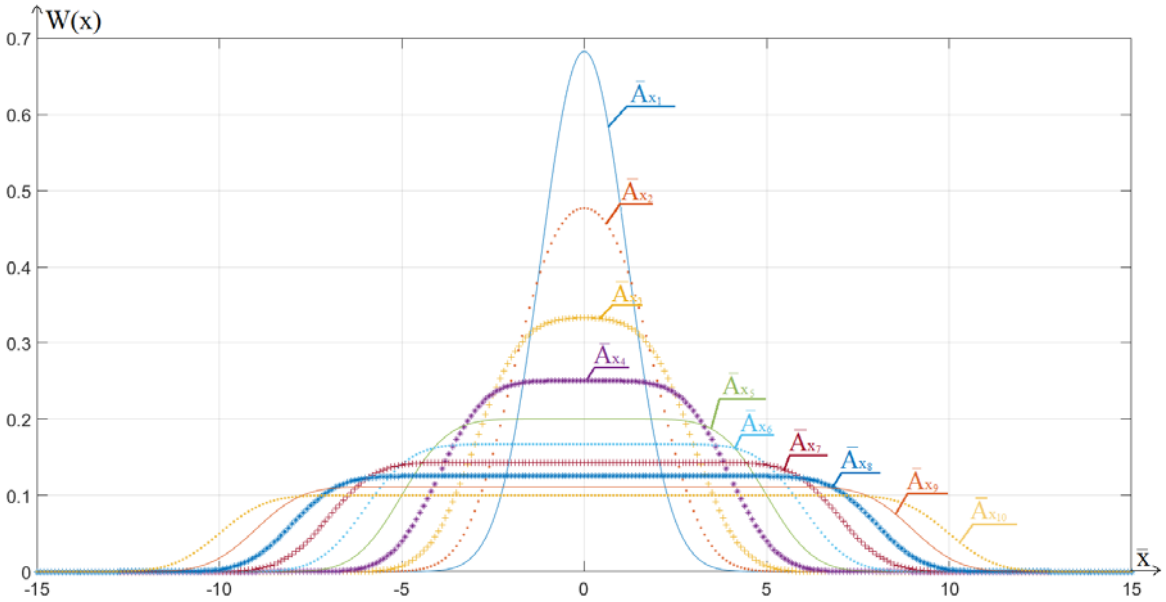

Fig. 5. Energy distribution on the surface for the case of a scanning trajectory in the form of a truncated raster:
$\overline{A_{x1}} = 1;\ \overline{A_{x2}} = 2;\ \overline{A_{x3}} = 3;\ \overline{A_{x4}} = 4;\ \overline{A_{x5}} = 5;\ \overline{A_{x6}} = 6;\ \overline{A_{x7}} = 7;\ \overline{A_{x8}} = 8;\ \overline{A_{x9}} = 9;\ \overline{A_{x10}} = 10$

Рис. 5. Распределение энергии пучка на поверхности детали при растровом сканировании:
$\overline{A_{x1}} = 1;\ \overline{A_{x2}} = 2;\ \overline{A_{x3}} = 3;\ \overline{A_{x4}} = 4;\ \overline{A_{x5}} = 5;\ \overline{A_{x6}} = 6;\ \overline{A_{x7}} = 7;\ \overline{A_{x8}} = 8;\ \overline{A_{x9}} = 9;\ \overline{A_{x10}} = 10$

Fig. 5 shows a figure with a normal energy distribution for the case of a scanning trajectory of an electron beam in the form of a raster across the junction.

Fig. 6 shows the scanning path of the electron beam in the form of a truncated raster. The scanning trajectory in the form of a raster is described by formula (8), but additional restrictions are added in the form of the following system [18]:

$$\begin{cases} A = 1, \text{ при } t \in [0.7; 1.2], \\ A = -1, \text{ при } t \in [2.6; 3.2]. \end{cases} \quad (8)$$

Note that when scanning with a truncated raster on the definite areas at a definite period the amplitude takes a fixed value. Therefore, in the formula (7) we add the expressions with the help of which the peaks, arising at values equal to the amplitude, are described. We get the following expression:

$$W(\bar{x}) = \frac{T - 2 \cdot M}{T} \cdot \int_{-1}^{1} \frac{1}{\sigma \cdot \sqrt{2 \cdot \pi}} \cdot \exp\left(-\frac{\left(\bar{x} - \left(\bar{A}_x \cdot k \cdot t + m\right)\right)^2}{2 \cdot \sigma^2} \right) dt + \quad (9)$$
$$+ \frac{M}{T} \cdot \left(\exp\left(-\frac{\left(\bar{x} - \left(\bar{A}_x\right)\right)^2}{2 \cdot \sigma^2} \right) + \exp\left(-\frac{\left(\bar{x} + \left(\bar{A}_x\right)\right)^2}{2 \cdot \sigma^2} \right) \right),$$

where $\bar{x}$ is the dimensionless coordinate across the junction, $\bar{A}_x$ – is the dimensionless amplitude across the junc-

tion, σ is the standard deviation, $m = 0$, $k = 1$, M is the saturation time, T is the scanning period.

In formula (9), with an amplitude equal to 3 and, taking into consideration that the area of the figure with a normal energy distribution, we change the limits of the saturation zone boundaries $\frac{M}{T} = [0.05; 0.1; 0.15; 0.2; 0.25; 0.3; 0.4]$ and obtain the following energy distribution curves shown in fig. 7.

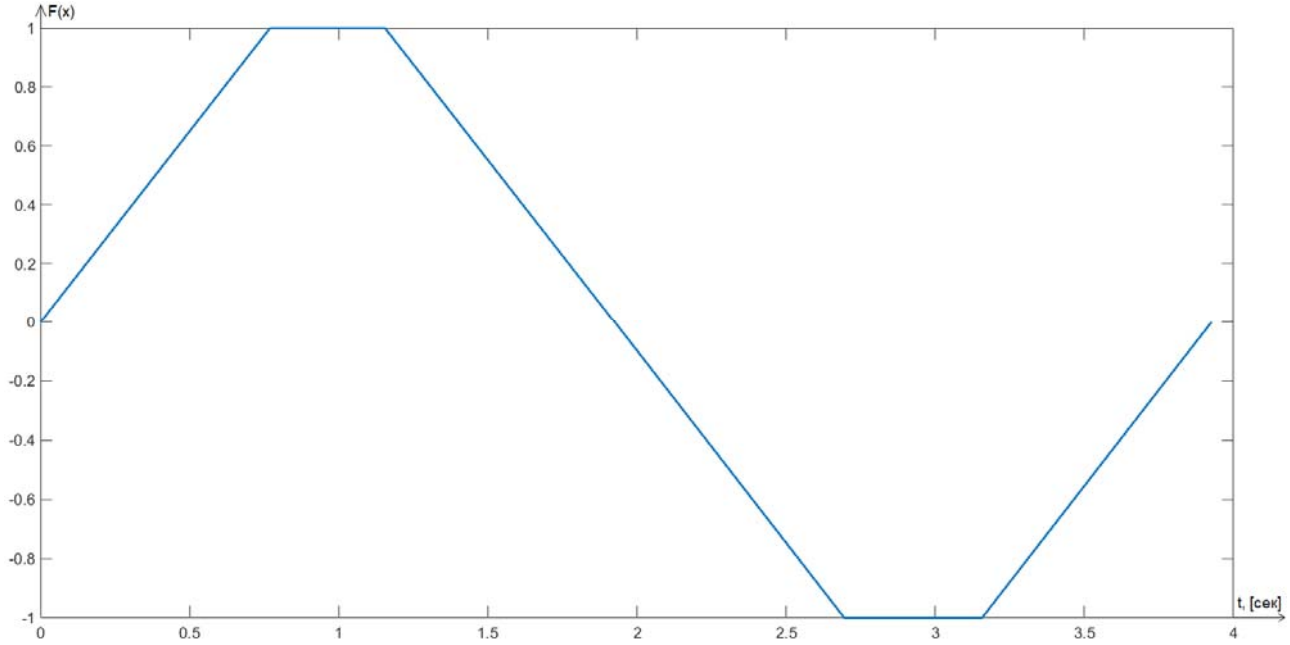

Fig. 6. The shape of the controlling signal in the form of a triangle with saturation zones

Рис. 6. Форма управляющего сигнала в виде треугольника с зонами насыщения

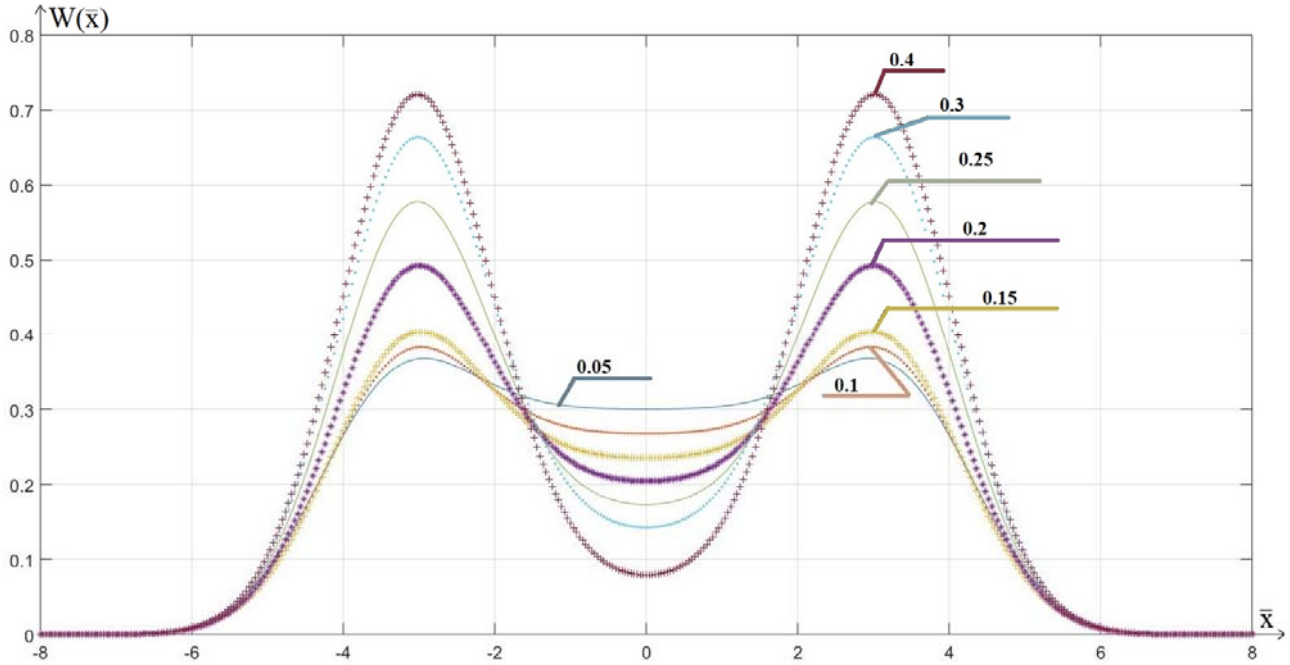

Fig. 7. Beam energy distribution on the surface of a detail when scanning with a truncated raster and changing the boundaries of the saturation zone

Рис. 7. Распределение энергии пучка на поверхности детали при сканировании усеченным растром и при изменении границ зоны насыщения

From the obtained graphs it can be seen that by changing the value of the saturation zone M, it is possible to control the amplitude of the two-hump energy distribution over the heating spot and achieve the best shape of the weld. In order to use the obtained calculated characteristics, it is necessary to get from dimensionless coordinates to dimensional coordinates, for this it is necessary to carry out the following actions [18]:

$$y = \bar{y} \cdot \sigma ;\ x = \bar{x} \cdot \sigma ;\ A = \bar{A} \cdot \sigma ;$$

$$W(x) = \frac{W(\bar{x})}{\sigma} ;\ W(y) = \frac{W(\bar{y})}{\sigma} .$$

As a result of the conducted research, a program was developed to control the energy distribution over the heating spot using various scans [19].

Conclusion. 1. For conducting investigations to optimize the process of electron beam welding, it is reasonable to use scanning electron beam in the form of a raster, which allows to obtain a stable penetration cavity and high quality welded joints.

2. The scanning shape in the form of a truncated raster allows to obtain a two-hump distribution of energy along the coordinate across the joint, which is necessary to form a weld with parallel walls and a significant radius in the root, excluding the appearance of root defects.

3. Numerical modelling of thermal processes to determine the parameters of EWB will significantly reduce the cost of developing technologies for structures made of new materials and various thicknesses.

References

1. Rykalin N. N., Zuev I. V., Uglov A. A. *Osnovy elektronno-luchevoy obrabotki materialov* [Fundamentals of electron beam processing of materials]. Moscow, Engineering, Publ., 1978, 239 p.

2. Sobko S. A., Kulikov V. A. *Sposob kontrolya elektronno-luchevoy svarki* [The method of control of electron-beam welding]. Available at: http://www.freepatent.ru/patents/2495737 (accessed 13.05.2020).

3. Shcherbakov A. B., Rodyakina R. V., Novokreschenov V. V., Lastovirya V. N. *Sistemy upravleniya elektronno-luchevykh ustanovok* [Technology of material processing. Equipment of electron-beam complexes]. Moscow, Yurayt Publ., 2018, P. 114–130.

4. Akopianc K. S., Nesterenko V. M. [Electron-beam welding of steels up to 600 m thick with longitudinal oscillations of the beam]. *Avtomaticheskaya svarka.* 2002, No. 9, P. 3–5 (In Russ.).

5. Ohmine M., Hiramoto S., Jamane J. Fundamental study on the plused electron beam welding // Intern. Inst. of Welding; Doc. IV-348-83 – S. I. 1983, 13 p.

6. Belenkiy V. Ya. [Scanning of an electron beam along an x-shaped trajectory as a means of reducing defects in the root of a weld in EBW]. *Avtomaticheskaya svarka*. 1986, No. 9, P. 35–37. (In Russ.).

7. Barishev M. S., Redchic A. A. [Optimization of welding modes by oscillating electron beam]. *Tez. dokladov 4-y Vserocs. soyuz. konferentsii po svarke tsvetnykh metallov* [Abstracts of the 4th. Rus. Union Conf. on welding of non-ferrous metals]. 1990, 34 p. (In Russ.).

8. Zenker R. Electron beam surface treatment and multipool welding – state of the art. *Proceedings of the EBEAM 2002. International Conference on High-Power Electron Beam Technology*. 2002, P. 12-1–12-5.

9. Shilov G. A., Akopianc K. S., Kasatkin O. O. [Influence of the frequency and diameter of the circular scan of the electron beam on the penetration in EBW]. *Avtomaticheskaya svarka*. 1983, No. 8, P. 25–28 (In Russ.).

10. Akopianc K. S., Emchenko-Ribko A. V., Neporohin V. Yu., Shilov G. A. [Prevention of the formation of root defects in EBW with non-penetration of up to 60 mm depth]. *Avtomaticheskaya svarka*. 1989, No. 4, P. 30–34 (In Russ.).

11. Komiro Y., Punshon C. S., Gooch T. G., Blakaley P. S. Effects of process parameters on centerline solidification in EB weld. *Metal Constr.* 1986, No. 2, P. 104–111.

12. Vasil'ev A. M., Goncharov V. A., Krivkov B. G., Solyankin V. V., Sharonov N. I. [Electronic beam control device by welding]. *Sudostroitel'naya promyshlennost'. Seriya Svarka*. 1988, No. 6, C. 11–12 (In Russ.).

13. Mara C. l., Funk E. R., McMaster R. C., Pence P. E. Penetration mechanism of electron beam Welding and spiking phenomenon. *Welding Journal*. 1974, Vol. 53, No. 6, C. 246–251.

14. Béraud N., Vignat F., Villeneuve F., Dendievel R. New trajectories in Electron Beam Melting manufacturing to reduce curling effect. *Proceedings of the 47th CIRP Conference on Manufacturing Systems*. 2014, P. 738–743.

15. Seregin Yu. N., Laptenok V. D., Uspenskiy N. V., Nikitin V. P. [Experimental research on the optimization of the technology of electron-beam welding of aluminum alloys]. *Tekhnologii i oborudovanie ELS-2011*. 2011. P. 71–80 (In Russ.).

16. Seregin Yu. N., Laptenok V. D., Murygin A. V., Bocharov A. N. Experimental research on electron-beam welding technology with a scanning electron beam. *21st Int. Sci. Conf. Resetnev Readings-2017*. 2019, Vol. 467, 8 p.

17. Venttsel' Ye. S. *Teoriya veroyatnostey* [Probability theory]. Moscow, Vysshaya shkola Publ., 1999, 576 p.

18. Kurashkin S. O., Laptenok V. D., Murygin A. V., Seregin Yu. N. Analytical characteristics of the electron beam distribution density over the heated spot for optimizing the electron-beam welding process. *Welding in Russia 2019: State-of-the-Art and Perspectives.* 2019, Vol. 681, 7p.

19. Kurashkin S. O., Seregin Yu. N., Tynchenko V. S., Petrenko V. E., Myrugin A. V. [The program for the formation of the scanning path of the electron beam in the form of a sine wave in electron beam welding]. *Certificate of state registration of a computer program № 2020611327*. 2020.

Библиографические ссылки

1. Рыкалин Н. Н., Зуев И. В., Углов А. А. Основы электронно-лучевой обработки материалов. М. : Машиностроение, 1978. 239 с.

2. Собко С. А., Куликов В. А. Способ контроля электронно-лучевой сварки [Электронный ресурс]. URL: http://www.freepatent.ru/patents/2495737 (дата обращения: 13.05.2020).

3. Системы управления электронно-лучевых установок / А. В. Щербаков, Р. В. Родякина, В. В. Новочеркасов и др. М. : Юрайт, 2018. С. 114–130.

4. Акопьянц К. С., Нестеренко В. М. Электронно-лучевая сварка сталей толщиной до 600м с продольными колебаниями луча // Автоматическая сварка. 2002. № 9. С. 3–5.

5. Ohmine M., Hiramoto S., Jamane J. Fundamental study on the plused electron beam welding // Intern. Inst. of Welding; Doc. IV-348-83 – S. I. 1983. 13 p.

6. Беленький В. Я. Развертка электронного луча по х-образной траектории как средство уменьшения дефектов в корне шва при ЭЛС // Автоматическая сварка. 1986. № 9. С. 35–37.

7. Барышев М. С., Редчиц А. А. Оптимизация режимов сварки колеблющимся электронным лучом // Тез. докладов 4-й Всеросс. союз. конференции по сварке цветных металлов. 1990. 34 с.

8. Zenker R. Electron beam surface treatment and multipool welding – state of the art // Proceedings of the EBEAM 2002. International Conference on High-Power Electron Beam Technology. 2002. P. 12-1–12-5.

9. Шилов Г. А., Акопьянц К. С., Касаткин О. О. Влияние частоты и диаметра круговой развертки электронного луча на проплавление при ЭЛС // Автоматическая сварка. 1983. № 8. С. 25–28.

10. Предотвращение образования корневых дефектов при ЭЛС с несквозным проплавлением глубиной до 60мм / К. С. Акопьянц, А. В. Емченко-Рыбко, В. Ю. Непорохин и др. // Автоматическая сварка. 1989. № 4. С. 30–34.

11. Komiro Y., Punshon C. S., Gooch T. G., Blakaley P. S. Effects of process parameters on centerline solidification in EB weld // Metal Constr. 1986. No. 2. P. 104–111.

12. Прибор управления электронным пучком при сварке / А. М. Васильев, В. А. Гончаров, Б. Г. Кривков и др. // Судостроительная промышленность. Серия «Сварка». 1988. № 6. С. 11–12.

13. Mara C. l., Funk E. R., McMaster R. C., Pence P. E. Penetration mechanism of electron beam Welding and spiking phenomenon // Welding Journal. 1974. Vol. 53, No. 6. C. 246–251.

14. Béraud N., Vignat F., Villeneuve F., Dendievel R. New trajectories in Electron Beam Melting manufacturing to reduce curling effect // Proceedings of the 47th CIRP Conference on Manufacturing Systems. 2014. P. 738–743.

15. Экспериментальные исследования по оптимизации технологии электронно-лучевой сваркой алюминиевых сплавов / Ю. Н. Серегин, В. Д. Лаптенок, Н. В. Успенский и др. // Технологии и оборудование ЭЛС-2011. 2011. С. 71–80.

16. Seregin Yu. N., Laptenok V. D., Murygin A. V., Bocharov A. N. Experimental research on electron-beam welding technology with a scanning electron beam // 21st Int. Sci. Conf. Resetnev Readings-2017. 2019. Vol. 467. 8 p.

17. Вентцель Е. С. Теория вероятностей. М. : Высш. шк., 1999. 576 с.

18. Kurashkin S. O., Laptenok V. D., Murygin A. V., Seregin Yu. N. Analytical characteristics of the electron beam distribution density over the heated spot for optimizing the electron-beam welding process // Welding in Russia 2019: State-of-the-Art and Perspectives. 2019. Vol. 681. 7 p.

19. Курашкин С. О., Серегин Ю. Н., Тынченко В. С., Петренко В. Е., Мурыгин А. В. Программа для формирования траектории развертки электронного пучка в виде синусоиды при электронно-лучевой сварке. Свидетельство о государственной регистрации программы для ЭВМ №2020611327. Дата регистрации: 19 февраля 2020.

Kurashkin Sergei Olegovich – graduate student; Reshetnev Siberian State University of Science and Technology. Email: scorpion_ser@mail.ru.

Seregin Yrui Nikolaevich – Cand. Sc., assistant professor of department of ICS; Reshetnev Siberian State University of Science and Technology. Email: ius_ceregin@mail.ru.

Murygin Aleksandr Vladimirovich – D. Sc., administrator of department of ICS of the Reshetnev Siberian State University of Science and Technology. Email: avm514@mail.ru.

Petrenko Vyacheslav Evgenievich – graduate student; Reshetnev Siberian State University of Science and Technology. Email: dpblra@inbox.ru.

Курашкин Сергей Олегович – аспирант; Сибирский государственный университет науки и технологий имени академика М. Ф. Решетнева. Email: scorpion_ser@mail.ru.

Серегин Юрий Николаевич – кандидат технических наук, доцент кафедры ИУС; Сибирский государственный университет науки и технологий имени академика М. Ф. Решетнева. Email: ius_ceregin@mail.ru.

Мурыгин Александр Владимирович – доктор технических наук, заведующий кафедрой ИУС; Сибирский государственный университет науки и технологий имени академика М. Ф. Решетнева. Email: avm514@mail.ru.

Петренко Вячеслав Евгеньевич – аспирант, Сибирский государственный университет науки и технологий имени академика М. Ф. Решетнева. Email: dpblra@inbox.ru.

UDC 621.793
Doi: 10.31772/2587-6066-2020-21-2-274-278

For citation: Mikheev A. E., Girn A. V., Yakubovich I. O., Rudenko M. S. Plasmotron for coating internal surfaces of component parts. *Siberian Journal of Science and Technology.* 2020, Vol. 21, No. 2, P. 274–278. Doi: 10.31772/2587-6066-2020-21-2-274-278

Для цитирования: Плазмотрон для нанесения покрытий на внутренние поверхности изделий / А. Е. Михеев, А. В. Гирн, И. О. Якубович, М. С. Руденко // Сибирский журнал науки и технологий. 2020. Т. 21, № 2. С. 274–278. Doi: 10.31772/2587-6066-2020-21-2-274-278

PLASMOTRON FOR COATING INTERNAL SURFACES OF COMPONENT PARTS

A. E. Mikheev*, A. V. Girn, I. O. Yakubovich, M. S. Rudenko

Reshetnev Siberian State University of Science and Technology
31, Krasnoyarskii rabochii prospekt, Krasnoyarsk, 660037, Russian Federation
*E-mail: michla@mail.ru

Plasma spraying is one of technologically appropriate, productive and effective methods of applying protective coatings to component parts produced by aerospace, metallurgical and other industries, objects exposed to high temperatures, dynamic loads, aggressive media, etc. Plasma spraying makes it possible to apply quite a variety of materials, such as metals, oxides, carbides, nitrides, etc. to different surfaces. Certain problems may arise, though, in applying protective coatings to the inner surfaces of cylinders and complex parts of small size (about 100 mm). These complexities depend on the dimensions of the plasma generator proper. There are no home-produced small-size plasma torches, they are all imported from other countries. That causes certain problems with delivery, to say nothing of very high commercial price. One of the ways to improve the situation is to develop small-size plasmatrons capable of applying high-quality coatings to the internal surfaces of limited-size parts; that may significantly reduce expenses through import substitution.

The effectiveness of the proposed device is in working out a method of applying high-quality coatings to the inner surfaces of orifices as small as 60 mm in diameter (operating a plasmatron of smaller size), as well as in significant cost reduction due to domestic production. Sample calculations show that the price of that plasmatron type will not exceed 0.5 million rubles.

Keywords: plasmatron, plasma spraying, internal surface coating.

ПЛАЗМОТРОН ДЛЯ НАНЕСЕНИЯ ПОКРЫТИЙ НА ВНУТРЕННИЕ ПОВЕРХНОСТИ ИЗДЕЛИЙ

А. Е. Михеев*, А. В. Гирн, И. О. Якубович, М. С. Руденко

Сибирский государственный университет науки и технологий имени академика М. Ф. Решетнева
Российская Федерация, 660037, Красноярск, просп. им. газ. «Красноярский рабочий», 31
*E-mail: michla@mail.ru

Плазменное напыления является одним из технологичных, производительных и эффективных способов нанесения защитных покрытий на изделия аэрокосмической, металлургической и других отраслей промышленности, подвергаемых воздействию высоких температур, динамических нагрузок, агрессивных сред и т. д. Плазменным напылением практически можно наносить любые материалы, такие как металлы, оксиды, карбиды, нитриды и т. п. на различные поверхности. Но существуют проблемы по нанесению защитных покрытий на внутренние поверхности цилиндрических деталей и деталей сложной формы с небольшими размерами (до 100 мм). Эти сложности связаны с габаритами самих плазмотронов. Малогабаритные плазмотроны в России не производятся, а импортируются из зарубежных стран, что причиняет ряд неудобств, связанных с поставками и очень высокой коммерческой ценой. Одним из путей решения этой проблемы является разработка малогабаритных плазмотронов, которые позволят наносить качественные покрытия на внутренние поверхности деталей с ограниченными размерами и существенно снизить их цену за счет импортозамещения.

В результате использования предлагаемого устройства стало возможным наносить качественные покрытия на внутренние поверхности отверстий с минимальным диаметром 60 мм за счет уменьшения габаритов плазмотрона, а также существенно снизить его стоимость за счет собственного производства. Предварительные расчёты показывают, что цена плазмотрона не превышает 0,5 млн руб.

Ключевые слова: плазмотрон, плазменное напыление, напыление на внутренние поверхности.

Introduction In many industries, such as aerospace, metallurgy, oil production, etc., there are increasing requirements for reliability, durability and safety of products operated in extreme conditions (exposure to high temperatures, dynamic loads, aggressive media, etc.). These requirements create a demand for special protective coatings. One of the most effective methods of applying such coatings is plasma spraying, and the application of the method is growing from year to year [1–17]. The problems arising in application of protective coatings to the inner surfaces of cylinders and complex parts of small size (about 100 mm), refer to the dimensions of the plasma torches in use – there is not enough space for them in the sprayed area. Small-size plasma torches are not produced in Russia, they are all imported; that involves problems of shipment and delivery, of paying high commercial prices. One of the ways to avoid these problems is to develop home-produced small-size plasmatrons capable of applying high-quality coatings to the inner surfaces of limited-size parts – import substitution means considerably reduced prices.

The model currently used most widely is F1 plasma torch, intended for applying various high-quality coatings by the method of plasma-powder spraying to inner surfaces of orifices as small as 70 mm in diameter [18]. The manufacturer is "Innatech" company (Dinse – www.dinse.eu, AMT – www.amt-ag.net). The drawbacks of the plasmotron are the limited period of plasma torch operation (not more than 50 hours) and the unit's high cost – more than 1.5 million rubles. This article presents a comparison of capacities demonstrated by the F1 plasma torch and the currently developed small-size plasmatron PM-2, capable of applying coatings to inner surfaces of orifices as small as 60 mm in diameter.

Experimental parameters. The proposed plasma torch make comprises coaxially and sequentially mounted cathode assembly, insulating bushing, anode assembly, working (plasma forming) gas and cooling water supply systems, injector for supplying powder under the nozzle edge. In the developed plasmatron design, the nozzle with the sealing gaskets is removed from the anode assembly; its function is overtaken by water-cooled anode assembly, into which a tungsten insert is pressed to increase the endurance of the nozzle. The cathode and anode assemblies have separate cooling systems. The cooling channels are formed by covers soldered to the cathode and anode assemblies – that eliminates the need for gaskets, which often wear out. These changes allow smaller dimensions of the plasma torch. The insulating bushing is installed between the cathode and anode assemblies, and these are held together with three screws in insulating cover.

Fig. 1 is the cross section view of the plasmotron construction.

Fig. 2 is a 3D graphic presentation of the cathode *1* and anode *3* assemblies with cooling channels *6* and *7*.

The proposed plasmotron design comprises cathode assembly *1* with cathode *2* and anode assembly also performing the nozzle function *3*, into which a tungsten insert *4* is pressed to increase the endurance; covers *5* are soldered to the cathode and anode assemblies to form cooling channels *6* and *7*; electrical insulator *8* separating the cathode assembly from the anode assembly; tungsten cathode *8*; three screws *9* in insulating covers *10* to hold the cathode and anode assemblies together; plugs *11* for fixing the cathode; feeder *12* of the working (plasma-forming) gas to channel *13* in the cathode assembly body, to the gas distribution ring *14* installed at the entrance to discharge chamber *15* comprising cathode assembly *1*, ceramic ring *16* and anode assembly *3* (that provides uniform distribution of the gas inside); tubes *17* to feed cooling water to channels *6* and *7*; injector *18* for feeding the spraying powder, and orifices *19* in insert *4* for the plasma jet.

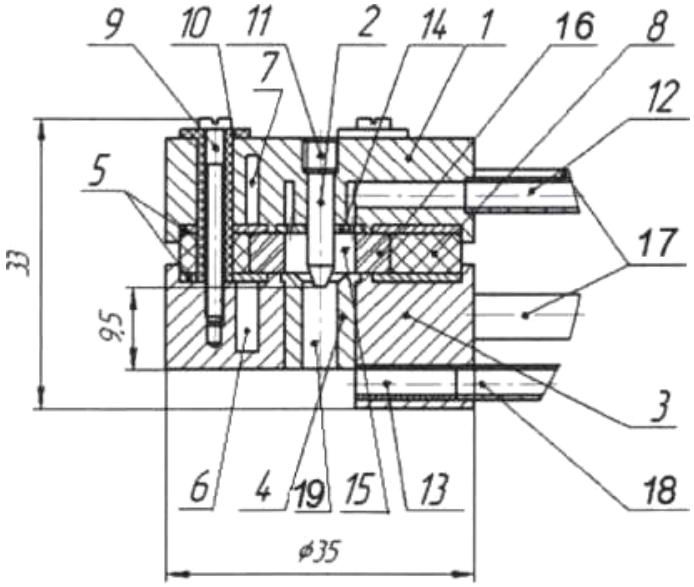

Fig. 1. Plasmotron PM-2

Рис. 1. Плазмотрон ПМ-2

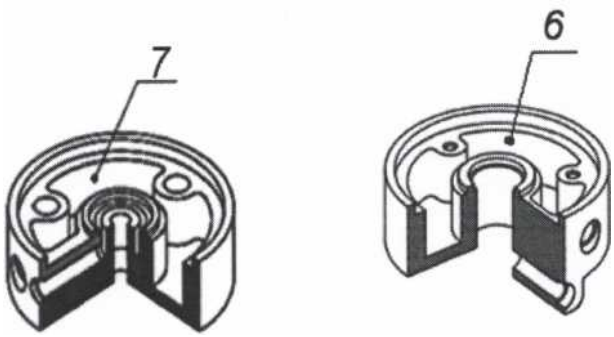

Fig. 2. Cathode and anode assemblies

Рис. 2. Катодный и анодный узел

Comparative characteristics of the plasmotrons

Parameter	Plasmotron F1 (GTV)	Plasmotron PM-2
Maximum power, kW	25	20
Arc current, A	Up to 500	Up to 400
Immersion length at spraying, mm	500	600
Min diameter of the orifice for spraying, mm	70	60
Max plasmotron overall size, mm	50	35
Operation time at medium current, hr	50 ≤	50 ≤
Type of cooling	Water	Water
Technological powder	Metal, composite, ceramic	Metal, composite, ceramic

The plasma torch works as follows: water is fed through cooling tubes *16*, plasma-forming gas is fed to tube *12*, and an electric arc is initiated between cathode *2* and tungsten insert *4* pressed into the anode assembly. The working (plasma-forming) gas is fed through the inlet channel *13* and gas distribution ring *14* into plasmotron discharge chamber *15* (fig. 1), formed by cathode assembly *1*, ceramic ring *16* and anode assembly *3*; the gas gets ionizes and escapes through orifice *18* of insert *6* at high speed, producing a jet of plasma, into which the powder material is fed through injector *11*, mounted in anode assembly *3*.

In the developed design of the plasma torch (PM-2), the overall dimensions are minimized: 33 mm vertically, 35 mm in diameter. The plasma torch is capable of applying coatings inside smaller orifices (as small as 60 mm in diameter). The make allows to adjust the immersion length at spraying by installation of longer nozzles.

The operational parameters of two small-size plasmotrons are compared in table.

Tests were carried out to check the adherence of coatings applied by the plasmatrons at their maximum power. The strength of the coating adhesion to the substrate was determined by pull-off method (adhesive binding, VK-9 glue) according to GOST (State standard specification) 209-75 with the use of Eurotest T-50 universal test machine. The obtained data showed that the adhesion strength of aluminum oxide coating applied to steel samples by the experimental plasmotron PM-2 comes between 8 and 10 MPa, which is close to the results of plasmatron F1 (GTV) coating strength tests, showing 9-10.5 MPa. But the min diameter of the orifice for spraying allowed by plasmatron F1 is 70 mm – the limit determined by the overall plasmotron dimensions (see table).

Conclusion. The efficiency of the proposed plasmotron design is in the potential of applying high-quality coatings to the inner surfaces of orifices as small as 60 mm in diameter by reducing the overall dimensions of the plasma torch; the cost of the device can also be significantly reduced. Sample calculations show that the price of the plasmotron will not exceed 0.5 million rubles.

References

1. Khasuy A. *Tekhnika napyleniya* [Spraying technique]. Moscow, Mashinostroyeniye Publ., 1975, 288 p.

2. Kudinov V. V. *Plazmennye pokrytiya* [Plasma coatings]. Moscow, Nauka Publ., 1977, 270 p.

3. Kudinov V. V, Ivanov V. M. *Naneseniye plazmoy tugoplavkikh pokrytiy* [Plasma application of refractory coatings]. Moscow, Mashinostroyeniye Publ., 1981, 212 p.

4. Borisov Yu. S., KHarlamov Yu. A., Sidorenko S. L., Ardatovskaya E. N. *Gazotermicheskiyye pokrytiya iz*

poroshkovykh materialov: Spravochnik [Gasothermic coating with powder materials: Reference book]. Kiev, Naukova dumka Publ., 1987, 544 p.

5. Kopylov V. I, Shatinskiy V. F. [Investigation of processes in plasma spraying contact zone and estimation of their parameters]. *Neorganicheskiye i organosilikatnyye pokrytiya.* 1975, P. 96– 106 (In Russ.).

6. Puzryakov A. F. *Teoreticheskiyye osnovy tekhnologii plazmennogo napyleniya* [Theoretical Foundations of the Technology of Plasma Sputtering]. Moscow, MGTU im. N. E. Baumana Publ., 2008, 235 p.

7. Kharlamov Yu. A. [Factors influencing the adhesion strength of gas-thermal coatings]. *Zashchitnye pokrytiya na metallakh.* 1988, No. 22, P. 30–34 (In Russ.).

8. Polak L. S., Surov N. S. [Investigation of the interaction of powder particles with plasma flow in the nozzle]. *Fizika i khimiya obrabotki materialov*. 1969, No. 2, P. 19–29 (In Russ.).

9. Mikheev A. E., Kolmykov V. A. *Povysheniye ekspluatatsionnykh kharakteristik poverkhnostey elementov konstruktsiy letatel 'nykh apparatov. Avtomatizatsiya protsessov obrabotki* [Upgrading of operational characteristics of aircraft components' surfaces. Automation of treatment processes]. Moscow, MAKS Press Publ., 2002, 224 p.

10. Mikheev A. E., Statsura V. V., Nikushkin N. V. [Equipment for high-quality gas-thermal coating application]. *III otraslevaya nauchno-tekhnicheskaya konferentsiya "Primeneniyye gazotermicheskikh pokrytiy v mashinostroyyenii"* [III Industry science and technology conference "Application of gas-thermal coatings in mechanical engineering"]. Moscow, 1990, P. 84–87 (In Russ.).

11. Mikheyev A. E., Statsura V. V., Ivasev S. S., Gim A. V. [Processing of refractory oxides in low-temperature plasma]. *Sb. nauchnykh trudov Vserossiyskoy nauchno-tekhnicheskoy konferentsii "Materialy i tekhnologii XXI veka"* [Proceedings of Russian science and technical conference "Materials and technologies of the XXI century"]. Penza, 2001, P. 123–125 (In Russ.).

12. Donskoy A. V., Klubnikin V. S. *Elektroplazmennyye protsessy i ustanovki v mashinostroyenii* [Electroplasma processes and equipment in mechanical engineering], Leningrad, Mashinostroyyeniye Publ., 1979, 221 p.

13. Zhukov M. F., Smolyakov V. Ya, Uryukov B. A. *Elektrodugovye nagrevateli gaza (plazmotrony)* [Electric arc gas heaters (plasmatrons)]. Moscow, Nauka Publ., 1973, 232 p.

14. *Yavleniya perenosa v nizkotemperaturno-y plazme* [Transference phenomena in low- temperature plasma]. Ed. A.V. Lykova et al. Minsk, Nauka i tekhnika Publ., 1969, 248 p.

15. Saunin V. N. *Elektrodugovoy plazmotron Saunina* [Saunin electric arc plasmatron]. Patent RF, No. 2276840, 2006.

16. Ivanchenko A. F., Lavrinenko M. Z., Mel'nik B. I., Prisevok A. F., Sannikov V. A., Solovey A. I., Fedortsev V. A. *Sposob naneseniya pokrytiy na vnutrennie poverkhnosti tsilindricheskikh izdeliy i ustroystvo dlya ego osushchestvleniya* [Method of coating inner surfaces of cylinders and device for the coating application]. Patent No. 2009027, 1994.

17. BY 8930 U 2013.02.28 Plasmatron for coating internal surfaces of component parts.

18. FI plasma torch of innatech.ru (manufacturers: Dinse – www.dinse.eu, AMT www.amt-ag.net).

Библиографические ссылки

1. Хасуй А. Техника напыления. М. : Машиностроение, 1975. 288 с.

2. Кудинов В. В Плазменные покрытия. М. : Наука, 1977. 270 с.

3. Кудинов В. В, Иванов В. М. Нанесение плазмой тугоплавких покрытий. М. : Машиностроение. 1981. 212 с.

4. Газотермические покрытия из порошковых материалов: Справочник / Ю. А. Харламов, С. Л. Сидоренко, Е. Н. Ардатовская, Ю. С. Борисов. Киев : Наукова думка, 1987. 544 с.

5. Шатинский В. Ф., Копылов В. И. Исследование процессов в контактной зоне при плазменном напылении и оценка их параметров // Неорганические и органосиликатные покрытия. Л. : Наука, 1975. С. 96–106.

6. Пузряков А. Ф. Теоретические основы технологии плазменного напыления. М. : Издательство МГТУ им. Н. Э. Баумана, 2008. 235 с.

7. Харламов Ю. А. Факторы, влияющие на адгезионную прочность газотермических покрытий // Защитные покрытия на металлах. 1988. Вып. 22. С. 30–34.

8. Суров Н. С., Полак Л. С.. Исследование взаимодействия частиц порошка с потоком плазмы в сопле // Физика и химия обработки материалов. 1969. № 2. С. 19–29.

9. Михеев А. Е., Колмыков В. А. Повышение эксплуатационных характеристик поверхностей элементов конструкций летательных аппаратов. Автоматизация процессов обработки. М. : МАКС Пресс, 2002. 224 с.

10. Михеев А. Е., Стацура В. В., Никушкин Н. В. Оборудование для нанесения качественных газотермических покрытий // Применение газотермических покрытий в машиностроении : III отраслевая науч.-техн. конф. Москва, 1990. С. 84–87.

11. Обработка тугоплавких оксидов в низкотемпературной плазме / В. В. Стацура, С. С. Ивасев, А. В. Гирн, А. Е. Михеев // Материалы и технологии XXI в. : сб. науч. тр. Всероссию науч.-техн. конф. Пенза, 2001. С. 123–125.

12. Донской А. В., Клубникин В. С. Электроплазменные процессы и установки в машиностроении. Л. : Машиностроение, 1979. 221 с.

13. Жуков М. Ф., Смоляков В. Я., Урюков Б. А. Электродуговые нагреватели газа (плазмотроны). М. : Наука, 1973. 232 с.

14. Явления переноса в низкотемпературной плазме / под ред. А. В. Лыкова и др. Минск : Наука и техника, 1969. 248 с.

15. Патент России RU 2276840, МКИ H05H1/26, C23C4/00, 20.05.2006. Электродуговой плазмотрон

Саунина / Саунин В. Н. Заявл. 07.07.2004 ; Опубл. 20.05.2006. Заявка № 2004120804/06.

16. Патент № 2009027 Способ нанесения покрытий на внутренние поверхности цилиндрических изделий и устройство для его осуществления / Иванченко А. Ф., Лавриненко М. З., Мельник Б. И. и др. Заявл. 18.10.1991 ; опубл. 15.03.1994.

17. BY 8930 U 2013.02.28 Плазмотрон для нанесения покрытия на внутренние поверхности деталей.

18. Плазмотрон F1 компании innatech.ru (производители: Dinse – www.dinse.eu, AMT –www.amt-ag.net).

Miheev Anatolii Egorovich – D. Sc., Professor, head of the Department of Flying vehicles; Reshetnev Siberian State University of Science and Technology. E-mail: michla@mail.ru.

Girn Aleksei Vasilyevich – Cand. Sc., associate professor, associate professor of the Department of Flying vehicle; Reshetnev Siberian State University of Science and Technology. E-mail: gim007@gmail.com.

Yakubovich Ivan Olegovich – postgraduate student; Reshetnev Siberian State University of Science and Technology. E-mail: flversin@mail.ru.

Rudenko Mikhail Sergeevich – engineer; Reshetnev Siberian State University of Science and Technology. E-mail: mister.m.rudenko@gmail.com.

Михеев Анатолий Егорович – доктор технических наук, профессор, заведующий кафедрой летательных аппаратов; Сибирский государственный университет науки и технологий имени академика М. Ф. Решетнева. E-mail: michla@mail.ru.

Гирн Алексей Васильевич – кандидат технических наук, доцент, доцент кафедры летательных аппаратов; Сибирский государственный университет науки и технологий имени академика М. Ф. Решетнева. E-mail: gim007@gmail.com.

Якубович Иван Олегович – аспирант, Сибирский государственный университет науки и технологий имени академика М. Ф. Решетнева. E-mail: flversin@mail.ru.

Руденко Михаил Сергеевич – инженер; Сибирский государственный университет науки и технологий имени академика М. Ф. Решетнева. E-mail: mister.m.rudenko@gmail.com.

UDC 620.192
Doi: 10.31772/2587-6066-2020-21-2-279-288

For citation: Filippenko N. G., Larchenko A. G. Automated experiment systems for studying the properties of transport polymer materials in high-frequency electrothermia. *Siberian Journal of Science and Technology.* 2020, Vol. 21, No. 2, P. 279–288. Doi: 10.31772/2587-6066-2020-21-2-279-288

Для цитирования: Филиппенко Н. Г., Ларченко А. Г. Системы автоматизированного эксперимента для исследования свойств полимерных материалов транспортного назначения при высокочастотной электротермии // Сибирский журнал науки и технологий. 2020. Т. 21, № 2. С. 279–288. Doi: 10.31772/2587-6066-2020-21-2-279-288

AUTOMATED EXPERIMENT SYSTEMS FOR STUDYING THE PROPERTIES OF TRANSPORT POLYMER MATERIALS IN HIGH-FREQUENCY ELECTROTHERMIA

N. G. Filippenko, A. G. Larchenko*

Irkutsk State Transport University
15, Chernyshevsky St., 664074, Irkutsk, Russian Federation
*E-mail:Larchenkoa@inbox.ru

Recent decades have been characterized by increased activity in the use of polymer and composite materials in transport engineering. In this paper, the authors give a generalizing analysis of previously created systems of scientific research and analyze the principles of building automated systems of scientific research (ASSR) that allow solving the problems of determining the parameters of heat exchange, electrophysical parameters and phase transformations in polymer and composite materials when exposed to the HF field. The authors continue the research of the ASSR HF developed by the Irgups team, a number of other scientific schools working in the same direction.therefore, within the framework of the hardware created by these teams, both similar and original developments and solutions are viewed. The analysis of the software parts of the ASSR HF presented by a number of mathematical models and software complexes is given. Thus, the analysis of the structure of the developed systems of scientific research allows us to speak about its dynamic development. The developed and presented flowcharts of automated experiment and automated research systems allow the author to assert that the systems of automated experiment for studying the properties of polymer materials in RF electrothermia created for certain tasks, despite the fact that they were conducted independently and separately, have a single construction methodology. Comparing the results of the research, the author concludes that the construction of a complex system of ASSR HF polar thermoplastic polymers is generally complete

Keywords: automated scientific research systems, high-frequency electrothermics, polymer products, methodology for building research systems.

СИСТЕМЫ АВТОМАТИЗИРОВАННОГО ЭКСПЕРИМЕНТА ДЛЯ ИССЛЕДОВАНИЯ СВОЙСТВ ПОЛИМЕРНЫХ МАТЕРИАЛОВ ТРАНСПОРТНОГО НАЗНАЧЕНИЯ ПРИ ВЫСОКОЧАСТОТНОЙ ЭЛЕКТРОТЕРМИИ

Н. Г. Филиппенко, А. Г. Ларченко*

Иркутский государственный университет путей сообщения
Российская Федерация, 664074, Иркутская область, г. Иркутск, ул. Чернышевского, 15
*E-mail:Larchenkoa@inbox.ru

Последние десятилетия характеризуются повышенной активностью использования полимерных и композитных материалов в транспортном машиностроении. В данной работе авторами дается обобщающий анализ ранее созданных систем научных исследований и анализируются принципы построения автоматизированных систем научного исследования (АСНИ), позволяющие решать задачи определения параметров теплообмена, электрофизических параметров и фазовых превращений в полимерных и композитных материалах при воздействии на них ВЧ-поля. Авторы продолжают исследования разработанных АСНИ ВЧ коллективом ИрГУПС, ряда других научных школ, работающих в том же направлении, поэтому в рамках аппаратной части, созданной этими коллективами, просматриваются как схожие, так и оригинальные разработки и решения. Дается анализ программных частей АСНИ ВЧ, представленных рядом математических моделей и комплексами программного обеспечения. Таким образом, анализ структуры разработанных систем научного исследования позволяет говорить о динамическом ее развитии. Разработанные и представленные блок-схемы систем автоматизированного эксперимента и автоматизированных исследований позволяют авторам утверждать, что созданные под определенные задачи системы автоматизированного эксперимента по изучению свойств полимерных материалов при ВЧ-электротермии, несмотря на то что велись самостоятельно

и разрознено, имеют единую методика построения. Сопоставив результаты исследований, авторы делают вывод о том, что построение комплексной системы АСНИ ВЧ полярных термопластичных полимеров в целом завершено.

Ключевые слова: системы автоматизированных научных исследований, высокочастотная электротермия, полимерные изделия, методология построения систем исследований.

Introduction. The driving force of the growth of the polymer industry is still the ever-increasing standard of living of mankind. It should be noted that continuous growth is primarily demonstrated by the transport sector of the engineering industry.

In the modern world, polymer industry companies are building new capacities with minimal capital expenditures due to the use of advanced technologies that can reduce costs by reducing electricity consumption rates, and this primarily refers to high-frequency electrothermal technologies [1–15]. However, the introduction of these technologies is constrained by the lack of reliable data on the electrophysical properties of modern materials necessary for the organization of control processes. Therefore, the solution of this problem is an important national economic task.

In this regard, the aim of this work was to analyze existing scientific research automation systems (ASSR) and experimental automation systems (SAE) of the effects of high-frequency electrothermia on the properties of polymeric materials processed in the HF field over a wide temperature range.

Analysis of the state of ASSR and SAE HF-electrothermics. In plastics processing, the HF heating method, as has been repeatedly noted, is one of the most advanced. The effectiveness of the use of HF heating is judged by the value of the dielectric loss factor of the dielectric constant –ε′, and the dielectric loss tangent –tgδ [16–23]. The authors of an automated research system for determining the permittivity – ε′ and dielectric loss tangent –tgδ, polyamide-610 performed the work using an E9 meter (Q-meter) using two and three-dimensional resonance methods [5]. The functional measurement scheme and the location of the processed material are presented in fig. 1 and 2, respectively, where a sample of material placed between two plates of the working capacitor 2 was affected by an HF field. Temperature control was carried out by pyrometer 3 and thermocouples TE 4-1. The calculation of dielectric indicators was carried out by computing device 1.

The results of the work were the obtained data on the characteristic changes in the electrophysical parameters of PA-6 polyamide (ε′ and tgδ) depending on temperature. Nevertheless, even the authors themselves in the work point out the difficulties of using such a research system in determining the melt moment of a material, referring to a difficult to control process accompanied by gas formation at the time of a phase transition. The obvious drawbacks of the developed automated experiment are also the absence of immunity systems, and the mathematical model does not correspond to the real technological system and consists of one layer of material to be welded.

The mathematical apparatus of the HF heating model proposed by the authors [15; 20] describes the temperature distribution in the thickness of the thermoplastic, taking into account the design features of technological equipment (fig. 3).

The calculation of the welding process was carried out by numerically solving the equation for variable values of *y* and dependencies obtained by calculation and experimental methods were used.

The disadvantage of this system, as with previous authors, is also associated with the mathematical model. The model underwent changes, was expanded, but considers only a special case of processing, namely welding. The schematic diagram of the experimental setup is shown in fig. 4.

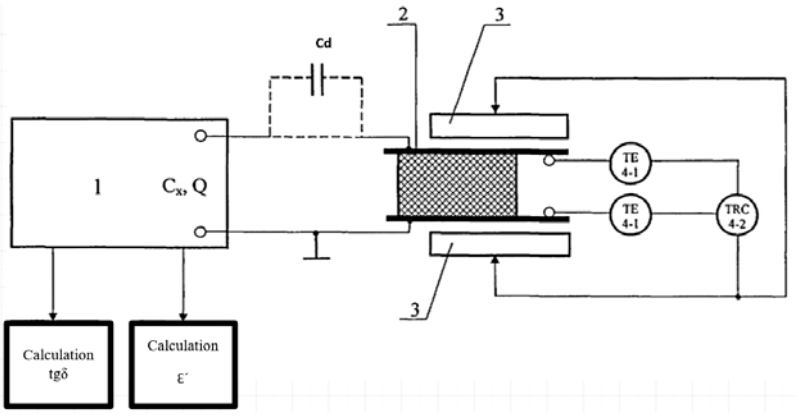

Fig. 1. Functional measurement scheme:
1 – computing device; *2* – upper and lower plates of the working capacitor;
3 – windows for temperature pyrometry

Рис. 1. Функциональная схема измерений:
1 – вычислительное устройство; *2* – верхняя и нижняя обкладки рабочего конденсатора; *3* – окна для пирометрии температуры

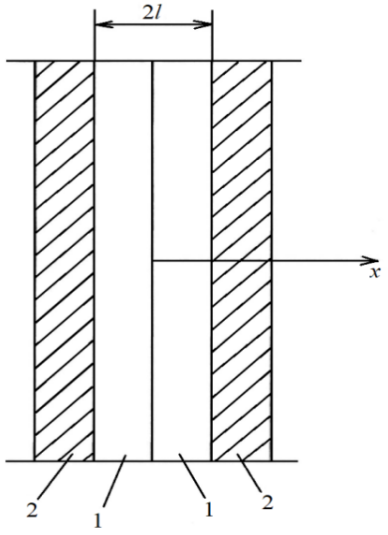

Fig. 2. The location of the welded material
in the working capacitor:
1 – materials to be welded; *2* – electrodes

Рис. 2. Расположение свариваемого материала
в рабочем конденсаторе:
1 – свариваемые материалы; *2* – электроды

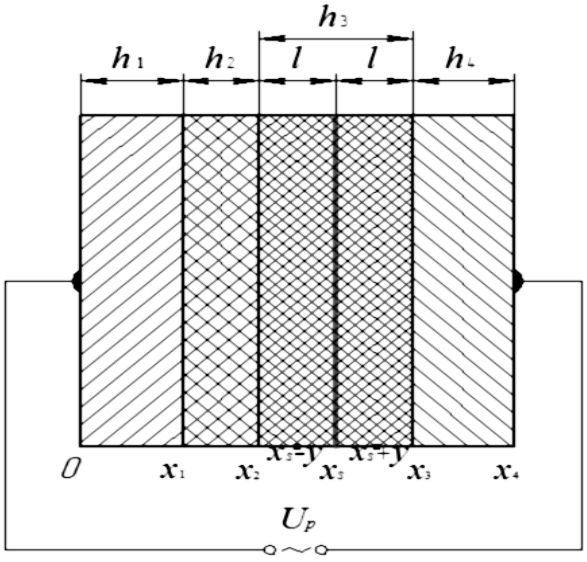

Fig. 3. High-frequency welding of plastic parts in industrial
equipment with one insulated electrode, where h_1, h_4
is the thickness of the high potential and grounded electrodes;
h_2 is the thickness of the insulating liner; $l = h_3/2$ – thickness
of the welded part; x_i is the coordinate of the layer boundary;
x_s is the coordinate of the weld; y is the distance from
the weld; U_p is the voltage at the working capacitor

Рис. 3. Высокочастотная сварка деталей из пластмасс
в технологической оснастке с одним изолированным
электродом, где h_1, h_4 – толщина высокопотенциального
и заземленного электродов; h_2 – толщина изоляционного
вкладыша; $l = h_3/2$ – толщина свариваемой детали;
x_i – координата границы слоя; x_s – координата сварного
шва; y – расстояние от сварного шва; U_p – напряжение
на рабочем конденсаторе

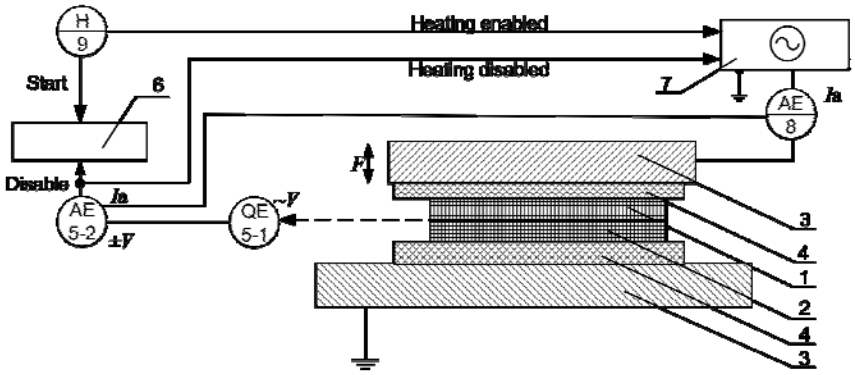

Fig. 4. Schematic diagram of the experimental setup:
1 is a product sample; *2* is a product sample; *3* is for electrodes of the working capacitor; *4* is an insulating liner; *5-1* is an acoustic sensor; *5-2* is an analog-to-digital converter (ADC); *6* is a computing device; *7* is a HF generator; *8* is an ammeter of the anode current; *9* is a "START" button

Рис. 4. Принципиальная схема экспериментальной установки:
1 – образец изделия; *2* – образец изделия; *3* – электроды рабочего конденсатора; *4* – изоляционный вкладыш; *5-1* – акустический датчик; *5-2* – аналогово-цифровой преобразователь (АЦП); *6* – вычислительное устройство; *7* – ВЧ-генератор; *8* – амперметр анодного тока; *9* – кнопка «ПУСК»

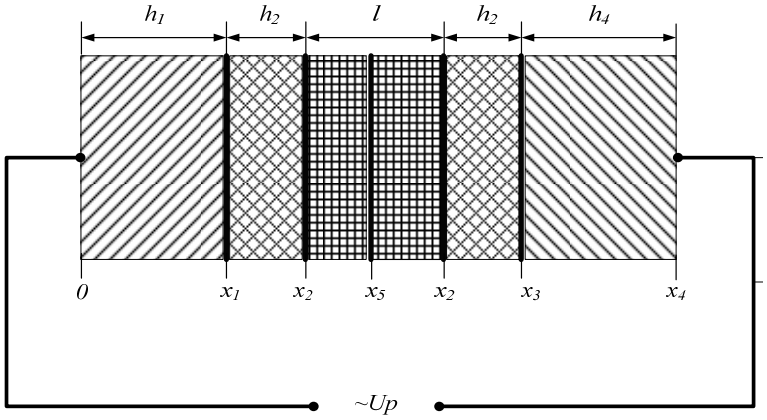

Fig. 5. Applience for high-frequency processing of parts:
h_1, h_4 are thickness of high-potential and grounded electrodes; h_2 is the thickness of the insulating liners; l is the thickness of the processed (welded) part; x is the coordinate of the layer boundary; x_s is the coordinate of the connection; y is the distance from the junction; U_p is the voltage at the working capacitor

Рис. 5. Приспособление для высокочастотной обработки деталей:
h_1, h_4 – толщина высокопотенциального и заземленного электродов; h_2 – толщина изоляционных вкладышей; l – толщина обрабатываемой (свариваемой) детали; x – координата границы слоя; x_s – координата соединения; y – расстояние от места соединения; U_p – напряжение на рабочем конденсаторе

In [12], the shortcomings indicated in previous versions of automated experiments are not so obvious, but nevertheless, the presented SAE has limited capabilities and is applicable only in the study of polar thermoplastics. The device for high-frequency processing of parts is shown in fig. 5.

A solution was found to organize the calculation and measurement of temperature on the surface and inside the material and to protect the electrodes from breakdown, which was implemented both in the hardware and in the mathematical program part of the research system [4; 14; 23].

The ASSR hardware also underwent changes. Switching systems and control units were added.

Nevertheless, the presented model, although it expanded the capabilities of the technological system (the quantity of layers of material is increased up to five), but the possibility of its application is limited by a number of HF processing processes such as welding, drying, and acclimatization.

A feature of the works presented [7; 8] is the expansion of the capabilities of scientific HF research regarding diagnostic processes. A mathematical model was developed for measuring the capacitance of a working capaci-

tor, and a software package was created for calculating the effective diagnostic parameters (fig. 6) under HF exposure, depending on the shape and size of the samples [7; 14; 22].

This automated system (fig. 7) of scientific research has expanded the possibility and list of technological processes of HF electrothermics, but concerns only one type of research, namely diagnostics

An analysis of one of the latest works of scientific research systems [8; 12] on the study of the interconnections of electrophysical parameters of electrothermal equipment and polymer materials widely used in transport engineering shows that a number of problems that were not included in the work of previous authors were solved.

A mathematical model of the technological system was developed in a 3D setting (fig. 8, 9), which included a variable number of electrodes, insulators and processed materials, and the developed algorithm made it possible to calculate the temperature field taking into account the heating of the technological system.

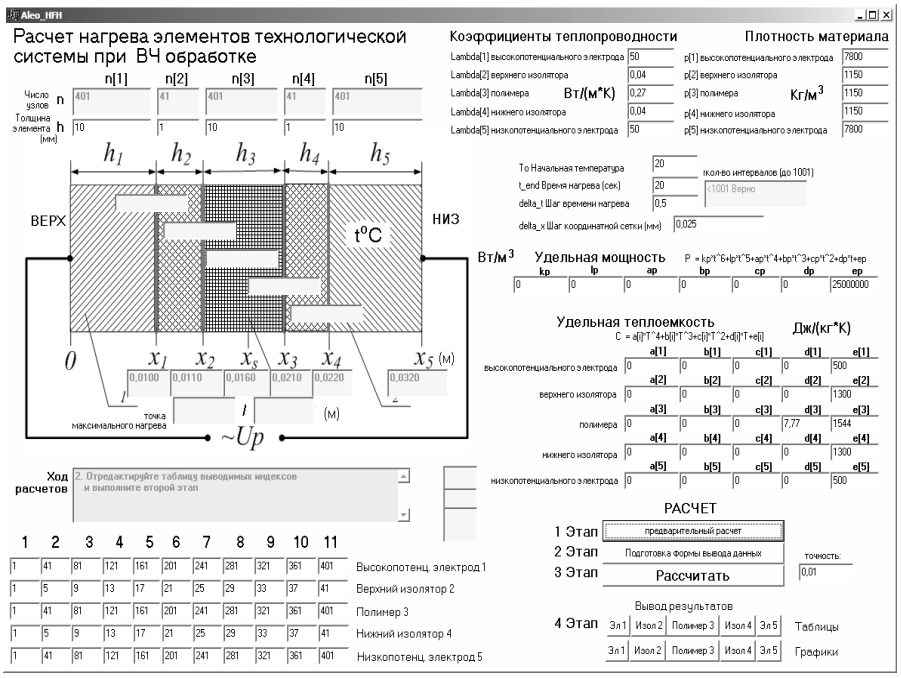

Fig. 6. Interface of Aleo_HFH software complex

Рис. 6. Интерфейс программного комплекса Aleo_HFH

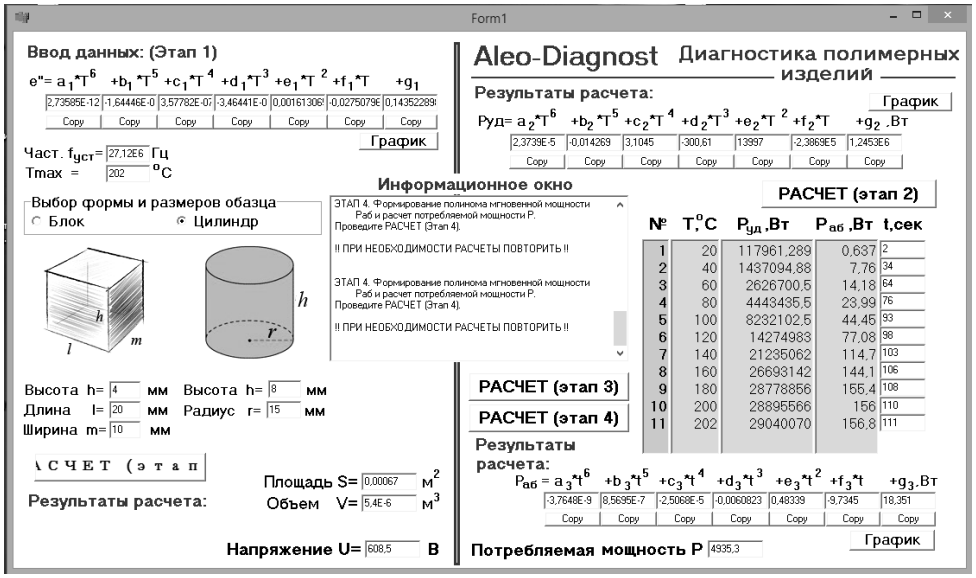

Fig. 7. Aleo-Diagnost software interface

Рис. 7. Интерфейс программного комплекса Aleo-Diagnost

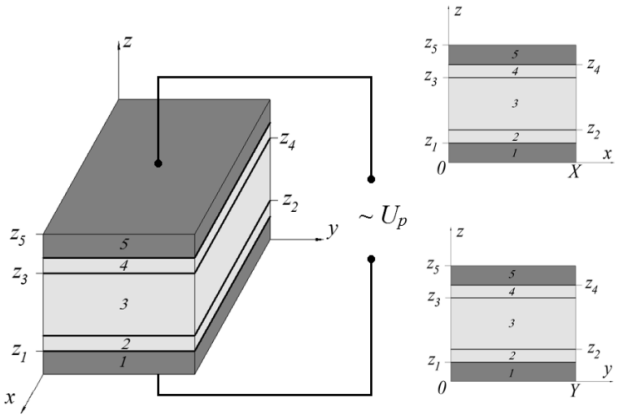

Fig. 8. 3D five-layer high-frequency processing technological scheme.
The first group of the technological scheme consists of:
1 – low-potential electrode of the working capacitor; *2* – insulator; 2nd group: *3* – processed polymer (internal heat source); 3rd group: *5* – high-potential electrode of the working capacitor; *4* – insulator; *X*, *Y*, *Z* are coordinates of the boundaries of the layers; U_p is the voltage at the working capacitor

Рис. 8. 3D пятислойная технологическая схема ВЧ-обработки.
1-я группа технологической схемы:
1 – низкопотенциальный электрод рабочего конденсатора; *2* – изолятор; 2-я группа: *3* – обрабатываемый полимер (внутренний источник тепла); 3-я группа: *5* – высокопотенциальный электрод рабочего конденсатора; *4* – изолятор; *X*, *Y*, *Z* – координаты границ слоев; *Up* – напряжение на рабочем конденсаторе

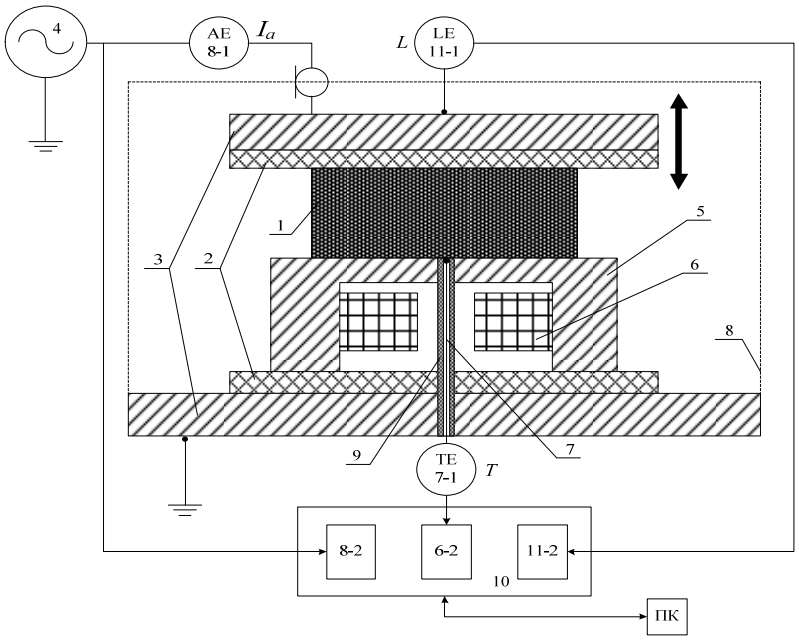

Fig. 9. Scheme of an automated experimental setup for determining the amperometric dependence of dielectric loss in polymeric materials:
1 is a processed sample; *2*, *9* are heat-electric insulators; *3* is for electrodes of the working capacitor; *4* is a HF generator; *5* is a device for contact heating of the sample; *6* is an electric heating element; *7* is a thermocouple; *7-1* is a thermocouple thermometer; *8* is a protective screen; *8-1* is a current sensor; *10* is a computing unit; *11-1* is a linear thermal expansion sensor

Рис. 9. Схема автоматизированной экспериментальной установки по определению амперометрической зависимости диэлектрических потерь в полимерных материалах:
1 – обрабатываемый образец; *2*, *9* – тепло-, электроизоляторы; *3* – электроды рабочего конденсатора; *4* – ВЧ-генератор; *5* – приспособление для контактного нагрева образца; *6* – электронагревательный элемент; *7* – термопара; *7-1* – термопара-термометр; *8* – защитный экран; *8-1* – датчик тока; *10* – вычислительный блок; *11-1* – датчик линейного теплового расширения

To date, a full-fledged automated system of scientific research (ASSR HF) developed at the Irkutsk State Transport University (IrGUPS) can be considered the most system-developed one. It was finally formed and indicated in [1; 8; 12].

Two versions of the ASSR HF with different hardware have been developed chronologically. An industrial HF processing unit of the UZP-2500 model was used as a source of electromagnetic radiation. The developed and patented automation unit [4], performed registration, processing and transmission of information. It was implemented on the basis of the programmable controller ATmega 328.

We should note that this system, in addition to the hardware, was also provided with a software component, consisting of a number of software systems that implement automated research programs.

The basic principles for constructing a fully functional ASSR HF hardware and its structural scheme for studying the process of heat treatment of polymeric materials are presented in fig. 10.

The work of the unit is organized as follows. Simultaneously with turning on the high-frequency generator, the control unit and the automation unit are turned on. A linear Hall sensor measures the anode current of a high-frequency generator, and acoustic sensors detect partial discharges that occur on the polymer during HF processing. Data on anodic current of high frequency generator and partial discharges is transmitted to the computing device of a microcontroller assembled on the basis of the ATmega8 processor [2].

The microcontroller calculates the magnitude of the change in the anode current; drying time; interdischarge time; number of partial discharges. Installation of the unit and sensors was carried out without re-equipment of existing electrical circuits of HF installations [6; 17; 18].

The integration of ACS elements with reference to the HF equipment scheme of the UZP-2500 model is shown in fig. 11.

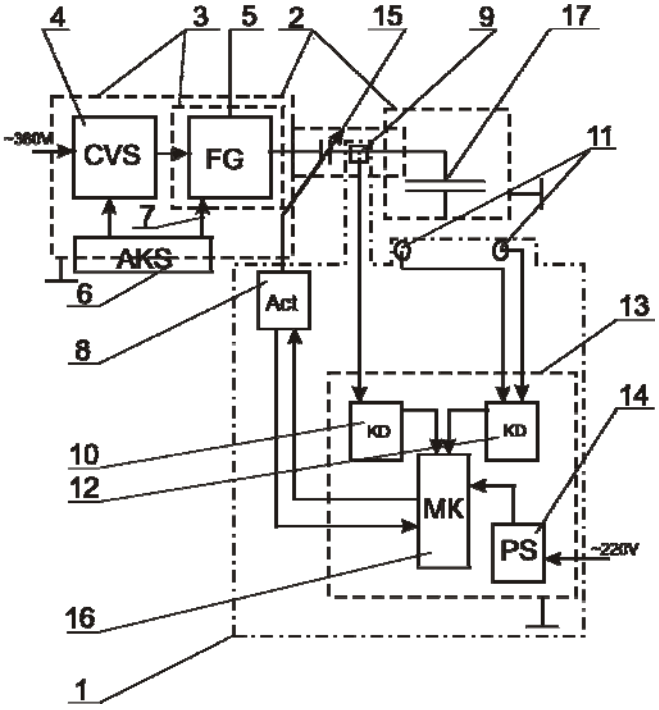

Fig. 10. Block diagram of the ASSR HF hardware:
1 is an automation unit; *2* is a shielding case; *3* is a coaxial cable; *4* is a constant voltage source; *5* is a high-frequency generator; *6* is an alarm control system; *7* is a generator control circuit; *8* is an actuator; *9* is a linear current sensor; *10* is a computing device; *11* are acoustic sensors for detecting partial discharges; *12* is a computing device; *13* is anti-interference housing; *14* is power supply; *15* is a variable capacitor; *16* is a microcontroller; *17* is a working capacitor

Рис. 10. Структурная схема аппаратной части АСНИ ВЧ:
1 – блок автоматизации; *2* – экранирующий корпус; *3* – коаксиальный кабель; *4* – источник постоянного напряжения; *5* – высокочастотный генератор; *6* – система управления сигнализацией; *7* – цепь управления генератором; *8* – исполнительный механизм; *9* – линейный токовый датчик; *10* – вычислительное устройство; *11* – акустические датчики регистрации частичных разрядов; *12* – вычислительное устройство; *13* – помехозащищенный корпус; *14* – блок питания; *15* – переменный конденсатор; *16* – микроконтроллер; *17* – рабочий конденсатор

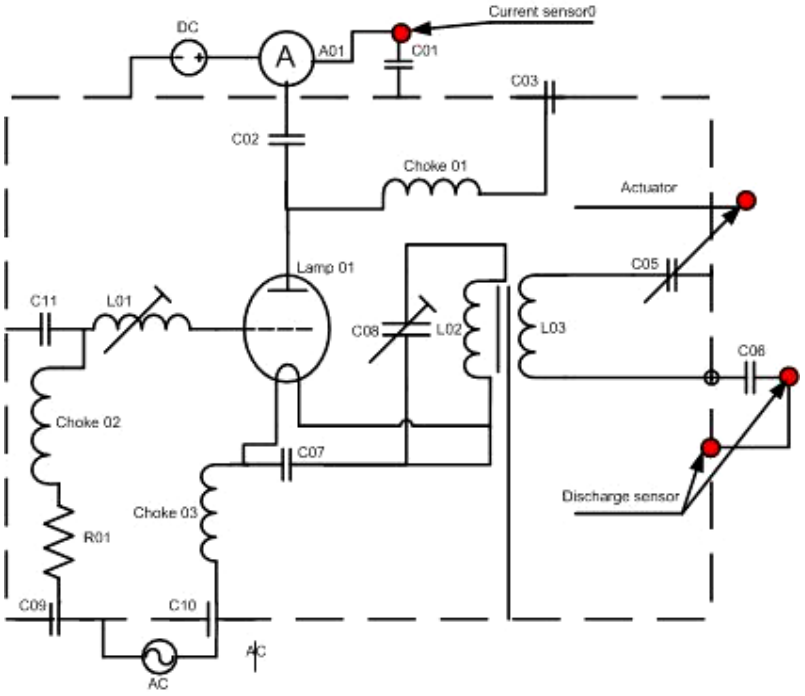

Fig. 11. Integration of ACS elements with reference to the HF scheme of the installation of the model UZP-2500

Рис. 11. Интеграция элементов АСУ с привязкой к схеме ВЧ установки модели УЗП-2500

The unit of the registration and control device was implemented with the following technical characteristics:

– number of measurement channels – 6;

– measured current: 0.01...10 AC, VC;

– measured voltage: 100...4000 V AC;

– measurement interval: 0.005 s, (expansion to 8.10-6 s is possible);

– maximum measurement error: ± 1.5 %;

– non-volatile memory, 64 Kb;

– power –100...380 in VC;

– power consumption – 50 mA.

As it was mentioned above, along with the team of IrGUPS, a number of other scientific schools work in the same direction, therefore, within the hardware created by these teams, both similar and original developments and solutions are viewed. The software parts of ASSR HF are also represented by a number of mathematical models and software complexes.

Thus, the analysis of the structure of the developed systems of scientific research allows us to talk about its dynamic development. To date, comparing the research results, it is safe to say that the construction of an integrated ASSR HF system as a whole is completed. As can be seen from the block diagrams of automated experiment and automated research systems presented below, although they were created separately, specifically for certain tasks, a specific construction methodology is seen in all the works.

Conclusion. Thus, an analysis of the structure of the developed scientific research systems allows us to conclude that the dynamic development of ASSR and SAE by various scientific schools of electrothermists has led to a uniform methodology for constructing ASSR HF.

Comparing the research results, it can be argued that the construction of an integrated system of ASSR HF of polar thermoplastic polymeric materials as a whole is completed.

References

1. Shastin V. I., Kargapoltcev S. K., Gozbenko V. E., Livshits A. V., Filippenko N. G. Results of the complex studies of microstructural, physical and mechanical properties of engineering materials using innovative methods. *International Journal of Applied Engineering Research*. 2017, Vol. 12, No. 24, P. 15269–15272.

2. Baranov V. N. *Primeneniye mikrokontrollerov AVR: skhemy, algoritmy programmy* [Application of AVR microcontrollers: circuits, program algorithms]. Moscow, Dodeka Publ., 2004, 288 p.

3. Bezmenov F. V., Fedorova I. G. *Vysokochastotnaya svarka plastmass* [High frequency welding of plastics]. Moscow, Mashinostroyeniye Publ., 1989, 89 p.

4. Filippenko N. G., Livshits A. V., Mashovich A. Ya., Kargapol'tsev S. K. *Blok avtomatizatsii ustroystva vysokochastotnoy termoobrabotki polimernykh materialov* [Automation unit for high-frequency heat treat-ment of polymer materials]. Patent RF, No. 118916. 2011.

5. *GOST 22372–77. Materialy dielektricheskiye. Metod opredeleniya dielektricheskoy pronitsayemosti i tangensa ugla dielektricheskikh poter' v diapazone chastot ot 100 do 5·10(6) Gts* [State Standard 22372–77. Dielectric materials. The method for determining the dielectric constant and the dielectric loss tangent in the frequency range from 100 to 5 · 10 (6) Hz]. Moscow, Standartinform Publ., 1977. 52 p.

6. Kiseleva T. F. *Tekhnologiya sushki* [Drying technology]. Kemerovo, Kemerovskiy tekhnologicheskiy institut pishchevoy promyshlennosti Publ., 2007.

7. Larchenko A. G. *Sistema avtomatizirovannogo upravleniya vysokochastotnym diagnostirovaniem pri pro-izvodstve i ekspluatatsii izdelii iz polimernykh materialov. Kand. Diss.* [Automated control sys-tem for high-frequency diagnostics in the production and operation of products from polymeric materials. Cand. Diss.]. Irkutsk, 2014. 164 p.

8. Larchenko A. G. [Automated Device for Diagnosing Polymeric Products of Complex Configuration by the Method of High-Frequency Radiation]. *Kontrol'. Diagnostika.* 2016, No. 2, P. 61–65 (In Russ.).

9. Livshits A. V. *Avtomatizirovannoye upravleniye tekhnologicheskimi protsessami vysokochastotnoy elektrotermii polimerov*. *Dokt. diss*. [Automated process control of high-frequency electrothermal pol-ymers. Doct. diss.]. Irkutsk, 2016. 351 p.

10. Markova T. E. [The current state and development trends of the polymer industry]. *Ekonomika i upravleniye*. Available at: https://ecsn.ru/files/pdf/201406/ 201406_94.pdf (accessed 15.04.2020).

11. Matsyuk L. N., Vishnevskaya N. V., Kotovshchikova O. A. [The effect of melt flow on the weldability of polymeric materials]. *Svarochnoye proizvodstvo.* 1975. P. 25–26.

12. *Obzor mirovoy polimernoy industrii* [Overview of the global polymer industry]. Available at: https://polyprofi.ru/blogs/Blog_Poly_and_Pro/obzor-mirovoy-polimernoy-industrii.php (accessed 15.04.2020).

13. Popov S. I. *Avtomatizatsiya upravleniya tekhnologicheskimi protsessami vosstanovleniya ekspluatatsion-nykh svoystv polimerov*. *Kand. diss*. [Automation of control of technological processes of restoration of operational properties of polymers. Cand. Diss.]. Irkutsk, 2013.150 p.

14. [The order of Rosstat dated April 23, 2017 The industrial production index is calculated by type of activity: "Mining", "Manufacturing"]. Available at: https://www.gks.ru/bgd/free/B04_03/IssWWW.exe/Stg/d04/7.htm (accessed 15.04.2020).

15. Rumynskiy S. N. *Avtomatizirovannaya sistema upravleniya protsessom vysokochastotnoy svarki izdeliy iz poliamida*. *Kand. diss*. [Automated control system for the process of high-frequency welding of products made of polyamide. Cand. Diss]. St. Petersburg, 2005. 133 p.

16. Zaytsev K. I. Matsyuk L. N. *Svarka polimernykh materialov* [Welding of polymeric materials]. Moscow, Mashinostroenie Publ., 1988, 312.

17. Sukhoguzov A. P., Kosyakov A. A [Investigation of partial discharges in electrical isolation]. *Vestnik UGTU–UPI*. 2003, No. 5 (25), Part 1, P. 363–371 (In Russ.).

18. *Skhemy upravleniya v ASUTP* [Control schemes in process control systems]. Available at: http://automation-system.ru/main/item/42-sxemy-upravleniya-v-asutp.html (accessed 15.04.2020).

19. Trostyanskaya Ye. B., Komarov G. V., Shishkin V. A. *Svarka plastmass* [Welding plastics]. Moscow, Mashinostroenie Publ., 1967, 251 p.

20. Trofimov N. V., Markov A. V. [Mathematical model of the optimal mode of high-frequency welding of plastics]. *Matematicheskiye metody v tekhnike i tekhnologiyakh (MMTT-21)* [Mathematical methods in engineering and technology (MMTT-21)]. Pskov, 2009, P. 71–73.

21. Trofimov N. V. *Upravleniye rezhimom vysokochastotnoy svarki izdeliy iz plastmass slozhnoy formy*. *Kand. diss.* [Control of high-frequency welding of plastic products of complex shape. Cand. Diss]. St. Petersburg, 2011. 112 p.

22. Shengeliya R. G. [On the application of the method of three measurements on a meter when measuring ε and tanδ of materials with large losses]. *Elektrichestvo.* 1966, P. 79–81 (In Russ.).

23. Larchenko A. G. [Evaluation of the quality of products from polymeric materials for engineering purposes]. *Vestnik Irkutskogo gosudarstvennogo tekhnicheskogo universiteta*. 2019. Vol. 23, No. 3, P. 463–471 (In Russ.).

Библиографические ссылки

1. Results of the complex studies of microstructural, physical and mechanical properties of engineering materials using innovative methods / V. I. Shastin, S. K. Kargapoltcev, V. E. Gozbenko et al. // International Journal of Applied Engineering Research. 2017. Vol. 12, No. 24. P. 15269–15272.

2. Баранов В. Н. Применение микроконтроллеров AVR: схемы, алгоритмы программы. М. : Додека, 2004. 288 с.

3. Безменов Ф. В., Федорова И. Г. Высокочастотная сварка пластмасс. Л. : Машиностроение, 1989. 89 с.

4. Пат. №118916 РФ МПК B29C 65/04. Блок автоматизации устройства высокочастотной термообработки полимерных материалов / Филиппенко Н. Г., Лившиц А. В., Машович А. Я., Каргапольцев С. К. Заяв. 21.10.2011.

5. ГОСТ 22372–77. Материалы диэлектрические. Метод определения диэлектрической проницаемости и тангенса угла диэлектрических потерь в диапазоне частот от 100 до 5·10(6) Гц. М. : Изд-во стандартов, 1977. 52 с.

6. Киселева Т. Ф. Технология сушки. Кемерово : Кемеровский технологич. ин-т пищевой промышл-ти, 2007.

7. Ларченко А. Г. Система автоматизированного управления высокочастотным диагностированием при производстве и эксплуатации изделий из полимерных материалов : дис. … канд. тех. наук. Иркутск, 2014. 164 с.

8. Ларченко А. Г. Автоматизированное устройство диагностирования полимерных изделий сложной конфигурации методом высокочастотного излучения // Контроль. Диагностика. 2016. № 2. С. 61–65.

9. Лившиц А. В. Автоматизированное управление технологическими процессами высокочастотной электротермии полимеров : дис. … докт. тех. наук. Иркутск, 2016. 351 с.

10. Маркова Т. Э. Современное состояние и направления развития полимерной индустрии. Экономика и управление [Электронный ресурс]. Самара,

2014. URL: https://ecsn.ru/files/pdf/201406/201406_94.pdf11 (дата обращения: 15.04.2020).

11. Мацюк Л. Н., Вишневская Н. В., Котовщикова О. А. Влияние текучести расплава на свариваемость полимерных материалов // Сварочное производство. 1975. С. 25–26.

12. Обзор мировой полимерной индустрии [Электронный ресурс]. URL: https://polyprofi.ru/blogs/Blog_Poly_and_Pro/obzor-mirovoy-polimernoy-industrii.php (дата обращения: 15.04.2020).

13. Попов С. И. Автоматизация управления технологическими процессами восстановления эксплуатационных свойств полимеров : дис. … канд. тех. наук. Иркутск, 2013. 150 с.

14. Приказ Росстата от 23 апреля 2017 Индекс промышленного производства исчисляется по видам деятельности: «Добыча полезных ископаемых», «Обрабатывающие производства» [Электронный ресурс]. URL: https://www.gks.ru/bgd/free/B04_03/IssWWW.exe/Stg/d04/7.htm (дата обращения: 15.04.2020).

15. Румынский С. Н. Автоматизированная система управления процессом высокочастотной сварки изделий из полиамида : дис. … канд. тех. наук. СПб., 2005. 133 с.

16. Зайцев К. И. Мацюк Л. Н. Сварка полимерных материалов. М. : Машиностроение, 1988. 312 с.

17. Сухогузов А. П., Косяков А. А. Исследование частичных разрядов в изоляции электрических // Вестник УГТУ–УПИ. 2003. № 5(25). Ч. 1. С. 363–371.

18. Схемы управления в АСУТП [Электронный ресурс]. URL: http://automation-system.ru/main/item/42-sxemy-upravleniya-v-asutp.html (дата обращения: 15.04.2020).

19. Тростянская Е. Б., Комаров Г. В., Шишкин В. А. Сварка пластмасс. М. : Машиностроение, 1967. 251 с.

20. Трофимов Н. В., Марков А. В. Математическая модель оптимального режима высокочастотной сварки пластмасс // Математические методы в технике и технологиях (ММТТ-21). Псков, 2009. С. 71–73.

21. Трофимов Н. В. Управление режимом высокочастотной сварки изделий из пластмасс сложной формы : дис. … канд. тех. наук. СПб., 2011. 112 с.

22. Шенгелия Р. Г. О применении метода трех измерений на куметре при измерении ε и tgδ материалов с большими потерями // Электричество. 1966. № 3. С. 79–81.

23. Ларченко А. Г. Оценка качества изделий из полимерных материалов машиностроительного назначения // Вестник Иркутского гос. технич. ун-та. 2019. Т. 23, № 3. С. 463–471.

Filippenko Nikolay Grigorievich – Cand. Sc., Associate Professor of the Department Automation of Production Processes; Irkutsk State Transport University. E-mail:Pentagon@mail.ru.

Larchenko Anastasia Gennadyevna – Cand. Sc., Associate Professor of the Department Automation of Production Processes; Irkutsk State Transport University. E-mail: Larchenkoa@inbox.ru.

Филиппенко Николай Григорьевич – кандидат технических наук, доцент кафедры автоматизации производственных процессов; Иркутский государственный университет путей сообщения. E-mail: Pentagon@mail.ru.

Ларченко Анастасия Геннадьевна – кандидат технических наук, доцент кафедры автоматизации производственных процессов; Иркутский государственный университет путей сообщения. E-mail: Larchenkoa@inbox.ru.